Are Epigenetic Mechanisms Involved in Axonal Regeneration?

Dissertation

der Mathematisch-Naturwissenschaftlichen Fakultät
der Eberhard Karls Universität Tübingen
zur Erlangung des Grades eines
Doktors der Naturwissenschaften
(Dr. rer. nat.)

vorgelegt von
Ricco Lindner
aus Leipzig

Tübingen
2013

Tag der mündlichen Qualifikation:

Dekan:	Prof. Dr. Wolfgang Rosenstiel
1. Berichterstatter:	Prof. Dr. Philipp Kahle
2. Berichterstatter:	Prof. Dr. Robert Feil

Index of Contents

I. Eidesstattliche Erklärung

Ich erkläre hiermit,

1. dass ich bisher genau ein Promotionsverfahren begonnen aber vorzeitig abgebrochen habe (Universität Tübingen, Institut für Physiologie, von September 2006 bis April 2008, betreut durch Prof. Dr. Florian Lang und Prof. Dr. Michael Duszenko).

2. dass die vorgelegte Dissertation noch nie ganz oder teilweise als Dissertation oder sonstige Prüfungsarbeit eingereicht worden ist, allerdings bereits teilweise zur Veröffentlichung eingereicht worden ist:

"PCAF-dependent epigenetic changes promote axonal regeneration in the central nervous system" - Radhika Puttagunta, Andrea Tedeschi, Marilia Grando Soria, ***Ricco Lindner****, Perrine Gaub, Khizr Rathore, Yashashree Joshi, Tuan Nguyen, Tony Schmandke, Frank Bradke, and Simone Di Giovanni - submitted to Nature Letters (under revision)*

"Epigenetic regulation of axon outgrowth and regeneration in CNS injury: the first steps forward" (Review) – ***Ricco Lindner****, Radhika Puttagunta, and Simone Di Giovanni - submitted to Neurotherapeutics*

3. dass ich die zur Promotion eingereichte Arbeit mit dem Titel: *„****Are Epigenetic Mechanisms Involved in Axonal Regeneration?****"* selbstständig verfasst habe, nur die angegebenen Quellen und Hilfsmittel benutzt habe und wörtlich oder inhaltlich übernommene Stellen als solche gekennzeichnet habe. Ich versichere an Eides statt, dass diese Angaben wahr sind und dass ich nichts verschwiegen habe.

4. dass ich bisher weder strafrechtlich verurteilt, noch Disziplinarmaßnahmen und anhängigen Straf- und Disziplinarverfahren unterzogen worden bin.

5. dass ich meine eigenen Anteile und die Anteile anderer an dieser Dissertation, wie folgt, wahrheitsgemäß und vollständig angegeben habe:
Ricco Lindner: Entnahme von DRG, Durchführung der MeDIP und Probenvorbereitung zur MeDIP-chip, Microarray-Analysen zur DNA-Methylierung, CGI-Analyse, qRT-PCR für DNMTs, RAG (Zeitpunkte: 1, 3, 7 Tage), *Sprr*-Gene und DM-Gene (TaqMan Expression Array und dessen Verifizierung) [wesentlicher Anteil an dieser Dissertation (50-55 %)]
Dr. Radhika Puttagunta: DRG- und CGN-Kultur inklusive PCAF-AAV-Infektion und Behandlungen; Immunfärbungen und Analysen zum Neuritenwachstum; qRT-PCR für RAG; ChIP für Histon-Modifikationen von CGN; Western Blot für H3-K9ac von CGN; Luciferase-Assay [wesentlicher Anteil an dieser Dissertation (25-30 %)]
Dr. Elisa Floriddia: (ChIP-Experimente zu Histon-Modifikationen an Maus-DRG inklusive Axotomie bei Mäusen (SNA, DCA); qRT-PCR (Zeitpunkt: 2 Tage); Western Blot für H3-K9/K14ac/me2 [wichtiger Anteil an dieser Dissertation von kleinerem Umfang (10 %)]
Dr. Andrea Tedeschi: Applikation der zentralen Axotomie bei Mäusen (DCA) für MeDIP-chip
Dr. Tuan Nguyen: Applikation der peripheren Axotomie bei Mäusen (SNA) für MeDIP-chip

Leipzig, 26. April 2013

II. Acknowledgment

I want to thank Dr. Simone Di Giovanni, the principle investigator of my research group "NeuroRegeneration & Repair", for the kind opportunity to accomplish the presented thesis and to do interesting, challenging, and high quality research in a great, international, and friendly atmosphere. I owe special thanks to him for the competent advice and support as my supervisor.

I want to thank Prof. Dr. Philipp Kahle and Prof. Dr. Robert Feil for the assessment of my thesis, and Prof. Dr. Michael Duszenko for his kind and competent advice as second supervisor.

Great thank to my colleagues from the Hertie Institute for a wonderful work atmosphere and their friendship. Special thanks to Dr. Tuan Nguyen, Dr. Andrea Tedeschi, Dr. Radhika Puttagunta, and Dr. Elisa Floriddia for the valuable data contribution, performed experiments or techniques, instructions, advice, and moreover their friendship.

Last but not least, I want to thank my lovely and encouraging girlfriend, my dear friends, and my parents for everlasting support, patience, and understanding.

III. Zusammenfassung

Das Ziel dieser Studie war, die Rolle epigenetischer Mechanismen bei der Genregulation im Zusammenhang mit Axonregeneration aufzuklären. Insbesondere wurden hierzu zwei Typen von Nervenverletzung verglichen, die Axotomie des peripheren Ischiasnervs (sciatic nerve axotomy; SNA) und die Schädigung des dorsalen Rückenmarks (dorsal column axotomy; DCA). Die Regeneration von Axonen ist normalerweise nur im peripheren Nervensystem erfolgreich. Der Hypothese entsprechend wurde erwartet, dass differenzielle Veränderungen des Genexpressions-Musters, abhängig vom Verletzungstyp, mit entsprechenden Änderungen im epigenetischen Code korrelieren. Insbesondere sollte eine verstärkte Genpromotor-DNA-Methylierung infolge der Axotomie, im Vergleich zur Scheinoperation als Kontrolle, mit einer Herunterregulierung von regenerations-assoziierten Genen (RAG) verbunden sein. Umgekehrt sollte eine verminderte Promoter-Methylierung mit einer entsprechenden Hochregulierung korrelieren. Des Weiteren könnten auch spezifische Histon-Modifikationen mit der induzierten RAG-Expression zusammenhängen (**Abb. 1**).

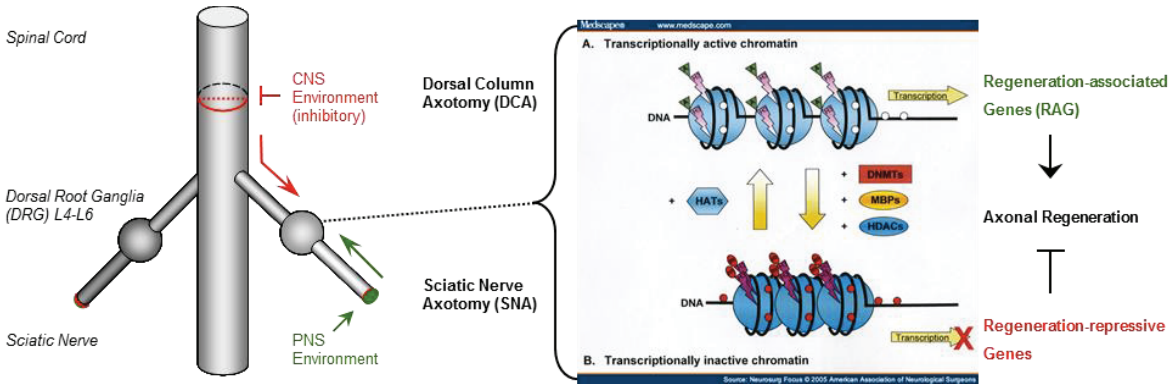

Abbildung 1 – Schematische Darstellung des verwendeten Modells für Nervenverletzung und der hypothetisierten epigenetischen Regulierung von regenerations-assoziierten Genen (RAG). 2 bis 3 Monate alte Mäuse erhielten entweder eine beidseitige Axotomie des Ischiasnervs (SNA), eine Axotomie des dorsalen Rückenmarks oder eine Scheinoperation, jeweils im gleichen Abstand zu den Spinalganglien L4-L6 (DRG), welche ein geeignetes Regenerationsmodell sind. Die axotomie-induzierte Expression von RAG in DRG korrelierte zum Teil mit differenzieller Promotor-DNA-Methylierung und mit spezifischen Histon-Modifikationen (H3-K9ac/me2).
Rechter Teil der Abbildung von www.medscape.com; Neurosurg Focus 2005

Maus-Spinalganglien (dorsal root ganglia; DRG) wurden als geeignetes *in vivo* Modell für die Axonregeneration verwendet, welches erlaubt, differenzielle Effekte und Reaktionen auf beide Verletzungstypen im selben neuronalen System zu untersuchen. Ein, drei oder sieben Tage nach durchgeführter SNA beziehungsweise DCA wurden induzierte Veränderungen der promotorgebundenen epigenetischen Markierungen untersucht und in Bezug zu entsprechenden Genexpressions-Veränderungen im Rahmen der Axonregeneration gesetzt. Zunächst wurde eine Immunpräzipitation von methylierter DNA mit einem speziellen Microarray-Typ kombiniert (MeDIP-chip), um genomweit die Methylierungsmuster von Genpromotoren und sogenannten CpG-Inseln (CGI) zu analysieren. Insgesamt wurden 179 hyper- beziehungsweise hypomethylierte Gene für beide Arten von Nervenverletzungen identifiziert. Diese

Gene waren zum Teil differenziell methyliert (DM), das heißt, sie wiesen verletzungsbedingte Veränderungen des Methylierungsmusters nur für einen Verletzungstyp auf. Viele von diesen Genen konnten mit Funktionen bei der Chromatin-Umgestaltung, der Transkriptions-regulation oder in der (neuralen) Entwicklung beziehungsweise Zelldifferenzierung assoziiert werden. Jedoch nur für einen Teil der differenziell methylierten Gene konnten der Hypothese entsprechende Genexpressions-Muster gefunden werden. Zusätzlich wurde in dieser Arbeit die Hochregulierung einiger bekannter RAG exklusiv infolge der peripheren Axotomie verifiziert, beispielsweise für *Gap43*, *Sprr1a* und *Bdnf*. Allerdings waren die meisten dieser Gene nicht signifikant methyliert. Folglich wurde zusätzlich eine Promotor-CGI-Analyse von RAG und DM-Genen durchgeführt, um voraussagbare Beziehungen zwischen dem Promotor-Methylierungsmuster und der Verteilung von CpG-Dinukleotiden zu finden. Fast alle der untersuchten Gene, insbesondere RAG, und mit Ausnahme von *Sprr1a*, besaßen mindestens eine oder mehrere CpG-Inseln in deren proximalen Promotorregion oder nahe der Transkriptions-Startseite (TSS). Im Vergleich zu RAG zeigten DM-Gene durchschnittlich eine höhere normalisierte CpG-Dichte im Bereich der TSS. Dabei wiesen differenziell hypermethylierte Gene höhere normalisierte CpG-Werte auf als hypomethylierte Gene, und moderat regulierte RAG höhere Werte als stark induzierte RAG.

Anschließend konnte gezeigt werden, dass die Hochregulierung wichtiger RAG infolge der peripheren Nervenverletzung mit erhöhten Leveln von Azetyl-Histon-3-Lysin-9 (H3-K9ac) und verringerten Dimethyl-Leveln (H3-K9me2) in der Promotorregion zusammenhing. Die Überexpression von PCAF (KAT2B), einer spezifischen Histon-Azetyltransferase für H3-K9, in Kulturen von dissoziierten DRG-Neuronen oder zerebellären Neuronen, verstärkte das Auswachsen von Neuriten, sogar auf hemmendem ZNS-Myelin. In diesem Zusammenhang wurde die myelin-induzierte Reduktion von Promotor-H3-K9ac, im Vergleich zu einem wachstumsfördernden Substrat, verhindert beziehungsweise wurde die RAG-Expression gesteigert.

Zusammenfassend scheint die Promotor-DNA-Methylierung keine wesentliche Rolle bei der Regulierung regenerations-assoziierter Gene im Allgemeinen zu spielen, allerdings dennoch für bestimmte induzierte Gene. Hingegen ist speziell die H3-K9-Azetylierung für die RAG-Regulierung nach peripherer Axotomie von Bedeutung und fördert das Neuritenwachstum. Durch Überexpression von PCAF und durch die folgende erhöhte Promotor-Histonazetylierung konnte sogar der hemmende Effekt von Myelin *in vitro* überwunden werden und ein gewisses Maß an Regeneration in kultivierten DRG-Neuronen oder CGN erreicht werden. Diese Studie konnte erfolgreich zeigen, dass bestimmte epigenetische Mechanismen an der Genregulation im Rahmen der Axonregeneration beteiligt sind. Dennoch ist das Gesamtbild zum Verständnis dieser Regulierung noch lange nicht vollständig. Weitere Studien sind dringend erforderlich und könnten dazu beitragen, kombinierte klinische Therapien für die Behandlung traumatischer Rückenmarksverletzungen zu entwickeln.

IV. Executive Summary

The purpose of this study was to elucidate the role of epigenetic mechanisms for the regulation of genes associated with axonal regeneration following peripheral sciatic nerve axotomy (SNA) as compared to central dorsal column axotomy (DCA). Axon regeneration is usually only successful in the peripheral system. According to the hypothesis, injury type dependent differential changes of the gene expression pattern were expected to be associated with corresponding changes of the epigenetic code. Specifically, gene promoter DNA hypermethylation would correlate with downregulation of regeneration-associated genes (RAGs) following injury, compared to sham. Inversely, promoter hypomethylation would correlate with an upregulation. Furthermore, specific histone modifications might be associated with injury-induced RAG expression (**Figure 1**).

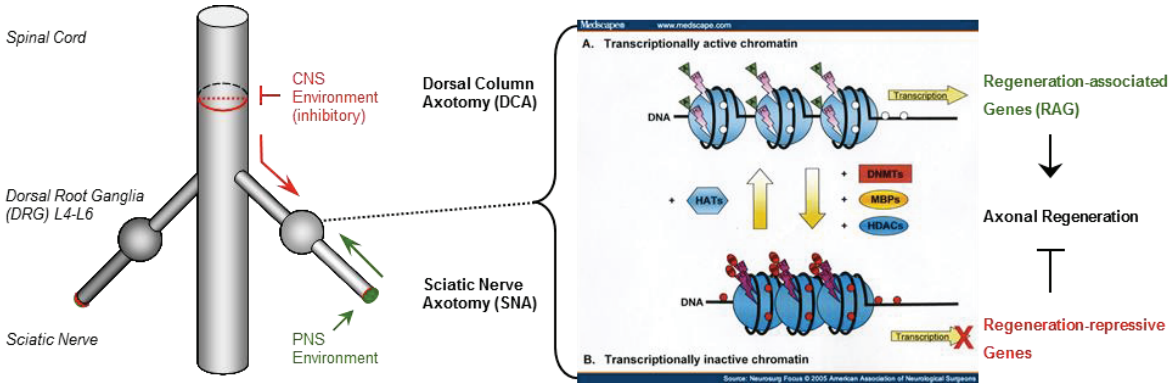

Figure 1 – Schematic of the nerve injury model and of the hypothesized epigenetic regulation of regeneration-associated gene (RAG) expression. Bilateral sciatic nerve axotomy (SNA), or dorsal column axotomy (DCA), or sham surgery was applied equidistally to L4-L6 dorsal root ganglia (DRG) in adult mice. Injury-induced RAG expression in DRG, which serve as unique regeneration model, correlated with differential promoter DNA methylation and specific histone modifications (H3-K9ac/me2). Right part of figure from www.medscape.com, Neurosurg Focus 2005

Mouse dorsal root ganglia (DRG) were used as a suitable *in vivo* model for axon regeneration that allows the investigation of differential responses and effects to both types of nerve lesion within the same neurons. One, three, or seven days following either SNA or DCA, injury-induced changes of promoter-bound epigenetic marks were assayed and correlated to gene expression changes associated with axon regeneration. First, methylated DNA immunoprecipitation was combined with a special microarray for methylated DNA (MeDIP-chip) in the frame of a genome-wide promoter and CpG island (CGI) DNA methylation analysis. Altogether, 179 hyper- or hypomethylated genes were identified for both injury conditions. A subset of these genes was differentially methylated (DM) exhibiting injury-induced changes of methylation levels only upon SNA or DCA. Many of these genes were associated with functions in chromatin remodeling, transcription regulation, or neural development or differentiation. For a subset of the DM genes, the promoter methylation status correlated with gene expression changes upon injury according to the hypothesis. Gene expression of known major RAGs such as *Gap43*, *Sprr1a*, and *Bdnf* was verified to be upregulated solely upon SNA. However, most of these genes were not significantly methylated. Consequently, a promoter

CGI analysis was performed for RAGs and DM genes to identify predictable correlations between promoter methylation status and CpG dinucleotide distribution. Almost all investigated genes, especially RAGs, have one or more CGIs within the proximal promoter region or close to the transcription start site (TSS), except *Sprr1a*. DM genes exhibited a higher normalized CpG density around the TSS than analyzed RAGs. Thereby, differentially hypermethylated genes had higher normalized CpG values than hypomethylated genes, and moderately induced RAGs had higher values compared to highly induced RAGs.

Second, increased expression of major RAGs was shown to be associated with increased promoter histone-3 lysine-9 acetylation (H3-K9ac), and decreased dimethylation (H3-K9me2) following peripheral injury. Overexpression of PCAF (KAT2B), a histone acetyltransferase for H3-K9, in dissociated mouse DRG neuron cultures, or in mouse cerebellar granule neurons enhanced neurite outgrowth, even on inhibitive CNS myelin. This was associated with the prevention of decreasing promoter H3-K9ac occupancy, and with increased RAG expression on myelin compared to a permissive substrate.

Altogether, promoter DNA methylation seems not to be majorly involved in regeneration-associated gene expression regulation although it seemed to be important for specific induced genes. However, H3-K9 acetylation specifically plays a role for RAG expression upon SNA and for promoting neurite outgrowth. Enhancing local promoter histone acetylation by overexpression of PCAF can even overpower the outgrowth inhibiting effects of CNS myelin *in vitro* inducing a certain degree of regeneration in cultured DRG neurons or CGN. This study succeeded to show that specific epigenetic mechanisms are involved in gene regulation in the frame of axonal regeneration, although the whole picture is still far from being complete. Further studies are mandatory and might help developing combinational clinical therapies for treatment of spinal cord injury.

1 Introduction

1 Introduction

1.1 Nerve injury and regeneration

1.1.1 Axonal regeneration in the peripheral and central nervous system

For more than 30 years, research on the molecular details of axonal regeneration has been promoted [Schwartz 1987; Caroni 1998] in order to understand underlying mechanisms and to find therapies allowing functional recovery after injury or lesion of the central nervous system (CNS). Stroke and traumatic injuries of the brain or spinal cord are the most frequent acute CNS neurological disorders. Still, such destructive incidents as well as neurodegenerative and some other disorders cannot be cured or functionally restored yet [Cafferty *et al.* 2008; Roshanpour *et al.* 2012]. CNS injuries often implicate severe and irreversible consequences like local tissue damage, cell loss, and impaired axonal injury, followed by a loss of neuronal and synaptic connections. This is accompanied by various degrees of ischemia and hemorrhage at the lesion site, inflammatory responses, and glial scar formation [Springer 2002; Allan *et al.* 2003]. In contrast to nerve injuries of the peripheral nervous system (PNS) where axonal regeneration happens spontaneously and is partially functional, injury of CNS neurons does not lead to substantial axon sprouting or regeneration or functional recovery under physiological conditions. The repair process at the lesion site is quite different for the two injury types. Detailed knowledge about the basic mechanisms that control the capacity of axons to sprout or regenerate is still lacking although several involved molecular pathways have been proposed [Yakovlev *et al.* 1995; Rossi *et al.* 2007; Huebner *et al.* 2009]. Long-term conse-

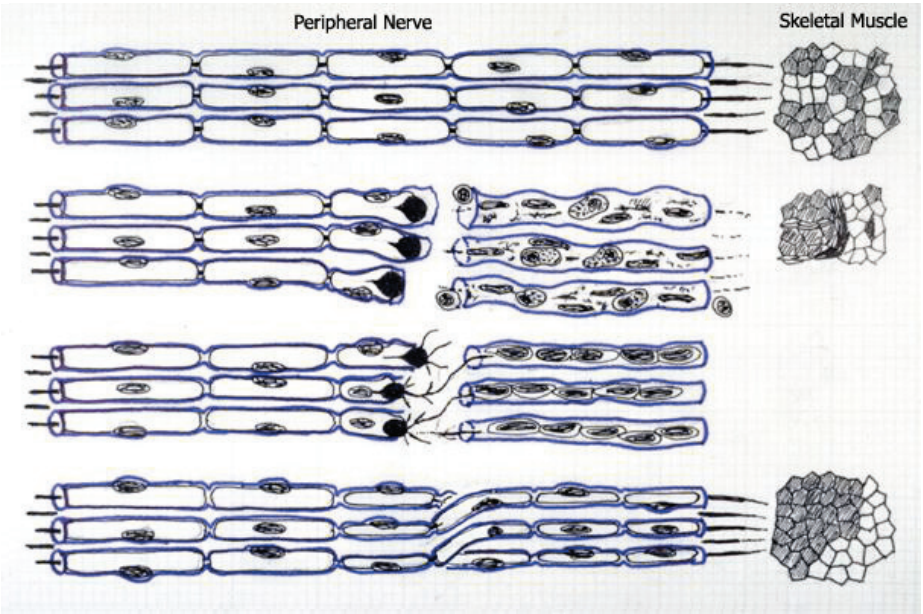

From former Multimedia Learning Modules @ UCSF

Figure 2 – Scheme of cellular regeneration processes upon peripheral nerve injury. Following transection, the peripheral axons distal to the injury site will undergo Wallerian degeneration sparing the basement membrane (blue). Thereby, macrophages enter the area around the injury site removing PNS myelin and debris. Then, Schwann cells (black) line up in the distal basement membrane tube to attract and remyelinate proximal axon sprouts. The proximal nerve terminals will grow into the Schwann cell sheaths and eventually reinnervate the muscle causing a neurogenic rearrangement.

quences of acute axonal CNS injury are loss of certain neurological functions and overall clinical disability. Patients with such injuries often suffer from substantial loss of brain functions or, in the case of spinal cord injury, paraplegia and several secondary complications such as incontinence, pneumonia, and thromboses [Navarro *et al.* 2007; Ditor *et al.* 2009].

The regeneration potential of adult mammalian CNS neurons is very limited compared to PNS neurons. Peripheral axons that innervate muscles or other organs can functionally regenerate upon nerve transection (**Figure 2**). Due to Wallerian degeneration, axons and peripheral myelin (produced by Schwann cells) distal to the lesion site are degraded. Debris and PNS myelin is quickly removed by invading activated macrophages. During this process, the basement membrane surrounding axons and Schwann cells remains intact. Thus, leaving a growth promoting sheath, Schwann cells settle in these basement membrane tubes and secrete growth factors for the chemotactical attraction of axons sprouts from the proximal end of severed nerves. During this process, innervated muscles become atrophic. Many axons successfully sprout into the membrane sheaths and eventually reinnervate the muscle causing a neurogenic rearrangement [Stoll *et al.* 1989; ZL Shen *et al.* 2000]. In contrast to peripheral nerve injury, tissue repair is deficient upon spinal cord injury complicated by secondary tissue damage, a more intensive inflammatory response, glial scar formation, and the axon growth inhibitory environment (**Figure 3**). Initially, macrophages are recruited to remove axonal and myelin debris although Wallerian degeneration occurs more slowly and protracted compared to peripheral injury. In addition to a more efficient removal of myelin debris in the PNS following injury, compared to the CNS, and in contrast to Schwann cells that downregulate the expression of myelin-associated genes, oligodendrocytes in the CNS continue their expression [Filbin 2003; TB Jones *et al.* 2005]. This process is accompanied by increased proliferation and activation of reactive astrocytes that produce glial fibrillary acidic protein (GFAP). Astro-

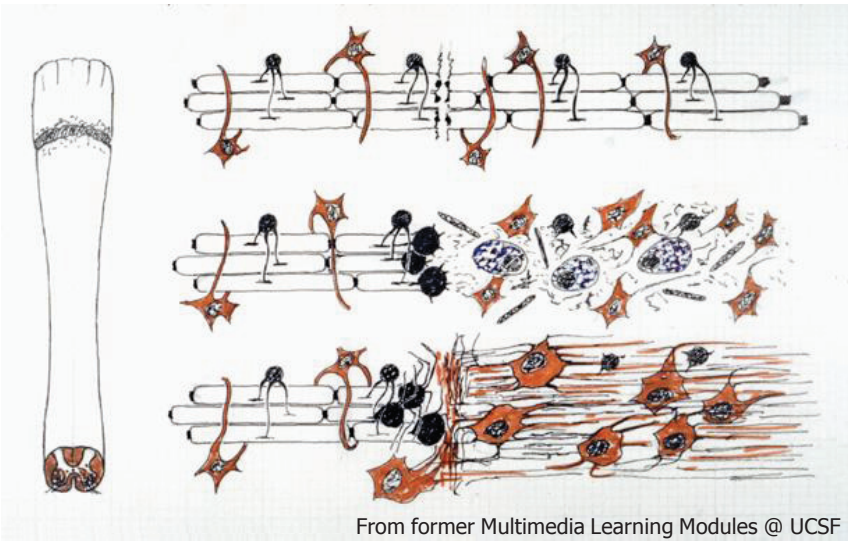

Figure 3 – Scheme of cellular processes upon central nerve injury. Following transection of central axons in the spinal cord, damaged axons (Wallerian degeneration) and tissue debris (necrosis) distal to the injury site are removed by invading activated macrophages (purple). Astrocytes (orange) begin to proliferate and get activated (reactive astrogliosis) to form a glial scar containing polymerized GFAP, blocking and inhibiting axonal growth. Oligodendrocytes (small black) are not responding as Schwann cells in the peripheral system.

cytes and polymerized GFAP, together, form a dense glial scar which blocks putative growth signaling, inhibits axonal regeneration as a physical barrier, and prevents even sprouting into or beyond the lesion site. However, such scar is not formed upon peripheral nerve injury and the PNS myelin sheath environment is much less inhibitory [Fawcett *et al.* 1999; Qiu *et al.* 2000; Silver *et al.* 2004]. The CNS environment around the injury site is typically rather hostile for axonal regeneration containing inhibitory myelin components and myelin-associated factors that are typically found in the CNS but rarely in PNS myelin. These extrinsic factors seem to play a central role as molecular signals to prevent axonal regeneration [Berry 1982; JK Lee *et al.* 2011].

1.1.2 Dorsal root ganglia - a model for axonal regeneration

Dorsal root ganglia (DRG) are nodular groups of the cell bodies of afferent neurons located at either site of the spinal cord between the vertebras grouped into cervical, thoracic, and lumbar DRG. Their neurons pass sensory information into the dorsal column of the spinal cord via the dorsal horn, eventually arriving in the brain. DRG contain different types of large and small neurons of a pseudo-unipolar type having one afferent axon with two branches that act as a single axon. These axons relay sensory information into the CNS such as nociception and thermal perception (small DRG neurons), mechanoception (large neurons), or proprioception (**Figure 4**). The specific morphology of DRG neurons allow action potentials, that arise in the periphery, to bypass the cell body and to be propagated into the dorsal horn, either to synapses with other interneurons, or along another branch into the dorsal columns of the spinal cord directed to the brain. Because of their special property to project axonal branches into both, the peripheral and the central nervous system, DRG neurons are a unique model of axonal regeneration. The same neurons can be investigated responding to different types of nerve injury, depending on a different local environment. DRG exhibit an intrinsic outgrowth capacity since the peripheral branch is capable of a robust regenerative response following peripheral nerve lesion. However, the central branch within the spinal cord does not spontaneously regenerate when the lesioned axon is exposed to the local inhibitory environment. DRG neurons are thus capable of a differential reaction showing successful peripheral regeneration and axon outgrowth but failing to regenerate in the inhibitory CNS environment.

To study the differential regenerative capacity of axons in the PNS versus the CNS, specifically neurons from mouse lumbar L4-L6 DRG, associated with the sciatic nerve, were of interest in this thesis. The sensory information from the sciatic nerve is a relevant feedback, for example, for fine movements of muscles in the hind limbs and feet, as well as for relaying heat and pain (nociceptive), or touch (mechanoceptive), or proprioceptive sensory information from innervated tissues such as skin, bone, tendon, or muscle [Caspary *et al.* 2003]. Nerve lesion of the peripheral branch of L4-L6 DRG neurons can easily be performed, usually at mid-thigh level. A central axotomy of the same neurons can be applied as dorsal hemisection, as a form of spinal cord injury, or as nerve crush at an equidistal position, for example,

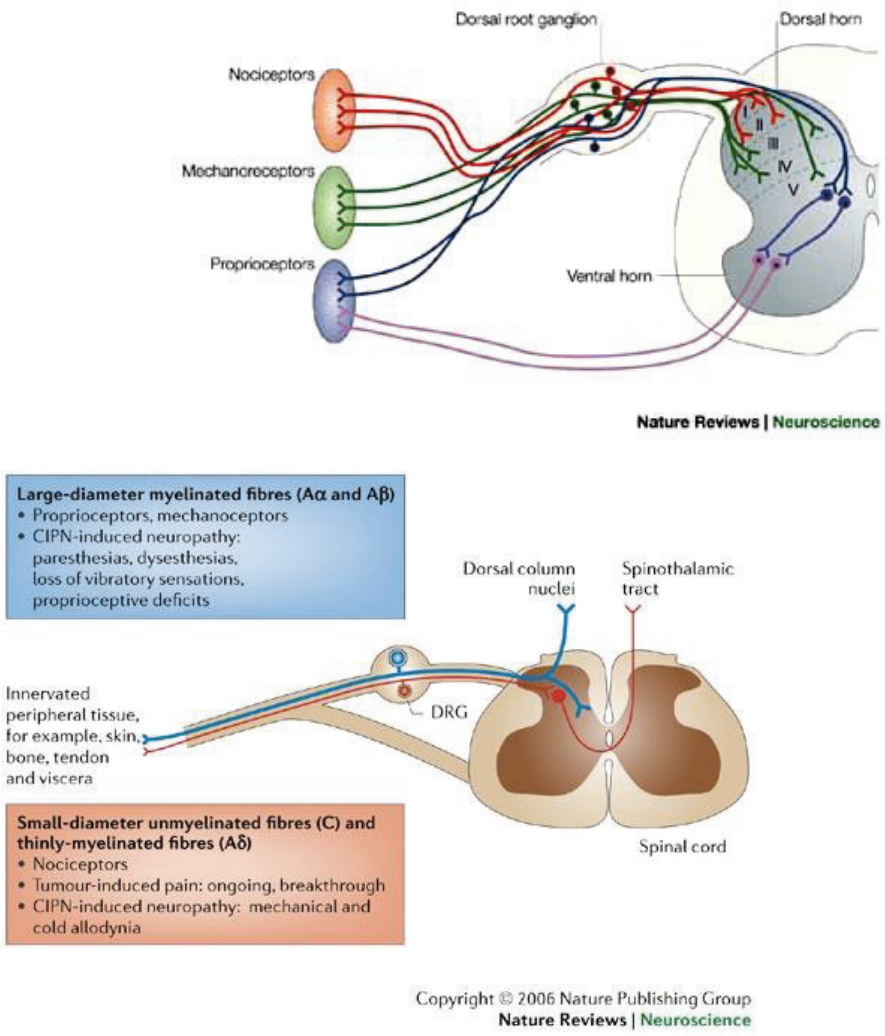

Figure 4 – Schematic of dorsal root ganglia (DRG), a model of axonal regeneration. DRG neurons are an interesting model for axonal regeneration since these unique pseudo-unipolar neurons possess a single afferent axon with two branches extending into the peripheral or central nervous system (spinal cord). Arising sensory signals in the periphery, for example, nociception (pain and temperature), mechanoception, or proprioception (upper and lower figure) are conveyed into specific laminae of the dorsal horn, or to ventrally located motoneurons, or through the spinal cord into the brain (lower figure). The upper figure is a schematic of neuronal circuits in a mouse spinal cord at embryonic day 18 [Caspary & Anderson 2003]. The lower schematic additionally shows the different types of sensory neurons and their projections into the spinal cord [Mantyh 2006].

between the thoracic vertebrae T9 and T10. This allows for the comparison of responses to the two injury types in different environments involving retrograde signaling, activated transcriptional mechanisms, and finally regeneration efficacy.

1.1.3 The extrinsic environment in the CNS inhibits axonal regeneration

Which mechanisms allow axonal sprouting and regeneration as well as functional recovery in the peripheral but not in the central nervous system? In the recent years, research focused on the identification of major factors responsible for the failure of CNS regeneration. Thereby, extrinsic and intrinsic factors can be distinguished. Extrinsic molecular factors are part of the myelin environment or the scar forming upon central nerve injury and are secreted by glial

cells. An increasing complexity of molecular players has led to a more detailed picture of the interactions between extracellular components and the axonal membrane proteins and subsequent signaling. Understanding the inhibitory mechanisms of extrinsic factors in the CNS environment is important to understand the failure of axon regeneration after a central lesion and to find out how this inhibition might be overcome. Since it was discovered that myelinating oligodendrocytes express neurite growth inhibitory proteins [Caroni *et al.* 1988b; Schwab *et al.* 1993], the concept of CNS neurons only being deficient of regeneration capability was put into question. Rather, the prohibitive environment seemed to prevent neurite outgrowth although central neurons, in principal, might be intrinsically able to regenerate [Kim *et al.* 2003]. Axon growth potential is highest in young neurons but diminishes with age. Reasons for this observation during the maturation of neurons might be a reduced intrinsic outgrowth capacity and/or an increasingly growth inhibitory molecular environment, once neuronal structures in the spinal cord are established. Accordingly, an increasing set of extrinsic growth inhibitory molecules and related signaling pathways have been described and characterized [Fawcett & Asher 1999; Filbin 2003; Schwab 2004; Yiu *et al.* 2006].

Major inhibitory components of the specific CNS myelin environment at the lesion site are, for example, myelin basic protein (MBP), oligodendrocyte myelin glycoprotein (OMG, previously OMGP), or myelin-associated glycoprotein (MAG). Additionally, chondroitin sulfate proteoglycans (CSPGs) are produced by astrocytes and specifically present in the scar that is formed after a central nerve injury. These components were found to inhibit the activation of a regeneration response to nerve injury [Mukhopadhyay *et al.* 1994; Huber *et al.* 2000; Filbin 2003; Fujita *et al.* 2011; JK Lee & Zheng 2011]. Such growth inhibiting myelin-associated molecules are present to a much lesser extent in the peripheral myelin environment, which is provided by Schwann cells, although at least MAG plays a role in both environments [Trapp *et al.* 1989; Latasa *et al.* 2010]. CSPGs have been shown to retract neurites and to cause growth cone collapse *in vitro*. Reactive astrocytes produce CSPG4 (NG2) in the glial scar that inhibits axonal growth, putatively acting through the receptor PTPRS [McKeon *et al.* 1991; Yiu & He 2006; Y Shen *et al.* 2009]. Several receptors for inhibitory signals from the CNS myelin have been characterized and are involved in the inhibition of axonal regeneration, for example, RTN4R (NOGOR/NGR) that responds to reticulon 4 (RTN4, previously NOGO-A), or LINGO1 and LILRB3 (PIRB), which in part functionally colocalize. Additionally, the nerve growth factor receptor NGFR (or Tumor necrosis factor receptor TNFRSF16, previously P75NTR) and its interacting receptor TNFRSF19 (TROY) were described to contribute to the mediation of inhibitory signals [He *et al.* 2004; Atwal *et al.* 2008; Akbik *et al.* 2011]. Best characterized, so far, is the RTN4R downstream signaling cascade via RHOA activation, which results in growth cone collapse and axonal outgrowth inhibition. Modulating this receptor-mediated signaling leads to partially promoted axonal sprouting and regeneration in different experimental regeneration models [MS Chen *et al.* 2000; GrandPre *et al.* 2000; Kim *et al.* 2004; Di Giovanni 2006].

Besides myelin-associated molecules, several other secreted inhibitory signaling molecules have been shown to inhibit axon outgrowth such as certain semaphorins, ephrins, and netrins [Moreau-Fauvarque *et al.* 2003; Goldberg *et al.* 2004; Goldshmit *et al.* 2004; Giger *et al.* 2010]. Semaphorin 3A (SEMA3A), for example, is a repulsive guidance factor for many developing neurons, which is continuously expressed into adulthood and involved in growth cone collapse, and it binds to the neuropilin 1/plexin A4 receptor complex (NRP1/PLXNA4) [Pasterkamp *et al.* 2001; Montolio *et al.* 2009; Nangle *et al.* 2011]. Several ephrins and ephrin receptors are upregulated in neurons or astrocytes upon spinal cord injury. The predominantly repulsive ephrin EFNB3 is strongly expressed in CNS myelin along with EFNB2 [Benson *et al.* 2005]. Important interacting ephrin receptors are EPHB3 and EPHA4 that mediate outgrowth inhibiting signals [Fabes *et al.* 2007]. Antagonization or deficiency of EPHA4 promotes sprouting of corticospinal tract (CST) axons. Additionally, netrin-1 is a repellent guidance molecule binding to netrin receptors UNC5A to UNC5C and functioning as inhibitor of sensory axonal regeneration [Masuda *et al.* 2009].

An anti-regenerative signaling following a central lesion might replace the activation of a pro-regeneration program, lacking appropriate activating factors. Several experiments have shown that it is possible to overcome growth limitations of the CNS and to trigger substantial neurite outgrowth with proper treatments, despite the presence of inhibitory myelin or a glial scar. To overcome the limitations for axonal outgrowth in the CNS, experiments have been performed in rodents modifying the inhibitory CNS environment at the injury site. For example, transplanted peripheral Schwann cell-derived nerve grafts allowed injured CNS axons to grow and extend into them, thereby simulating a PNS environment [Richardson *et al.* 1980; David *et al.* 1981; Benfey *et al.* 1982; Bunge 2001]. The inhibitory CNS myelin environment might serve as a therapeutic target to induce or enhance axonal regeneration. Blocking the effects of such extrinsic inhibitory molecules with antibody strategies promotes axon outgrowth. For example, the IN-1 monoclonal antibody neutralized myelin-mediated inhibition [Caroni *et al.* 1988a; Schnell *et al.* 1990]. In other studies, CSPG degrading enzymes were applied such as neuronal matrix metallopeptidase 2 (MMP2) [Zuo *et al.* 1998] or chondroitin sulfate ABCase which show de-inhibitive effects [Bradbury *et al.* 2002; Iaci *et al.* 2007]. Otherwise, the synthesis of proteoglycans was inhibited in order to make the CNS environment less hostile for axon regeneration [Smith-Thomas *et al.* 1995]. However, neutralizing regeneration inhibitors alone is not sufficient for substantial axonal regrowth. One of the reasons may be that most inhibitory molecules are also constitutively expressed in the uninjured nervous system and are therefore not specifically expressed in response to nerve injury [Schwab et al. 1993; Raisman 2004]. Certainly, they usually play a role in physiological conditions. Inhibitory factors might maintain the unchanged and intact postnatal structure of the spinal cord, and provide clear and distinct pathways for axonal growth during development preventing uncontrolled axon outgrowth [Mueller *et al.* 2006]. More recently, specific molecular mechanisms for regeneration have emerged to be of crucial importance, including intrinsic neuronal factors.

1.1.4 Intrinsic factors for successful or inhibited axonal regeneration

Blocking the regeneration inhibitory effects of extrinsic factors within the CNS environment has been shown to allow substantial neurite outgrowth, though not sufficient for successful functional regeneration. Moreover, the lack of growth factors upon central nerve lesion must be compensated to potentially trigger the intrinsic pro-growth program. Therefore, it is fundamentally important to identify and to understand intrinsic molecular players and pathways. After the embryonic to adult transition, the intrinsic neuronal growth activity is repressed to allow for proper synaptic development and function in the post-mitotic neurons [Abe *et al.* 2008]. Further, CNS neurons might even lose their axon outgrowth capacity during development [Goldberg *et al.* 2002]. Injured peripheral axons of post-mitotic neurons are able to activate a pro-outgrowth program in response to local growth signals. Since injured central neurons are capable to sprout neurites in certain experimental conditions, as well, they might not be completely deficient of an intrinsic regeneration capacity, as it was believed [Di Giovanni 2009]. Rather the CNS myelin-associated inhibitory signaling might just suppress the activation of a pro-outgrowth program. Dorsal root ganglia, as a model for axonal regeneration, allow to investigate the intrinsic regeneration potential of neurons in response to the glial environment. In DRG neurons, the differential intrinsic response to either peripheral or central nerve lesion can thus be observed and compared in the same neuronal model system.

Necessarily, there must be some retrograde signaling from the injury site to the cell body and into the nucleus to induce gene expression [Sung *et al.* 2006; Abe & Cavalli 2008]. Upon peripheral injury, certain major pathways were identified to be involved in the regeneration response, which are mostly not activated upon central nerve lesion. Specifically, these comprise several mitogen-activated protein kinase pathways such as MAPK3 and MAPK1 (ERK1 and ERK2) [Seira *et al.* 2010; Tsuda *et al.* 2011], or MAPK8 to MAPK10 pathways (JNK1 to JNK3) [Lindwall *et al.* 2005]. Besides the MAPK pathways, also PI3K/mTOR signaling [KK Park *et al.* 2008; Christie *et al.* 2013] and the JAK/STAT3 pathways are involved, altogether drawing a picture of complex activation patterns upon injury [RY Liu *et al.* 2001]. These pathways are triggered by growth promoting factors like nerve growth factor (NGF), brain derived neurotrophic factor (BDNF), or neurotrophin 3 (NTF3), which show increased protein levels following peripheral but not upon central nerve lesion. These factors can bind to nerve growth factor receptors to activate pro-growth processes in lesioned DRG neurons [Windebank *et al.* 1986; Klesse *et al.* 1999; Geremia *et al.* 2010; Weishaupt *et al.* 2012]. Various different approaches have been pursued to trigger the intrinsic molecular regeneration capacity. The application of BDNF, GDNF, NTF3, NGF, or cAMP (also induced upon PNS injury but not upon CNS injury) to the extracellular space, potentially together with peripheral Schwann cell grafts or antibodies against myelin components, could be shown to promote axon outgrowth [Schnell *et al.* 1994; R Grill *et al.* 1997a; RJ Grill *et al.* 1997b; Blits *et al.* 2000; LL Jones *et al.* 2001; L Zhou *et al.* 2003; Kadoya *et al.* 2009; Bretzner *et al.* 2010; Hou *et al.* 2012]. Additional factors like the cytokine interleukin 6 (IL6), the leukemia inhibitory

factor (LIF), and the ciliary neurotrophic factor (CNTF) from Schwann cells are participating in injury-related signaling [Richardson *et al.* 2009].

In response to peripheral injury, the expression of regeneration-associated genes (RAGs) is increased in regenerating neurons, specifically in DRG neurons. Lesser changes of RAG expression were observed after injury of the central branch of the same DRG neurons [Bosse *et al.* 2001; Kubo *et al.* 2002; Makwana *et al.* 2005; Bosse *et al.* 2006; Di Giovanni 2009]. To the expanding group of RAGs belong structural proteins, pro-axon growth signaling proteins, and transcription factors. The set of injury-induced structural proteins comprises GAP43 (BASP2), BASP1 (CAP23), STMN2 (SCG10), and SPRR1A that are involved in cytoskeleton dynamics within growth cones [Chong *et al.* 1994; Bonilla *et al.* 2002; MR Mason *et al.* 2002; Richardson et al. 2009; Starkey *et al.* 2009]. Further, cytoskeleton proteins such as alpha tubulins, coronin 1b (CORO1B), and RAB13 are associated with growth cones as well as cell adhesion molecules like L1CAM, CHL1, NCAM1, and contactin-2 (CNTN2), which contribute to the structural changes of regenerating axons. The galactose binding lectin LGALS1 (Galectin 1) is involved in apoptosis, cell proliferation and differentiation, and potentially also in both, axon regeneration and axon degeneration [Aubert *et al.* 1998; Y Zhang *et al.* 2000; MR Mason *et al.* 2003; Di Giovanni 2009]. Additionally, expression of cytokines (IL6) and signaling or neurotrophic peptides (GAL, BDNF), which are involved in neurogenesis and neuronal development, was increased upon peripheral injury [Tonra *et al.* 1998; J McGraw *et al.* 2004; Sachs *et al.* 2007; Kurihara *et al.* 2010]. Cell intrinsic mechanisms and a differential regulation of RAGs might determine the intrinsic regeneration potential of neurons in response to either peripheral or central nerve lesion [Neumann *et al.* 2002]. However, only few of the above mentioned factors have been demonstrated to promote axon outgrowth of CNS neurons under inhibitory conditions in *in vivo* models of axonal injury. Common mechanisms for the activation of these RAGs are not well deciphered by now.

The participating pathways that respond to nerve injury finally lead to the activation of transcription factors. Induction of RAG expression in neurons upon peripheral injury requires transcriptional activation in order to promote the switch to a regenerative status. Within hours after peripheral injury, transcription factor expression is increased while genes for neurotransmission are downregulated. Rather than one factor alone, the cooperative action of several transcription factors activate or repress target genes, thereby orchestrating the regeneration program. Intercepting early transcription factor activation after injury altered the regenerative response [DS Smith *et al.* 1997; Moore *et al.* 2011a]. One relevant transcription factor induced upon peripheral injury is the cAMP responsive element binding protein 1 (CREB1) which becomes phosphorylated by PRKACA (PKA) that is induced by the intracellular mediator cAMP. CREB1 is crucial for axon regeneration since it is involved in NGF signaling and in the activation of relevant target genes such as *Bdnf* [Tao *et al.* 1998; Riccio *et al.* 1999; Gao *et al.* 2004; Teng *et al.* 2006; Hannila *et al.* 2008]. Both treatments, cAMP analog application and CREB1 overexpression, are capable of overcoming myelin inhibition

and promote axon regeneration by increasing growth capacity upon subsequent dorsal column lesion [Qiu *et al.* 2002]. The transcription factor JUN (AP1), activated by MAPK8 to MAPK10, is expressed acutely following injury in successfully regenerating peripheral neurons but not in central neurons [Broude *et al.* 1997]. The expression of JUN, JUND, and further RAGs can be induced in non-regenerating adult rat Purkinje cells following axotomy if treated with either colchicine or with the IN-1 antibody. Cholchicine is an inhibitor of microtubule polymerization and retrograde transport, and the IN-1 antibody neutralizes a main inhibitory component of CNS myelin. These results speak for a constitutively suppressed RAG expression by CNS myelin-associated inhibitory factors [Zagrebelsky *et al.* 1998]. However, JUN seems to be necessary yet not sufficient for axon regeneration. It forms a heterodimer and synergizes with cAMP-dependent activating transcription factor 3 (ATF3) to regulate the expression of several genes such as galanin. Overexpression of ATF3 leads to increased SPRR1A and JUN levels in DRG but not of GAP43, BASP1 or STAT3 [Raivich *et al.* 2004; FQ Zhou *et al.* 2004; Seijffers *et al.* 2007]. STAT3 that is activated by IL6, LIF, or CTNF is also crucial for axon regeneration. Its phosphorylated form is retrogradely transported into the nucleus only in successfully regenerating neurons, specifically in DRG [Teng & Tang 2006]. Deletion or downregulation of the *Stat3* gene impairs regeneration of the lesioned peripheral nerve in DRG and decreases *Gap43* and *Bdnf* gene expression, whereas overexpression of STAT3 enhances outgrowth of the lesioned central branch. Interestingly, STAT3 also drives SPRR1A expression, promotes growth cone remodeling in injured axons, and prevents growth cone collapse [Qiu *et al.* 2005; YP Ng *et al.* 2006; Bareyre *et al.* 2011]. Furthermore, the tumor suppressor TRP53 is activated following neurotrophin and retinoic acid signaling and has been shown to be important for the prevention of growth cone collapse. Acetylated TRP53 binds promoters of the pro-neurite outgrowth genes *Coro1b* and *Rab13* [Di Giovanni *et al.* 2005; Tedeschi *et al.* 2009a; Tedeschi *et al.* 2009c]. Loss of function in *Trp53*-deficient mice led to decreased sprouting and impaired functional recovery after spinal dorsal hemisection injury [Floriddia *et al.* 2012]. The neuronal regeneration related protein NREP (P311) is a transcription factor for cellular differentiation that facilitates regeneration of injured facial motoneurons *in vivo*, and in postnatal DRG neurons or embryonic hippocampal neurons *in vitro* [Fujitani *et al.* 2004]. NFATC4 is required for axonal growth and guidance during vertebrate neuronal development and neurogenesis. It represses the *Gap43* gene promoter and therefore might regulate axon outgrowth upon injury [Graef *et al.* 2003; Nguyen *et al.* 2009]. The retinoic acid receptor beta (RARB), if bound by retinoic acid (RA), is capable of transcriptionally blocking the regeneration-inhibitory effect of the myelin-activated receptor LINGO1 following CNS injury [Puttagunta *et al.* 2011]. Overexpression of RARB in DRG enabled axon regeneration and partial functional recovery across the inhibitory dorsal root entry zone of the spinal cord [LF Wong *et al.* 2006]. Finally, several other transcription factors have been reported to regulate neurite outgrowth, often in the DRG regeneration model, further complicating the picture of axonal regeneration: SKIL, TCF3, SOX11, cAMP-dependent ATF2, RELA/NFkappaB, and Kruppel-like factors (KLFs) [Di Giovanni 2009; Moore et al. 2011a; Moore *et al.* 2011b].

Interestingly, a conditioning peripheral lesion of the sciatic nerve can trigger RAG and transcription factor expression (GAP43, BDNF, cAMP, STAT3, CREB1, KLF4, and others) and enhancing the intrinsic growth capacity of DRG neurons following a central lesion [Qiu et al. 2005; Teng & Tang 2006; P Yang *et al.* 2012]. In contrast to former studies, a conditioning peripheral lesion was proven to enhance axon sprouting before and even after a central lesion, *in vitro* and *in vivo* [Ylera *et al.* 2009]. Indeed, conditioning lesion has been shown to have greater effects than cAMP and NTF3 administration [Blesch *et al.* 2012], whereby endogenous BDNF is a crucial factor required to propagate pro-regenerative effects of a conditioning lesion [Song *et al.* 2008]. However, such experiments prove that injured axons can principally overcome the inhibitory central environment and unfold an intrinsic outgrowth capacity.

Altogether, much is known about the participation of diverse intrinsic factors but their cooperation as a complex pro-regeneration program is still poorly understood. As indicated before, adult CNS neurons show little capacity of pro-axonal outgrowth gene expression, which is different for neurons at an embryonic or early post-natal stage. Therefore, lesioned embryonic central neurons seem to have a better potential to grow axons, and the embryonic CNS environment less forcefully inhibits this outgrowth. It has also been thought that axonal regeneration might occur along a recapitulation of earlier developmental stages necessary for axon outgrowth [Emery *et al.* 2003; Gris *et al.* 2003; Harel *et al.* 2006]. Although regenerating neurons show some signs of de-differentiation following peripheral injury, the signaling that leads to axon outgrowth upon injury seems to be different from those during development [RY Liu & Snider 2001]. Understanding the neuronal developmental processes will help to comprehend axon regeneration of adult neurons. The complex cooperative transcriptional regulation and the differential expression of RAGs might essentially be regulated or accompanied by a putative master switch. Such a switch mechanism could be of epigenetic nature.

1.2 Epigenetic mechanisms

Nowadays, the field of Epigenetics is one of the fastest growing research areas in biomedicine. Originally, epigenetic changes were only associated with inheritable genomic imprinting during early embryogenesis. During the past years, epigenetic modifications and mechanisms attracted more and more attention, and they have been intensively studied in various other research areas, as well. The two major classes of epigenetic modifications are cytosine-specific DNA methylation and a variety of different histone protein modifications. Different epigenetic modifications lead to either a more condensed or relaxed chromatin structure tightly connected to gene expression regulation in a cell-type and developmental stage dependent manner [Berger 2007; BE Bernstein *et al.* 2007]. The epigenetic information is inheritably encoded, additionally to the genomic sequence information, and preserved through mitosis or meiosis. Still, mechanisms of epigenetic inheritance are only incipiently understood [Daxinger *et al.* 2012]. Independently from the DNA sequence, epigenetic modifications crucially influence temporal and spatial gene expression patterns, specifically during embryonic

development. Additionally, non-coding RNAs that are important for gene transcription regulation are nowadays considered another epigenetic mechanism [Ma *et al.* 2010; Qureshi *et al.* 2010]. It became clear that epigenetic mechanisms are essential for genome structure and gene expression regulation, not only during embryonic development but also in cancer [Momparler *et al.* 2000] and in the pathogenesis of non-cancerous diseases like immunological, cardiovascular, and developmental disorders. Furthermore, chromatin modifications have been brought into context with CNS development, adult neurogenesis, neurological functions, and several developmental and neurodegenerative disorders. Their roles in mature neurons, specifically for synaptic plasticity, memory and learning, and upon nerve injury indicate a possible involvement in axonal regeneration [Tucker 2001; RP Sharma *et al.* 2005; Feng *et al.* 2007; Day *et al.* 2010; Ma et al. 2010; Meaney *et al.* 2010; NK Yu *et al.* 2011]. Few recent reports suggested a role for epigenetic players such as histone acetyltransferases in axonal regeneration [Gaub *et al.* 2010; Iskandar *et al.* 2010; Kronenberg *et al.* 2010; Gaub *et al.* 2011]. Epigenetic marks in adult CNS, specifically in post-mitotic neurons, might be more dynamic than it was believed in the past. Thus, many of these marks indeed seem to be reversibly established during development and can undergo changes. Epigenetic mechanisms might also respond to dynamic neurophysiological changes or to nerve injury, which has only been partly investigated so far. Therefore, epigenetic mechanisms are worthwhile to be studied in the frame of axonal regeneration in order to better understand the complexity of this process.

1.2.1 DNA methylation

DNA methylation is the only epigenetic mechanism modifying DNA directly. Already in 1975, it was proposed that cytosine DNA methylation in eukaryotes could affect gene regulation and cellular differentiation as a stably inherited modification [Holliday *et al.* 1975; Riggs 1975]. Interestingly, in higher organisms, specifically in mammals and other vertebrates, cytosine-C5 methylation seems to be the dominant base methylation modification as compared to plants or bacteria, for example [Dunn *et al.* 1955; Gardiner-Garden *et al.* 1987]. This epigenetic mark is already known to be fundamentally involved in various biological and genetic processes such as in parental genomic imprinting, in X-chromosome inactivation in females, and during embryonic development and gametogenesis. Thereby, next to histone modifications, DNA methylation is required for the organization of the chromatin structure associated with gene expression or silencing, and for the suppression of viral genes and repetitive or deleterious elements that accumulated in the host genome over time [S Lindsay *et al.* 1985; Kochanek *et al.* 1993; Miranda *et al.* 2007; Maksakova *et al.* 2008].

1.2.1.1 Cytosine methylation and CpG islands

Analyzing DNA methylation patterns means understanding their chemical properties and distribution, first. Most abundant in mammals is methylation of cytosine at the C5 position

occurring predominantly in CpG dinucleotides (where ‘p’ denotes for a phosphate group) although there might also be substantial non-CpG methylation at cytosines [Lister *et al.* 2009]. CpG dinucleotides are underrepresented throughout the genome at only 21 percent of the statistically expected rate [Ehrlich *et al.* 1981; Gardiner-Garden & Frommer 1987; Lander *et al.* 2001]. This disproportion might have evolved during evolution because of a relatively higher chemical instability of methylated CpG dinucleotides compared to other dinucleotides, due to spontaneous oxidative deamination [DH Lee *et al.* 2002; Ikehata *et al.* 2003; Jabbari *et al.* 2004]. Numerous genomic regions exhibit non-random accumulations of CpGs, so-called CpG islands (CGIs), which seem to be protected from deamination [Caiafa *et al.* 2005]. Such CGIs are rather conserved, for example, between human and mouse. Characteristically, CGIs exhibit a high (G+C) content and a much higher concentration of CpG dinucleotides compared to the genomic average. Their minimum size is usually defined as 200 bp (classic definition, formalized as “NCBI-relaxed”) or even 500 bp (“NCBI-strict”). The modern NCBI-strict algorithm seemed to better match human DNA libraries of CGI clones. Different methods were tested and refined to predict CGIs. CpG islands often stretch over several hundred base pairs although typically not exceeding 2 kb. However, they contribute to only 2 percent of the total genomic sequence. Two thirds of the about 25,000 CGIs in human (about 23,000 in mouse) are found in the proximal gene promoter region or within 1,500 bp around the transcription start site (TSS) of genes that especially comprise the majority of constitutively active housekeeping genes and about 40 percent of tissue-associated genes [A Bird 2002]. About half of the CpG islands associated with gene promoters are located around the TSS of annotated genes and mostly extend into the first exon or intron. Less often, CpG islands were also found more distal to transcription start sites in intergenic or even in intragenic regions, so-called “orphan CGIs”. Some of these CGIs that are remote from annotated gene promoters have a functional promoter potential, nevertheless [Ponger *et al.* 2002; Maunakea *et al.* 2010]. Promoter CpG islands likely influence gene expression although absolute gene expression levels do not generally correlate with the CpG density of gene promoters. Many genes with promoters containing a high CpG content seem to be expressed rather ubiquitously [Su *et al.* 2004]. Altogether, about 70 percent of human gene promoters (50 to 60 percent in mouse) exhibit a high concentration of CpG dinucleotides mostly forming CpG islands. These genes are often associated with housekeeping functions like gene expression mechanisms, DNA replication in the nucleus, metabolism, or cell cycle. Contrary, a second fraction of about 30 percent of human gene promoters has a distinctly lower CpG content rarely exhibiting a CGI. Many of these genes fulfill more tissue-specific functions often associated with physiological processes and stimulus response signaling [Antequera *et al.* 1993; Saxonov *et al.* 2006; Weber *et al.* 2007; Deaton *et al.* 2011]. CpG islands are predominantly unmethylated, only 6 to 8 percent are supposed to be significantly methylated. Intriguingly, altogether 70 to 80 percent of all CpG dinucleotides scattered throughout the genome are methylated including promoters with a low CpG density. Furthermore, CGIs are found in repetitive regions like *Alu* elements that are not associated with genes and often exhibit high methylation levels [AP Bird 1986; Kochanek et al. 1993; Antequera 2003; Fazzari *et al.* 2004].

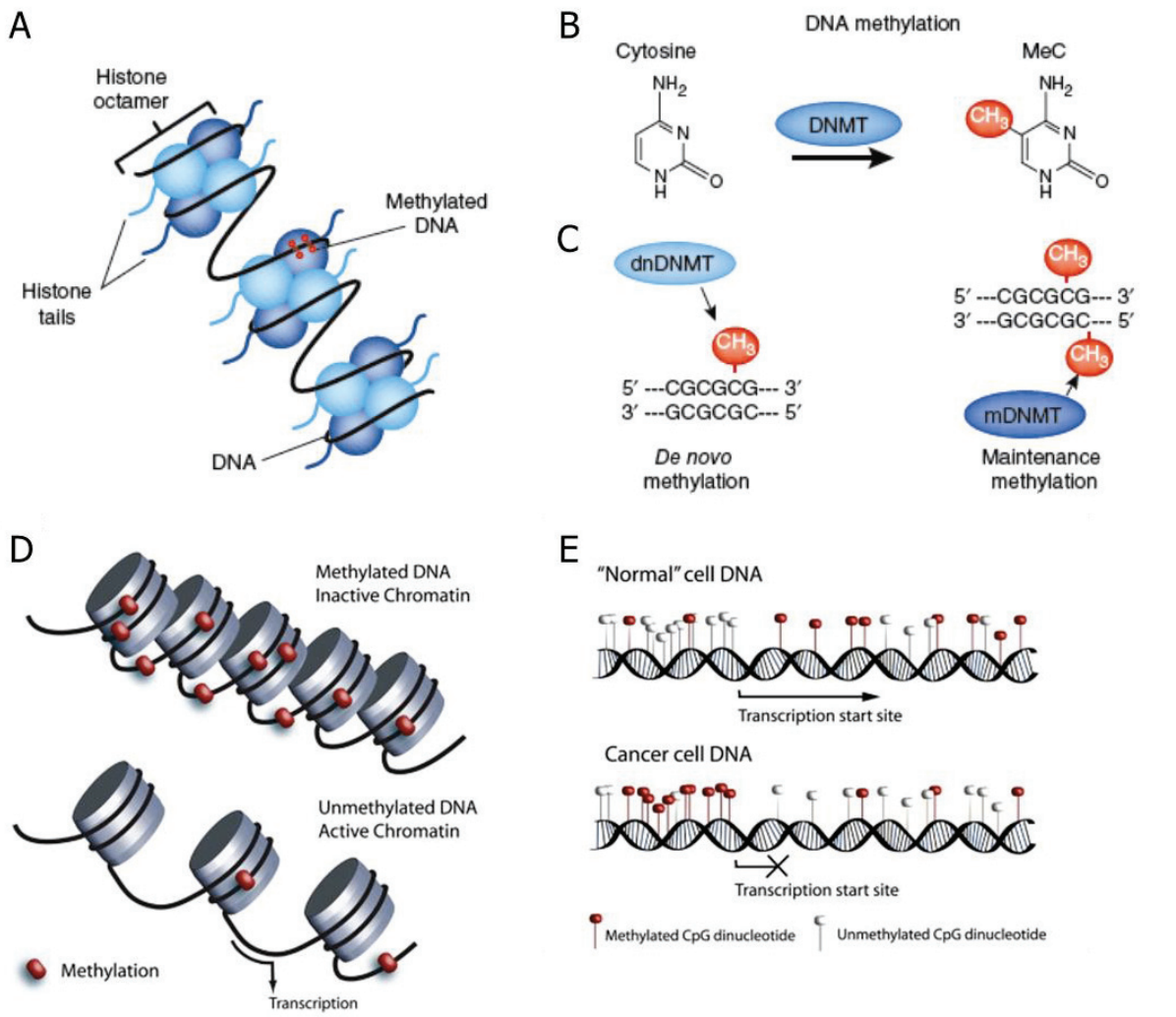

Figure 5 – DNA cytosine methylation influences chromatin structure. (A) Schematic of chromatin as a compact form of genomic DNA winding around highly basic histone octamers. **(B)** DNA methylation in mammals usually occurs at cytosine bases. DNA methyltransferases (DNMT; *De novo* methyltransferase) covalently add a methyl group to the C5 position of the pyrimidine ring. **(C)** Different DNMTs show preferences for either unmethylated DNA (DNMT1), or hemimethylated DNA (maintenance DNMT3A or DNMT3B). **(D)** Inactive, condensed chromatin is associated with elevated CpG methylation and active, relaxed chromatin with little CpG methylation. **(E)** Promoter CpG methylation can influence gene expression, as it has been found for many tumor suppressor genes or oncogenes in cancer. (A-C) from [Day & Sweatt 2010], (D-E) modified from [Barton *et al.* 2008].

In general, high gene promoter methylation is supposed to contribute to a condensed state of chromatin that prevents transcriptional activity (**Figure 5**). In contrast, low promoter methylation is associated with transcription-permissive (relaxed) chromatin [Berger 2007; Miranda & Jones 2007]. The question is, can promoter methylation be dynamic, specifically in response to physiological or pathological changes that might stimulate hyper- or hypomethylation of specific regions? Several examples, given further below, will demonstrate the discovery and importance of DNA methylation in genomic imprinting, embryonic development, and in the nervous system. Thus complex changes in the tissue environment, for example upon nerve injury, could cause dramatic changes in cellular gene expression patterns correlating with changes of epigenetic marks at gene promoters.

1.2.1.2 DNA methyltransferases and DNA demethylation

In order to understand how DNA methylation patterns are established, changed, or erased, it must be disclosed which enzymes are involved and how these are regulated. Mechanisms of DNA methylation and demethylation have been intensively investigated but, still, they are only in part understood [ZX Chen *et al.* 2011c; Auclair *et al.* 2012]. So far, more is known about the process of DNA methylation and involved enzymes than about mechanisms of active or passive DNA demethylation. De novo methyltransferases (DNMTs) are responsible to either establish CpG methylation at unmethylated double strands ("*de novo*"), or to maintain and re-establish it. Three major methyltransferases (DNMT1, DNMT3A, and DNMT3B) are essential during embryonic development, in carcinogenesis, and importantly in neurogenesis and in the adult CNS [Bestor 2000; Hermann *et al.* 2004; Klose *et al.* 2006a; Serman *et al.* 2006; Jurkowska *et al.* 2011a]. DNA methyltransferases transfer a methyl group to the C5 position of specific cytosines, predominantly at CpG dinucleotides, yielding 5-methylcytosine (5mC). Thereby, S-adenosyl-L-methionine (AdoMet), a product of the folate metabolism cycle, serves as methyl donor required in the context of brain disorders and axonal regeneration [Kronenberg *et al.* 2009; Iskandar et al. 2010; Kronenberg & Endres 2010]. Enzymatic properties have been best characterized for DNMT1 that is, for example, responsible to re-establish methylation patterns on the newly synthesized unmethylated strand during in S-phase of the cell cycle. DNMT1 is a processive enzyme preferring hemimethylated DNA potentially within a certain sequence context. Additionally, DNMT1 exhibits a *de novo* methylation activity [Tollefsbol *et al.* 1995; Flynn *et al.* 1996; Pradhan *et al.* 1999; Jeltsch 2006]. DNMT3A and DNMT3B, distinguished from DNMT1, show equal preferences for unmethylated or hemimethylated DNA potentially for site-specific cytosine methylation [Okano *et al.* 1999; Robertson *et al.* 1999; Oka *et al.* 2006; Chedin 2011]. Additionally, few other proteins were identified that are at least similar to DNA methyltransferases or that are isoforms of known DNMTs such as DNMT3L, DNMT3A2, DNMT1B, as well as DNMT3B isoforms. These might play specific roles during development, and thereafter, and in the regulation of major DNMTs acting as cofactors. DNMT3L, for example, seems to act as a crucial cofactor for DNMT3A in the germ line although not exhibiting a DNA methyltransferase activity itself, despite its sequence similarity to DNMTs [Bonfils *et al.* 2000; Aapola *et al.* 2001; Jurkowska *et al.* 2011b; O'Doherty *et al.* 2011]. DNMT2, in contrast, seems rather associated with RNA methyltransferase activity [Goll *et al.* 2006].

It shall be mentioned that research has mainly focused on DNA methyltransferases and on the presence or changes of DNA methylation. However, putative DNA demethylases and mechanisms of complementary demethylation are largely unknown or speculated on [SC Wu *et al.* 2010; Bhutani *et al.* 2011; Dalton *et al.* 2012]. To explain hypomethylation, passive DNA demethylation was assumed, first, since inhibition of DNA methyltransferases caused global hypomethylation [Singh *et al.* 2009]. A prominent and obvious role of active demethylation was assumed in genomic imprinting when methylation patterns are first erased during game-

togenesis and then re-established [Daxinger & Whitelaw 2012], and further during embryonic development [B Zhu *et al.* 2001; Klug *et al.* 2010; Wossidlo *et al.* 2010; Auclair & Weber 2012]. Of note, DNA demethylation was additionally reported in brain development and brain functions [Kriaucionis *et al.* 2009; Guo *et al.* 2011b]. Proposed mechanisms include the demethylation of 5-methylcytosines via an intermediate modified base, 5-hydroxymethylcytosine, which then is replaced by an unmethylated cytosine through a deamination-base excision repair mechanism [Cortellino *et al.* 2011; Kriukiene *et al.* 2012]. Specific DNA glycosylases were proposed to act as processive DNA demethylases [Cervoni *et al.* 1999].

1.2.1.3 CpG-binding proteins

How DNA methyltransferases are regulated, how are their specific target sites recognized, and how do these enzymes get directed to them? Mechanisms of DNA methylation regulation are only incipiently understood. A family of methylated DNA binding proteins shall be briefly introduced, consisting of MECP2 and MBD1 to MBD4 that exhibit a methyl-CpG binding domain (MBD). These proteins provide a "read-out" mechanism for DNA methylation. However, they are not in the focus of this study. MBD proteins mediate information that is encoded in DNA methylation patterns. They supply a connecting platform for different chromatin-modifying enzymes and transcription factors within a transcription repressor complex bound at methylated DNA sections [Bogdanovic *et al.* 2009; Buck-Koehntop *et al.* 2013]. All members of the MBD family act as transcriptional repressors *in vitro*, except MBD4 which is a thymine glycosylase and associated with DNA repair, specifically excising mutated methylated and unmethylated CpGs [Hendrich *et al.* 1999]. MBD proteins can bind to DNA methyltransferases. Furthermore, MBD2 and MECP2 interact with histone deacetylases HDAC1 and HDAC2, and MBD1 can interact with histone methyltransferase SUV39H1. Moreover, MBD proteins can bind to other auxiliary proteins like the corepressor SIN3A [Nan *et al.* 1998; Boeke *et al.* 2000; HH Ng *et al.* 2000; Fournier *et al.* 2012]. Thus, MBD proteins provide a link between different repressive chromatin remodeling mechanisms like DNA methylation and histone deacetylation in the frame of transcriptional regulation. Additionally such factors, and also regulative non-coding RNAs, even bind the promoters of *Dnmt* genes to regulate their expression in turn [Kinney *et al.* 2011].

A substantial research effort during the last few years has demonstrated the important role of methyl-CpG binding proteins (MBPs), specifically MECP2, and of DNA methylation for brain-related functions and neural disorders. Both, loss of function as well as increased MECP2 expression can cause various neuropsychiatric disorders like mental retardation, autism, or the Angelman syndrome [Watson *et al.* 2001; Chahrour *et al.* 2008; Diaz de Leon-Guerrero *et al.* 2011]. Best characterized is the disruption or certain mutations of *Mecp2* that affect DNA binding causing X-linked Rett syndrome, a post-natal neurological disorder that is associated with cognitive and motor abnormalities, and autistic symptoms [Amir *et al.* 1999; CM McGraw *et al.* 2011; Samaco *et al.* 2011]. Although binding of MBPs to methylat-

ed DNA is usually associated with transcriptional repression, MECP2 is found in a dual role as gene repressor and activator. MECP2 is expressed in neurons but also in glial cell types like astrocytes and oligodendrocytes, however not in microglia, oligodendrocyte precursor cells, and Schwann cells [Shahbazian *et al.* 2002; Nagai *et al.* 2005; Maezawa *et al.* 2009; Singleton *et al.* 2011; Tochiki *et al.* 2012]. Indicating a potential RAG expression regulation through binding of methylated DNA, BDNF expression is lower in *Mecp2*-deficient mice [W Li *et al.* 2012]. Neuronal activity-dependent membrane depolarization triggers phosphorylation of MECP2 and its release from the *Bdnf* promoter thereby facilitating *Bdnf* transcription. BNDF synthesis in neurons after depolarization correlated with decreased CpG methylation and with the release of MECP2/SIN3A repression complex from its promoter [Martinowich *et al.* 2003]. Binding of MECP2 to the *Bdnf* promoter can be regulated by acetylation and deacetylation via the histone modifying enzymes EP300 and SIRT1, respectively [Zocchi *et al.* 2012], or by phosphorylation of MECP2 [Khoshnan *et al.* 2012]. Controversially, binding of MECP2 was also reported to repress *Bdnf* expression depending on the specific promoter region III. *Bdnf* expression is therefore expressed exon-specifically [WG Chen *et al.* 2003]. Furthermore, MECP2 also associates with the transcriptional activator CREB1 at promoters of its activated target genes, like the growth-hormone release inhibitor somatostatin, but not at repressed target gene promoters [Chahrour et al. 2008]. Taken together, MBPs are essential during neurodevelopment and for cognitive functions, mediating proper transcription factor binding and transcriptional regulation. They might also be required for the regulation of genes associated with axonal regeneration upon nerve injury.

1.2.1.4 DNA methylation in genomic imprinting and embryonic development

DNA methylation was initially identified in the context of genomic imprinting in germline cells and during early embryogenesis, respectively [Reik *et al.* 1987]. Genomic imprinting describes the monoallelic expression of a small subset of genes (about 1 percent in the human genome) whereby one allele is methylated and thus silenced. Many of these genes are involved in embryonic development and placental growth. Epigenetic regulation of these genes occurs in the pronuclear zygote. DNA methylation patterns are supposed to be initially erased or masked in germline cells, and then re-established in a parent-of-origin-specific manner about the time of implantation of the zygote [Gold *et al.* 1994; Reik *et al.* 2001]. Imprinted genes can influence brain functions and behavior already during neuronal development [Wilkinson *et al.* 2007]. Dysregulated imprinting majorly influences gene expression from fetal development into adulthood, associated with disorders such as the reciprocally inherited Prader-Willi syndrome and the Angelman syndrome, or cancer [Wilkins 1988; Knoll *et al.* 1989; Nicholls *et al.* 1989; Uribe-Lewis *et al.* 2011; Millan 2013].

Beyond genomic imprinting, DNA methylation and other chromatin modifications appear to be rather general mechanisms to coordinate cell-type specific and temporal gene expression profiles during embryogenesis, stem cell differentiation, and somatic tissue development.

Both classes of epigenetic marks seem to tightly interact with each other, although in part with diverting functions [K Mason *et al.* 2012; ZD Smith *et al.* 2013]. During and after embryonic development, and for postnatal stages, DNA methylation is involved in the suppression of tissue-associated genes in the frame of cell differentiation [Brandeis *et al.* 1993; Hashimshony *et al.* 2003; Fisher *et al.* 2011]. For example, multipotential neural stem cells/precursor cells (NSCs/NPCs) are partly regulated by DNA methylation [Singh et al. 2009; Juliandi *et al.* 2010]. NPCs can differentiate into neurons during midgestation or into glial cells in late gestation. Astrocytic differentiation can be induced by IL-6 family cytokines and is dependent on activation of the transcription factor STAT3. Astrocyte-specific gene promoters, such as *Gfap* and *S100b*, are hypermethylated in early developmental stages but get demethylated in induced late-stage NPCs that differentiate into astrocytes. Thereby, STAT3-driven *Gfap* expression requires demethylation of the STAT3 binding site at the *Gfap* promoter [Takizawa *et al.* 2001; Namihira *et al.* 2004; Hatada *et al.* 2008].

1.2.1.5 DNA methylation in the CNS and upon nerve injury

DNMT3A and DNMT3B have similar and, in part, complementary roles suppressing tissue- and stage-specific genes during embryonic development, genomic imprinting, and for the silencing of repetitive elements. During early neurogenesis, DNMT3B is mainly expressed in embryonic stem cells (ESCs) and in NPCs. In contrast, DNMT3A is predominantly expressed in later developmental stages and in the adult brain, detectable in maturing neurons, oligodendrocytes, and in astrocytes [Watanabe *et al.* 2006]. Interestingly, DNMT1 is still expressed in post-mitotic neurons of the adult CNS, at higher levels than DNMT3A or DNMT3B. Coincidently, global DNA methylation levels are higher in adult brain than in other tissues. DNMTs are abundantly expressed in brain, in the spinal cord, and in DRG [Tawa *et al.* 1990; Goto *et al.* 1994; Feng *et al.* 2005; Chestnut *et al.* 2011]. Cytosine methylation seems to be dynamically regulated in the adult CNS and is maybe directly involved in active gene expression regulation upon physiological changes. DNA methylation and DNMT1 have both been shown to be involved in neurological functions, for example, neuronal plasticity and memory formation [Dulac 2010; NK Yu et al. 2011]. In excitatory neurons in mouse forebrain, DNMT1 and DNMT3A play a role in long-term plasticity in the hippocampal CA1 region and therefore in learning and memory [Feng *et al.* 2010; LaPlant *et al.* 2010]. Guo et al. demonstrated with a genome-wide sequencing analysis *in vivo* that adult mouse dentate granule neurons exhibit neuronal activity induced alterations of CpG methylation for many genes associated with neuronal plasticity [Guo *et al.* 2011a]. Epigenetic alterations were examined upon amygdala-dependent auditory Pavlovian fear conditioning associated with synaptic plasticity in the amygdala, demonstrating a training-related increase in histone H3 acetylation and DNMT3A expression. The DNA methyltransferase (DNMT) inhibitor 5'-Aza-dC thereby impaired fear memory consolidation [Monsey *et al.* 2011]. In contextual fear conditioning, exon-specific differential regulation of *Bdnf* transcription in the hippocampus is associated with changes of promoter DNA methylation. Blockade of NMDA receptor prevented memory-associated

changes of *Bdnf* promoter methylation and subsequently derogated memory formation [Lubin *et al.* 2008; Tian *et al.* 2009]. Upon fear conditioning, also the memory suppressor gene for protein phosphatase 1 becomes methylated and transcriptionally silenced whereas the synaptic plasticity-promoting gene reelin is activated [Levenson *et al.* 2006; CA Miller *et al.* 2007].

Consequently, rapid and dynamic changes of promoter DNA methylation patterns might also be involved in the transcriptional regulation of axon regeneration-associated genes upon peripheral nerve injury. However, not much is known about the role of DNA methylation in neurons following CNS nerve injury. DNA methylation levels were increased after mild focal brain ischemia following middle cerebral artery occlusion (MCAO) that is partly dependent on DNMT1 activity. Blocking of DNMT1 activity protected injured neurons improving their survival [Endres *et al.* 2000]. It was proposed that DNA methylation is involved in the enhancement of CNS repair via folate metabolism and a functional methylation cycle. Folic acid is a methyl donor required to produce the substrate for DNMTs, S-adenosyl-methionine [Iskandar et al. 2010; Kronenberg & Endres 2010]. Folate or homocysteine metabolism has already been implicated to play a role in the context of neurodegenerative or neuropsychiatric disease, and in neural plasticity [Mattson *et al.* 2003; AL Miller 2003; Kronenberg et al. 2009]. Altogether, these findings make it worthwhile to further investigate the role of DNA methylation in axonal regeneration and specific RAG expression regulation.

1.2.2 Histone modifications

Alongside with DNA methylation, a second group of chromatin features is important that comprises various histone modifications. These epigenetic marks have first been investigated and characterized in yeast, and more recently in mouse and human. Yeast and mammals display a high degree of similarity of the involved enzymes and mechanisms. Already in 1964, Allfrey et al. found that histone acetylation and methylation might be important for the regulation of RNA synthesis [Allfrey *et al.* 1964]. It became clear that certain histone modifications, or combinations of these, code for specific chromatin properties affecting local gene transcription. At least 8 different posttranslational modifications at various amino acid residues of N-terminal histone tails are known mostly at lysines and arginines, or serines and threonines. Altogether, more than 100 different combinations have been discovered, which mainly comprise acetylation, methylation, and phosphorylation besides other modifications such as ubiquitination, sumoylation, deamination, and ADP-ribosylation (**Figure 6**). This so-called histone code is only in part understood. Anyhow, some knowledge has already been acquired about the influence of certain histone modifications on the chromatin structure, the promoter availability for transcription factors, and the recruitment of chromatin binding or remodeling proteins, together affecting gene expression [Jenuwein *et al.* 2001; Kouzarides 2007; Bannister *et al.* 2011]. Histone modifications are essential for cell differentiation and tissue-fate determination during embryonic development, adult neurogenesis, and for neuronal functions in the adult brain [Mager *et al.* 2005; Margueron *et al.* 2005; Lilja *et al.* 2013]. In order

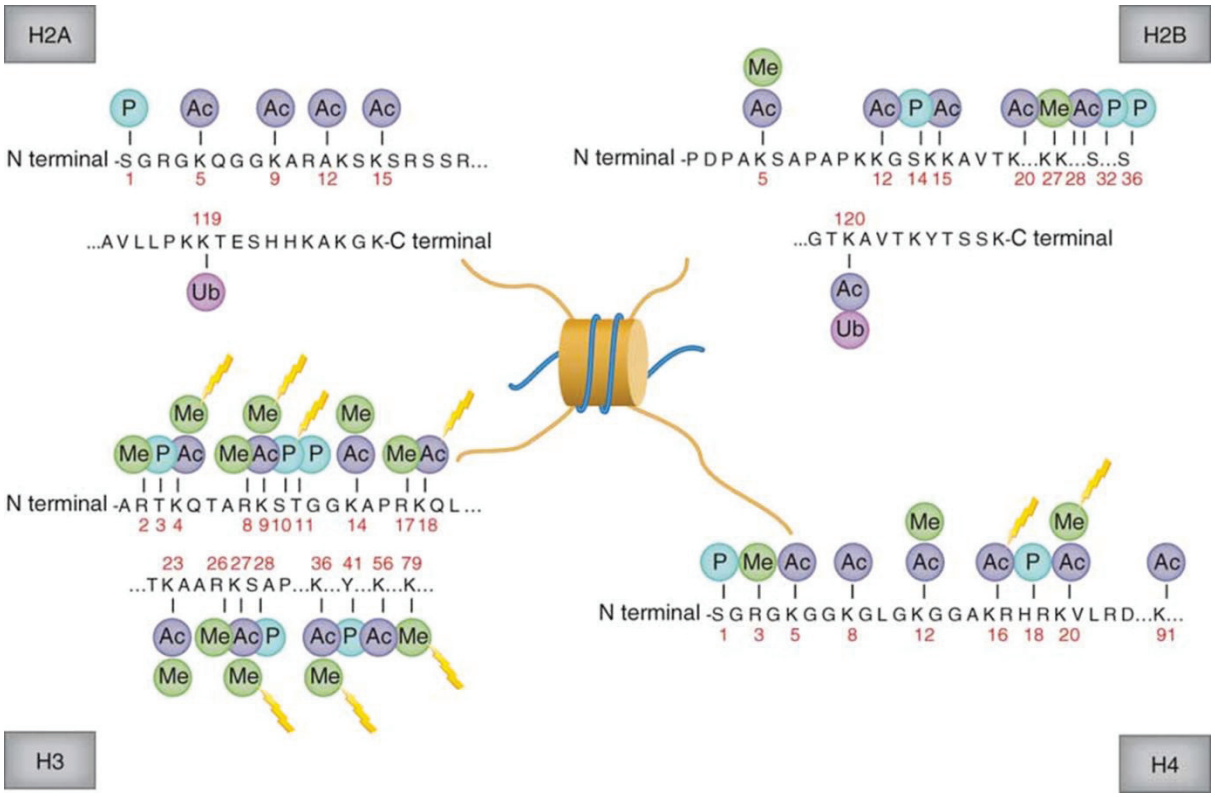

Figure 6 – Scheme of several known posttranslational histone modifications, which mainly involve acetylation (Ac), methylation (Me), or phosphorylation (P) of various amino acid residues of histones H2A, H2B, H3, and H4. These histones form octamers tightly binding DNA within the nucleosome substructure of chromatin. Usually, amino acids of the protruding N-terminal tails are targets of modifying enzymes such as histone acetyltransferases (HATs), deacetylases (HDACs), methyltransferases (HKMTs), or demethylases. Many lysine residues (K) can be either acetylated or methylated depending on the functional context. Several positions, highlighted in yellow, were reported to be involved in cancer. From [Rodriguez-Paredes *et al.* 2011].

to investigate the influence of certain histone modifications, many genome-wide studies analyzed their abundance at gene promoters and other genomic regions of interest. Thereby, promoter association of various epigenetic histone marks were in part correlated with gene expression levels, promoter CpG content, or with the presence of DNA methylation [Mikkelsen *et al.* 2007]. But which modifications have an influence on gene expression and which enzymes are involved? Of all known chemical modifications, the best-characterized and investigated types are histone acetylation and methylation, predominantly at the N-terminal tail of histones H3 and H4. These modifications are implicated in the regulation of both, global and local inducible chromatin structure, and gene expression although the exact mechanisms remain largely undetermined. Histone modifications can be dynamic and are often found in the proximal promoter region of genes or in intragenic regions [B Li *et al.* 2007a].

1.2.2.1 Histone acetylation, deacetylation, and modifying enzymes

Genome-wide studies have confirmed that histone acetylation usually correlates with gene activation. Specifically, histone H3 acetylation at lysine residues 9, 14, 18, and 27 (H3-K9/K14/K18/K27ac) and H4 acetylation are often found in active promoter regions and around the TSS. Besides histone acetylation, transcriptional activity also correlates with methylation of histone H3-K4 and K36, contributing to a relaxed and less condensed state of promoter chromatin (euchromatin). Thereby, acetyl groups neutralize the positive charge of Lys or Arg residues. Consequently, the negative backbone of DNA is bound less efficiently by acetylated histones [BE Bernstein et al. 2007; Z Wang *et al.* 2008]. Histone acetylation is mediated by histone acetyltransferases (HATs). There are two major classes of HATs. Type-B HATs predominantly acetylate unbound cytoplasmatic histones setting preliminary marks [Parthun 2007; XJ Yang *et al.* 2007; Q Jin *et al.* 2011]. HATs of type A are localized in the nucleus and can be classified according to their conformational structure and sequence homology: GNAT, MYST, and CBP/P300 families [Sterner *et al.* 2000; Hodawadekar *et al.* 2007]. Most of these enzymes are able to modify multiple histone tail residues and are found together with other chromatin modifying enzymes in large multiprotein complexes. Histone acetyltransferases are often functioning as transcriptional coactivators [Jenuwein & Allis 2001; XJ Yang & Seto 2007]. Well characterized are KAT2B (lysine (K) acetyltransferase 2b; PCAF; CBP/P300-associated factor) belonging to the GNAT family (GCN5-related N-Acetyltransferases), and the complex CBP/P300 (CREB-binding protein (CREBBP)/EP300; KAT3A/KAT3B). KAT2B will be subsequently called “PCAF” since this term is commonly used. PCAF is known to acetylate the core histones H3 and H4, thereby promoting transcriptional activation as a coactivator. Known target sites of PCAF are histone H3 lysine residues 9, 14, and 18 (H3-K9/K14/K18) whereby PCAF might be the major acetyltransferase for H3-K9 [Kouzarides 2007]. This enzyme usually activates gene expression by increasing promoter H3-K9 acetylation levels accompanied by its own phosphorylation and nuclear translocation, which is inducible by neurotrophins via NGF receptor signaling [K Wong *et al.* 2004]. PCAF interacts with the histone deacetylase SIRT1 and with CBP/P300 in a large multiprotein complex [Ogryzko *et al.* 1996; Wallberg *et al.* 2002]. *Pcaf*-knockout mice show deficits in memory formation and stress response [Maurice *et al.* 2008]. This enzyme is also able to acetylate and potentially activate non-histone proteins such as the transcription factor TRP53 that is involved in cell cycle arrest and in axonal regeneration [Xenaki *et al.* 2008; Di Giovanni 2009]. However, not many specific functions of PCAF or CBP/P300 are known in the CNS, as will be discussed later. Many H3 target sites of PCAF are shared by KAT2A and CBP/P300 (however not H3-K9). Despite the high degree of homology to PCAF, KAT2A seems to acetylate only free cytosolic but not nucleosomal histone H3 and, therefore, is likely not relevant for this study [Xu *et al.* 1998; Q Jin et al. 2011]. CBP/P300 is found in complexes with transcriptional activators such as CREB1, JUN, FOS, or TRP53 that are known to be involved in axonal regeneration [Kamei *et al.* 1996; Goodman *et al.* 2000]. CBP/P300 has functions in neuronal differentiation acting as a coactivator of neurogenic differentiation

factor 1 (NEUROD1) [A Sharma *et al.* 1999]. EP300 generally acetylates histones as a tag for transcriptional activity while CREBBP also specifically binds to phosphorylated CREB1, an important factor in axonal regeneration, thereby enhancing its transcriptional activity towards cAMP-responsive genes [Chrivia *et al.* 1993; Kwok *et al.* 1994]. CREB1 induction in sensory neurons by Serotonin (5-hydroxytryptamin, 5-HT) leads to promoter histone acetylation of CREB1 target genes through recruitment of CREBBP. The subsequent increased long-term facilitation, a form of synaptic plasticity, is counteracted by the CREB2/HDAC5 complex with consequent promoter histone deacetylation concluding in long-term depression [Guan *et al.* 2002]. CREB1 is activated upon peripheral injury of rat DRG together with JUN, RELA, ATF2, and ATF3. Epigenetic regulation of CREB1-mediated transcription might thus be relevant for sensory nerve injury in the DRG model applied for this study [Herdegen *et al.* 1997; Buschmann *et al.* 1998; MY Li *et al.* 2009].

Opposing the effects of HATs, histone deacetylases (HDACs) remove acetyl groups from lysine residues of histones H2A, H2B, H3 and H4, although with little substrate specificity, which has a general repressive effect on transcription [XJ Yang *et al.* 2008]. HDACs are usually recruited to chromatin as components of larger multiprotein complexes, for example, of the NuRD, SIN3A, or RCOR1 complexes. HDAC1 and HDAC2, the best characterized members, interact with histone acetyltransferases (like PCAF or CBP/P300), other histone deacetylases (like HDAC7, SIRT1), histone methyltransferases (like SUV39H1, SETDB1), histone demethylases (like KDM4A/5A), and with transcription factors. Additionally, they also interact with DNA methylation associated proteins (like DNMT1/3A, MECP2, MBD2/3), thus linking different transcription repression mechanisms [de Ruijter *et al.* 2003; Kouzarides 2007; XJ Yang & Seto 2007; McDonel *et al.* 2009]. Because of their interaction, enzymes of complementary mechanisms work together dynamically, allowing for a balance between transcriptional activity or repression [RP Sharma et al. 2005]. HDACs are further involved in negative regulation of certain transcription factors like SP1 and SP3 that can protect CpG islands from methylation. Thereby, SP1 or SP3 activity is abolished by deacetylation [Brandeis *et al.* 1994]. Additionally, certain histone modifications can influence each other and DNA methylation in a cross-talk manner [B Li et al. 2007a; T Chen 2011]. Histone deacetylation can be important for axonal regeneration since it is implicated in the differentiation of adult NPCs. Inhibiting HDAC activity by valproic acid (VPA) leads to decreased proliferation of these cells together with increased neuronal differentiation, without increasing gliogenesis [Hsieh *et al.* 2004]. Histone deacetylation plays a role in the adult brain, as well. In cortical neurons, HDAC3 interacts with nuclear receptor corepressor 2 (NCOR2), which controls neuronal responsiveness of several transcription factors thus regulating neurogenic and neuroprotective pathways. NCOR2 further interacts with HDAC1/2 and with retinoic acid receptors (RAR), some of which are involved in preventing regeneration-inhibiting CNS myelin signals upon nerve injury [Puttagunta et al. 2011; Soriano *et al.* 2011]. A balance between HDAC1/2 and EP300, interacting with RELA, is required during Schwann cell differentiation for proper myelination in the PNS, which is required in axonal regeneration. Mice lacking

HDAC1/2 exhibited a severe myelin deficiency with Schwann cells remaining at an immature stage [Y Chen *et al.* 2011b]. Therefore, specific gene promoter acetylation or deacetylation must be essential to drive the regeneration response following peripheral nerve injury, and it might be prevented upon central nerve lesion.

1.2.2.2 Histone methylation, demethylation, and modifying enzymes

As a second group of histone modifications, various methylated histone residues are involved in chromatin regulation and are essential for neural development. Aberrant methylation of histone lysines has been implicated in several diseases including cancer and X-linked mental retardation [Schneider *et al.* 2002; Y Shi 2007; SS Ng *et al.* 2009; Spannhoff *et al.* 2009]. Histone methylation mainly occurs at the side chain amino group of Lys and Arg residues whereby, in contrast to histone acetylation, the effective charge is not altered but the hydrophobic and steric properties. Interestingly, the grade of histone residue methylation has to be considered since lysines can be mono-, di-, or trimethylated, and arginines can be monomethylated as well as symmetrically or asymmetrically dimethylated. Different methyltransferases have already been assigned to specific histone residues targets [Bedford *et al.* 2009; Lan *et al.* 2009; Pedersen *et al.* 2010; Upadhyay *et al.* 2011]. As indicated by studies, methylation of H3-K4, H3-K36, and H3-K79 is associated with transcriptionally active chromatin while, in contrast, methylation of H3-K9, trimethylation of H3-K27, or H4-K20 methylation generally correlate with transcriptional repression or with silencing of repetitive elements [Martin *et al.* 2005; Kouzarides 2007]. Histone methylation patterns undergo changes during development. For example, promoter H3-K4me is more abundant in ESCs than in differentiated cells [BE Bernstein et al. 2007]. Among the modified histone positions, H3-K9 might be of special interest. This residue can either be acetylated, which is associated with an “open” or relaxed state of chromatin (transcriptionally active), or it can be methylated whereby at least its highly methylated forms are found in “closed” or condensed chromatin. All grades of H3-K9 methylation are associated with transcriptional repression. Thereby methylated H3-K9, together with methylated H3-K27, may have a key role in gene repression regulation. While higher levels of H3-K27me3 seem to be rather associated with low expressed genes, different modifications of H3-K9 might act as a switch for gene expression regulation [RP Sharma et al. 2005; Komashko *et al.* 2008]. However, in seeming contrast, H3-K9 methylation can occur both in denser heterochromatin and in more relaxed euchromatin. Mono- and dimethylated H3-K9 are important marks in euchromatin at gene promoters and will be investigated in this study, together with H3-K9ac.

Many histone lysine methyltransferases (HKMTs) and lysine (K) demethylases (KDMs) have been identified, up to now, many of them with specificity for certain residues [Rea *et al.* 2000; Fischle *et al.* 2003; Kouzarides 2007]. Almost all HKMTs share a common SET domain that is responsible for the methyl group transfer requiring S-adenosyl-l-methionine (AdoMet) as substrate. Thereby, HKMTs and DNMTs use the same methyl donor molecule. SET-

containing HKMTs are grouped into six different subfamilies: SET1, SET2, SUV39, EZH, SMYD, and PRDM. Additionally, HKMTs can contain other methylhistone binding domains such as chromodomain, polycomb, or trithorax, which show different preferences for the methylation status of a certain lysine residue [Dillon *et al.* 2005; BE Bernstein et al. 2007]. Different methylated histone residues and degrees of methylation levels seem to have differential functions. Associated with gene repression, methylated H3-K9 is of special interest in this study. H3-K9 methylation is in part established by the HKMTs EHMT2 (G9A; KMT1C) and EHMT1 (GLP; KMT1D) which can heteromize and play an important role during early embryonic development. As an example for complex interactions, EHMT2 is involved in silencing of neuronal genes [Roopra *et al.* 2004]. This enzyme also methylates non-histone proteins such as TRP53 (at Lys 373), CDYL, or KLF12, and enzymes like DNMT1, HDAC1, and itself. The presence of EHMT2 is required to mediate DNA methylation although not due to its HKMT activity, thus presenting another link between different repressive epigenetic mechanisms [Tachibana *et al.* 2008]. SUV39H1 and SUV39H2 (KMT1A and KMT1B) are important methyltransferases for H3-K9me3 and involved in processes such as chromatin organization, cell cycle regulation, and the regulation of telomere length [Lachner *et al.* 2001; Rice *et al.* 2003; Garcia-Cao *et al.* 2004]. SUV39H1, the first HKMT identified, is important for neuronal survival [Rea et al. 2000; DX Liu *et al.* 2005] and it interacts with DNMT3B, MBD1, HDAC1/2, or with recruited chromobox protein homologs CBX1/4/5 that "read" H3-K9me2/3. These interactions link different transcriptional repressive modifications [Jenuwein 2006]. For example, knocking-out SUV39H enzymes in murine ESCs led to impaired CpG dinucleotide methylation at major centromeric satellites, dependent on DNMT3B. Thus, H3-K9me3 seems to be necessary to direct DNA methylation [Lehnertz *et al.* 2003; D'Alessio *et al.* 2006]. Another important HKMT for H3-K9 trimethylation is SETDB1 (KMT1E) that has been reported to be coordinated with DNMT1-mediated re-methylation during S-phase of mitosis [CM Wong *et al.* 2011]. SETDB1 is usually expressed at low levels in mature neurons, and it might be involved in the regulation of affective and motivational behaviors [Jiang *et al.* 2010].

Histone methylation was first believed to be static unless mechanisms and enzymes for histone demethylation were found [Bannister & Kouzarides 2011]. There is a great number of known lysine-specific demethylases counteracting the action of HKMTs. Out of more than 30 histone demethylases, about 20 are phylogenetically related containing a Jumonji domain [Tsukada *et al.* 2006]. Most of Jumonji domain demethylases also exhibit at least one additional domain like the PHD-type zinc finger domain, so they are classified into at least seven subfamilies [Trewick *et al.* 2005; Klose *et al.* 2006b]. According to the current unified classification, they will be referred to as lysine (K) demethylases (KDMs). Several KDMs shall be exemplarily introduced that, in part, target methylated H3-K9 very specifically, which is relevant for this study. KDM3A and KDM3B (JHDM2A/B) preferably demethylate H3-K9me2 but also H3-K9me. KDM4A to KDM4D (JMJD2A to JMJD2D) specifically demethylate H3-K9me3, or H3-K9me2 (KDM4D), and H3-K36me3 [Kouzarides 2007; Horton *et al.* 2010;

Upadhyay & Cheng 2011]. KDM1A (LSD1) was found in histone modifying complexes with RCOR1, demethylating H3-K4me1/me2 and H3-K9me1/me2. Thereby, this enzyme acts as coactivator or corepressor, respectively. KDM1A also demethylates non-histone proteins like TRP53 (K370me2), which prevents TRP53-dependent transcriptional activation [YJ Shi *et al.* 2005; J Huang *et al.* 2007]. Interestingly, loss of KDM1A function in ESCs led to decreased DNA methylation and DNMT1 protein levels [J Wang *et al.* 2009]. Neuron-specific isoforms of KDM1A play an important role in early neurite morphogenesis and cortical development, particularly during perinatal stages [Zibetti *et al.* 2010].

Histone modifications have been proven important for neurophysiological processes such as memory and neuronal plasticity but also for neuropathological disorders. As an example for neuronal plasticity, the response to social defeat stress includes epigenetic remodeling like increased methylation of histone H3 at the BDNF promoter and consequent downregulation of this regeneration-associated gene [Tsankova *et al.* 2006; Lockett *et al.* 2010]. The example of epigenetic *Bdnf* regulation might give insights into the molecular regulation of axonal regeneration upon nerve injury as well. So far, there are little or no publications about specific roles of HKMTs or KDMs in axonal regeneration. However, there is some evidence for a brain-related role of epigenetic transcription regulation. Therapeutic approaches targeting repressive epigenetic mechanisms are already under investigation for neuropathological disorders or cancer. Because of their neuroprotective potential and evidence for epigenetic co-regulation of transcription factors induced after nerve injury, it seems important to explore the role of epigenetic mechanisms in axonal injury.

1.3 Hypothesis

For several decades now, axon regeneration and functional recovery of spinal cord injury, compared to peripheral nerve injury, have been intensively investigated. Injury-induced processes of either successful regeneration in the peripheral nervous system (PNS) or inhibited regeneration and scar formation in the central nervous system (CNS) were partly described. Despite various efforts, triggering functional axon regeneration in the spinal cord still achieves very limited success, and the whole picture of successful or failing regeneration is not yet revealed. Although many molecular regeneration-permissive or prohibitive players have already been identified, their subtle and complex regulation has not yet been completely understood. Specifically, the role of epigenetic mechanisms in the regulation of regeneration-associated genes (RAGs) is hardly known. DNA methylation and specific histone modifications might play a role in the differential transcriptional regulation following PNS versus CNS injury.

We hypothesize that expression of RAGs following nerve injury is regulated by a “master switch” represented by epigenetic modifications. Promoter DNA methylation and specific histone modifications are known to regulate gene expression by modulating transcriptional

accessibility to chromatin. These epigenetic modifications would be differentially affected by peripheral versus central axotomy in dorsal root ganglia (DRG) as a model of axonal regeneration resulting in an induction or inhibition of known and novel RAGs. Specifically, promoter/CpG island methylation levels and/or acetylation or methylation of H3-K9 would be expected to change globally or locally at promoters of specific regeneration-associated genes.

1.4 Project outline

This work will investigate the potential role of two major epigenetic mechanisms in mouse DRG as a mouse model for axonal regeneration. First, a genome-wide microarray analysis of DNA methylation patterns at gene promoters and CpG islands will be performed, following a methylated DNA immunoprecipitation (MeDIP-chip). Genomic DNA of dissected DRG will be analyzed for different conditions after 1, 3, or 7 days following either sciatic nerve axotomy (SNA) as peripheral injury, or dorsal column axotomy (DCA) as central injury of the spinal cord. To investigate the involvement of promoter DNA methylation, genes with differential hyper- or hypomethylation and known major RAGs will be analyzed for their mRNA expression levels for each condition. A CpG island analysis of selected genes and their promoters shall reveal correlations between the normalized CpG dinucleotide distribution and injury-induced changes of promoter methylation or gene expression.

Chromatin immunoprecipitation (ChIP) will be applied to detect RAG proximal promoter H3-K9 acetylation or dimethylation that are involved in the activation and repression of gene expression, respectively. Thereafter, the role of histone-3 lysine-9 (H3-K9) acetyltransferase PCAF in axonal regeneration will be investigated in cultured dissociated DRG or cerebellar granule neurons (CGN). Thereby neurite outgrowth on permissive or inhibitory substrates, and global or RAG promoter-specific H3-K9ac and H3-K9me2 levels will be assessed, specifically upon AAV-mediated overexpression of PCAF.

2 Results

2 Results

2.1 Involvement of gene promoter DNA methylation in axonal regeneration

2.1.1 Establishment of Methylated DNA immunoprecipitation (MeDIP)

Differential DNA methylation patterns were hypothesized to be involved in the transcriptional regulation of regeneration-associated genes (RAGs) following different types of nerve injury. Gene promoter methylation was already correlated with a silenced state of gene expression. The intention of this study was to measure levels of promoter and CpG island methylation genome-wide in order to identify induced or repressed genes with differential promoter methylation upon peripheral or central nerve injury. In the frame of the experimental setup, either a peripheral sciatic nerve axotomy (SNA) or a central dorsal column axotomy (DCA) was applied to young adult mice (aged between 2 and 3 months) and compared to corresponding sham controls or naive. Lumbar dorsal root ganglia (L4 to L6 DRG), as a model of axonal regeneration, were dissected after 1, 3, or 7 days following each injury type. Methylated DNA immunoprecipitation was performed on sonicated genomic DNA extracted from DRG. Immunoprecipitated methylated DNA fragments were subsequently whole-genome-amplified (WGA) and hybridized to DNA methylation sensitive tiling microarrays (MeDIP-chip).

Before performing the real MeDIP-chip experiments, the immunoprecipitation procedure needed to be established in the laboratory applying naive mice only. A modified MeDIP protocol was applied adopted from Komashko et al. [Komashko et al. 2008]. In pilot experiments, MeDIP was performed on 10 µg of genomic DNA from naive mouse DRG, sonicated to an average fragment size of 700 bp (100 to 2,000 bp) and incubated with a 5-methylcytosine antibody (IP) compared to a no-antibody control (no Ab). Genomic DNA (Input) was additionally used as reference sample. An initial verification of efficiency and specificity of the MeDIP protocol was performed with minor modifications according to the setup in Weber et al., where the high sensitivity of the antibody was demonstrated allowing for a quantifiable analysis [Weber *et al.* 2005]. Therefore, 4 described PCR primer sets were used for the *H19* imprinting control region (ICR; amplicons 1 to 4) that is completely methylated [Tremblay *et al.* 1997]. This genomic region serves as quantifiable positive methylation control. In Weber et al., genomic DNA was fragmented by the Alu1 restriction enzyme (cutting AG-CT) to yield defined fragments with distinct numbers of CpGs (21, 5, 11, or 12 CpGs for *H19* ICR 1 to 4). The more methylated CpGs are present in a sequence of interest, the more 5-methylcytosine antibody molecules should bind fragments representing this sequence, which will consequently be more enriched during immunoprecipitation. Unmethylated sequences should not be enriched. A primer set for the *Actb* promoter was used as negative control. The *Actb* housekeeping gene contains a large CpG island that is supposed to be largely unmethylated. Weber et al. used the AluI fragmentation only for the verification of the MeDIP. Else, genomic DNA was sonicated for the actual experiments following surgery, similar to this study. In contrast, MeDIP verification in this work was likewise performed on sonicated DNA

Gene Name	genomic DNA Primer forward	genomic DNA Primer reverse	Start Ampl.	Stop Ampl.
H19.1	ACATTCACACGAGCATCCAGG	GCTCTTTAGGTTTGGCGCAAT	-4.006	-3.861
H19.2	GCATGGTCCTCAAATTCTGCA	GCATCTGAACGCCCCAATTA	-3.382	-3.254
H19.3	TGCCAGAAAGCACAAAAGCC	TGGCCCTTGGACATTGTCAT	-2.947	-2.821
H19.4	GCCCAAATGCTGCCAACTT	ACCATTCCAGAGGTGCACACA	-2.600	-2.493
Actin	AGCCAACTTTACGCCTAGCGT	TCTCAAGATGGACCTAATACGG(	+241	+419

Gene Name	Size Ampl.	#CpGs AluI	#CpGs 200 bp	#CpGs 400 bp	#CpGs 700 bp	#CpGs 1,000 bp	#CpGs g-mean	IP/Inp Enrich.
H19.1	146	*22*	8	12	21	24	**15,2**	1,42
H19.2	129	*5*	5	7	16	22	**10,6**	0,91
H19.3	127	*11*	7	10	17	27	**13,3**	1,12
H19.4	108	*12*	6	12	22	35	**15,6**	1,71
Actin	179	*51*	15	34	65	96	**43,8**	0,02

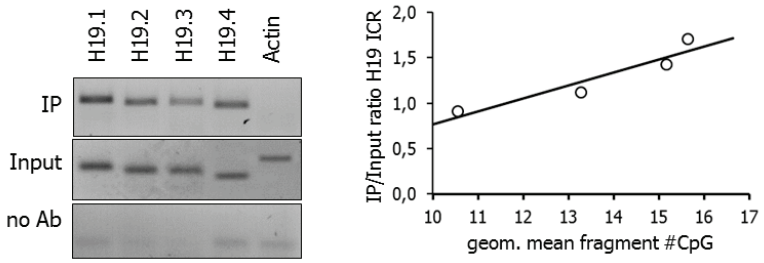

Figure 7 – Verification of Methylated DNA Immunoprecipitation (MeDIP) on the *H19* Imprinted Control Region (ICR). To establish MeDIP on sonicated genomic DNA from naive mouse DRG, enrichment of 4 sequence fragments from the fully methylated *H19* ICR locus was measured. 10 µg of sonicated input genomic DNA (Input) and equal amounts of immunoprecipitated DNA (IP) or a no-antibody control (no Ab) were PCR amplified. Primer sequences were selected from Weber et al. who used the AluI restriction enzyme to digest genomic DNA [Weber et al. 2005]. For all *H19* ICR sequences, the numbers of CpG dinucleotides are given for hypothetical sizes of sonication fragments around the center of each amplicon. The graph displays the quantitative correlation between enrichment (IP/Input ratio) and the weighted geometric mean number of CpGs, which represents the population of fragments. An unmethylated *Actb* region as negative control was not enriched. No-antibody controls yielded no specific signals.

in order to be close to the real experiments. Therefore, the alternative fragmentation method yielded different raw results compared to Weber et al. Quantification of enrichment for *H19* ICR sequences was adjusted to the weighted average of the sonicated fragment size range. **Figure 7** displays the applied primer sequences and the positions of amplicons relative to the TSS of the *H19* locus. Also, the numbers of CpGs are given for either the AluI fragments (produced by Weber et al.), or for representative hypothetical fragments centrically around the amplicons. The weighted geometric mean CpG number for each representative fragment was calculated from the numbers of CpGs for a given arbitrary fragment size (**Formula 1**) and correlated to the *H19* ICR enrichment ratios. The geometric mean was weighted because of the typical Gauss fragment size distribution of regular IP or whole genome amplified IP samples (200 to 1,000 bp) used afterwards for the microarray analysis.

Formula 1 Weighted #CpG = geometric mean of ($\#CpG_{200\ bp} \cdot \#CpG_{400\ bp}\text{^}2 \cdot \#CpG_{700\ bp}\text{^}2 \cdot \#CpG_{1,000\ bp}$)

PCR was performed for IP, no-Ab, or Input samples and PCR amplicons were separated on agarose gel for quantitative densitometry analysis using the GelPro32 software. IP/Input enrichment ratios, deduced from PCR signal intensities, roughly correlated with the expected

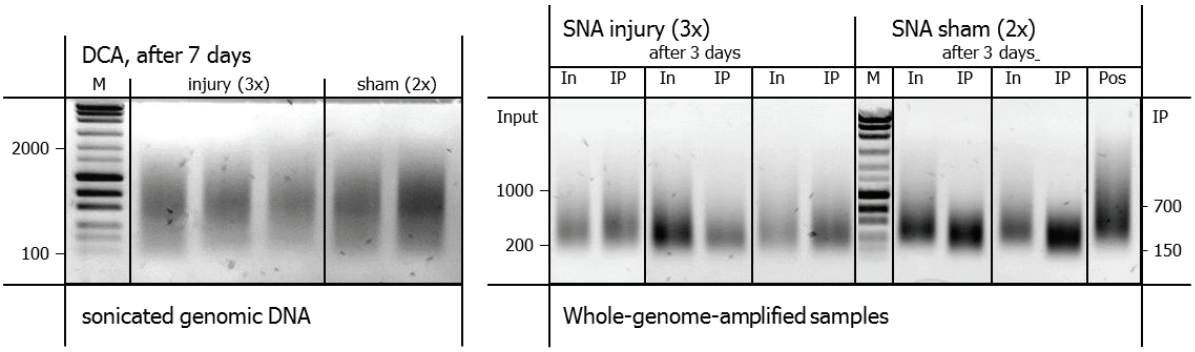

Figure 8 – Quality control of whole-genome-amplified (WGA) samples after MeDIP for DNA methylation microarray. Genomic DNA (Input for MeDIP) was extracted and pooled from each 2 adult mice following nerve injury, and sonicated to an average fragment size of approximately 700 bp (100 to 2,000 bp). For each injury condition (SNA/DCA, 3 time points) and naive, a triplicate of pooled samples was used, and duplicate sets for each sham condition. WGA samples displayed a smaller average fragment size of 400 bp (200 to 800 bp for Input, and 150 to 700 bp for IP). As positive control (Pos), non-fragmented commercial human genomic DNA, included in the kit, was whole-genome-amplified as well.

weighted average numbers of CpGs for the different *H19* fragments. The *Actb* negative control was not enriched, nor did the no-Ab controls yield any specific signals (**Figure 7**).

After establishing and verifying MeDIP, mice were either subjected to (sham) surgery (SNA or DCA) or kept as naive mice, according to the experimental setup described further below in the section for DNA methylation microarray analysis. For each MeDIP sample, genomic DNA of 2 mice per experimental condition group was pooled. The small-scale IP samples needed to be amplified in order to obtain enough material for a DNA methylation microarray study (at least 1 µg). Therefore, each 20 ng of IP samples and Input genomic DNA were amplified using the GenomePlex® Complete Whole Genome Amplification (WGA) Kit (Sigma-Aldrich) ensuring an equivalent treatment of samples. According to the manufacturer, this kit would be able to amplify fragmented genomic DNA representatively up to 1,000-fold thus largely preserving inter-sample ratios for enriched fragments compared to original genomic input samples. By applying WGA, triplicate sample sets for naive or injury, and duplicate sets for sham conditions were produced for each time point and injury type. These samples were further purified with the GenElute™ PCR Clean-Up Kit (Sigma-Aldrich) to remove nucleotides and small oligonucleotides that would disturb DNA concentration measurement and hybridization to the microarrays. Cleaned WGA samples were finally concentrated, if necessary, to match Roche/NimbleGen's instructions for DNA sample quality and concentration. Fragment size distribution and sample quality was verified on agarose gel (**Figure 8**).

2.1.2 DNA methylation microarray analysis

According to the experimental setup, bilateral sciatic nerve axotomy (SNA) or dorsal column axotomy (DCA) was applied. Thereby, bilateral surgery was preferred over an ipsilateral injury with contralateral sham control since in the latter case complete independence of samples is not given, specifically upon DCA. Consequently, corresponding sham control injuries

were performed in separate animals and naive mice were used as reference. L4-L6 DRG of each 2 mice were dissected for each sample after 1, 3, or 7 days following SNA or DCA. MeDIP was performed and processed to WGA IP and Input samples that were hybridized to DNA methylation sensitive microarrays (33 arrays in total) that were pre-analyzed by Roche/NimbleGen. For each experimental condition, triplicate sample sets for injury or sham, and duplicate sets for sham were applied, using 66 mice in total with n = 6 or n = 4 for each condition group (**Figure 10 A and B**). Further microarray analysis was performed based on the pre-analyzed dataset according to the workflow. This figure provides an overview for the experimental design and DNA methylation analysis process of the whole MeDIP-chip experiment. Subsequently, 12 distinct experimental conditions were defined regarding the injury type (SNA or DCA), the time point (1, 3, or 7 days), and injury or corresponding sham plus naive. For the analysis of (differentially) hyper- or hypomethylated genes, 6 instead of 12 experimental conditions were coherently defined for associated injury and sham microarray sets for each time point and injury type. Additionally, "Naive" was supposed to be the reference condition.

In detail, pairwise IP and Input samples were co-hybridized on promoter/CGI DNA methylation tiling microarrays (Roche/NimbleGen, "2007-02-27 MM8 CpG Island Promoter 385K RefSeq"). The applied microarray type represented 18,180 mouse genes annotated by their NCBI Entrez Gene IDs. Specifically, the promoter region, approximately -1,500 to +800 bp relative to the TSS, was covered by close-set (tiling) oligonucleotide probes. Additionally, the

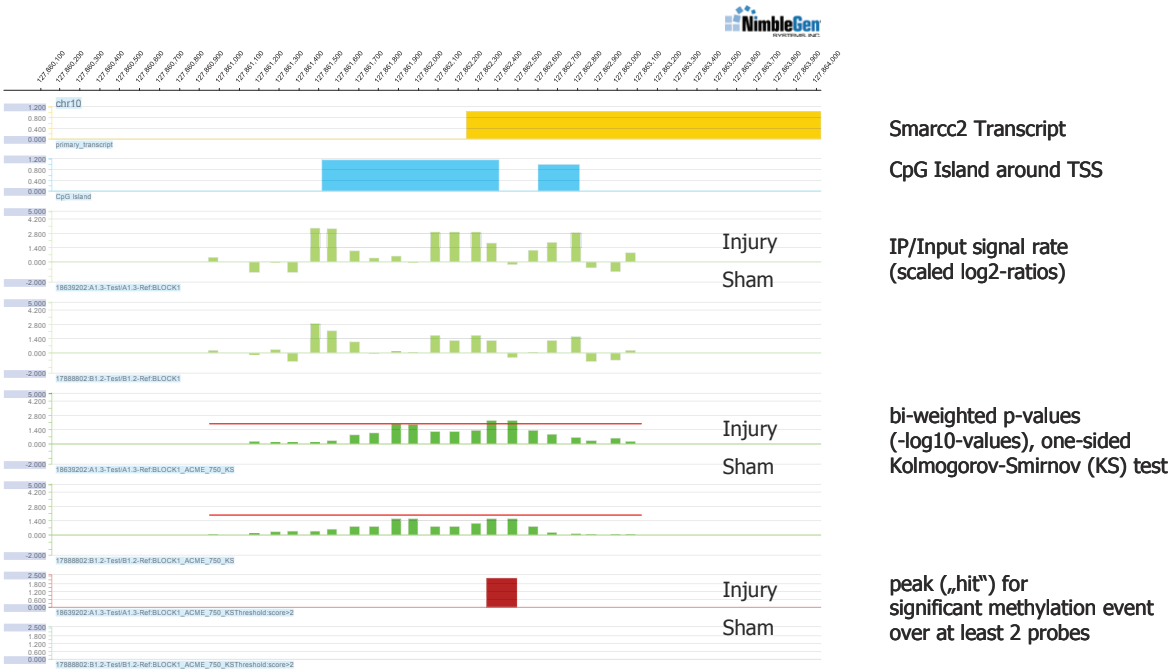

Figure 9 – Graphical analysis of DNA methylation tiling microarrays for gene promoters and CGIs using the example of the *Smarcc2* gene locus (yellow bar). Tiling probes covered the promoter region (approx. -1,500 to +800 bp to TSS). IP-to-Input ratios for either injury or sham sample sets were displayed as scaled log2-ratios (light green). Significant enrichment in a walking 200 bp window was assessed using a Kolmogorov-Smirnov test yielding log10 p-values. In case of an average log10 value higher than 2 in such a window, an output peak stated a significant methylation event. Pre-analysis was performed by Roche NimbleGen, displayed with the company's software tool SignalMap.

array covered promoter and non-promoter CGIs. Roche/NimbleGen provided a pre-analyzed qualitative dataset yielding probabilities (p-values) for significant methylation events in the covered regions, which are defined as IP/Input ratios significantly higher than background. Such an event only resulted from a high average enrichment over a sliding 200 bp window based on normalized and scaled log2-IP/Input ratios for each single oligonucleotide probe (Kolmogorov-Smirnov test). A graphical representation of the complete dataset was possible with the Roche/NimbleGen software "SignalMap" providing localization information for annotation genes with TSS and CGIs (status Feb. 2006, NCBI36/mm8). An exemplary SignalMap screen for the hypermethylated *Smarcc2* gene is shown in **Figure 9**. Significant methylation peaks (events) were usually located in the proximal promoter region, mostly within a CpG island close or around the TSS. This peak dataset was further analyzed in a Microsoft Office® Excel spreadsheet (for layout see **Table S1**). The term "gene" will be

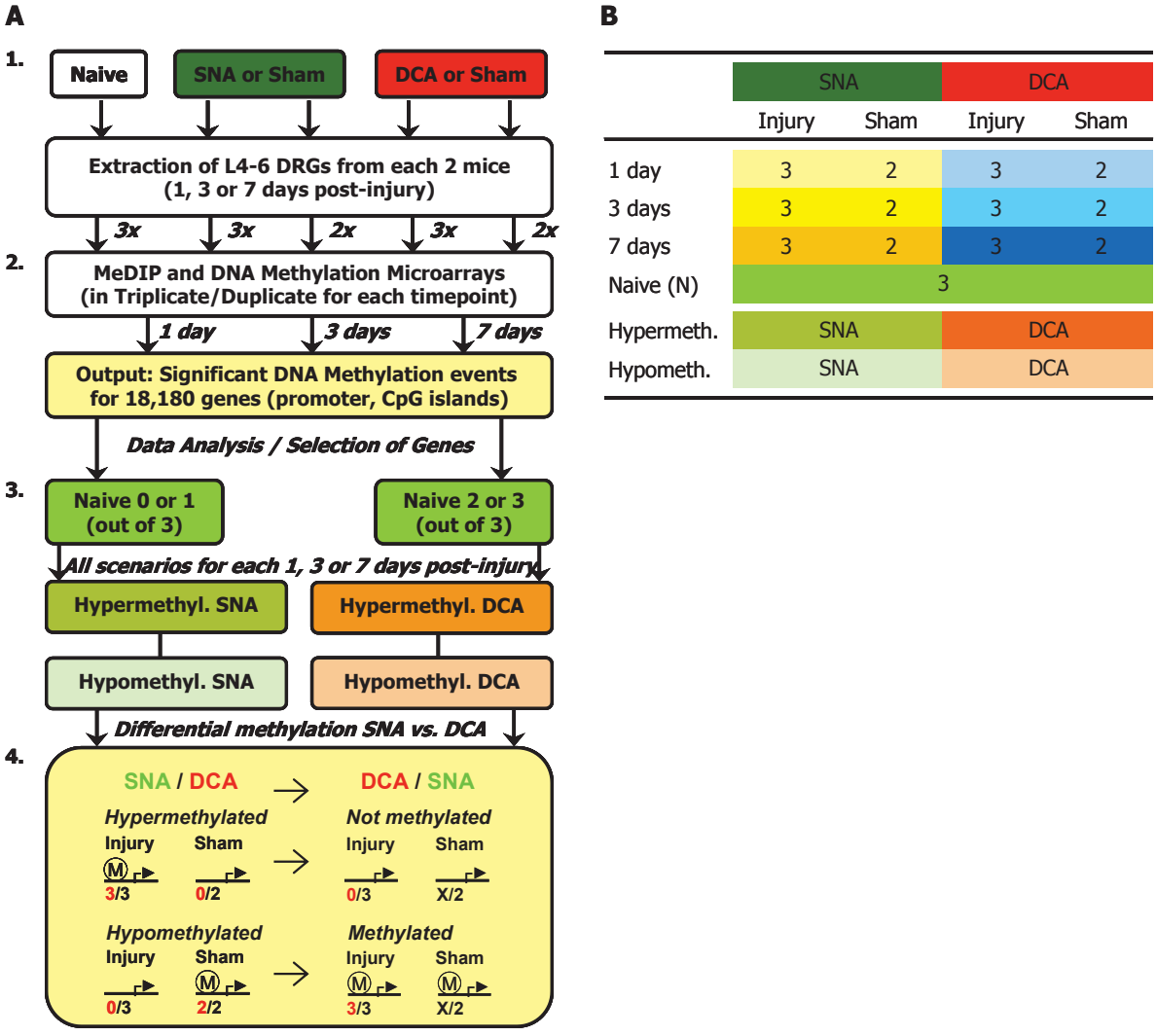

Figure 10 – DNA methylation microarray analysis algorithm and condition overview. (A) The schematic workflow displays the experimental conditions and sample sets chosen to perform MeDIP-chip with whole genome amplified IP and genomic Input samples. Genes were filtered for defined hyper- or hypomethylation and further filtered for differentially methylated genes. **(B)** Altogether, 33 microarrays were applied in this study for both injury types and 3 time points, with either triplicate array sets for injury and naive or duplicate sets for sham conditions. Different color codes were used to compare SNA with DCA or to distinguish hyper- or hypomethylated genes for single time points and injury type.

synonymously used for a covered proximal gene promoter region. Genes "hit" on a microarray if significantly methylated upon a certain experimental condition yielding a peak (mean of -log10 p-values > 2). Otherwise, insignificant or no promoter methylation yielded no hit.

For the 12 experimental conditions plus naive, altogether 33 data points were analyzed for each gene (see **Figure 10 B**). Naive samples functioned as reference control for basal gene promoter methylation being not affected by any kind of surgery. Sham surgeries themselves, at least in the case of laminectomy, might have an effect on gene expression similar to nerve injury [De Biase *et al.* 2005]. To clearly distinguish between perspectives and to better understand the following analysis process, a color code was defined (**Figure 10 B**). To distinguish single time points in the MeDIP-chip analysis (for 1, 3, or 7 days post-injury), SNA samples were subdivided into light yellow to orange (■■■), DCA samples into light blue to dark blue (■■■), and naive coded bright green (■). To compare hyper- and hypomethylated genes, respectively, green and light green (■■) was applied for SNA, and orange and light orange (■■) for DCA. For other results like mRNA expression analysis, a different code was used. SNA injury-to-sham fold change ratios were set dark green (■) and corresponding DCA values set red (■), naive was now set blue (■).

Because of the qualitative nature of the dataset, the analysis could only be performed semi-quantitatively by analyzing the frequency of significant methylation peaks for each gene within the multiple array sets. First, a global analysis approach was chosen to obtain results for changes of global methylation between different experimental conditions. The total number of 18,180 annotated genes was the reference for the maximum hit number on one array. The average real number of significant methylation hits from each condition array set represents the number of methylated genes (gene promoters), which is therefore a semi-quantitative measure for global DNA methylation levels without unit. First, average total hit numbers, interpreted as global methylation levels, were compared between conditions. The average total hit numbers resulted either, from triplicate injury or naive array sets, or from duplicate sham sets (**Figure 11 A**). The average global methylation level for the naive reference (919 ± 200 STD) was slightly lower but still comparable to average DCA shams (976 ± 83 STD, mean for all time points). Global methylation levels in SNA shams were much lower (756 ± 101 STD, average for all time points) than in DCA shams or naive. Interestingly, average global methylation levels for SNA injuries across all time points were higher (892 ± 174 STD) than the average of the corresponding shams (756 ± 101 STD), indicating an SNA injury-induced increase in global methylation. Thereby, highest global levels upon SNA injury were found at 1 day and then consequently decreasing during the time course (1 day: 1,065 ± 116 STD; 3 days: 913 ± 56 STD; 7 days: 697 ± 48 STD). The average total hit number for DCA injury across all time points (915 ± 131 STD) was slightly lower than for corresponding DCA shams (976 ± 83 STD) and as high as naive levels. Highest DCA injury values were found after 3 days post-injury (1 day: 970 ± 81 STD; 3 days: 992 ± 99 STD; 7 days: 784 ± 112 STD). Remarkably, highest overall levels of global methylation were found

for DCA sham after 7 days (1,070 ± 19 STD). To the end, average SNA injury levels (892 ± 174 STD) were comparable to average DCA injury levels (915 ± 131 STD) and to naive (919 ± 200 STD) although tendencies along the time course, and sham levels were different for both injury types. The injury-to-sham fold changes of global DNA methylation levels upon injury were highest upon SNA after 1 and 3 days (+27 and +26 percent) whereas there was no increase anymore after 7 days. Following DCA, fold change values were notably decreased after 7 days (-27 percent), in part due to high sham levels. Else rather no significant change was detected after 1 or 3 days upon DCA (-1 and +12 percent).

Second, the numbers of genes with specific "methylation levels" are shown in comparison between experimental conditions and across the time course (**Figure 11 B and C**). Genes were regarded as "unmethylated" if hitting in none of the arrays of a set (0/3 or 0/2), or as significantly "methylated" if hitting in all arrays (3/3 or 2/2). The other genes were regarded as "partly methylated" (1/3, 2/3 or 1/2) showing significant methylation only in at least one but not all arrays. However, due to the qualitative nature of the p-value dataset, no correlation with quantitative percent methylation levels could be deduced directly. Regarding the time course for both SNA and DCA, the combined numbers of methylated (3/3) and partially methylated genes (1/3 or 2/3) upon injury were generally decreasing from 1 to 7 days post-injury (SNA injury: from 1,904 down to 1,202 out of 18,180 genes; DCA injury: from 1,768 down to 1,331 – Naive: 1,662 genes) **(Figure 11 C)**. In average, the numbers of methylated

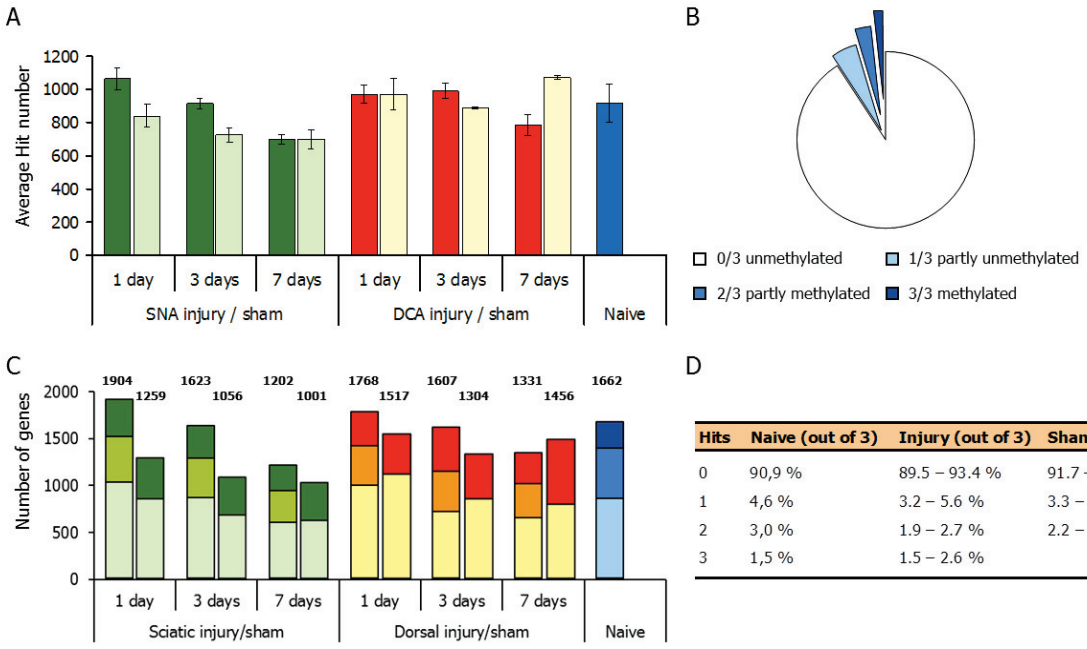

Hits	Naive (out of 3)	Injury (out of 3)	Sham (out of 2)
0	90,9 %	89.5 – 93.4 %	91.7 – 94.5 %
1	4,6 %	3.2 – 5.6 %	3.3 – 6.0 %
2	3,0 %	1.9 – 2.7 %	2.2 – 3.8 %
3	1,5 %	1.5 – 2.6 %	

Figure 11 – Global DNA methylation microarray analysis. **(A)** The total hit number of significant methylation events (mean) for all 18,180 annotated genes (by GeneID) was regarded as a measure for global methylation. The average total hit number for each multiple microarray set is graphed comparing SNA injury (green) and sham (light green), or DCA injury (red) and sham (yellow), or naive (blue). Triplicate arrays were applied for injury conditions and naive, duplicates for sham. **(B)** Most genes were not significantly methylated in each condition, as shown representatively for average naive microarrays. **(C)** The numbers of methylated and partially methylated genes were compared (hitting in at least 1/3 arrays for injury or naive, or in at least 1/2 arrays for shams). **(D)** The average percentage of methylated, partly methylated, or unmethylated genes was similar across all microarrays. Error bars: SEM.

and partially methylated genes across all time points were similar for both injury types (SNA injury: 1,576 ± 353 STD; DCA injury: 1,569 ± 221 STD) although steeper declining upon SNA. However, SNA sham average gene numbers (1,105 ± 136 STD) were clearly lower than for average DCA sham across the time course (1,426 ± 110 STD), which diminished the difference between injury and sham upon DCA. Regarding single injury, sham, or naive conditions in average, most gene promoters were not significantly methylated (not hitting) on any of the multiple arrays for each condition (unmethylated: 89.5 to 94.5 percent; in average 16,742 ± 274 STD out of 18,180 genes). However, 1.5 to 3.8 percent of all genes (in average 405 ± 104 STD) were always significantly methylated for each condition (**Figure 11 D**). Interestingly, in average of all conditions, 78.8 percent (14,325 genes) of all genes remained unmethylated whereas 0.2 percent (36 genes) showed significant methylation on every microarray across all conditions.

2.1.3 Gene expression of DNA methyltransferases upon nerve injury

Establishment, maintenance, and certain changes of global DNA methylation upon injury are mediated by DNA methyltransferases (DNMTs). Upon nerve injury, massive intracellular adaptations have to be realized, potentially accompanied by moderate alterations of global methylation levels that were detected by microarray analysis in this study. *Dnmt* mRNA expression levels might be consequently regulated, as well. This might lead to local changes of target gene promoter DNA methylation, as already described in brain-related contexts such as epilepsy, schizophrenia, or in gliomas [Zhubi *et al.* 2009; Rajendran *et al.* 2011; Q Zhu *et al.* 2012]. However, under physiological conditions chromatin-modifying enzymes might be carefully regulated. Therefore, qRT-PCR was applied following SNA and DCA covering the

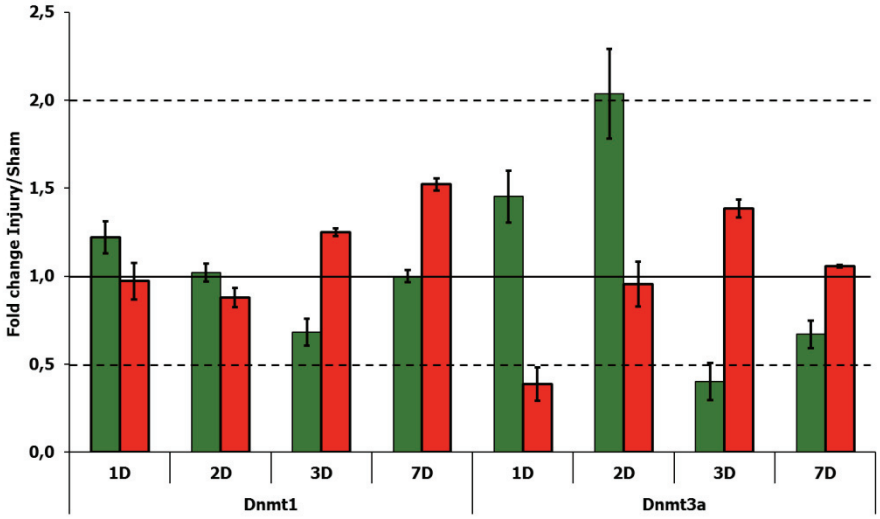

Figure 12 – *De novo* methyltransferases *Dnmt1* and *Dnmt3a* are differentially expressed upon SNA or DCA during the time course. Normalized mean injury-to-sham fold change expression of *Dnmt1* and *Dnmt3a* was detected by qRT-PCR whereby *Dnmt3a* was regulated more dramatically than *Dnmt1*. Thereby, *Dnmt* expression profiles exhibited an opposing or delayed relative expression pattern for DCA compared to SNA. *Dnmt3b* was not detectable by qRT-PCR (in triplicates from n = 3; error bars: SEM).

whole time course from 1 to 7 days post-injury including additionally 2 days (**Figure 12**). Relative *Dnmt1* mRNA expression (normalized injury-to-sham fold change ratio) increased at 1 day following SNA, was downregulated after 3 days, and normalized after 7 days. Upon DCA, in contrast, relative *Dnmt1* expression increased after 3 and 7 days post-injury. *Dnmt3a* was regulated more dramatically being upregulated 2 days after SNA but again downregulated after 3 to 7 days. Upon DCA, the *Dnmt3a* gene expression profile followed an opposing or delayed expression pattern compared to SNA. *Dnmt3b* was not detectable.

2.1.4 Hypermethylated or hypomethylated genes

Next, specific scenarios and algorithms were defined to filter potential genes of interest. First, hyper- or hypomethylated genes were identified for each condition. Thereby, "hypermethylated" meant being significantly methylated upon injury but not methylated in sham, with respect to naive values similar to sham. Consequently, "hypomethylated" was defined as not being methylated upon injury but methylated in sham for a specific condition (steps 3 and 4 of the work flow scheme, **Figure 10 A** and **Figure 13 B**). For a number of gene promoters, certain discrepancies for methylation levels were found across all shams and naive. That is why strict filters were applied for the main analysis to find genes that were clearest hyper- or hypomethylated for the single conditions (**Figure 14** and **Table S1**, Appendix).

Deduced from the qualitative dataset, "Methylation Values" (MV) were defined as a semi-quantitative measure for strong, medium, or weak hyper- or hypomethylation or neutral cases

A

	Scenario	MV	Inury (3)	Sham (2)
HYPERmeth.	strong	5	3	0
	medium	4	2	0
		3	3	1
	weak	2	1	0
		1	2	1
	neutral	0	3	2
		-0	0	0
HYPOmeth.	weak	-1	1	1
		-2	2	2
	medium	-3	0	1
		-4	1	2
	strong	-5	0	2

B

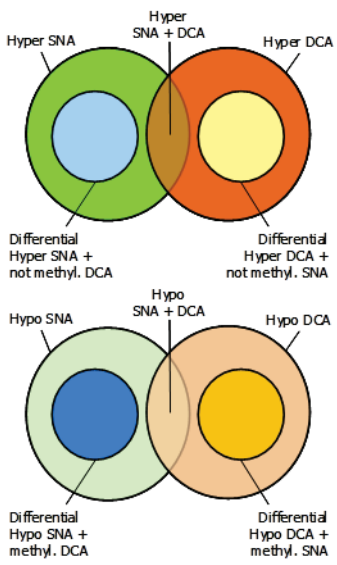

Figure 13 – Legend for Methylation Values and schematic for semi-quantitative analysis of the DNA methylation microarray dataset. (A) Arbitrary Methylation Values (MV) were defined according to the ranking of calculated differences between relative injury and sham hit numbers (see text) in order to determine genes with strong, medium, or weak hyper- and hypomethylation for each condition (with respect to naive being similar to sham). **(B)** The schematic visualizes the sets of hyper- or hypomethylated genes and the subset of differentially methylated genes exhibiting hyper- or hypo methylation only upon one injury type but no change upon the other.

(**Figure 13 A**). The arbitrary MVs were defined according to the ranking of calculated differences between relative hit numbers for injury and sham. These differences were ranked from highest to smallest and assigned to each level from strong hypermethylation down to strong hypomethylation (for example, 2 out of 3 hits for injury and 1 out of 2 hits for sham (2-1) are calculated as follows: one-half is substracted from two-thirds equaling one-sixth that is ranked as MV = +1). Thus, the maximum positive MV = +5 stands for strong hypermethylation (injury: 3/3 hits; sham: 0/2 hits), and MV = -5 for strong hypomethylation (injury: 0/3 hits; sham: 2/2 hits). Applying a strict analysis algorithm allowing only MV = +5/-5 and regarding naive values, required to be similar to shams, yielded sets of strong hypermethylated genes (with naive: 0/3 or 1/3) or strong hypomethylated genes (naive: 2/3 or 3/3) for each condition.

These genes were analyzed for functional annotations and further filtered for differentially methylated genes that exhibited an injury-induced change of the methylation status, clearly for only one injury type at a given time point. In an extended scenario, medium and weak hyper- or hypomethylated genes (MV = +4/+3 for hypermethylation, and MV = -4/-3 for hypomethylation) were additionally analyzed to determine genes with a consistent methylation status overlapping several time points. Strong hyper- or hypomethylated genes were filtered for each condition separately disregarding the relative changes of methylation in other

A

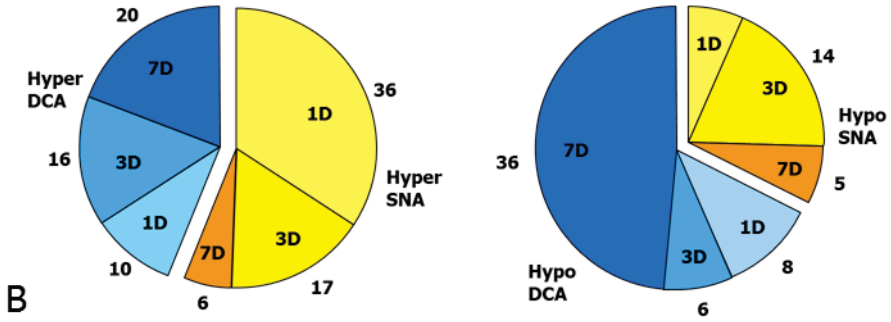

B

NCBI Gene ID	Gene Symbol	SNA 1 day Inj	Sh	MV	SNA 3 days Inj	Sh	MV	SNA 7 days Inj	Sh	MV	DCA 1 day Inj	Sh	MV	DCA 3 days Inj	Sh	MV	DCA 7 days Inj	Sh	MV	N
HYPERmethylated genes after 1 day upon Sciatic nerve axatomy (SNA) - with Naive 0 or 1																				
68094	Smarcc2	3	0	5	0	0	0	0	0	0	0	0	0	0	0	0	0	1	-3	1
269003	Sap130	3	0	5	1	0	2	0	0	0	0	0	0	2	1	1	0	0	0	0
HYPERmethylated genes after 3 days upon Dorsal column axatomy (DCA) - with Naive 0 or 1																				
26407	Map3k4	0	0	0	0	0	0	0	0	0	1	0	2	3	0	5	0	0	0	1
HYPOmethylated genes after 1 day upon Sciatic nerve axatomy (SNA) - with Naive 3 or 2																				
14685	Gnat1	0	2	-5	2	2	-2	3	2	0	3	2	0	3	2	0	3	2	0	3
HYPOmethylated genes after 1 day upon Dorsal column axatomy (DCA) - with Naive 3 or 2																				
140703	Emid1	2	2	-2	3	2	0	3	2	0	0	2	-5	3	1	3	3	2	0	3

Figure 14 – Hyper- and hypomethylated genes upon sciatic nerve axotomy (SNA) or dorsal column axotomy (DCA) were filtered according to a strict scenario (MV = +5 or -5) from the complete Roche/NimbleGen microarray dataset. **(A)** Altogether 179 genes were found (strong hypermethylated: 105, strong hypomethylated: 74). The numbers of SNA-related genes are shown in shades of yellow, for DCA-related genes in shades of blue. **(B)** An exemplary excerpt of the (strong) hyper- and hypomethylated genes list is displayed. For the relevant condition, the color code was removed for better visualization. A complete list can be viewed in **Table S1** (Appendix).

experimental conditions. An (experimental) condition, as indicated before, will now be defined for associated injury and sham microarray sets (3 plus 2) for each time point and injury type, for which a MV is defined. In total, 179 strong hypermethylated (105) or hypomethylated genes (74) were identified. **Figure 14 A** summarizes the numbers of hyper- or hypomethylated genes for each condition in a pie chart diagram and an exemplary excerpt of the full gene list spreadsheet is demonstrated in **Figure 14 B**. The complete list can be viewed in **Table S1** (Appendix). Comparing conditions, overall more genes were hypermethylated (total SNA for all time points: 59; total DCA: 46) than hypomethylated (total SNA: 24; total DCA: 50). Thereby, the number of hypermethylated genes upon SNA decreased during the time course (highest after 1 day: 36) but increased upon DCA (highest after 7 days: 20). Most hypomethylated genes upon SNA were found after 3 days (14), for DCA after 7 days (36).

The set of strong hyper- and hypomethylated genes was subjected to a functional annotation analysis utilizing the DAVID Bioinformatic Database (http://david.abcc.ncifcrf.gov/) and integrating information from the UniProtKB database (www.uniprot.org/uniprot/) and the NCBI Gene Database (www.ncbi.nlm.nih.gov/gene). Since more than one functional annotation term was usually found for most genes, they were manually grouped into 9 major functional categories according to their most important functional association, or else into a 10th category of "Other/Unknown function". **Figure 15** shows pie charts with gene numbers of all functional categories for the 4 main conditions (hyper- or hypomethylated genes, upon SNA or DCA, with each all 3 time points combined). The ranking of the functional categories, according to the included overall gene numbers, revealed that most genes were associated with functions in signal transduction, transcription and chromatin regulation, or cell structure:

Signal Transduction (37)
Transcription/Chromatin (25)
Cell Structure/ECM/Cytoskeleton (23)
Transport/Ion channels (22)
Metabolism (14)
Translation/mRNA processing (9)
Protein Modification (8)
(Neural) Development, Differentiation, Cell Cycle (6)
Stress response/Apoptosis (3)
Other/Unknown function (32)

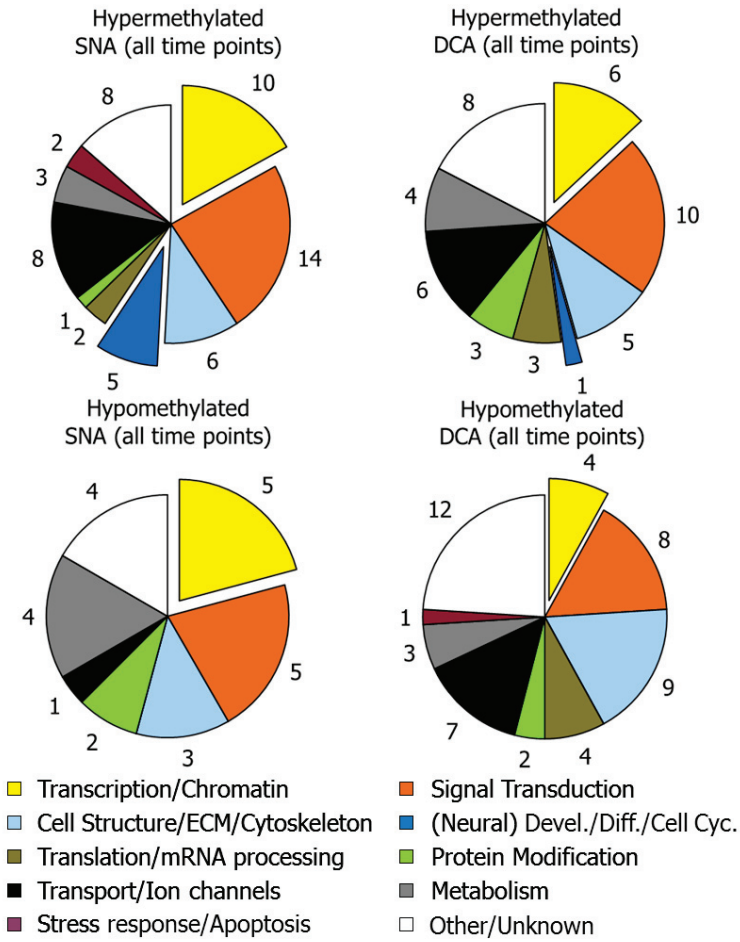

Figure 15 – Functional annotation analysis of 179 hyper- and hypomethylated genes from the strict scenario of the DNA methylation microarray analysis was performed separately for the 4 main conditions (hyper- or hypomethylated, SNA or DCA). According to their major annotation, all genes were assigned to 10 functional categories, for which gene numbers are given accumulated for all time points. Highlighted categories in yellow and blue were in the focus of this study. **Table S2** (Appendix) provides a complete list of annotated genes.

82 percent (147) out of 179 strong hyper- or hypomethylated genes could be properly assigned to the 9 functional categories. Most genes (107; 60 percent) belonged to the top 4 categories as listed above (complete gene list in **Table S2**, Appendix). No genes were found overlapping any of the 4 major conditions. In the largest functional categories, more genes were usually hypermethylated than hypomethylated, and more genes were found upon SNA than upon DCA. 35 genes are known to be specifically relevant in a neuronal context (highlighted in red). According to the topic of this thesis, special focus was set on the categories 'Transcription or Chromatin', and '(Neural) Development, Differentiation, or Cell Cycle'. Several of the highlighted genes in these categories might have functions in axonal regeneration because of known roles in neurons or a conspicuous injury type-dependent promoter methylation:

'Transcription, Chromatin': *Smarcc2*, *Cbx4*, *Sap130*, *Tcf3* (*Tcfe2a*), *Crct1*, *Rbpjl* (*Rbpsuhl*);
'(Neural) Development, Differentiation, Cell Cycle': *Metrn*, *Fyn*, *Neurl4*, *Dpysl5*).

Table 1 – Extended hyper- or hypomethylated genes were analyzed for persistent methylation changes for adjacent time points. (A and B) Number of genes filtered according to the extended scenario including strong, medium, and weak hyper- or hypomethylated genes (MV ≥ +3, and ≤ -3, respectively, regarding appropriate naive values). **(C)** Numbers of genes that overlap adjacent time points for each injury type (SNA/DCA) exhibiting the same methylation status (hypermethylated/hypomethylated). Additional genes were identified with the same methylation status for both injury types at a given time point that are not of interest in this study.

A

	Hypermethylated			Hypomethylated		
MV	5	> 4	> 3	-5	< -4	< -3
SNA 1D	36	188	231	5	35	75
SNA 3D	17	139	158	14	38	60
SNA 7D	6	57	74	5	23	57
DCA 1D	10	90	121	8	31	114
DCA 3D	16	115	173	6	26	64
DCA 7D	20	103	129	36	87	162

B

	Scenario	MV	Inury (3)	Sham (2)
HYPERmeth.	strong	5	3	0
	medium	4	2	0
		3	3	1
	weak	2	1	0
		1	2	1
	neutral	0	3	2
		-0	0	0
HYPOmeth.	weak	-1	1	1
		-2	2	2
	medium	-3	0	1
		-4	1	2
	strong	-5	0	2

C

Hypermethylated	SNA				DCA			
	1 D	3 D	7 D	total	1 D	3 D	7 D	total
MV > 3	231	158	74	463	121	173	129	423
1 D + 3 D	26				20			
3 D + 7 D		7				22		
1 D + 7 D		5				16		
1, 3 + 7 D		1				6		
SCA + DCA	12	26	10	48				

Hypomethylated	SNA				DCA			
	1 D	3 D	7 D	total	1 D	3 D	7 D	total
MV < -3	75	60	57	192	114	64	162	340
1 D + 3 D	11				13			
3 D + 7 D		6				22		
1 D + 7 D		4				43		
1, 3 + 7 D		0				5		
SCA + DCA	36	7	40	83				

In the next step, the focus of attention was directed to genes with persisting hyper- or hypomethylation overlapping more than one time point for a specific injury type. Only 2 genes were hypomethylated across 2 time points of the same condition within the strict scenario (*Rbpjl* and *Krt4*, previously *Rbpsuhl* and *Krt2-4*, respectively). No genes preserved a clearly altered methylation status across the full time course. Therefore, an extended scenario was analyzed including strong, medium and weak hypermethylated (MV ≥ +3) or hypomethylated genes (MV ≤ -3), respectively (**Table 1 A and B**). In the frame of this extended scenario, 886 hypermethylated genes (463 for SNA, 423 for DCA) and 532 hypomethylated genes (192 for SNA, 340 for DCA) were identified, accumulated for all time points. 75 persistently hypermethylated genes were found to overlap each 2 adjacent time points (33 for SNA, 42 for DCA) and 72 hypomethylated genes (17 for SNA, 55 for DCA). An important small subset of genes (total 12) exhibited the same methylation status upon one injury type across the whole time course (hyper SNA: *Tmco1*; hyper DCA: *Kcnj4*, *Rp2h*, *Sowahb* (*5730467H21Rik*), *Kdelr3*, *Otud7b* (*Za20d1*), *Map3k9*; hypo DCA: *Drosha* (*Rnasen*), *Kifc3*, *Meis3* (*Mrg2*), *Kcnk12*, *Tas2r144*).

2.1.5 Differentially methylated genes for both injury types

After analyzing strong hyper- and hypomethylated genes for each condition, the more relevant subset of "differentially methylated" (DM) genes was identified, which respond specifically to SNA or DCA. Such genes were either strongly hypermethylated for one injury type and remain unmethylated upon the other type, or they were strongly hypomethylated for one type, and remain fully methylated for the other type (**Figure 10**, step 4, and **Figure 13 A**). Thereby, the filter for the opposing injury condition without significant methylation status changes was selective only for the methylation level upon injury but disregarding sham. For example,

Table 2 – Differentially methylated genes were identified for each injury type. As a subset of strong hyper- and hypomethylated genes, 46 differentially methylated genes were filtered. These were hyper- or hypomethylated for one injury type (compared to sham) and not methylated or completely methylated for the other type, respectively (neutral MV). Genes highlighted in blue have known functions in the context of chromatin or transcriptional regulation, or in neuronal signal transduction. Most of these genes were further analyzed to correlate their methylation status with differential relative mRNA expression assessed by a qRT-PCR array. Genes in *italic* were not examined.

NCBI	Gene	SNA 1 day			SNA 3 days			SNA 7 days			DCA 1 day			DCA 3 days			DCA 7 days			N
Gene ID	Symbol	Inj	Sh	MV	Inj	Sh	MV	Inj	Sh	MV	Inj	Sh	MV	Inj	Sh	MV	Inj	Sh	MV	
Differentially HYPERmethylated genes after 1 day upon SNA - with Naive 0 or 1 - 9 Genes																				
72482	Acbd6	3	0	5	0	0	0	0	0	0	0	0	0	0	0	0	0	0	0	1
12418	Cbx4	3	0	5	1	1	-1	0	0	0	0	0	0	1	1	-1	0	0	0	0
26554	Cul3	3	0	5	1	1	-1	0	0	0	0	0	0	0	0	0	0	0	0	1
110033	Kif22	3	0	5	1	1	-1	3	0	5	0	0	0	0	0	0	1	0	2	0
269003	Sap130	3	0	5	1	0	2	0	0	0	0	0	0	2	1	1	0	0	0	0
53896	Slc7a10	3	0	5	0	2	-5	1	1	-1	0	0	0	0	0	0	1	1	-1	1
68094	Smarcc2	3	0	5	0	0	0	0	0	0	0	0	0	0	0	0	0	1	-3	1
22063	Trpc1	3	0	5	0	0	0	0	0	0	0	1	-3	2	0	4	1	1	-1	1
69380	*17...G24Rik*	3	0	5	0	0	0	1	0	2	0	0	0	1	0	2	0	0	0	0
Differentially HYPERmethylated genes after 3 days upon SNA - with Naive 0 or 1 - 4 Genes																				
75796	Cdyl2	0	1	-3	3	0	5	0	0	0	0	0	0	0	1	-3	0	1	-3	1
16570	Kif3c	3	1	3	3	0	5	2	1	1	0	0	0	0	0	0	2	0	4	1
56294	Ptpn9	2	2	-2	3	0	5	0	0	0	1	1	-1	0	1	-3	0	1	-3	1
228994	Ythdf1	2	0	4	3	0	5	0	0	0	0	1	-3	0	0	0	0	0	0	1
Differentially HYPERmethylated genes after 7 days upon SNA - with Naive 0 or 1 - 2 Genes																				
654812	Angptl7	1	0	2	0	1	-3	3	0	5	0	0	0	0	0	0	0	0	0	0
239766	*Rtp1*	0	0	0	0	0	0	3	0	5	0	0	0	0	0	0	0	0	0	0
Differentially HYPERmethylated genes after 1 day upon DCA - with Naive 0 or 1 - 2 Genes																				
433586	Maml3	0	1	-3	0	0	0	0	1	-3	3	0	5	0	2	-5	1	0	2	0
229603	*Za20d1*	0	1	-3	2	1	1	1	0	2	3	0	5	3	0	5	2	0	4	0
Differentially HYPERmethylated genes after 3 days upon DCA - with Naive 0 or 1 - 5 Genes																				
78514	Arhgap10	1	0	2	0	0	0	0	2	-5	2	2	-2	3	0	5	0	0	0	0
65254	Dpysl5	2	0	4	0	2	-5	0	0	0	2	2	-2	3	0	5	1	0	2	0
67102	Eurl	0	0	0	0	0	0	0	0	0	1	0	2	3	0	5	0	0	0	0
16564	Kif21a	3	1	3	0	0	0	0	0	0	0	1	-3	3	0	5	0	0	0	1
26407	Map3k4	0	0	0	0	0	0	0	0	0	1	0	2	3	0	5	0	0	0	1
Differentially HYPERmethylated genes after 7 days upon DCA - with Naive 0 or 1 - 5 Genes																				
403205	Agr3	0	0	0	0	0	0	0	0	0	0	0	0	0	0	0	3	0	5	1
269109	Dpp10	0	0	0	1	1	-1	0	1	-3	0	1	-3	1	1	-1	3	0	5	1
237987	Otop2	0	0	0	0	0	0	0	0	0	0	0	0	0	0	0	3	0	5	0
18846	Plxna3	1	1	-1	1	0	2	0	1	-3	1	0	2	0	1	-3	3	0	5	0
637749	*LOC637749*	0	0	0	1	1	-1	0	1	-3	0	1	-3	1	1	-1	3	0	5	1

NCBI Gene ID	Gene Symbol	SNA 1 day			SNA 3 days			SNA 7 days			DCA 1 day			DCA 3 days			DCA 7 days			N
		Inj	Sh	MV	Inj	Sh	MV	Inj	Sh	MV	Inj	Sh	MV	Inj	Sh	MV	Inj	Sh	MV	
Differentially HYPOmethylated genes after 1 day upon SNA - with Naive 3 or 2 - 3 Genes																				
14685	Gnat1	0	2	-5	2	2	-2	3	2	0	3	2	0	3	2	0	3	2	0	3
16682	Krt2-4	0	2	-5	0	2	-5	0	0	0	3	1	3	3	1	3	3	2	0	2
19668	Rbpsuhl	0	2	-5	0	2	-5	1	0	2	3	2	0	3	1	3	2	2	-2	3
Differentially HYPOmethylated genes after 3 days upon SNA - with Naive 3 or 2 - 6 Genes																				
11639	Ak3l1	2	0	4	0	2	-5	0	0	0	2	1	1	3	1	3	2	2	-2	2
11717	Ampd3	2	1	1	0	2	-5	2	2	-2	1	2	-4	3	1	3	2	2	-2	3
320982	Arl4c	3	1	3	0	2	-5	2	0	4	3	2	0	3	2	0	3	2	0	3
16682	Krt2-4	0	2	-5	0	2	-5	0	0	0	3	1	3	3	1	3	3	2	0	2
19668	Rbpsuhl	0	2	-5	0	2	-5	1	0	2	3	2	0	3	1	3	2	2	-2	3
619306	B4...F04Rik	2	1	1	0	2	-5	2	2	-2	1	2	-4	3	1	3	2	2	-2	3
Differentially HYPOmethylated genes after 7 days upon SNA - with Naive 3 or 2 - 2 Genes																				
320237	63...J24Rik	1	1	-1	2	1	1	0	2	-5	3	1	3	2	2	-2	3	0	5	2
109050	65...L21Rik	3	2	0	1	1	-1	0	2	-5	2	2	-2	2	1	1	3	2	0	2
Differentially HYPOmethylated genes after 1 day upon DCA - with Naive 3 or 2 - 4 Genes																				
72685	Dnajc6	2	2	-2	3	1	3	3	1	3	0	2	-5	1	1	-1	3	2	0	2
140703	Emid1	2	2	-2	3	2	0	3	2	0	0	2	-5	3	1	3	3	2	0	3
231290	Slc10a4	2	2	-2	2	2	-2	1	1	-1	0	2	-5	1	1	-1	2	2	-2	2
22414	Wnt2b	2	0	4	1	0	2	2	0	4	0	2	-5	1	1	-1	0	1	-3	2
Differentially HYPOmethylated genes after 3 days upon DCA - with Naive 3 or 2 - 2 Genes																				
11550	Adra1d	1	1	-1	3	0	5	1	0	2	1	1	-1	0	2	-5	1	2	-4	2
56274	Stk3	3	2	0	3	1	3	1	0	2	1	1	-1	0	2	-5	2	2	-2	2
Differentially HYPOmethylated genes after 7 days upon DCA - with Naive 3 or 2 - 2 Genes																				
67808	Tprgl	1	1	-1	2	2	-2	2	2	-2	3	2	0	3	1	3	0	2	-5	3
320538	Ubn2	2	1	1	2	1	1	2	1	1	1	1	-1	3	1	3	0	2	-5	2

differentially hypermethylated genes could have the following values: SNA 3-0 (MV = +5), DCA: 0-0 or 0-1 (MV = -0 or -3), and a differentially hypomethylated gene: SNA: 0-2 (MV = -5), DCA: 3-2 or 3-1 (MV = +0 or +3). Less strict requirements for the sham of the opposite injury type were exceptionally allowed due to sample variability and the higher emphasis on the methylation levels of the injury samples microarrays. Applying this filter, 46 DM genes were identified and listed in **Table 2**. Altogether, 27 differentially hypermethylated genes were found upon SNA (15) and DCA (12), respectively, and 19 differentially hypomethylated genes were identified for SNA (11) and DCA (8), respectively. Some of the identified genes were not yet characterized and were only represented by a numerical ID (RIKEN Mouse Encyclopedia Index; Riken-MEI). Genes highlighted in blue were annotated for the two functional categories of special interest: ‘Transcription or Chromatin’ and ‘(Neural) Development, Differentiation or Cell Cycle’.

2.1.6 Gene expression levels of differentially methylated genes correlated with the promoter methylation status

Relative mRNA expression of most differentially (DM) methylated genes from the microarray analysis was assayed in order to test the hypothesis that injury-induced gene promoter hypermethylation would correlate with decreased mRNA expression, and vice versa for hypomethylated genes (**Table 2**). For this part of the study, a commercial Custom TaqMan Gene Expression Array (Applied Biosystems (ABS)/Life Technologies) was applied for 38 of the 46 genes, based on quantitative real-time PCR (qRT-PCR). Excluded genes were labeled in *italic*. Genes that have relevant functions in the nervous system, or particularly in the context of axonal regeneration, were highlighted in blue in this table. *Actb* and *Gapdh* as reference

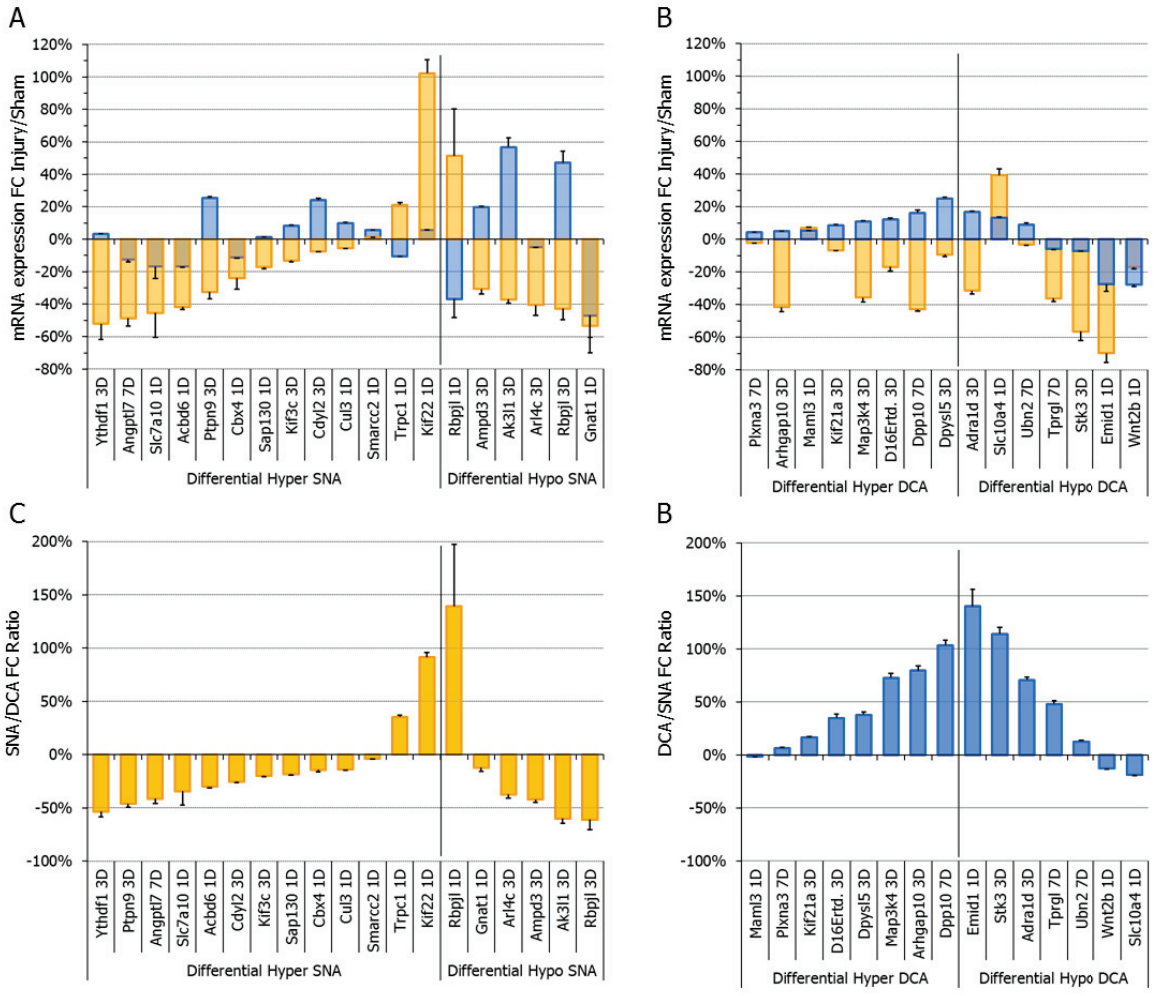

Figure 16 – Relative mRNA expression of differentially methylated genes upon SNA or DCA did correlate with the differential methylation status but not as a general rule. For most differentially methylated (DM) genes, mean mRNA expression was detected for the relevant time point for SNA and DCA samples (injury and sham; mean). According to the hypothesis, hypermethylated genes are supposed to be downregulated and, vice versa, hypomethylated genes upregulated. A stronger fold change expression was expected for the injury type causing hyper- or hypomethylation. **(A)** Relative gene expression of differentially hyper- or hypomethylated genes upon SNA (injury/sham fold change (FC), upon SNA: orange, upon corresponding DCA: blue). **(B)** Relative expression (FC) for differentially hyper- or hypomethylated genes upon DCA. **(C+D)** SNA/DCA FC ratio was calculated from individual FC ratios for each gene. A Custom TaqMan Gene Expression Array (Applied Biosystems) was applied based on qRT-PCR with all samples from n = 3 mice, in triplicates, Error bars: SEM.

genes, and 18s rRNA as internal loading control were detected in parallel. For each gene, the sample set of the 4 main conditions (SNA/DCA, injury/sham) was measured in triplicate only for the specific time point of observed differential methylation. The results of the TaqMan Gene Expression Array, grouped for the main conditions, are graphed in **Figure 16** that shows percentaged up- or downregulation of the selected genes upon SNA or DCA injury compared to sham. The fold changes of relative gene expression were arranged in a way to highlight the relevant condition and sorted according to the best fit to the hypothesis. Most of the differentially hypermethylated genes upon SNA were downregulated or unregulated upon SNA, partly according to the hypothesis (for example, *Ythdf1*, *Angptl7*, *Slc7a10*, *Acbd6*, *Ptpn9*, *Cbx4*, *Sap130*, and *Kif3c*). Exceptions were *Trpc1* and *Kif22*. The corresponding relative expression levels of the aforementioned genes varied upon DCA. However, most of the examined differentially hypomethylated genes upon SNA were downregulated, except *Rbpjl*. Upon DCA, differentially hypermethylated genes were not regulated or marginally upregulated, not supporting the hypothesis. Nevertheless, some hypomethylated genes upon DCA were upregulated (*Adra1d*, *Slc10a4*, and *Ubn2*), as would have been expected, while others were downregulated (*Tprgl*, *Stk3*, *Emid1*, and *Wnt2b*).

Since DNA methylation is not the only regulation mechanism in response to nerve injury, the ratio of mRNA expression fold changes (FC) upon SNA and DCA revealed the relative contribution of this epigenetic mechanism. For DM genes upon SNA, the SNA-to-DCA FC ratio was thus calculated, and vice versa the DCA-to-SNA FC ratio for DM genes upon DCA (**Figure 16 C and D**). Genes were arranged again according to the FC ratio ranking correspondingly to the hypothesis. Altogether, the relative effects were stronger although still several genes did not exhibit the hypothesized correlation between the differential methylation status and mRNA expression upon injury. Additional qRT-PCR experiments for DM gene expression have been performed with self-designed primers to confirm the TaqMan Gene Expression Array data (data not shown). Of note, many of the aforementioned genes were not amongst the (differentially) hyper- or hypomethylated genes. These were either unmethylated or exhibited a variable weak methylation status across conditions. The methylation status of a relevant selection of such genes determined by microarray analysis is shown in **Table S3**.

2.1.7 Gene expression of regeneration-associated genes following nerve injury

Several major RAGs are induced upon SNA although their promoter methylation status was largely inconspicuous. RAG expression was assessed by qRT-PCR in this study, also serving as control for successful surgeries and for the initiated regeneration in the DRG model. RAG expression levels were detected for both injury types (SNA or DCA) after 1, 2, 3 or 7 days following injury or corresponding sham. Injury-to-sham FC ratios of these genes were graphed comparatively in **Figure 17**. RAGs were either dramatically induced after 1 or 2 days following SNA but not upon DCA (*Sprr1a*, *Gap43*, *Gal*, *Bdnf*, *Chl1*), or they showed only marginal or no changes for each injury type (*Stmn2*, *Basp1*, *Lgals1*, *L1cam*).

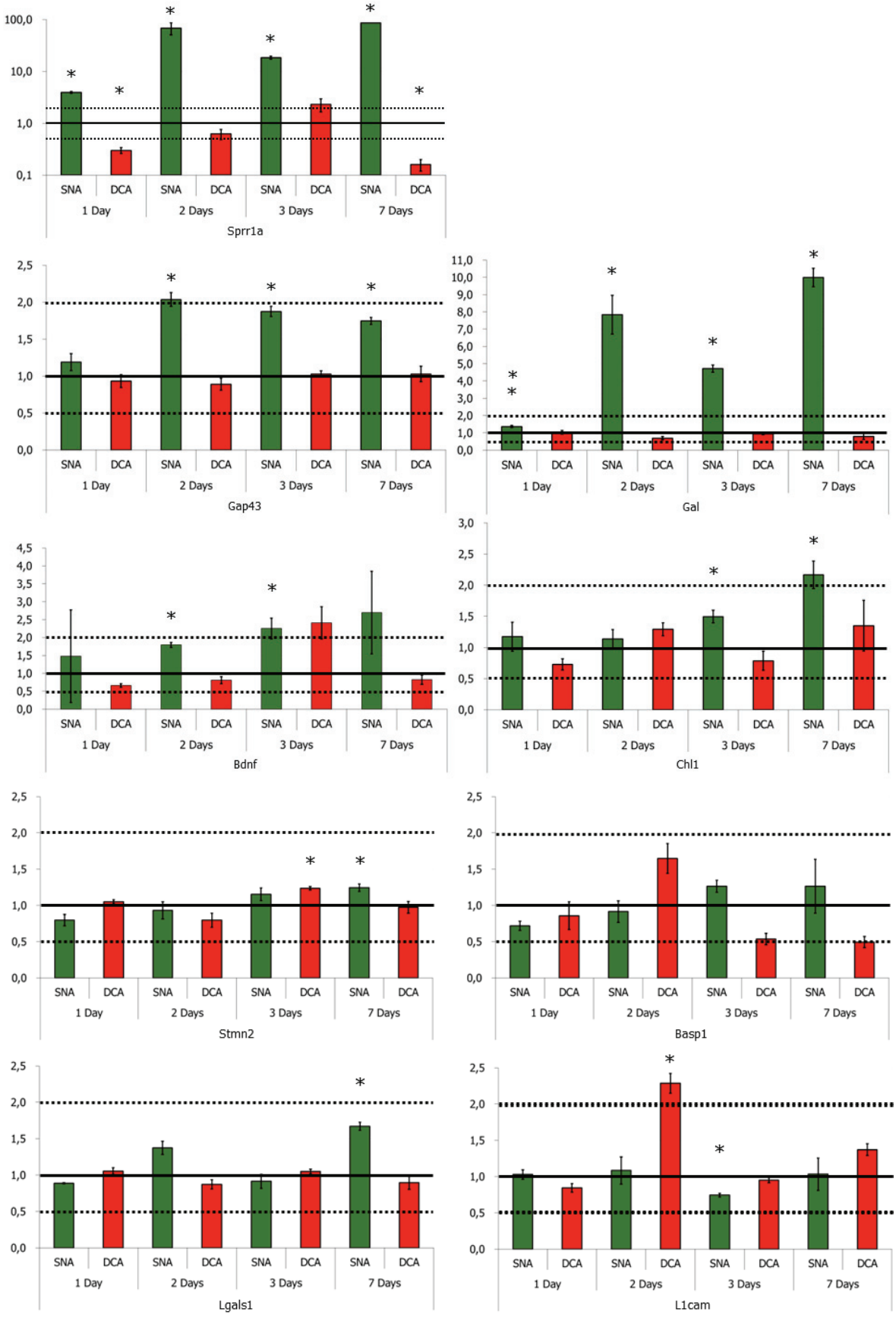
Sprr1a
Gap43
Gal
Bdnf
Chl1
Stmn2
Basp1
Lgals1
L1cam
SNA
DCA
1 Day
2 Days
3 Days
7 Days

Figure 17 – Relative mRNA expression of regeneration-associated genes (RAGs) was quantified for a time course from 1 to 7 days post-injury verifying successfully applied injuries. 5 RAGs (*Sprr1a, Gap43, Gal, Bdnf,* and *Chl1*) were considerably induced upon SNA but rather unchanged or decreased upon DCA. Another 4 RAGs (*Stmn2, Basp1, Lgals1,* and *L1cam)* were marginally induced upon SNA. Detection occurred quantitatively by qRT-PCR as mean of n = 3, in triplicate. Significant FC ratios indicated by "*". Error bars: SEM. qRT-PCR was conducted by the author (1, 3, 7 days) or by Dr. Elisa Floriddia (2 days).

Because of the outstanding gene expression changes of *Sprr1a* (Small proline-rich protein 1a) upon SNA, mRNA expression of further members of the whole *Sprr* gene family was investigated. Best characterized is *Sprr1a* that is known as the cross-linked envelope protein of keratinocytes in cornifying epithelia but also in various other epithelia. However, at least *Sprr1a* was already described in the context of axon regeneration although, else, *Sprr* genes have been rarely linked at all to functions in neuronal tissues [Kartasova *et al.* 1996; Bonilla et al. 2002; Starkey et al. 2009]. Sprr genes are closely co-localized in a gene cluster with the subgroup of *Sprr2a* to *Sprr2k* located on the coding strand and *Sprr1a*, *Sprr2b*, *Sprr3*, and *Sprr4* on the complementary strand. Therefore, injury-induced gene expression of all *Sprr* genes along the time course was measured in this study, which has not been investigated in this context before, besides for *Sprr1a*. Some of these genes exhibited expression profiles similar to *Sprr1a* with highest fold changes at 3 days (*Sprr2h* to *Sprr2k*) or already after 1 day following SNA (*Sprr2g*). *Sprr1a* and *Sprr2a* were expressed highest after 7 days. Other fami-

A

		1 day post-injury		3 dayspost-injury		7 dayspost-injury	
Gene ID	Gene	SNA	DCA	SNA	DCA	SNA	DCA
20753	**Sprr1a**	**3.9**	-3.3	**68.6**	-1.6	**86.1**	-6.3
20755	**Sprr2a**	**5.8**	3.1	**6.2**	-1.6	**11.6**	-3.4
20761	**Sprr2g**	**70.3**	-1.7	**23.0**	-1.1	**14.9**	-3.4
20762	**Sprr2h**	**4.7**	1.7	**42.5**	1.4	**21.0**	-4.2
20763	**Sprr2i**	**5.1**	-4.2	**58.8**	-2.8	**14.7**	-10.8
20764	**Sprr2j**	**16.5**	-1.1	**23.9**	1.2	**14.8**	-2.6
20765	**Sprr2k**	**5.8**	-1.1	**30.7**	1.3	**21.6**	1.2

B

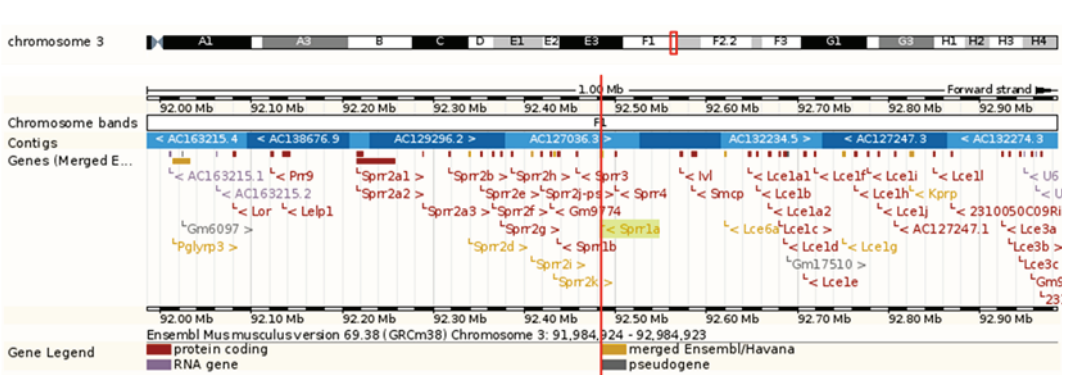

Figure 18 – *Sprr* gene family members were analyzed for relative mRNA expression upon SNA or DCA.
(A) Most of the 14 members in mouse had an increased injury-to-sham fold change (FC) gene expression (mean) only upon SNA, as already known for *Sprr1a*. Time points for highest fold change expression are indicated in red. *Sprr1b*, *Sprr2b*, *Sprr2d* to *Sprr2f*, *Sprr3*, and *Sprr4* did not show increased expression levels in L4-L6 DRG for any condition with the applied primers. Detection by qRT-PCR with n = 3, in triplicates. **(B)** *Sprr* genes are co-localized in a gene cluster on Chr 3 whereby *Sprr1a*, *Sprr1b*, *Sprr3*, and *Sprr4* are coded on the complementary strand. In proximity to this cluster, also *Sprr-like* genes (late cornified-envelope; *Lce*) are located indicating differential functions of the extended *Sprr* gene family members.

ly members (*Sprr1b/2b/2d/2e/2f*) either did not show dramatic upregulation or were not properly detectable with the applied primers. *Sprr* genes were prominently upregulated only upon SNA injury compared to very low levels in shams and only moderate changes upon DCA, suggesting a literally switched-on gene expression (qRT-PCR results summarized in **Figure 18**). Expression of *Sprr-like* (*Lce*) gene family members was not examined in this study. However, none of the *Sprr* genes exhibited any significant DNA methylation in the microarray dataset (exemplarily for *Sprr1a* in **Table S3**).

2.1.8 CpG island analysis of regeneration-associated genes and of differentially methylated genes

In addition to the genome-wide DNA methylation analysis via MeDIP-chip, and to gene expression analysis for RAGs and differentially methylated genes, it was interesting to test if the promoter CpG distribution of the investigated genes would correlate with these results. Thereby, analyzing the CpG dinucleotide content and density, the presence, positions, and sizes of CpG islands (CGIs) should help to understand the relations between sequence structure, DNA methylation patterns, and their influence on gene expression upon nerve injury. CGIs are regions with a high CpG density displaying a non-random accumulation of CpGs, often located in the proximal promoter region close to the TSS. A high promoter CpG content (and high CpG density) usually inversely correlates with low levels of DNA methylation and active gene expression. Specifically, promoters with larger CpG islands are mostly unmethylated. Else, low CpG content promoters exhibit more often methylated CpGs at lower density [Caiafa & Zampieri 2005; Saxonov et al. 2006; Deaton & Bird 2011].

15 selected major RAGs, 18 DM genes identified by MeDIP-chip in this study, and 2 housekeeping genes (*Actb* and *Gapdh*) were analyzed with the EMBOSS CPGPlot online tool from EMBL-EBI to detect promoter CGIs. The murine genomic sequences, extended by the 5 kb promoter region upstream of the TSS, were obtained from the Ensembl genome browser (www.ensembl.org). The graphical CGI analysis output of the CPGPlot online tool is exemplarily demonstrated for the *Gal* gene in **Figure 19 B**. The detailed analysis list can be viewed in **Table S4**. To identify CpG islands with CPGPlot, standard parameters for the classical CGI definition (“NCBI relaxed”; see Introduction) were applied requiring a minimum size of 200 bp. Multiple CGIs in very close proximity to each other were combined to one larger CGI. In certain cases, CGIs between 100 bp and 200 bp of length were considered as still significant and were included if it seemed appropriate. Such small CGIs in the proximal promoter region might still be involved in transcriptional regulation if co-located with relevant transcription factor binding sites, for example. Thereby most genes exhibited either one CGI (7/15 RAGs, 5/18 DM genes), or more than one CGI (7/15 RAGs, 13/18 DM genes) larger than 200 bp, usually close to the TSS. Exceptions were *Sppr1a* without CGI and *Gap43* with only a combined CGI close to the TSS. The proportion of investigated genes with CGIs was high compared to about 50 to 60 percent of annotated genes described for the murine genome

(about 70 percent in human) [Antequera & Bird 1993; Saxonov et al. 2006]. Of note, the official translation start site (Ensemble) was often located quite distant from the TSS and correlated in part well with CGI positions. For example, the translation start sites of most genes were located up to several hundred to 1,500 bp downstream of the TSS, for some of them between 1.5 kb and up to 11 kb (*L1cam*, *Lif*, *Matn4*, *Sap130*, *Trp53*), and for a few even up to 130 kb (*Basp1*, *Bdnf*, *Chl1*). These facts complicated the CGI analysis. Taken together, many CGIs were found rather close (within 1.5 kb) to the TSS. Most (combined) CGIs were significantly larger than the defined minimum size of 200 bp and ranged from 210 bp to 2,260 bp. The accumulated size for all CGIs associated with a single gene was in average higher for DM genes (1,939 bp) than for RAGs (1,524 bp). Overall, CGIs larger than 200 bp had an average size of 642 bp (single and combined CGIs; RAG mean: 542 bp, DM mean: 709 bp). Of note, some genes exhibited no CGIs larger than 200 bp in close proximity to the TSS. Specifically for several RAGs, a larger CpG island was only identified about 1,200 bp downstream of the TSS (*Calca*, *Chl1*, and *Lgals1*) or even 9 kb downstream of the TSS (*Lif*). Additionally, the DM genes *Gnat1* and *Rbpjl* only exhibited CGIs larger than 200 bp outside of a proximal region around the TSS (1,000 bp). If applying the more recently proposed "NCBI strict" parameters for CGI identification, that require a minimum size for CpG islands of 500 bp instead of 200 bp (Introduction), several genes would not exhibit large enough promoter CGIs close to the TSS anymore. Amongst the excluded genes are the RAGs *Calca*, *Chl1*, *Gal*, *Gap43*, *L1cam*, *Lgasl1*, *Stmn2*, *Tnfrst12a*, as well as some DM genes (*Emid1*, *Kif3c*, *Kif22*, *Rbpjl*). According to this scenario, still 6/15 RAGs and 12/18 differentially methylated genes possess at least one CGI of at least 500 bp size, disregarding the frequent discrepancy between the positions of TSS and translation start site.

In addition to the sizes and positions of CGIs, genes of both groups were analyzed according to their normalized CpG value (**Figure 19 A**), as already performed genome-wide by Saxonov et al. The normalized CpG value thereby is the observed-to-expected (obs/exp) CpG ratio for the 3 kb region symmetrically around the TSS. This region usually shows highest concentrations of CpG dinucleotides and allows a categorization into genes with high and low promoter CpG content [Saxonov et al. 2006]. The distribution of normalized CpG values for the complete set of analyzed genes roughly matched the genome-wide results. Differentially methylated genes exhibited in average higher normalized CpG values than known major RAGs (DM mean: 0.578, RAG means: 0.374). Thereby, differentially hypermethylated genes had the highest values (mean 0.650, ranging from 0.439 to 0.813) compared to differentially hypomethylated genes (mean 0.490, from 0.366 to 0.682). Slight differences were also found for the subset of 9 RAGs whose injury-induced gene expression was measured in this study. Strongly regulated RAGs (*Sprr1a*, *Gal*, *Gap43*, and *Bdnf*) had lower obs/exp CpG ratios (mean 0.310, from 0.041 to 0.561) than the moderately induced RAGs *Lgals1*, *L1cam*, *Stmn2*, *Chl1*, and *Basp1* (mean 0.425, from 0.302 to 0.724).

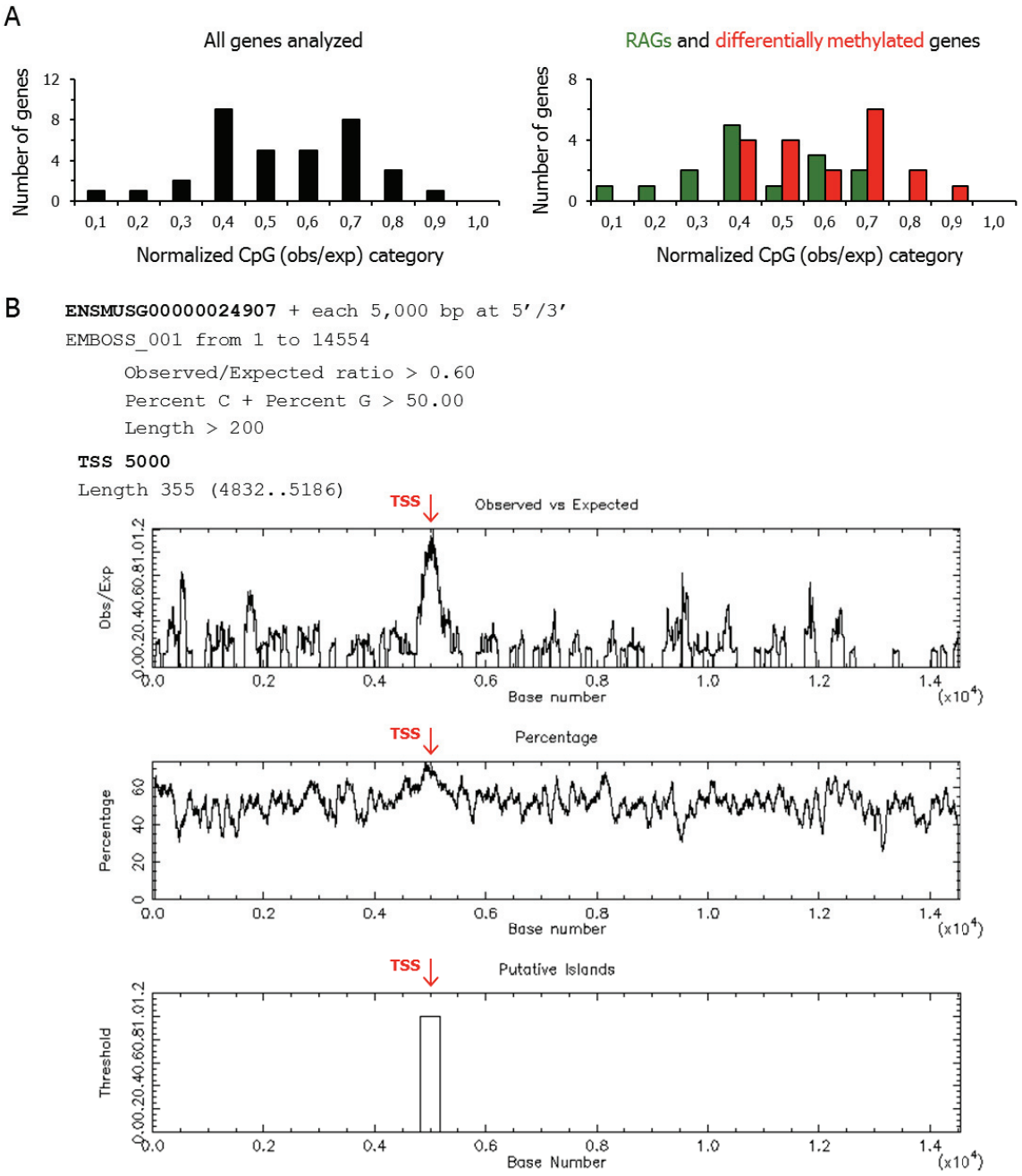

Figure 19 – CpG island (CGI) analysis for major regeneration-associated genes (RAGs) and differentially methylated (DM) genes. For 15 RAGs, 18 DM genes, and 2 housekeeping genes, the genomic sequences (obtained from Ensembl genome browser) were analyzed, including the 5 kb promoter region upstream of the TSS. Almost all genes exhibited one or more CGIs, usually within the proximal (promoter) region or around the TSS, except *Sprr1a*. **(A)** Analyzed genes were categorized according to their normalized CpG value calculated as the obs/exp ratio of the 3 kb region around the TSS, according to [Saxonov et al. 2006]. Either all genes were graphed together (left) or separately for RAGs and DM genes (right). **(B)** Exemplary graphical CGI analysis for *Gal* with a CGI around the TSS (position 5,000). Standard parameters were applied for CGI analysis (obs/exp ratio > 0.6; G+C content > 50 %; size > 200 bp, exceptionally 100 bp). The detailed CGI analysis list for all selected genes can be viewed in **Table S4**.

2.2 Involvement of gene promoter histone modifications in axonal regeneration

2.2.1 Gene promoter H3-K9 acetylation and dimethylation were differentially regulated upon SNA or DCA

The experiments within this chapter were performed by Dr. Radhika Puttagunta [Puttagunta et al. (under revision)] and by Dr. Elisa Floriddia from the author's research group. In addition to DNA methylation, specific histone modifications at gene promoters are important for gene expression regulation and chromatin remodeling, and potentially for RAG regulation upon nerve injury. Different types of histone acetylation and methylation are known to be involved in either gene activation (H3-K9ac, H3-K18ac, and H3-K4me2) or repression (H3-K9me2 and H3-K27me3). Specifically, H3-K9/K14ac correlates with a rather relaxed and transcription-permissive state of chromatin and activation of transcription, whereas H3-K9me2 is rather associated with inactive, condensed chromatin and gene repression [Nakayama *et al.* 2001; Z Wang et al. 2008]. Both modifications of the same histone tail residue might compete with each other. Global H3-K9/K14 acetylation and H3-K9 dimethylation were examined by Western Blot analysis of L4-L6 DRG of each 3 mice per condition after 1 day following either SNA or DCA, or corresponding shams. Overall H3-K9me2 levels were lower than H3 K9/K14ac levels. However, only moderate global changes of either modification were observed for SNA or DCA, usually higher upon injury compared to sham (**Figure 20**).

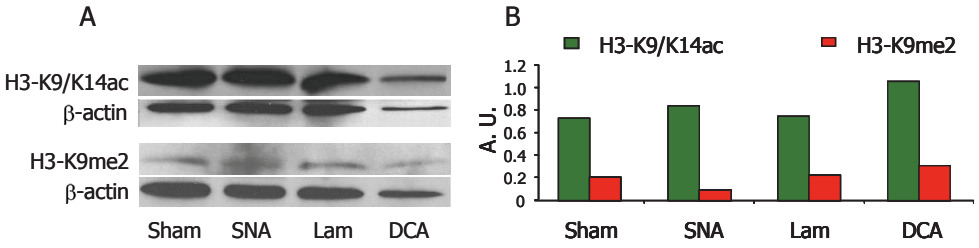

Figure 20 – Detection of global histone-3 lysine-9/14 acetylation (H3-K9/14ac) or dimethylation (H3-K9me2) by Western Blot analysis of L4-L6 DRG from each 3 mice after 1 day following SNA or DCA injury, sham or laminectomy (Sham/Lam), respectively, **(A)** and quantified by densitometry analysis normalized to beta-Actin (GelPro32 software) **(B)**. A.U. = arbitrary units. Immunoblot data was contributed by Dr. Elisa Floriddia for n = 3 mice in triplicates, representative blot.

Despite only moderate global changes of the selected histone modifications upon injury, potentially, local changes at specific gene promoters might be important and more dynamic. Following nerve injury, a complex pattern of gene expression is initiated with a differential regulation of RAGs. This is likely associated with oppositional changes of local histone acetylation or methylation patterns that might have only moderate effects on average global changes. Chromatin immunoprecipitation (ChIP) was utilized to investigate the local abundance of H3-K9 acetylation or dimethylation at the proximal promoter regions of major RAGs. Therefore, all L4-L6 DRG from each 6 mice were pooled for each ChIP experiment after 1 day following SNA or DCA, and enrichment of occupied promoter fragments was detected by qRT-PCR. Cross-linked chromatin was sonicated to a fragment size range of approximately 200 to 1,500 bp, and ChIP was performed using 2 antibodies specifically

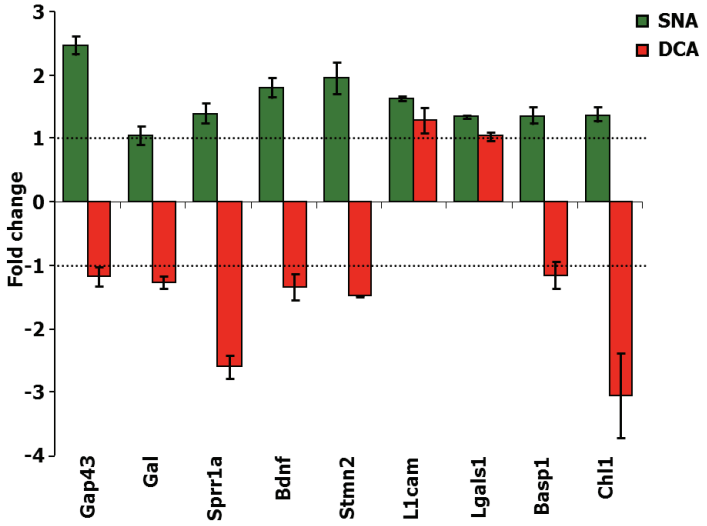

Figure 21 – Chromatin immunoprecipitation (ChIP) for H3-K9ac occupancy of RAG proximal promoters revealed increased acetylation for major RAGs after SNA but diminished levels after DCA. Mean injury-to-sham fold change enrichment (IP-to-input ratio) was calculated for both injury types after 1 day post-injury. Highest increase of H3-K9ac was found for *Gap43*, *Bdnf*, and *Stmn2* upon SNA. Highest decrease was found for *Chl1* and *Sprr1a* upon DCA. ChIP was performed on L4-L6 DRG chromatin from 6 mice and qRT-PCR was performed in triplicate targeting proximal promoter regions. Error bars: SEM. ChIP data was contributed by Dr. Elisa Floriddia.

targeting either H3-K9ac or H3-K9me2. Extracted DNA from immunoprecipitated (IP) samples was compared to chromatin input samples (Input) and negative controls (no Ab). A high IP-to-Input signal ratio (regarding no-Ab control) indicated high enrichment of the specific modification. Calculating the individual injury-to-sham fold change enrichment ratios yielded a quantitative measure for an increased or decreased presence of the given modification at a certain gene promoter. All investigated RAGs (*Gap43*, *Gal*, *Sprr1a*, *Bdnf*, *Stmn2*, *L1cam*, *Lgals1*, *Basp1* and *Chl1*) had increased H3-K9ac levels upon SNA, with highest injury-to-sham fold change enrichment for *Gap43*, *Stmn2*, and *Bdnf* (**Figure 21**). In contrast, promoter occupancy of the same modification was, by trend, decreased or not significantly changed upon DCA for all RAGs (highest decrease for *Chl1* and *Sprr1a*).

In contrast to H3-K9ac, proximal promoter H3-K9me2 occupancy decreased, by trend, for most RAGs upon SNA, except *Sprr1a* and *Bdnf* (**Figure 22**). Upon DCA, most RAG promoters exhibited slightly elevated levels of H3-K9me2 upon injury compared to laminectomy sham. Although some RAGs exhibited slightly decreased H3-K9me2 upon DCA, the negative fold change enrichment was significantly higher upon SNA compared to DCA (*Gap43*, *Gal*, and *Lgals1*). Additionally, the semaphorin receptor gene *Nrp1* was analyzed for which H3 K9ac enrichment could not be reliably measured. While most of the analyzed RAGs followed the trend of decreased promoter H3-K9me2 upon SNA (and increased upon DCA), *Sprr1a* showed the opposite trend. This might be associated with its exceptional CpG promoter distribution or gene expression compared to other RAGs. For several genes such as *Bdnf*, *L1cam*, or *Basp1*, H3-K9m2 levels were not significantly regulated.

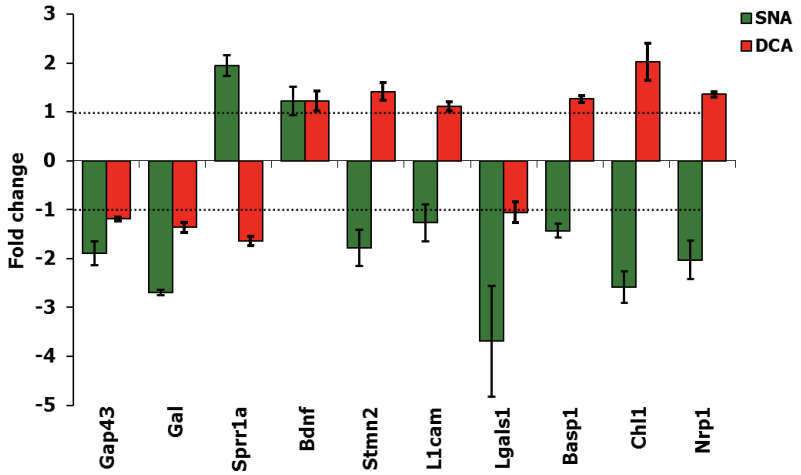

Figure 22 – Chromatin immunoprecipitation (ChIP) for H3-K9me2 occupancy of RAG proximal promoters. Mean injury-to-sham fold change enrichment values were calculated from ChIP IP-to-Input ratios after 1 day post-injury. Upon SNA injury, most RAG promoters were less enriched for H3-K9me2 compared to sham, except *Sprr1a* and *Bdnf*. In contrast, promoter occupancy of H3-K9me2 was slightly increased or showed no significant difference upon DCA. ChIP was performed on L4-L6 DRG chromatin from 6 mice for each condition, and qRT-PCR was performed in triplicate. Error bars: SEM. ChIP data was contributed by Dr. Elisa Floriddia.

2.2.2 PCAF enhanced neurite outgrowth, RAG expression, and H3-K9 acetylation of cultured DRG or cerebellar granule neurons (CGN)

The experiments and results of this chapter were partly prepared by the author but essentially performed and analyzed by Dr. Radhika Puttagunta from our research group.

In order to test if the manipulation of H3-K9 promoter acetylation might induce RAG expression in conditions similar to DCA, dissociated DRG neurons from naive mice (6 to 8 weeks) were cultured on two different substrates, either on axon growth permitting laminin or inhibitive rat CNS myelin. Laminins are collagen-like glycoproteins that are part of the extracellular matrix and basal laminas, relevant for cell-cell contacts. CNS myelin was extracted from rat spinal cord and served as regeneration inhibiting substrate. Cultured DRG neurons were infected with either control GFP-AAV or PCAF-GFP-AAV to overexpress the acetyltransferase for H3-K9. Neurite outgrowth was measured after 48 hours following AAV infection after immunofluorescence staining using the Neurolucida software. Infection efficiency and successful transgene expression was verified by visualization of the GFP reporter. Additionally, DRG neurons were stained for a marker of differentiated neurons, the neuronal class III beta-tubulin (TUJ1/TUBB3), and nuclei were stained with DAPI (**Figure 23 A**). As already known, only little neurite outgrowth occurs on myelin compared to laminin. However, with PCAF overexpression but not with GFP control, a robust regeneration response was observed. The length of longest neurites was dramatically increased more than 3-fold on laminin. Intriguingly, neurite outgrowth is also significantly enhanced almost 2-fold on inhibitory myelin compared to GFP control, although to a lesser extent than on laminin (**Figure 23 B**). Increased neurite sprouting and axonal regeneration upon PCAF overex-

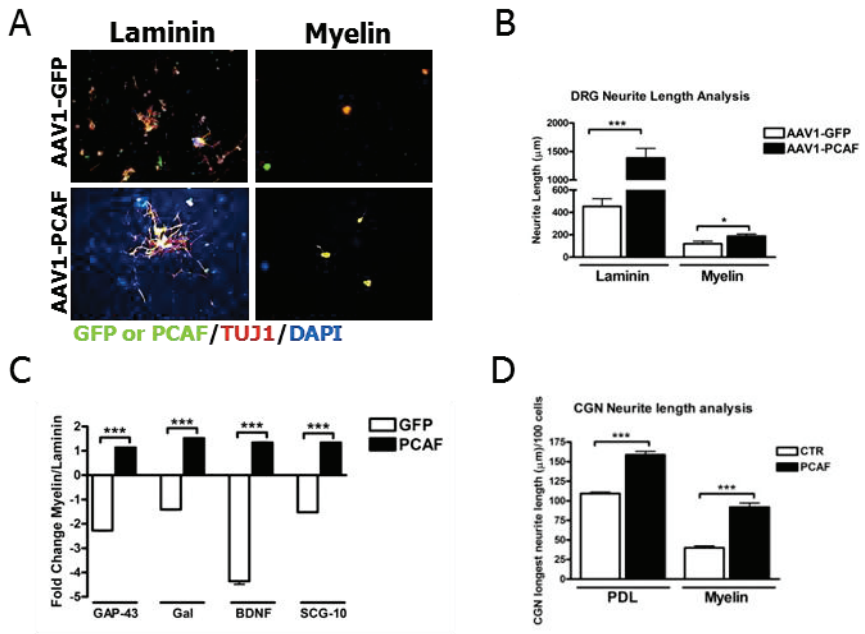

Figure 23 – Enhanced neurite outgrowth and increased RAG expression upon PCAF overexpression in dissociated DRG neurons. (A) Immunocytochemistry for dissociated DRG neurons from naive mice (6 to 8 weeks) on growth promoting laminin or inhibiting rat CNS myelin upon infection with PCAF-GFP-AVV or GFP-AAV control. Staining for neuronal marker TUJ1 (TUBB3) and DAPI. **(B)** Neurite outgrowth analysis resulted in a significant increase of neurite length on both substrates upon PCAF overexpression compared to GFP control. Counted in triplicate with 50 neurons each, analysis with Neurolucida software. **(C)** Normalized mean myelin-to-laminin fold changes revealed inhibitory myelin-dependent reduction in RAG expression, which was restored by PCAF overexpression detected 48 hours post-AAV infection. qRT-PCR in triplicate. **(D)** Similar to (B): longest neurite length of cerebellar granule neurons (CGN) on permissive PDL or myelin was increased upon PCAF overexpression compared to GFP control. Final experiments and analysis were performed by Dr. Radhika Puttagunta [Puttagunta et al. (under revision)]. For all experiments: n = 3 mice (6 to 8 weeks). Error bars: SEM.

pression was accompanied by equally increased mRNA expression levels of the RAGs *Gap43*, *Gal*, *Bdnf*, and *Stmn2* (*Scg10*) on myelin and laminin (**Figure 23 C**). In addition to cultured DRG neurons, cerebellar granule neurons (CGN) were cultured on axon outgrowth promoting poly-D-lysine (PDL), or on rat CNS myelin. The cell soma of CGN is located within the CNS, unlike for DRG neurons. Therefore, these cells show limited neurite outgrowth *in vivo* and on myelin *in vitro*. Upon infection with PCAF-GFP-AAV, compared to GFP control, longest neurites grew more than 50 percent longer on PDL and about 2.5-fold longer on myelin, almost reaching the values of CGN cultured on PDL without PCAF expression (**Figure 23 D**).

Western Blot analysis showed a decreased abundance of H3-K9ac in CGN plated for 24 hours on myelin compared to PDL (**Figure 24 A and B**). ChIP for H3-K9ac was performed on CGN cultured on PDL or myelin after 48 hours following infection with either PCAF-GFP-AAV or GFP-AAV control. The proximal promoter H3-K9ac occupancy of the RAGs *Gap43*, *Bdnf*, *Gal*, and *Stmn2* (*Scg10*) was assessed. All tested RAGs showed a dramatically lower H3-K9me2 promoter occupancy when CGN were cultured on myelin compared to PDL, in particular *Gap43*. With PCAF overexpression, H3-K9ac enrichment on myelin was restored

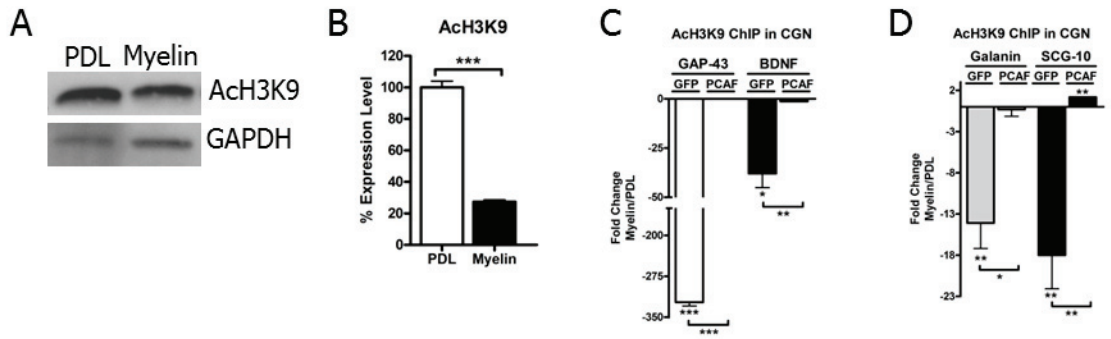

Figure 24 – Total H3-K9ac levels and local RAG promoter H3-K9ac occupancy in cultured CGN were decreased on CNS myelin but restored by PCAF overexpression. CGN were cultured on PDL or CNS myelin for 24 hours. **(A+B)** Total H3-K9ac levels were detected by Western Blot and quantified as expression levels normalized to GAPDH, comparing myelin and PDL (GelPro32 software). **(C+D)** H3-K9ac chromatin immunoprecipitation (ChIP) was performed for CGN infected with PCAF-GFP-AAV or GFP-AAV control. Mean proximal promoter H3-K9ac occupancy for the RAGs *Gap43*, *Bdnf*, *Gal*, and *Stmn2* (*Scg10*) was significantly lower on myelin compared to PDL (by qRT-PCR in triplicate). Upon PCAF overexpression but not GFP control, H3-K9ac levels on myelin were restored to levels comparable to PDL. All experiments were performed with n = 3 mice (6 to 8 weeks). Error bars: SEM. Experiments and final analysis were performed by Dr. Radhika Puttagunta [Puttagunta et al. (under revision)].

to levels on PDL (**Figure 24 C and D**). Finally, CGN cultured on PDL were treated 24 hours with 5 µM Garcinol, a potent natural inhibitor of histone acetyltransferases EP300 and PCAF [Balasubramanyam *et al.* 2004]. Neurite outgrowth was assessed for treated CGN compared to untreated controls after staining for H3-K9ac, TUJ1, and with DAPI. Garcinol treatment caused a 2-fold reduction of average neurite length (**Figure 25 A and B**). Further, a *Gap43*-proximal promoter luciferase construct was transfected into cultured CGN showed reduced luciferase reporter expression after 24 hours treatment with 5 µM Garcinol (**Figure 25 C**).

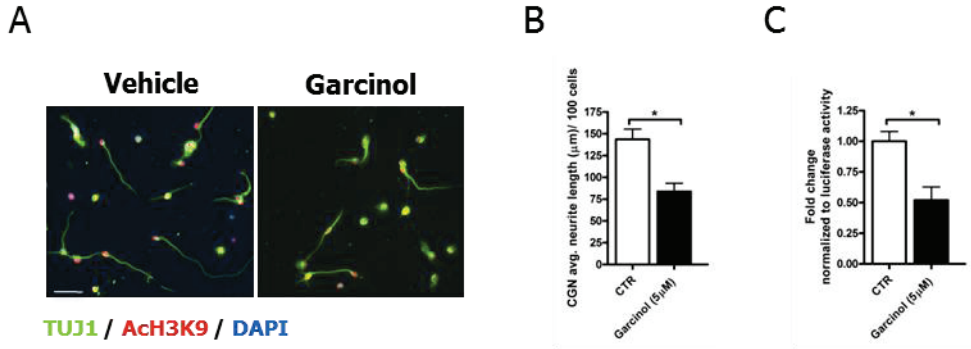

Figure 25 – Reduced regenerative neurite outgrowth of CGN cultured on PDL upon treatment with PCAF inhibitor Garcinol. (A+B) Immunofluorescence staining of cultured CGN for H3-K9ac, TUJ1 (TUBB3), and with DAPI revealed almost 2-fold decreased average neurite lengths upon treatment with 5 µM Garcinol. **(C)** A *Gap43*-proximal promoter luciferase construct showed decreased luciferase reporter expression after 24 hours treatment with Garcinol. Errors bars: SEM. Experiments and analysis were performed by Dr. Radhika Puttagunta [Puttagunta et al. (under revision)].

3. Discussion

3 Discussion

3.1 Summary of Results

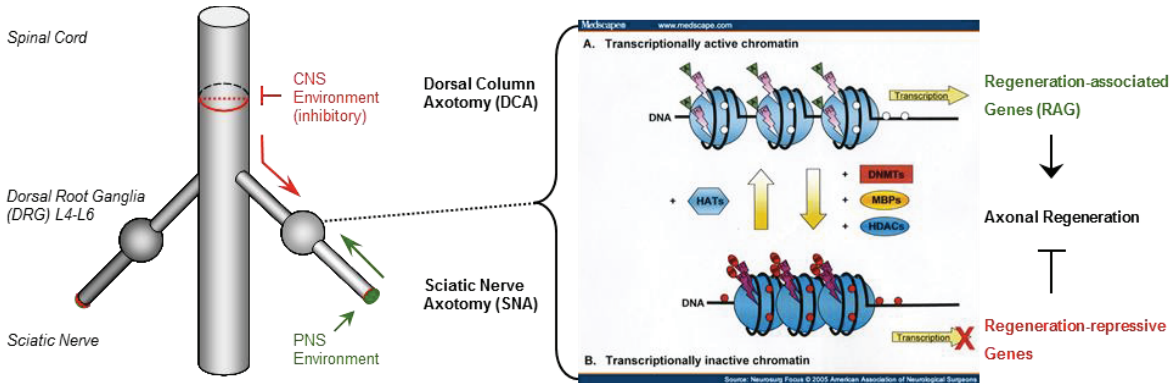

Figure 26 – Schematic of the nerve injury model and of the hypothesized epigenetic regulation of RAG expression. Mouse dorsal root ganglia (DRG) were chosen as a suitable model of axonal regeneration following peripheral or central nerve injury. The correlation of regeneration-associated gene expression with promoter DNA methylation or H3-K9ac/me2 promoter occupancy was investigated to identify an epigenetic influence on axonal regeneration. Right part of the figure from www.medscape.com, Neurosurg Focus 2005

The purpose of this study was to elucidate the role of epigenetic mechanisms for the regulation of axonal regeneration-associated genes (RAGs) following peripheral sciatic nerve axotomy (SNA) as compared to central dorsal column axotomy (DCA). Successful axonal regeneration is usually only successful in the peripheral system and associated with the expression of RAGs but not upon central lesion. According to the hypothesis, differential changes of the gene expression pattern upon either injury type were expected to be associated with corresponding changes of the epigenetic code. Specifically, DNA hypermethylation of gene promoters would correlate with downregulation of RAGs, and hypomethylation with upregulation. Furthermore, acetylation and dimethylation of histone-3 lysine-9 (H3-K9ac or H3-K9me2) might be associated with injury-induced RAG expression (**Figure 26**). Mouse dorsal root ganglia (DRG) were used as a suitable *in vivo* model for axon regeneration that allows the investigation of effects and differential responses to both types of nerve lesion within the same neurons. After 1, 3, or 7 days following either SNA or DCA in young adult mice injury-induced changes of promoter-bound epigenetic marks were assayed and correlated to gene expression changes associated with axon regeneration. Methylated DNA was assayed MeDIP-chip for a genome-wide promoter and CpG island (CGI) methylation analysis. 179 hyper- or hypomethylated genes and 46 differentially methylated (DM) genes for a specific injury type were identified for all conditions. Several of these genes were associated with functions in chromatin remodeling, transcription regulation, or neural development or differentiation. For a subset of the DM genes, gene expression changes upon injury correlated with the methylation status, although not as a general rule. Expression of known major RAGs such as *Gap43*, *Sprr1a*, and *Bdnf* was verified to be upregulated solely upon SNA. However, many of these genes were not significantly methylated in any condition. A promoter CGI analysis

was performed to identify predictable correlations between the methylation status and promoter CpG dinucleotide distribution. Interestingly, almost all investigated RAGs and DM genes have at least one CGI, except *Sprr1a*, usually close to the transcription start site (TSS) or to the translation start site. Thereby, differences for the normalized CpG density around the TSS were found between the differentially hyper- or hypomethylated genes and RAGs.

However, promoter DNA methylation seems to be a minor epigenetic mechanism involved in RAG expression regulation. Expression of major RAGs was increased only upon SNA accompanied by increased promoter H3-K9 acetylation and decreased H3-K9 methylation. Overexpression of PCAF (KAT2B), a histone acetyltransferase for H3-K9, in dissociated mouse DRG neuron cultures or in cerebellar granule neurons (CGN) enhanced neurite outgrowth even on CNS myelin. This was accompanied by a restored increase of RAG expression on inhibitory myelin and by elevated promoter H3-K9 acetylation.

3.2 Role of DNA methylation in axonal regeneration

3.2.1 Experimental setup and MeDIP-chip

The first part of this study focused on the analysis of differential changes of genome-wide promoter DNA methylation patterns in DRG as a model of axonal regeneration. An immunoprecipitation of methylated genomic DNA (MeDIP) was performed with a 5-methylcytosine antibody for direct enrichment of methylated DNA fragments. This method was combined with a DNA methylation tiling microarray for gene promoters and CpG islands with whole genome amplified immunoprecipitation samples (IP) and Input (genomic DNA) reference samples (MeDIP-chip). The advantage of this combined method was the possibility to address the presence of this epigenetic mark genome-wide and, at the same time, obtaining detailed information about the distribution of methylated CpGs in gene promoter regions. Alternatively, genomic DNA can be bisulfite-converted. Thereby, unmethylated CpG dinucleotides but not methylated CpGs are chemically converted to TpGs [Clark *et al.* 1994; Adorjan *et al.* 2002]. Subsequent sequencing or the use of methylation-sensitive PCR allows a CpG-specific methylation analysis at base-pair level if compared to a reference genomic sequence. However, these methods have only been of limited availability in the present study, therefore MeDIP-chip was selected as method of choice. The use of random DNA fragmentation for MeDIP allowed an unbiased enrichment of methylated sequences, as compared to restriction enzyme digestion methods [Fazzari & Greally 2004].

The tiling microarray approach facilitated a direct and specific assessment of 18,180 mouse genes for which the proximal promoter region and CpG islands were covered (approximately -1,500 to +800 bp to TSS). Since patterns of CpG methylation are supposed to be roughly similar across smaller regions of about 100 bp, the applied tiling array has been sensitive enough to detect significant changes. The microarray raw data of enriched IP over Input

signals was pre-analyzed by Roche/NimbleGen and yielded qualitative probability peaks (p-values) for significant methylation events that represented specific gene promoter/CGI regions ("genes"). Thus, no absolute methylation values could be extracted, precluding a direct quantification of fold change enrichment, analog to gene expression microarrays. A quantitative evaluation and interpretation of the dataset was complicated for several reasons. The applied 5-methylcytosine antibody recognized methylated cytosines (almost exclusively in CpG dinucleotides) but not unmethylated CpGs that are mostly found in CpG islands. Therefore, enrichment of partially methylated DNA fragments gave no direct information about the CpG density, CpG distribution, or the presence of unmethylated or hemimethylated CpGs. It is not possible with this antibody to directly distinguish between a high ratio of methylated to unmethylated CpGs within a low CpG density region, and the other way round. Relative methylation levels could be assessed by comparing microarray results to the enrichment of completely methylated genomic regions and to a reference genomic sequence, which is technically difficult. Better analytical tools for qualitative DNA methylation datasets were developed to partly compensate for the lack of quantifiability, specifically the Bayesian tool for methylation analysis (Batman) algorithm based on a Bayesian deconvolution strategy [Down *et al.* 2008; Mo 2012]. Unfortunately, the appropriate software and know-how was eventually not accessible for an additional or alternative data analysis in this study.

Furthermore, the results from the DNA microarray analysis are of limited accuracy, for several reasons. First, WGA-MeDIP samples for each microarray were pooled from only 2 mice, which increased variation due to inter-individual and surgery-associated differences. This was compensated by utilizing triplicate or duplicate sets of microarrays for each condition. Although raw results for each multiple array set seemed to be reproducible, the pre-analysis algorithms for raw data normalization and computation seemed to yield slightly different thresholds. These thresholds affected the decision for significant methylation of a gene within a set of microarrays. Therefore, partially methylated genes can yield different results for each array. Finally, it needs to be noted that the real extent of injury-induced effects has likely been subdued, because whole DRG were processed for MeDIP. About half the DRG cells are of non-neuronal types that would not directly respond to injury or in a different way, which constrains analysis. Further, truncated axons attached to the dissected DRG were majorly excluded from analysis. Axons were shown to contain and translate mRNA molecules close to the injury site in quick response to nerve injury [Taylor *et al.* 2009; Walker *et al.* 2012].

3.2.2 DNA methylation and expression of DNA methyltransferases

Genome-wide DNA methylation analyses were usually conducted in cells like fibroblasts or cancer cell lines, or comparing somatic cells with germ line cells, however, rarely in DRG or other neuronal cells [RP Sharma et al. 2005; Saxonov et al. 2006; Weber et al. 2007; RP Sharma *et al.* 2010]. Changes of DNA methylation patterns were never shown for DRG in the

context of nerve injury and axonal regeneration. Therefore, this study wanted to identify specific genes with injury-induced differential promoter/CGI DNA methylation correlating with gene expression and axonal regeneration.

As first analysis approach to the microarray dataset, injury-induced changes of global methylation were examined for each condition, deduced from the average total number of significant methylation events across all genes. Global promoter methylation changed only moderately and was increased already at 1 day after SNA compared to sham, then normalized during the time course. Upon DCA, overall methylation was decreased after 7 days. Interestingly, global hypermethylation was found rather upon SNA than DCA although increasing RAG expression upon peripheral injury might be expected to correlate with overall reduced DNA methylation levels. This could be explained by an acute extensive shut-down of genes that are relevant for regular neuronal function, followed by a stepwise activation of a pro-regeneration and repair program. Shutting down tissue-specific genes for regular neuronal functions would be accompanied or caused by promoter hypermethylation. Consequently, upregulated RAGs would be expected to be hypomethylated. This correlation was excluded in this study because RAG promoters were already unmethylated or not significantly methylated in shams or naive, and remained unmethylated even upon central injury. Inhibitory signals from the environment at the central injury-site prevent an acute regeneration response. Still, gene expression might be later enhanced (global hypomethylation after 7 days) in an effort to compensate the functional loss of severed axons or in response to inflammation. It is already known that promoter CpG islands in mouse or human are usually rather unmethylated. Most genes in DRG seemed to exhibit little proximal promoter CpG methylation for any condition, which implies that chromatin in these regions might be in a principally accessible state, with regard to DNA methylation. Although most genes are likely additionally regulated by transcriptional or post-translational mechanisms, such as histone modifications, low levels of promoter methylation may speak at least for latent activity of most genes. Despite a largely unmethylated promoter region, gene body DNA methylation or local CpG-specific promoter methylation can still influence gene expression, for example, at transcription factor binding sites or for methyl-CpG binding proteins (MBPs) [Laurent *et al.* 2010]. Thereby, moderate changes of total promoter methylation levels would already be sufficient. Such small effects could easily be missed by the pre-analysis algorithms of the applied commercial microarray aiming at average methylation events for larger regions. Nerve injury might induce marginal methylation changes rather than extensive alterations as, for example, known for certain tumor-suppressor genes or proto-oncogenes in tumor cells [Esteller 2008; Schoofs *et al.* 2011]. Thus, an additional detailed DNA methylation analysis for RAGs at base-pair level seems necessary.

DNA methyltransferases like DNMT1, DNMT3A or DNMT3B are involved in gene expression regulation [Reik et al. 2001; Turek-Plewa *et al.* 2005; Chedin 2011]. All DNA methyltransferases were reported to have functions in nervous system development, in neuronal precursor cells (NPCs), and in post-mitotic neurons of the adult brain. Expression of DNMT

proteins was shown in the spinal cord and rarely in DRG [Heintz 2004; CA Miller & Sweatt 2007; Feng *et al.* 2009; Feng et al. 2010; LaPlant et al. 2010; Chestnut et al. 2011]. DNMTs are involved in neuronal plasticity, memory formation but also in neuropsychiatric disorders and in ischemic brain injury. These previous findings support the idea of an important role of DNA methylation and DNMTs in axonal regeneration. Injury-induced changes of global DNA methylation might require adequate *Dnmt* expression regulation. Up to now, only few studies have been published demonstrating changes of DNMT protein levels upon brain injury or DRG nerve injury [Endres et al. 2000; Iskandar *et al.* 2004; Kronenberg & Endres 2010]. After 3 days following combined (dorsal column) spinal cord and conditioning sciatic nerve injury, DNMT3A and DNMT3B protein levels were downregulated in mouse spinal cord, together with decreased global DNA methylation while DNMT1 levels did not change [Iskandar et al. 2010]. In the present study, injury-induced *Dnmt* mRNA expression was detected in DRG from 1 to 7 days upon both types of nerve injury. *Dnmt3a* mRNA expression followed opposing courses for both injury types while *Dnmt1* expression varied only moderately, consistent with Iskandar et al. Significant *Dnmt3b* expression was not detectable in DRG in this study. Thereby, *Dnmt3a* expression increased within 2 days post SNA and then dropped down again. Upon DCA, *Dnmt3a* was downregulated already after 1 day, then increased to normal levels. These results were consistent with global DNA methylation levels in DRG that initially increased upon SNA and afterwards decreased during the time course, while they were downregulated after 7 days following DCA. Iskandar et al. have further shown that an intact functional DNA methylation cycle, based on folate metabolism, is necessary for axonal regeneration of spinal axons of afferent neurons. Folate is a methyl donor that is converted into S-adenosyl-methionine serving as substrate for DNMT and HKMT enzymes. Combined central and peripheral injury was accompanied by upregulation of the folate receptor 1 (*Folr1*), and of *Gadd45a* that is known as a negative regulator of neurite outgrowth [Yamauchi *et al.* 2007], controlling neuronal damage and cell death [Di Giovanni *et al.* 2003]. Supplementation of folic acid improved DRG axon sprouting in culture following combined injury, accompanied by increased DNMT3A and DNMT3B but not DNMT1 protein levels, as well as *Gadd45* promoter hypermethylation [Ma *et al.* 2009; Iskandar et al. 2010]. However, definite evidence that folate exerts its regenerative effects via DNA methylation of regeneration-associated promoters in neurons was not provided, neither was the specific cellular subtype for these expression changes clarified (glia or neurons). As a next step, gene promoters were approximately categorized as ‘methylated’, ‘partly methylated’, or ‘unmethylated’, depending on the number of significant methylation events of a gene in each triplicate (injury) or duplicate set (sham) of microarrays. As indicated before, most of the 18,180 annotated gene promoters were not significantly methylated upon any experimental condition or in naive. However, up to 10 percent of genes for each condition were at least partly methylated, and very few were significantly methylated across all conditions. The number of methylated and partly methylated genes decreased during the time course for both injury types, though more clearly upon SNA. Meanwhile, little gene number differences were observed in shams.

3.2.3 Hypermethylated and hypomethylated genes

Because of the qualitative nature of the microarray dataset, significant methylation 'hits' from multiple arrays for each condition were utilized to define a semi-quantitative measure for identifying hyper- or hypomethylated genes. For each gene, a Methylation Value (MV) was calculated comparing injury to sham sets of microarrays, respecting naive. The MV would estimate the extent of strong, medium, or weak promoter hyper- or hypomethylation upon nerve injury. This correlation is not very accurate because of the comparison of triplicate to duplicate microarray sets for injury and sham. Still, the MV represents a comparable indicator for the extent of hyper- or hypomethylation and to detect differentially methylated genes. Only strong hyper- and hypomethylated genes with extreme MVs were further analyzed, except for the identification of genes with a persisting methylation status during the time course, for which an extended scenario was applied. Although important candidates with weaker methylation changes upon injury likely slipped the analysis as false-negatives, otherwise, the number of false-positives was reduced by choosing this strict scenario. Overall, more hypermethylated genes were found upon SNA, specifically after 1 day, compared to DCA. Contrary, more hypomethylated genes were found upon DCA, specifically after 7 days, compared to SNA (**Table S1**; Appendix). A high number of hypermethylated genes early upon SNA (matching increased global DNA methylation after 1 day) were unexpected since the activation of a pro-regeneration program leads to majorly increased RAG expression. However, this perspective concentrates on emerging genes upon injury for inducing regeneration. Indeed, transcription factors and other gene products that are important for regular neuronal functions might be initially repressed either before or while concurrently switching to pro-regeneration processes. Especially genes that suppress axon regeneration-related functions in mature neurons, regarding neurite outgrowth and axon guidance, have to be repressed in response to nerve injury.

In order to identify specific functions of the strong hyper- or hypomethylated genes, major functional annotations were assigned, separately for the main conditions (SNA/DCA; hyper- or hypomethylated), according to 9 major functional categories. The largest functional groups for all conditions were 'Signal Transduction', 'Transcription and Chromatin remodeling', 'Transport and Ion channels', or 'Cell Structure' which are relevant for primary changes in injured neurons (**Figure 15**). Genes related to transcription or chromatin remodeling were more often identified upon SNA compared to DCA, and more often hypermethylated (like *Smarcc2*, *Sap130*, *Cbx4*, *Cdyl2*, or *Crtc1*) than hypomethylated like *Rbpjl* (**Table S2**). Additionally, the focus was set on genes with functions in '(Neural) Development, Differentiation, or Cell cycle' that might play a role specifically in neurite outgrowth. Interestingly, all genes within this functional group were exclusively hypermethylated, mostly upon SNA (for example, *Fyn*, *Metrn*, *Neurl4*, or *Dpysl5*). The gene product of the SNA-hypermethylated tyrosine-protein kinase gene *Fyn* plays a role in neural processes by interacting with ARHGAP32 and DPYSL2 (CRMP2). DPYSL2 is involved in neuronal development, axon growth and guidance, and growth cone collapse [Takahashi *et al.* 2003]. It is required for microtubule

reorganization in degenerating axons during Wallerian degeneration in injured DRG neurons [Wakatsuki *et al.* 2011]. DPYSL2 can heteromize and interact with similar proteins like DPYSL5 (CRMP5) that inhibits neurite outgrowth antagonizing DPYSL2-mediated regulation of neurite outgrowth [Fukada *et al.* 2000; Brot *et al.* 2010]. *Dpysl5* mRNA expression was upregulated upon DCA although it was differentially hypermethylated. Promoter hypermethylation might have been established to counteract its upregulation. The other interaction partner of FYN, ARHGAP32, is a GTPase-activating protein for RHOA involved in neuronal differentiation and in the reorganization of dendritic spines [Nasu-Nishimura *et al.* 2006]. A similar activator for the GTPase RHOA, *Arhgap10*, was differentially hypermethylated upon DCA, together with *Dpysl5*. Finally, *Metrn* is highly expressed in brain, typically in undifferentiated neural progenitors. METRN is a neurotrophic factor that induces axonal extension in small and intermediate DRG neurons by activating satellite glial cells, promoting neurogenesis after ischemic stroke in the adult brain [Nishino *et al.* 2004; Z Wang *et al.* 2012].

Noticeably, many hypomethylated genes were found after 7 days upon DCA, which might indicate a late and broad response within DRG, even though – or because – axon regeneration is inhibited. Several of these genes were involved in transcription regulation, such as *Gtf2i*, *Cnot2*, and *Meis3* (*Mrg2*), but only few of them were indeed differentially methylated for DCA. This fact relativizes the importance of the high number of hypomethylated genes for this specific condition. GTF2I is a general transcription factor known to interact with histone modifying enzymes. *Gtf2i* deletion is associated with the Williams-Beuren syndrome exhibiting unique neurocognitive features and behavior including low IQ and hypersociability [Sakurai *et al.* 2011]. CNOT2 is involved in the general modulation of gene expression by destabilizing mRNAs. It is highly expressed during neural development and in neural stem cells (NSCs), but it is rapidly downregulated during NSC differentiation and weaker expressed in mature neurons [C Chen *et al.* 2011a]. CNOT2 showed increased promoter methylation up to 3 days post-DCA but was hypomethylated after 7 days, which speaks for the aforementioned putative induction of gene expression to compensate the loss of neuronal functions upon DCA. The homeobox protein MEIS3 is expressed at high levels in brain, and it functions as a coordinator of neural tissue maturation in Xenopus hindbrain [Lernmark *et al.* 1990], and it is involved in cell faith regulation during early nervous system development [Gutkovich *et al.* 2010]. MEIS3 is required for axonal path-finding in dopaminergic neurons in mouse [Sgado *et al.* 2012]. Many hypomethylated genes upon DCA might have specific functions in centrally injured DRG neurons that could induce an alternative gene expression pattern, despite the inhibition of a pro-regeneration response.

The set of hypermethylated genes upon DCA included some genes with specific functions in differentiated neurons. For example, CRTC1, a coactivator of the transcription factor CREB1, is involved in dendritic growth in developing cortical neurons, regulated by BDNF [Finsterwald *et al.* 2010], and in long-term hippocampal plasticity responding to specific neuronal activity and stimuli [Ch'ng *et al.* 2012]. The homeobox protein GSX2 (GSH2) is a

putative transcription factor expressed in developing brain [Hsieh-Li *et al.* 1995]. Interestingly, GSX2 was found to regulate neurogenesis by abetting a quiescent and undifferentiated state of NSCs, thereby negatively regulating NSC proliferation and differentiation. It is further required for the specification of neuronal subtypes [Mendez-Gomez *et al.* 2012]. Since this gene is hypermethylated early upon DCA, its putative downregulation might promote neuronal progenitor maturation that can be mediated by GSX1, a potential counter player for GSX2 [Pei *et al.* 2011]. This effect supports the idea of an attempted compensation of CNS injury-induced cell loss and inhibited intrinsic axon outgrowth capacity. Gene expression for the above mentioned genes was not tested since they were not differentially methylated.

Surprisingly, the set of strong hyper- and hypomethylated genes was not suitable to yield a substantial number of genes maintaining a persistent injury-induced change of promoter methylation across several time points. For this reason, an extended scenario was used including genes with medium or weaker hypermethylation (MV > +3), or hypomethylation (MV < -3) (**Table 1**). Far more genes were expected than observed, since injury-induced gene expression often lasts for several days to weeks. Persistent hyper- or hypomethylation would potentially correlate with a continued down- and upregulation of these genes, respectively. The low number of genes overlapping time points was likely limited by the insufficient accuracy of the microarray raw data in combination with the manufacturer's qualitative computing algorithms. As mentioned before, detection of significant methylation was crucially dependent on the calculation of a significance threshold above the global average, which could vary between individual microarrays although raw data enrichment patterns seemed reproducible. Medium or weak levels of promoter methylation seemed therefore often to yield inconsistent p-values for the same condition, accounting for a lower probability of persistently high MVs. This effect was particularly visible when comparing naive or sham methylation levels of a specific gene across time points for both injury types, which varied to a certain extent. However, the identified genes with continuous hyper- or hypomethylation have rarely been associated with injury-induced expression in DRG, yet. For example, the potassium channel gene *Kcnj4* (*Kir2.3*) is hypermethylated for all time points upon DCA (only in extended scenario) – in contrast to many other *Kcnj* genes – while it remains unmethylated upon SNA. This channel was found highly expressed in forebrain and is involved in the control of basal ganglia function [Pruss *et al.* 2003], in dopamine-dependent structural plasticity of striatal neurons [Cazorla *et al.* 2012]. A differential expression of potassium channel subunits, and their combinations, contributes to the functional diversity of sensory DRG neurons and would be important to adapt to the injury-induced situation [Rasband *et al.* 2001]. *Map3k9* was also hypermethylated upon DCA, which is an essential upstream activator of the MAP kinase signaling including MAPK8 to MAPK10 and JUN that is induced in axonal regeneration [Jenkins *et al.* 1993; Buschmann et al. 1998]. Contrary, persistently hypomethylated genes upon DCA were, for example, the kinesin-like protein gene *Kifc3* and the already mentioned *Meis3*. KIFC3 is a microtubule-dependent motor protein expressed in brain and involved in apically targeted axon transport [Hoang *et al.* 1999]. This gene should not be confused with

the similar *Kif3c* that was hypermethylated and downregulated upon SNA. However, such opposite results for similar transport proteins indicate a differential adaptation of transport mechanisms to both injury types in DRG neurons. Additionally, 114 genes exhibited a persistent status across only two adjacent time points within the extended scenario. Among these were several genes that might have a role in axon regeneration, for example: *Ythdf1* (hyper SNA), *Map3K9* (hyper SNA and DCA), *Ptpre* (hyper SNA), *Camk2a* (hypo SNA), *Map4k4* (hypo SNA), *Drosha* (hypo SNA and DCA, previously *Rnasen*), *Spast* (hyper DCA).

3.2.4 Differentially methylated genes

Finally, the most interesting set of differentially methylated (DM) genes was identified being hyper- or hypomethylated only for one injury type. Relative gene expression levels of many but not all DM genes inversely correlated with the injury-induced methylation status according to the hypothesis. In general, this speaks for a role of DNA methylation for gene regulation upon nerve injury, at least for specific genes, although not including most major RAGs. Exemplary, *Smarcc2*, *Sap130*, *Cbx4* and *Cdyl2* are hypermethylated upon SNA whose gene products are components of chromatin remodeling complexes and associated with gene repression. The gene product of *Smarcc2* (SWI/SNF related, matrix associated, actin dependent regulator of chromatin, subfamily c, member 2) is associated with both, transcriptional activation or repression. SMARCC2 is a component of several chromatin remodeling complexes such as the neuronal cell specific SWI/SNF-type complexes, npBAF and nBAF, that are important for neuronal differentiation. Further, it has a role in gene expression regulation for dendrite outgrowth and for repression of neuronal specific gene promoters in non-neuronal cells [JI Wu *et al.* 2007b; Kazantseva *et al.* 2009]. However, *Smarcc2* mRNA expression levels did not yet change after 1 day, the time point of detected differential methylation, neither upon SNA nor DCA. Potentially, *Smarcc2* expression was decreased only after 24 hours post-SNA and following promoter hypermethylation. The SNA-hypermethylated gene *Sap130*, coding for the subunit of a histone deacetylase complex, is downregulated solely upon SNA. It acts as a transcriptional repressor within the SIN3A corepressor complex. However, no specific functions in the nervous system are published, yet. The chromobox protein and E3 SUMO-protein ligase CBX4 (PC2) and the chromodomain protein CDYL2, differentially hypermethylated upon SNA, are capable of binding and "reading" H3-K9me3 [E Bernstein *et al.* 2006; Fischle *et al.* 2008]. So far, little is known about CDYL2 in a brain-related context. More enlightening is the role of CBX4, for example, in differentiated cells during mouse brain development, being a component of PRC1 multiprotein complexes involved in maintaining a repressive state of many genes [Vogel *et al.* 2006]. CBX4 can interact with the H3-K9 methyltransferase SUV39H1, whereby H3-K9 methylation can serve as signal to establish DNMT3B-dependent DNA methylation patterns involving SUV39H1 [Lehnertz et al. 2003]. CBX4 further affects DNMT3A function through SUMOylation *in vitro* [B Li *et al.* 2007b]. Decreased expression of hypermethylated *Cbx4* upon SNA corre-

lated with reduced RAG promoter H3-K9me2 and increased H3-K9ac following peripheral injury. Else, not much is known about most of the other differentially hypermethylated and downregulated genes upon SNA in a neuronal context (*Ythdf1*, *Angptl7*, *Acbd6*, or *Ptpn9*). *Kif22*, in contrast, was upregulated despite its hypermethylated promoter.

In contrast, fewer genes were found differentially hypomethylated upon SNA. As an example, the putative transcription factor *Rbpjl* that is expressed in brain was persistently hypomethylated after 1 to 3 days. Surprisingly, *Rbpjl* gene expression was upregulated after 1 day upon SNA (and downregulated upon DCA) but upregulated after 3 days, even though at low absolute levels. RBPJL seems to interact antagonistically to its similar paralogue, RBPJ, which can associate with NOTCH proteins (important for cell-fate determination). RBPJL might prevent RBPJ-mediated NOTCH signaling activation that includes HDAC1/2 or EP300 recruitment [Minoguchi *et al.* 1997; Masui *et al.* 2010; Meier-Stiegen *et al.* 2010]. Furthermore, RBPJ binds to specific methylated DNA regions, which is not yet known for RBPJL [Bartels *et al.* 2011]. It has to be noted, that the hypomethylated promoter region of RBPJL overlaps with the promoter of matrilin 4 (*Matn4*) on the complementary strand, which is an extracellular matrix protein expressed in brain and other tissues. Expression analysis revealed highest expression of both genes in lung and brain, partially overlapping [Wagener *et al.* 2001]. Surprisingly, most differentially hypomethylated genes upon SNA were downregulated (*Ampd3*, *Ak3l1*, or *Gnat1*), thus not matching the hypothesis.

Unexpectedly, all differentially hypermethylated genes upon DCA were marginally upregulated for this condition and often downregulated upon SNA, contradicting the hypothesis as well. These results might speak for a less dramatic correlation of local promoter methylation changes and gene expression upon injury, not comparable to heavy promoter methylation of specific repressed tumor suppressor genes in cancer, for example [Santini *et al.* 2001]. A more likely explanation is that methylation-induced changes of gene expression were delayed relative to the observed preceding injury-induced promoter methylation for a specific time point that could not be tested by the qRT-PCR array in this study. Besides the aforementioned *Dpysl5* and *Arhgap10*, mastermind-like 3 (*Maml3*) is also differentially hypermethylated at 1 day following DCA but only weakly regulated for the same time point. All three MAML isoforms are coactivators of NOTCH signaling that is important, for example, in brain development, and they form DNA-binding complexes with NOTCH proteins and RBPJ [Lin *et al.* 2002; L Wu *et al.* 2002; Sivasankaran *et al.* 2009]. Thus, a hypermethylated *Maml3* gene promoter upon DCA might correlate with the observed hypomethylation of *Rbpjl* upon SNA. MAML1 has further been reported to coactivate TRP53, and to interact with the histone acetyltransferase EP300 enhancing its activity, for example towards NOTCH1 [Zhao *et al.* 2007; Hansson *et al.* 2012]. In centrally injured DRG neurons, MAML3 might thus have opposing functions to MAML1, maybe similar to RBPJL and opposing RBPJ.

Taken together, correlations between gene expression, differential promoter methylation, and gene function were either matching or in seeming contrast to the hypothesis for many genes. These results indicate that the hypothesis might not be plausible for all regulated genes, or too much simplified. Otherwise, injury-induced effects of promoter DNA methylation on gene expression could not be assessed isolated from the whole context of gene regulation. It must be considered that other regulation mechanisms and additional signals caused by collateral surgery effects, such as inflammation, overlay with epigenetic mechanisms. Such effects might cause false-positive or false-negative results. For example, laminectomy, as a sham control for spinal cord injury, has already been shown to cause expression profiles that are rather similar to mild traumatic spinal cord injury than to naive [De Biase et al. 2005]. For each injury type, the non-injured axon branch was still intact in this injury model, and the DRG nodes should still be susceptible to signals aside of the injury site. Upon DCA, sensory feedback information can still arise in the hind limbs, though potentially distorted due to impaired motion control. Hereby, nerve activity and gene expression patterns might have been affected. DRG neurons with an injured central branch might have sustained peripheral nerve activity, opposed by the inhibition of a pro-regenerative response causing different transcription signals. On the other hand, sensory and motor fibers within the mixed spinal nerve tract were truncated upon SNA while nerve fibers within the spinal cord were left intact. At least, the phenomenon of neuropathic pain after nerve injury can be the consequence of additional dramatic molecular changes. Consequently, neuronal survival and axon regeneration are promoted to a certain extent, including the modulation of pain transmission and sprouting of nerve fibers within the dorsal horn [Hokfelt *et al.* 1994; Scholz *et al.* 2007]. Further, it was observed that injury-induced DNA methylation patterns of many genes seemed to follow a similar course for DCA as for SNA, though delayed. Since both injury types were performed equidistally, a quicker retrograde signaling upon SNA can be assumed. This delaying effect can lead to false-positive differential methylation results for a specific time point.

3.2.5 Regeneration-associated genes

A differential retrograde signaling from the distinct injury sites is supposed to cause either activation (peripheral injury), or inhibition (central injury) of an intrinsic axon regeneration program, including the expression of regeneration-associated genes (RAGs). Upon SNA, significant improvement of motion control was observed, but not upon DCA. Consequently, gene expression of major RAGs was assessed by qRT-PCR upon injury. Several RAGs were prominently induced only upon SNA at increasing levels along the time course (*Sprr1a*, *Gal*, *Gap43*, and *Bdnf*). Other RAGs were only moderately induced upon SNA (*Chl1*, *Stmn2*, *Basp1*, *Lgasl1*, and *L1cam*). The time points were chosen in a way to cover acute events, established after 1 day, and later events after up to 7 days when functional axon regeneration is usually already initialized. Consistent with the literature, the expression profile of these genes verified the success of the surgery procedure and the DRG model for axonal regenera-

tion. DNA methylation microarray analysis revealed that the investigated RAGs and further known injury-associated genes showed either no significant promoter methylation for any condition (like *Basp1*, *Bdnf*, *Calca*/*Cgrp1* or *Gap43*), or occasionally weak methylation (like *Gal* or *Stmn2*). These findings suggest that many RAGs were not transcriptionally regulated by significant promoter DNA methylation changes. For this reason, their SNA-induced up-regulation could not be accompanied by a hypothesized hypomethylation. In contrast, the leukemia inhibitory factor 1 (*Lif*) was methylated on all arrays for each condition. LIF is another upregulated and retrogradely transported RAG that induces expression of the neuropeptide GAL [Ozturk *et al.* 2001]. So far, little is known about DNA methylation as a regulatory mechanism for RAGs in a neuronal context. Dysregulation of *Bdnf* expression in the brain, associated with altered promoter DNA methylation, was reported in the context of cocaine addiction [Bilinski *et al.* 2012]. Interestingly, epigenetic regulation of the *Bdnf* gene plays a role in long term potentiation in learning and memory, and in object recognition [Munoz *et al.* 2010; Sui *et al.* 2012]. Promoter methylation of *Bdnf* is further involved in bipolar disorder and its treatment [D'Addario *et al.* 2012] and also in schizophrenia [Kordi-Tamandani *et al.* 2012]. *Gap43* regulation during olfactory receptor neuron differentiation was suggested to be regulated by DNA methylation [Macdonald *et al.* 2010]. Expression of the regeneration-associated neuropeptides calcitonin and calcitonin gene-related peptide (*Cgrp1*) from the *Calca* gene locus can be enhanced in glial cells by treatment with the DNA methyltransferase inhibitor 5-Aza-dC, which leads to demethylation of an enhancer element [KY Park *et al.* 2011]. Further, 5-Aza-dC treatment of a murine hepatoma cell line induced the expression of *Sprr1a* and *Sprr2a*, proving a principal role of DNA methylation for this genes [B Jin *et al.* 2004]. These results are interesting, although in a non-neuronal context, since all *Sprr* genes and *Sprr-like* genes were not significantly methylated in DRG neurons for any condition in the present work. Nevertheless, treatment of centrally-injured DRG with DNMT inhibitors might induce expression of *Sprr* genes since these are usually not expressed in naive DRG. For this activation, CpG methylation of small promoter regions might be responsible. Since the *Sprr* gene family cluster exhibits low promoter CpG density (no CGI), most CpGs should theoretically be methylated and therefore sensitive to 5-Aza-dC treatment. The density of potentially methylated CpGs might have been below the sensitivity threshold of the applied MeDIP-chip for significant methylation. *L1cam* is an interesting RAG with two promoter regions. Its gene expression seemed to correlate with hypermethylated promoter I in endometrial carcinomas and was inducible by DNMT or HDAC inhibition [Schirmer *et al.* 2013]. However, hypomethylated *L1cam* was aberrantly expressed in colon cancer [Kato *et al.* 2009]. Else, little information is available for an involvement of DNA methylation in RAG expression regulation upon injury, which coincides with the results of the microarray analysis in this study [Kiryu-Seo *et al.* 2011].

The majority of known RAGs encode for protein categories relevant for axon repair such as cytoskeletal proteins, neurotransmitter metabolizing enzymes, neurotrophins, and neurotrophin receptors, neuropeptides, and cytokines [Bonilla et al. 2002]. Most of the major RAGs

are highly expressed during neural development and, usually at lower levels, in the adult nervous system and in mature neurons [Starkey et al. 2009]. In fact, most identified RAGs were already expressed in naive DRG neurons. The present study, for example, confirmed relatively high basal expression of *Gap43* in DRG with subsequent further increase upon SNA but not upon DCA. The same sustained upregulation and its rapid transport into growth cones was reported for most types of DRG neurons. GAP43 is a structural protein and the prototypic RAG localized primarily in axons and growth cones, associated with the plasma membrane [Schreyer *et al.* 1993; Chong et al. 1994; Di Giovanni et al. 2005]. It plays a role in axonal and dendritic filopodia induction, in a neurotrophin-dependent manner, and it is highly expressed during target innervation in brain development but downregulated in adult. It is preferentially expressed in forebrain and in highly plastic CNS regions such as the olfactory bulb, hippocampus, and in DRG [Skene *et al.* 1981; De la Monte *et al.* 1989; Mahalik *et al.* 1992; Benowitz *et al.* 1997]. *Gap43* and *Basp1* are similarly regulated and involved in actin structure modulation, specifically in growth cones. Combined overexpression of *Gap43* and *Basp1* in a double transgenic mouse model induced robust axon extension of adult DRG neurons, *in vitro*. Further, regenerative growth into peripheral nerve grafts following dorsal column lesion was dramatically increased, *in vivo* [Bomze *et al.* 2001]. And co-expression of *Gap43* together with *L1cam* promoted regenerative growth of Purkinje cells [Y Zhang *et al.* 2005]. Increased levels of the neuropeptide GAL have been detected in axotomized sensory neurons, together with other neuropeptides, implying a role in peripheral axon regeneration [Klimaschewski *et al.* 1994; Shadiack *et al.* 1998]. This neuropeptide was one of the highest upregulated genes only following SNA [Reimer *et al.* 1999], as confirmed in this study. BDNF was described to be involved in axonal regeneration and neuron development [RM Lindsay 1988; Schecterson *et al.* 1992]. This growth factor is a potent promoter of axonal regeneration in injured sensory neurons and in the spinal cord [Geremia et al. 2010; Weishaupt et al. 2012] where it promotes neuronal survival and differentiation, and reduces axon degradation [Clatterbuck *et al.* 1994]. *Sprr1a* (Small proline-rich protein 1a/Cornifin-A) belongs to a multigene family for cornifying proteins important for the differentiation of keratinocytes and squamous epithelial cells. SPRR1A is usually involved in the construction of cell envelopes in cornifying epithelia that require increased thickness or extreme flexibility [Kartasova et al. 1996]. Usually, SPRR1A is not neuronally expressed except in few neurons in the neocortex [Marklund *et al.* 2006]. Thus, *Sprr1a* mRNA was not expressed in naive or sham mouse DRG in this study. Its neuronal expression was first detected by microarray analysis of mouse DRG that successfully regenerated after SNA. *Sprr1a* was co-induced with other epithelial differentiation genes such as *S100a11* (*S100c*) and *Cdkn1a*. Thereby, SPRR1A augments neurite outgrowth upon injury by co-localizing with fibrous actin in membrane ruffles. Depletion or blockade of this protein caused less outgrowth of injured peripheral neurons of adult mice [Bonilla IE, 2002 J Neurosci]. Overexpression, on the contrary, enhanced outgrowth even on inhibitory substrates. *Sprr1a* is a unique and interesting RAG because it is not already expressed during the axonal outgrowth period of embryonic development, in contrast to other major RAGs. For this reason, *Sprr1a* was proposed to be a

marker for pro-regenerative processes in neurons [Starkey et al. 2009]. In this study, *Sprr1a* gene expression was dramatically induced solely upon SNA injury, confirming what was previously shown. Additionally, and maybe for the first time, gene expression of the other *Sprr* family members was examined in this study in DRG following either SNA or DCA. These include 14 genes (*Sprr1a* and *Sprr1b*, *Sprr2a* to *Sprr2j*, *Sprr3*, and *Sprr4*) that are found clustered within a narrow genomic region, likely to share common regulation mechanisms. None of them could be detected as significantly expressed in naive mice or upon sham but several of them (*Sprr2a/g/h/l/j/k*), if not all, were induced strongly upon SNA, similar to *Sprr1a*. This speaks for a more complex role of these genes in axon and tissue regeneration, which should be further investigated. The *Sprr1a* gene seems to be regulated by the transcription factor CCAAT/enhancer binding protein delta (CEBPD) that is known to be induced upon peripheral nerve injury [De Biase et al. 2005]. *Cebpd*-deficient mice show an impaired axon regeneration-related upregulation of SPRR1A in DRG, in contrast to GAP43 or GAL. As a surprising result, a quick recovery after sciatic nerve injury was also severely impaired or significantly delayed, which speaks for a crucial role of this transcription factor and/or SPRR1A [de Heredia *et al.* 2012].

Importantly, the acute expression of several transcription factors, specifically JUN/FOS (AP1 complex), ATF3, CREB1, and CEBPD, upon peripheral injury is crucial for the successful initialization of regeneration [Jenkins et al. 1993; De Biase et al. 2005; Hyatt Sachs *et al.* 2007]. Upon nerve injury, JUN seems to be a crucial general activator of pro-regeneration genes [Raivich et al. 2004] and its activity is linked to the activating transcription factor 3 (ATF3) in this context [Pearson *et al.* 2003]. ATF3 is also induced upon peripheral but not upon central nerve lesion. Transgenic mice that constitutively express ATF3 showed enhanced peripheral axon regeneration of adult DRG neurons, and this factor increased SPRR1A expression in non-injured DRG neurons although not that of other RAGs such as GAP43 [Seijffers et al. 2007]. Together with rising cAMP levels upon peripheral nerve injury, the cAMP response element binding 1 (CREB1) transcription factor was demonstrated to be sufficient to trigger axonal regeneration within the spinal cord myelin environment upon DCA of DRG [Neumann et al. 2002; Qiu et al. 2002; Gao et al. 2004].

In addition to research studies that focused on single RAGs, microarray studies were applied during the last 12 years to explore axon regeneration-related changes of gene expression patterns genome-wide following nerve injury of mouse or rat DRG neurons [Fan *et al.* 2001; Costigan *et al.* 2002]. These studies identified a number of up- or downregulated RAGs upon peripheral or central injury. However, the resulting lists of identified candidates showed only limited parallels between these studies, and did not always reveal the participation of all known major RAGs. Important common players whose injury-induced expression was identified were, for example, transcription factors (*Jun*, *Fos*, *Atf3*, *Atf2* (*Creb2*), *Sp2*, *Gata4*, or *Sox11*), or neuropeptides and neurotrophic factors (*Gal*, *Npy*, *Pacap*, or *Bdnf*). Further, *Sprr1a*, *Gap43*, 5-HT receptor genes, *Akt*, or *Gadd45* were reproducibly identified and

strongly regulated [Tanabe *et al.* 2003; Nilsson *et al.* 2005; Taylor et al. 2009]. Most recently, the body of evidence is growing for an additional involvement of microRNAs [Strickland *et al.* 2011; D Wu *et al.* 2011; HY Zhang *et al.* 2011] and long non-coding RNAs in the promotion of injury-induced axon outgrowth in DRG and brain [Bhalala *et al.* 2012; B Yu *et al.* 2013]. However, most publications about injury-associated gene expression of the last 10 years often concentrated on proofing the relative importance of specific gene products for axonal regeneration, rather than being able to draw a complete mechanistic picture.

3.2.6 CpG island analysis

Finally, it was tested if the promoter DNA methylation status of identified DM genes and known major RAGs correlated with the promoter structure, regarding CpG dinucleotide distribution and density, specifically with CpG islands. A CGI analysis was performed to elucidate, first, the properties of CGIs for each set of examined genes. Second, it was asked whether the promoter CpG density (as "normalized CpG value" or observed-to-expected (obs/exp) CpG ratio) around the TSS correlated with injury-dependent promoter methylation and gene expression levels. However, examination of the promoter structure was not in the focus of this work and was therefore analyzed only to a certain extent. Sequence-based CpG island analysis revealed the presence of CGIs for almost all investigated RAGs and DM genes, except *Sprr1a*. Almost all analyzed genes exhibited one or more CGI larger than 200 bp, usually within the core promoter region or around the TSS. This is surprising since only about 50 to 60 percent of all annotated genes of the murine genome were supposed to exhibit promoter CGIs [Antequera & Bird 1993; Saxonov et al. 2006]. If modern "NCBI strict" parameters (CGI size defined as larger than 500 bp) were applied, instead of the classical "NCBI relaxed" (larger than 200 bp), only 8 out of 15 RAGs, and 16 out of 18 DM genes would still exhibit a CpG island [Illingworth *et al.* 2008; Hackenberg *et al.* 2010]. The proximal promoter region around the TSS is important for the binding of transcription factors, other regulators, and RNA polymerase II. Active gene expression requires a relaxed state of chromatin, which might be triggered or supported by CpG island hypomethylation, together with specific histone modifications. Gene promoters with CGIs are highly hypomethylated, in genome-wide average, compared to gene body or intergenic methylation levels. These narrow hypomethylated regions around the TSS often stretch into the first exon, especially for high CpG content promoters. Even promoters with lower CpG content are hypomethylated as well although to a lesser extent [Saxonov et al. 2006; Laurent et al. 2010]. Thus, core promoter methylation is up to 10-fold lower for CGI-containing gene promoters than for non-CGI promoters. In this context, the CpG density inversely correlates with promoter methylation levels. However, promoter regions are usually not completely methylated or unmethylated having a potential for both, hyper- or hypomethylation associated with gene expression regulation. Additionally, the presence of CGIs indicates the existence of mechanisms that promote accumulation and conservation of CpG dinucleotides. In more detail, genome-wide analyses

in the literature showed that genes could be roughly divided into two categories with low or high promoter CpG content, represented by the obs/exp CpG ratio (normalized CpG value). The average obs/exp CpG ratio is usually highest at the TSS [Saxonov et al. 2006; Weber et al. 2007; Meissner *et al.* 2008]. Consequently, gene promoters with high normalized CpG values contain more often larger CGIs. According to the literature, in particular Saxonov et al., the normalized CpG values for selected genes were calculated, in this study, for the 3 kb region around the TSS (± 1.5 kb). Interestingly, major RAGs exhibited significantly lower normalized CpG values than DM genes. This was surprising, since the major RAGs were usually unmethylated which would speak for the presence of larger CpG islands and a high obs/exp CpG ratio. Specifically, strongly upregulated RAGs exhibited a relatively low promoter CpG content/density. Further, differentially hypermethylated genes had higher normalized CpG values than differentially hypomethylated genes correlating with the methylation status in corresponding shams. These results match genome-wide findings of usually unmethylated CpG islands (with high obs/exp CpG ratio). However, the normalized CpG value of a specific gene did not generally correlate with its relative mRNA expression upon the type of injury, for which it showed differential methylation. Anyhow, differentially hypermethylated genes, in average, had about 2-fold higher normalized absolute expression levels in sham controls than differentially hypomethylated genes, as deduced from the qRT-PCR TaqMan Gene Expression Array. Conspicuously, several RAGs possessed CGIs further away from the TSS, either as the only one (*Calca*, *Chl1*, *Lgals1*, *Lif*, and *Stmn2*) or as additional CGI (*Bdnf* and *Trp53*). Of note, the official translation start site of many genes (Ensemble), which is usually close to the TSS, was often further away downstream of the TSS, for some genes more than 1.5 kb up to even 131 kb, mostly for RAGs (7) rather than for DM genes (1). Lower normalized CpG average values for RAGs can therefore be partly explained by the frequent accumulation of (additional) CGIs distant from the TSS. Like this, genes can be regulated by several "subpromoters" or alternative promoters such as for *Bdnf* or *L1cam*, which might have emerged during evolution by beneficial "incorrect" recombinations of gene-coding sequences [WG Chen et al. 2003; Schirmer et al. 2013].

Taken together, injury-induced RAGs might be regulated either by just marginal changes of promoter DNA methylation patterns or at other genic regions, besides other (epigenetic) mechanisms. For example, increased H3-K9ac and decreased H3-K9me2 occupancy was detected for all RAGs upon SNA, in contrast to DCA, as will be discussed further below. As indicated by others, the presence of promoter CpG methylation alone seems not to generally correlate with absolute gene expression levels [Komashko et al. 2008]. Nevertheless, relative changes of promoter/CGI methylation of active genes might at least modulate gene expression, independently of basal expression levels. Further, DNA methylation can be an indicator for other epigenetic mechanisms, potentially determining the grade or duration of gene repression. Else, no specific correlations between presence, size, or position of promoter CGIs and gene function, or tissue specificity could be evaluated, in part due to the small sample size of analyzed genes.

3.3 Role of histone modifications in axonal regeneration

The epigenetic histone code is more complex than DNA methylation, regarding the variety of different histone modifications associated with different functions for chromatin structure, and for gene expression regulation [Jenuwein & Allis 2001; Z Wang et al. 2008; Bannister & Kouzarides 2011]. Distinct types of histone acetylation and methylation have been characterized in the literature that are involved in chromatin remodeling, and either in gene activation (H3-K9ac, H3-K18ac, H3-K4me2), or repression (H3-K9me2, H3-K27me3). The focus of this study was set on proximal promoter H3-K9 modifications that are known to activate (H3-K9ac) or repress genes (H3-K9me2). Several histone modifying enzymes, responsible for establishment or erasure of both modifications of the same residue, can interact with each other and with DNA methyltransferases, potentially depending on differential regulatory signals (Introduction) [D'Alessio & Szyf 2006]. Chromatin immunoprecipitation (ChIP) was applied to assess promoter occupancy of both modifications for selected major RAGs. Prominently, increased RAG expression, only upon SNA, positively correlated with increased promoter H3-K9 acetylation (except *Sprr1a*) and decreased H3-K9 dimethylation in this study. So far, few studies investigated the role of epigenetic histone modifications upon nerve injury or in axonal regeneration. The histone acetyltransferases CBP/P300 and PCAF have already been found to be repressed in cultured primary cerebellar neurons, whereas their expression was triggered by HDAC1/2 inhibition with Trichostatin A (TSA), promoting neurite outgrowth even on inhibitory myelin substrates dependent on H3-K9/K14ac and acetylated TRP53. These results were confirmed by loss or gain of function experiments for CBP/P300 or PCAF, demonstrating that these HATs and acetylated TRP53 are required for neurite outgrowth [Gaub et al. 2010]. Additionally, overexpression of EP300 promoted axon regeneration in retinal ganglia cells (RGCs) after optic nerve crush (ONC). Thereby, EP300 acetylated histone H3 and TRP53, and occupied promoters of the RAGs *Gap43*, *Coronin1b*, and *Sprr1a*, driving RAG expression following ONC. HDAC inhibition via TSA improved survival of injured RGCs although axon regeneration was not enhanced [Gaub et al. 2011]. Interestingly, neuronal survival and axon regeneration seem to be regulated, at least in part, by different mechanisms. This was demonstrated, for example, by pro-survival HDAC inhibition and pro-regeneration EP300 expression, or by the effect of the transcription factor KLF4 on axon regeneration of RGCs after optic nerve injury [Moore *et al.* 2009; Gaub et al. 2011]. Moreover, the transcriptional complex of acetylated TRP53 and its acetyltransferase CBP/P300, binding to the *Gap43* promoter in facial motor neurons following axotomy, likely acts as a switch to axon regeneration [Tedeschi *et al.* 2009b]. Similar beneficial effects on RGC survival following ONC were found upon treatment with MS-275, an inhibitor for HDAC1-3 [Chindasub *et al.* 2013]. Several studies have demonstrated that valproic acid (VPA), another inhibitor of HDACs, was able to provide neuroprotection and to enhance axonal regeneration following either sciatic nerve injury *in vivo* or in RGCs following ONC. Upon spinal cord injury, VPA application had neuroprotective effects and improved locomotor recovery [Cui *et al.* 2003; Biermann *et al.* 2010; Lv *et al.* 2011]. HDAC inhibitors were

also tested upon acute CNS injury leading to some improvement of neurobehavioral recovery and reduction of tissue damage [B Zhang *et al.* 2008; Shein *et al.* 2011]. In contrast, neither methylated histone residues, nor their corresponding enzymes, nor methyl-CpG binding proteins have been brought into context with axonal regeneration upon nerve injury.

However, PCAF has rarely been described in the context of axonal regeneration before. Specifically, PCAF seemed to be highly relevant for H3-K9 acetylation. Consequently, the role of this major acetyltransferase for H3-K9 acetylation in the frame of RAG expression regulation and axonal regeneration was further investigated. Dr. Elisa Floriddia contributed initial ChIP data for H3-K9ac and H3-K9me2, and Dr. Radhika Puttagunta (both from the author's research group) contributed results concerning PCAF overexpression and effects of H3-K9 acetylation in DRG and CGN [Puttagunta et al. (under revision)]. Several methods were partly prepared, and several preliminary results obtained by the author of this thesis (dissociated DRG culture, ChIP, qRT-PCR). Increased total levels of H3-K9/K14 acetylation (targets of PCAF) as well as increased nuclear PCAF localization and nuclear H3-K9 acetylation were detected upon SNA in DRG but not upon DCA, compared to sham. Enhanced PCAF occupancy of RAG promoters (*Gal*, *Bdnf*, and *Gap43*) was assured by additional ChIP experiments on dissected DRG regarding relative injury-to-sham fold change enrichment upon SNA compared to DCA [Puttagunta et al. (under revision)]. These results suggest a quick peripheral injury-dependent and PCAF-mediated induction of gene expression. Together, nuclear PCAF localization, and increased PCAF and H3-K9ac promoter occupancy coincided with injury-induced RAG expression, which supported an important role of PCAF upon injury. To further test the pro-regenerative effect of PCAF-mediated promoter H3-K9 acetylation, dissociated DRG neurons or primary cerebellar granule neurons (CGN) were cultured on either growth-permissive substrate (laminin or PDL) or inhibitory substrate (CNS myelin). Cultured DRG and CGN are appropriate models for axon regeneration since both are able to grow neurites on permissive substrate but not on myelin, simulating conditions in the PNS or CNS environment. In accordance to these properties, DRG or CGN cultured on growth-permissive substrates exhibited increased overall H3-K9ac levels. AAV-mediated overexpression of PCAF in DRG or CGN could significantly increase neurite outgrowth on both substrates, compared to AAV-GFP expression. This is a surprisingly positive effect since, first, the normal outgrowth potential seemed to be even further enhanced on laminin and, second, PCAF activity alone already allowed the regeneration of neurites overcoming the inhibitory myelin. PCAF also reversed the myelin-dependent repression of RAGs such as *Gap43*, *Gal*, *Bdnf* and *Stmn2*. This effect correlated with the restoration of decreased promoter H3-K9 acetylation for these RAGs in CGN, when cultured on myelin and upon PCAF overexpression. Taken together, PCAF overexpression alone was able to increase promoter acetylation on myelin, sufficient to induce RAG expression and neurite outgrowth, similar to SNA in DRG. Additionally, endogenous PCAF and EP300 acetyltransferase activities were inhibited in cultured CGN with the natural inhibitor Garcinol [Balasubramanyam et al. 2004]. Hereupon, CGN neurite outgrowth was reduced almost by half, which confirmed a major role

of H3-K9 acetylation and PCAF activity in neurite outgrowth and axonal regeneration. To specify this effect, a *Gap43*-proximal promoter luciferase construct was designed that showed decreased luciferase reporter expression in CGN in the presence of Garcinol, confirming previous results. Similar effects might be achieved *in vivo* following nerve injury, specifically upon spinal cord injury. Enhancing *in vivo* PCAF activity could be a target of future therapies for spinal cord injury. Inhibition of HDAC activity by TSA or VPA that are already in clinical use, can improve the outcome of acute spinal cord injury having neuroprotective effects, as described above. Additional application of neurotrophic factors, specific axon guidance factors, glial scar and CNS myelin inhibitors, or stimulation of HATs might further improve locomotor recovery for patients.

Taken together, the contribution of epigenetic regulation mechanisms to successful axonal regeneration in injured peripheral nerves, or its prevention at central lesion sites is only incipiently understood so far. It becomes clear that the complex mechanisms in axonal regeneration cannot be considered anymore just a phenomenon of transcriptional RAG regulation and protein-protein interactions. The interplay of different epigenetic mechanisms seems to be essentially involved in the signal integration and the carefully orchestrated temporal and spatial gene expression regulation. Elucidating this additional level of regulation might provide more opportunities for therapeutic approaches for brain or spinal cord injuries.

4 Conclusions and Outlook

4 Conclusions and Outlook

Axon regeneration upon peripheral nerve injury, or its inhibition upon central nerve injury, is better understood nowadays. However, the larger picture of the cellular processes and complex molecular regulations is still far from being complete. Axonal regeneration requires adaptations of the gene expression pattern in injured neurons to switch from a mature functional state to a pro-outgrowth regenerative state. A successful switch depends on the interaction with the specific molecular environment, a subsequent pro-regenerative signaling, and on changes of the epigenetic pattern at the promoters of induced regeneration-associated genes (RAGs) [Kiryu-Seo & Kiyama 2011], and [R Lindner et al. (review, submitted)]. Thereby, it is still not clear if induced epigenetic modifications at gene promoters accompany or precede gene regulation.

Up to now, very little is known about an involvement of epigenetic mechanisms in axonal regeneration. Some reports demonstrated the importance of an intact DNA methylation cycle for axonal regeneration, and a contribution of epigenetic mechanisms to the regulation of RAGs such as for *Sprr1a*, *Gap43* or *Bdnf*. This work could show that epigenetic mechanisms, specifically histone-3 lysine-9 acetylation (H3-K9ac) and dimethylation (H3-K9me2) are involved in the regulation of RAGs upon sciatic nerve axotomy (SNA). An opposing pattern of these marks was detected upon dorsal column axotomy (DCA) when RAG induction was prevented. Overexpression of PCAF (KAT2B), a specific H3-K9 acetyltransferase, could be shown to enhance neurite outgrowth due to enhanced H3-K9 acetylation and RAG expression in cultured neurons, even on non-permissive myelin. However, promoter DNA methylation might either play a minor or more subtle role for RAG regulation, or it is required only for specific genes. The field of basic and clinical Epigenetics research has been accelerating to expand in different areas in the recent few years. More insights into mechanisms of axonal regeneration are likely to emerge soon.

Since promoter H3-K9 acetylation was increased for upregulated RAGs upon SNA, it would be interesting to further investigate the injury-induced presence of this epigenetic mark genome-wide with sensitive ChIP microarrays to identify more differentially induced genes. Expression and activity of other selected H3-K9 modifying enzymes such as CBP/P300, HDAC1/2, SUV39H1/2, or KDM1A should be detected. Furthermore, overexpression or knock-down studies for such enzymes could be performed in dissociated DRG or in primary CGN cultures to explore their contributions [Lander et al. 2001; BE Bernstein et al. 2007; Kouzarides 2007]. Some of these enzymes might be potential therapeutic targets for *in vivo* nerve injury studies in rodents. Of more immediate importance for clinical trials could be strategies to enhance H3-K9 acetylation. Triggering histone acetylation in patients with spinal cord crush or contortion injury might have potent therapeutic effects, probably in combination with a mixed application of intrinsic growth capacity enhancing factors such as BDNF, NTF3 and cAMP (described above). In order to recapitulate the *in vitro* effects, AAV-mediated

PCAF overexpression will be performed *in vivo*, in mouse or rat, as already planned by this author's research group [Puttagunta et al. (under revision)]. Stimulation of endogenous PCAF activity in injured human neurons, however, might be achieved by phorbol ester treatment, *in vivo* [Masumi *et al.* 1999]. Further, treatment with valproic acid (VPA), a histone deacetylase inhibitor, has already been demonstrated to be beneficial upon spinal cord injury in rodents (also see Discussion). VPA treatment has been clinically tested and shown to induce neurotrophic factors and to suppress hypoacetylation caused by spinal cord injury [F Wu *et al.* 2008; Abdanipour *et al.* 2012; Lv *et al.* 2012].

The role of promoter DNA methylation should be studied in more detail since the MeDIP-chip procedure in this study might not have been sensitive enough. RAG promoter-specific or genome-wide bisulfite-sequencing would yield precise information about genes regulated by DNA methylation upon nerve injury, even for the hypothesized small regional changes. Moreover, several publications indicated that gene body methylation, regarding the exon-intron structure, might be additionally relevant [Laurent et al. 2010]. These results should be carefully correlated with injury-related patterns of the above-mentioned histone modifications. Like this, information on the cross-talk interactions between the different epigenetic mechanisms can be obtained in the context of axonal regeneration, due to co-localization of different marks. For example, dimethylation of H3-K9 is known to approximately cooperate with DNA methylation and to inversely correlate with H3-K9 acetylation in gene repression for larger genomic regions [D'Alessio & Szyf 2006; J Wu *et al.* 2007a; T Chen 2011]. Instead of direct CpG methylation, binding patterns of methyl-CpG binding proteins, such as MECP2, could be assessed by ChIP as a good indicator for methylated promoter regions. MECP2 also facilitates local methylation of H3-K9 by SUV39H1 that binds DNMT proteins. This would enlighten the coordination of different epigenetic marks upon injury or pro-regenerative treatments [Fuks *et al.* 2003]. In addition, the set of injury-induced transcription factors should be comprehensively characterized to understand these connective links between injury site specific signals, chromatin-modifying enzymes, and functional target gene expression.

However, functional regeneration in the severely injured spinal cord is still unachievable. Altogether, the focus of basic and clinical research must be on understanding the mechanisms and coordinated orchestration of successful regeneration, on the one hand, and how to adapt or trigger them upon brain or spinal cord injury, on the other hand. Thereby, a complex combination of glial scar prevention, CNS myelin inhibition, neurotrophic factor application, and histone deacetylase inhibition might be promising, rather than single factors alone. Future strategies might further comprise anti-inflammatory treatment, or electrophysiological stimulation of neuronal function [Dooley *et al.* 1978; Kadoya et al. 2009; F Liu *et al.* 2009; SF Huang *et al.* 2011]. Additionally, a potent trigger, such as cAMP, might be found that resembles the promising effects of a conditioning peripheral lesion, which is a very potent inducer of axon sprouting.

5 Material and Methods

5 Material and Methods

5.1 Material

5.1.1 Buffers and Solutions, Chemicals and Reagents, Enzymes

Table 3 – Buffers and Solutions used for experiments performed by the author and by others, in part. Sterile distilled water or RNase-free water was used for buffers and solutions. Additional Buffers and solutions were used for DRG and CGN cell culture and treatment, and subsequent experiments (see text) [Puttagunta et al. (under revision)].

Buffers and Solutions	Composition
Hank's Balanced Salt Solution (HBSS)	Invitrogen, GIBCO, #14185-045
Phosphate Buffered Saline (PBS)	Invitrogen, GIBCO, #14190-094
Dulbecco's PBS	Invitrogen, #14080-048
DMEM +4,5g/l Glucose	PAA, #E15-843
HEPES Buffered Saline (HBS)	Sigma-Aldrich/Fluka, #51558-50ml
Fetal Bovine Serum (FBS)	Invitrogen, GIBCO. #10270-098
MeDIP Lysis Buffer	10 mM Tris/HCl, pH 8.0, 100 mM NaCl, 25 mM EDTA, 0.5 % SDS, 0.2 mg/ml Proteinase K
ChIP SDS Lysis Buffer (Millipore)	50 mM Tris, 1% SDS, 10 mM EDTA, pH 8.1
ChIP Dilution Buffer (Millipore)	16.7 mM Tris-HCl, 0.01% SDS, 1.1% Triton X-100, 1.2 mM EDTA, pH 8.1, 167 mM NaCl
Low Salt Wash Buffer (Millipore)	20 mM Tris-HCl, 0.1% SDS, 1% Triton X-100, 2 mM EDTA, pH 8.1,
High Salt Wash Buffer (Millipore)	20 mM Tris-HCl, 0.1% SDS, 1% Triton X-100, 2 mM EDTA, pH 8.1,
LiCl Wash Buffer (Millipore)	10 mM Tris, 0.25 M LiCl, 1% IGEPAL-CA630, 1% deoxycholic acid, 1 mM EDTA, pH 8.1
TE Buffer, pH 8.0 (Millipore)	10 mM Tris-HCl, 1 mM EDTA, pH 8.0
Elution Buffer	0.1 M NaHCO3, 1% SDS
EDTA Solution (Millipore)	0.5 M EDTA, pH 8.0
Tris/HCl Solution (Millipore)	1 M Tris-HCl, pH 6.5
Sodium Acetate Solution	3 M NaOAc, pH 5.2
Glycogen solution	20 mg/ml
Formaldehyde Solution	1% CH2O
SDS-PAGE Stacking Gel Buffer	0.5 M Tris (pH 6.8), 0.4% SDS
SDS-PAGE Separating Gel Buffer	1.5 M Tris (pH 8.8), 0.4% SDS
SDS-PAGE Running Buffer	25 mM Tris, 193 mM Glycin, 3.5 mM SDS
SDS-PAGE 6x Sample Buffer (Laemmli)	0.312 M Tris/HCL (pH 6.8), 10% SDS, 25% β-Mercaptoethanol, 50% Glycerol, 0.05% Bromophenol Blue
Western Blot Transfer Buffer	25 mM Tris, 192 mM Glycin
Tris Buffered Saline (TBS)	50 mM Tris (pH 7.4), 150 mM NaCl
TBS-Tween, Wash Buffer	50 mM Tris (pH 7.4), 150 mM NaCl, 0.1% Tween-20
Blocking Solution	TBS-T, 5% non-fat dried milk
Western Blot Stripping Solution	62.5 mM Tris (pH 7.6), 2% SDS, 100 mM β-Mercaptoethanol
Primary Antibody Solution	TBS-T, 5% non-fat dried milk, 0.02% Sodium Azide
Secondary Antibody Solution	TBS-T, 5% non-fat dried milk

The listed buffers, solutions, chemicals, reagents, and enzymes were used in experiments performed by the author (DRG extraction, DNA/RNA isolation, MeDIP-chip, qRT-PCR, preliminary ChIP on DRG, or preliminary DRG culture), or by Dr. Andrea Tedeschi and Dr. Tuan Nguyen (animal surgery), or by Dr. Elisa Floriddia (ChIP on DRG, Western Blot – see **Figure 20**). Additional materials (not shown) have been used for experiments contributed by Dr. Radhika Puttagunta (animal surgery, DRG or CGN cultures and treatment, AAV infection, Immunocytochemistry, ChIP on CGN; Western Blot, qRT-PCR, Luciferase assay - see **Figures 23 to 25** [Puttagunta et al. (under revision)].

Table 4 – Chemicals, reagents, and enzymes used in this thesis. The materials described in this table were used for (preliminary) experiments performed by the author and by others as explained in the text. Additional chemicals were used for DRG and CGN cell culture and treatment, and subsequent experiments (see text) [Puttagunta et al. (under revision)].

Chemical / Reagent / Enzyme	Company
Ammonium persulfate	Roth
Ampicillin	Roth
Chloroform	Merck
Collagenase Type II	Worthington Bioch. Corp.
Collagenase Type IA	Sigma-Aldrich
Cystine-L hydrochloride (anhydrous)	Sigma-Aldrich
DEPC water	Roth
Dispase II	Sigma-Aldrich
DMSO	Sigma-Aldrich
DNase I, Amplification Grade	Invitrogen
EDTA	Sigma-Aldrich
Ethanol (EMSURE®, for analysis)	Merck
Ethidium bromide	Roth
Formaldehyde, ≥ 37 %	Merck
Garcinol, ≥ 95 %	Sigma-Aldrich
HEPES	Roth
Isoamyl alcohol	Merck
Isoba®, Isofluran	Essex Tierarznei
Isopropanol/2-Propanol (EMSURE®, for analysis)	Merck
Laminin, mouse	Millipore
MassRuler™ 6x DNA Loading Dye	Fermentas
MassRuler™ Express Forward DNA Ladder Mix + Dye	Fermentas
Nerve Growth Factors (NGF), 2.5 S, mouse	BD Biosciences
Non-fat dried milk powder	AppliChem
Orange 6x DNA Loading Dye	Fermentas
O'Range Ruler™ 50bp DNA Ladder + Dye	Fermentas
Papain Suspension	Worthington/Cellsystems
Penicillin/Streptomycin	Invitrogen
PhosSTOP Phosphatase Inhibitor Cocktail tablets	Roche
Poly-D-Lysine (PDL) hydrobromide	Sigma-Aldrich
Protein A Agarose Salmon Sperm DNA (50% slurry)	Millipore/Upstate
Protein-G Magnetic Beads	Millipore/Upstate
Proteinase K	Invitrogen
Roti-Phenol/Chloroform/Isoamyl Alcohol (25:24:1)	Roth
Sodium chloride (NaCl)	Merck
Sodium dodecyl sulfate (SDS; for Molecular Biology)	AppliChem
Sigmacote (silicone solution)	Sigma
Sodium bicarbonate (NaHCO3)	Roth
TEMED	Roth
TriFast™ peqGold	peqGOLD
Tris Hydrochloride	Roth
Trizma® Base	Sigma-Aldrich
Trypsin, 0.25% with EDTA	Invitrogen
Tween® 20	Roth
UltraPure™ Agarose	Invitrogen
Yeast Extract	Sigma-Aldrich

5.1.2 Commercial Kits

Table 5 – Commercial kits and materials applied in this study by the author were summarized here and were indicated at appropriate positions in the Methods and Results sections. Additional kits and materials were used for DRG and CGN cell culture and treatment, and subsequent experiments (see text) [Puttagunta et al. (under revision)].

Commercial Kits / Material	Company
ABsolute QPCR SYBR® Green ROX Mix and Seals	Thermo Scientific
Chromatin Immunoprecipitation (ChIP) Assay Kit	Millipore/Upstate
GenElute™ PCR Clean-Up Kit	Sigma-Aldrich
GenomePlex® Complete Whole Genome Amplification (WGA) Kit	Sigma-Aldrich
High Pure RNA Parafin Kit	Roche
Phase Lock Gel™ (PLG) tubes, 1,5 ml, Heavy	5prime
QIAquick® PCR Purification Kit	Qiagen
SuperScript™ II RT, First-Strand cDNA Synthesis Kit	Invitrogen/Life Technologies
Taq PCR Master Mix Kit	Qiagen
TaqMan® Gene Expression Master Mix	ABS/Life Technologies

Furthermore, hardware and software used for MeDIP-chip analysis or for qRT-PCR will be described at the appropriate positions in the Methods and Results sections.

5.2 Methods

5.2.1 Animal Model and Surgery

All mice used for this work were treated according to Animal Welfare Act and to the ethics committee guidelines of the University of Tuebingen. C57BL/6 wild type mice (Charles River Laboratories International) were used for all experiments presented here, aged from 2 to 3 months or 6 to 8 weeks, respectively. Any treatment or surgery was performed in a way to avoid stress as much as possible. All surgical procedures were performed under aseptic technique and general anesthesia. For surgeries, mice were anesthetized with ketamine (100 mg/kg body weight) or with xylazine (10 mg/kg body weight), and with Isofluran/O_2 (Isoba®; initially 5 percent, maintained at 2 percent). Either sciatic nerve axotomy (SNA), or dorsal column axotomy (DCA), or the corresponding sham injury was performed on different sets of mice. Another set of naive mice received no surgery. Animal surgery was either performed by Dr. Andrea Tedeschi (DCA) or Dr. Tuan Nguyen (SNA; aged 2 to 3 months, for MeDIP-chip and qRT-PCR TaqMan Gene Expression Array), or by Dr. Elisa Floriddia (for ChIP on DRG and Western Blot), or by Dr. Radhika Puttagunta (aged 6 to 8 weeks, for DRG culture and subsequent experiments).

5.2.1.1 Sciatic nerve axotomy

Mice were anesthetized, and bilateral surgery was successively performed. At a distance of approximately 20 mm from L4-L6 DRG, a 10 mm skin incision was performed on the gluteal region at mid-thigh level. Muscles were displaced to expose the sciatic nerve for a complete

transection with spring micro-scissors. Finally, skin was closed with two suture clips. The nerve fiber was left intact for sham surgeries else, the same procedure was applied.

5.2.1.2 Dorsal Column Axotomy

Mice were anesthetized. Surgeries were performed as previously reported [Floriddia et al. 2012]. A T10 laminectomy was performed, approximately 20 mm far from L4-L6 DRG. An incision from T7 to T10 was made and superficial tissue displaced or carefully removed. Holding the spinous process, the side connecting bone was cut and the top half of the vertebrae was lifted away. A few drops of Xylocain were applied to anaesthetize the spinal cord. Then, the dura mater was removed taking care of not damaging the spinal cord. A bilateral dorsal hemisection until the central canal (0.3 to 0.4 mm depth) was performed with a microknife. For the control laminectomy surgery, the dura mater was removed but the dorsal hemisection was not performed. Finally, skin and tissue was closed with two suture clips.

5.2.2 DRG dissection and sample preparation for MeDIP

For each of the 3 time points and for each injury conditions (1, 3, 7 days after bilateral SNA or DCA, injury or sham, and naive), all L4-L6 DRG were collected from 2 mice and pooled for each one sample (in triplicate for injury and naive, and in duplicate for sham). Animals were deeply anesthetized and killed by cervical dislocation by stretching. As dissection method of choice, the spinal cord and DRG were exposed from the ventral direction. DRG were quickly dissected, kept in HBSS buffer on ice, cleaned, and frozen in liquid nitrogen. Frozen tissue was ground, lysed in 200 µl MeDIP lysis buffer and digested with 0.2 mg/ml Proteinase K overnight at 50 °C and shaking at 400 rpm. The lysate was then sonicated on ice to a chromatin size range of 100 to 2,000 bp, with 700 bp average (Bandelin Sonopuls GM70, type UW 70 sonication device with micropestle; 6 times, 10 seconds, 50 % pulse, 30 % power). Genomic DNA was extracted from the cleared lysate by standard phenol-chloroform extraction and ethanol precipitation procedure. Sonication efficiency was optimized and tested on agarose gel before performing Methylated DNA immunoprecipitation (MeDIP). DNA concentration and quality was assessed with a peqlab NanoDrop ND-1000 and on agarose gel.

5.2.3 Methylated DNA Immunoprecipitation

MeDIP procedure, subsequent Whole Genome Amplification (WGA), and sample preparation for Roche/NimbleGen DNA methylation microarrays (**Figure 27**) were performed by the author and according to a modified protocol adapted from Komashko et al. and, in part, from Weber et al., established and verified by the author [Weber et al. 2005; Komashko et al. 2008].

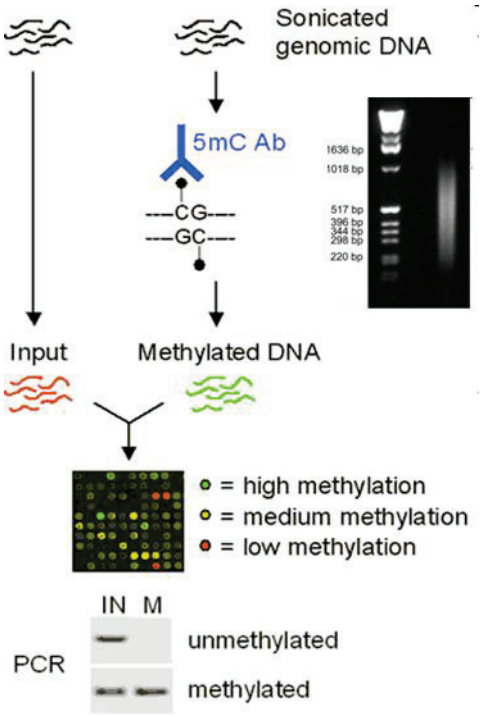

Figure 27 – Schematic of MeDIP-chip procedure. Sonicated genomic DNA was immunoprecipitated (IP) with a 5-methylcytosine antibody. IP (M) and genomic DNA (Input) samples were amplified supposedly up to 1,000-fold with a Whole Genome Amplification (WGA) Kit (Sigma-Aldrich) and purified. Each set of IP and Input sample libraries were conjugated with either Cy3 or Cy5 and co-hybridized on a DNA methylation sensitive tiling microarray (Roche/NimbleGen). Relative IP-to-Input enrichment of methylated DNA fragments was verified by PCR [modified from Weber, M. and Schübeler, D.; The Epigenome Network of Excellence; http://www.epigenesys.eu].

MeDIP was performed according to the protocol of the Chromatin Immunoprecipitation (ChIP) Kit from Upstate/Millipore. 10 µg of sonicated purified genomic DNA were added to a total volume of 150 µl of ChIP SDS lysis buffer, denatured for 10 min at 95 °C, and quickly chilled on ice. Samples were then diluted 10-fold in ChIP Dilution Buffer. To reduce non-specific background, diluted samples were pre-incubated with 75 µl of Protein A/G agarose beads (50 percent slurry with salmon sperm DNA) and incubated for 30 min at 4 °C with agitation. The supernatant was incubated with 5 µg of a 5-methylcytosine antibody (Eurogentec, BI-MECY-0100) to immunoprecipitate methylated DNA fragments overnight and under agitation at 4 °C. A no-antibody negative control was used in parallel. Antibody-DNA complexes were incubated with 60 µl of Protein A/G agarose beads for 1 hour at 4 °C with agitation. Beads were briefly pelleted and the supernatant kept at -20 °C. Immune complexes were successively washed with Low Salt, High Salt, LiCl, and twice with TE Wash Buffer followed by elution of the DNA/antibody/bead complexes by adding twice 250 µl of freshly prepared Elution Buffer and incubating for 15 min at RT under agitation. The eluated complexes were digested with 0.1 mg/ml Proteinase K for 1 hour at 45 °C under agitation after adding 10 µl of 0.5 M EDTA and 20 µl of 1 M Tris/HCl, pH 6.5 to 500 µl eluate. DNA was the recovered from IP or no-antibody control samples by standard phenol/chloroform extraction and ethanol precipitation (EtOH/NaOAc/glycogen). Finally, samples were resuspended in 40 µl TE buffer. Regular PCR was employed to test MeDIP efficiency prior to performing the

real MeDIP-chip experiments upon nerve injury. IP and Input samples from naive mice were tested for 4 primer sets targeting the methylated *H19* imprinting control region (ICR). This verification was conducted as a modified procedure after Weber, M. et al. performed on sonciated genomic DNA. Primer sequences for *H19* ICR, *Act* as negative control, or "*CSa"* as positive control were obtained from the same publication [Weber et al. 2005]. Standard PCR was performed with 5 to 10 ng of IP or Input DNA, using the Taq PCR Master Mix Kit (Qiagen) and the following cycling program: 1. 94 °C for 3 min, 2. 94 °C for 30 s, 3. 60 °C for 30 s, 4. 72 °C for 45 s (45 cycles for steps 2. to 4.), 5. 72 °C for 3 min, 6. holding 4 °C.

5.2.4 Whole genome amplification

Due to the low IP sample yield in the range of a few hundred nanograms, the GenomePlex® Complete Whole Genome Amplification (WGA) Kit (#WGA2, Sigma-Aldrich) was performed to amplify 20 ng of IP and Input samples to a maximum yield of 3 to 7 µg. Representation analysis has been verified before in order to prove representative amplification with minimal sequence bias [Barker *et al.* 2004; Gribble *et al.* 2004]. This kit utilized a proprietary amplification method based on random fragmentation of genomic DNA and conversion of the resulting smaller fragments to PCR-amplifiable OmniPlex® Library molecules that exhibit flanking universal priming sites. The OmniPlex library was then PCR amplified using universal oligonucleotide primers. Since in this study genomic DNA was already fragmented due to sonication, the first step of the WGA kit was modified to eliminate the fragmentation step. IP or Input samples were amplified, together with a positive Human Control DNA sample to verify amplification success (provided). According to the manufacturer's protocol, Fragmentation Buffer, Library Preparation Buffer, and Library Stabilization Solution were added to the sample. The reaction mix was incubated for 2 min at 95 °C, cooled on ice, and Library Preparation enzyme was added. Library formation was achieved with the recommended thermocycler program: 1. 20 min at 16 °C, 2. 20 min at 24 °C, 20 min at 37 °C, 5 min at 72 °C, and holding 4 °C. Further, Amplification Master Mix, nuclease-free water, and WGA DNA Polymerase were added. The complete reaction mix was amplified according to the following thermocycler program: 1. 3 min at 95 °C, 20 cycles of: 2. 15 sec at 94 °C, 3. 5 min at 65 °C, and holding 4 °C. Samples were subsequently column-purified, as recommended, using the GenElute™ PCR Clean-Up Kit (Sigma) to remove residual nucleotides and fragments smaller than 100 to 200 bp, according to the manufacturer's protocol. DNA concentration and quality was assessed with a peqlab NanoDrop ND-1000. Samples were adjusted to a concentration of 250 ng/µl in order to meet Roche/NimbleGen's instructions for DNA sample quality (see "NimbleChip™ Arrays User's Guide for DNA Methylation Analysis"). For all samples, very good ratios were measured (A_{260}/A_{280} = 1.92 ± 0.04 and of A_{260}/A_{230} = 2.3 ± 0.05).

5.2.5 DNA Methylation Microarray

Preparation of MeDIP-WGA samples for the DNA methylation microarray analysis was described before [Komashko et al. 2008]. 5 µg of each WGA sample (triplicate or duplicate sample sets of IP and Input for each condition) were sent to the Roche/NimbleGen facility for proceeding with DNA methylation sensitive tiling microarrays. Briefly, for each microarray a corresponding pair of IP and Input samples was prepared for hybridization. Each 1 µg was labeled with Cy3 and Cy5, respectively, and co-hybridized on a "2007-02-27 MM8 CpG Island Promoter (385K RefSeq)" tiling microarray. This array type covered the proximal promoter regions and CpG islands (CGIs) of more than 18.000 genes, each represented by several close-set oligonucleotide probes. Genes and promoters were thus represented by regions of approximately 1,500 bp upstream and 800 bp downstream of a transcription start site (TSS). Fluorescence intensity raw data was obtained from scanned images of the tiling arrays using NimbleScan extraction software. For each spot on the array, Cy5/Cy3 ratios were calculated and normalized to obtain log2 values for enrichment. Then, the bi-weight mean of log2 values for each region was subtracted from each data point to center the ratio data to zero, similar to a mean-normalization.

5.2.6 Quantitative Real-Time RT-PCR

5.2.6.1 RNA extraction and cDNA synthesis

Total RNA was extracted and pooled from dissected L4-L6 DRG of 3 mice for each experimental condition applying the High Pure RNA Parafin Kit (Roche) following the manufacturer's protocol. RNA concentration was determined with a peqlab NanoDrop ND-1000. cDNA was synthesized from 1 µg of total RNA using the SuperScript™ II Reverse Transcriptase kit (Invitrogen) with oligo(dT) primers, according to the manufacturer's protocol. 5 µl of 1:25 diluted cDNA was used in qRT-PCR experiments using ABsolute QPCR SYBR® Green ROX Mix (Thermo Scientific) on an ABI 7000 Real Time PCR System (ABS/Life Technologies).

5.2.6.2 Custom TaqMan Gene Expression Array

A qRT-PCR-based Custom TaqMan® Gene Expression Array (ABS/Life Technologies) was applied to test injury-induced gene expression of differentially methylated (DM) genes from the microarray study. TaqMan primer sets (sense, antisense, and FAM-probe) for 38 DM genes were provided by the manufacturer, together with controls (18S RNA, *Act*, *Gapdh*). For each gene, samples for the 4 main conditions and for the specific time point of differential methylation were assayed using TaqMan® GEx Master Mix on an ABI 7000 Real Time PCR System (ABS/Life Technologies). TaqMan primer sets (assays) were delivered in a lyophilized form in suitable 96-well plates arranged in a customized array pattern. Standard cycling

parameters were applied for qRT-PCR: 1. 94 °C for 10 min, 2. 95 °C for 15 s, 3. 60 °C for 60 s (40 cycles for steps 2. to 4.), 5. holding 4 °C. Relative quantification of fold change expression ratios were calculated according to standard delta-ct method normalized to the *Act* reference gene. Additional qRT-PCR experiments for DM gene expression were performed with self-designed primers to verify TaqMan Gene Expression Array data (data not shown).

5.2.7 Promoter CGI analysis

Several major RAGs and DM genes (from DNA methylation microarray analysis) were analyzed for CGI and CpG dinucleotide distribution. The complete genomic plus promoter region (5,000 bp upstream of the TSS) was obtained from the Ensembl genome browser database (www.ensembl.org) updated for 2011 entries. The identity of the major transcript was confirmed by the UniProtKB database (www.uniprot.org/uniprot/). Genomic sequences were analyzed with the EMBOSS CPGPlot online tool from EMBL-EBI, applying standard parameters: observed-to-expected (obs/exp) ratio > 0.6 and (C+G) content > 50 percent for at least 200 bp. In several cases, a CGI size of 100 bp was allowed. Multiple CGIs in very close proximity were combined to one large CGI. Additionally, the normalized CpG values were calculated as the obs/exp CpG ratio (**Formula 2**) for the symmetrical 3 kb region around the TSS of the selected RAGs and DM genes, according to Saxonov et al. [Saxonov et al. 2006].

Formula 2 obs/exp CpG ratio = (Number of CpG · 3 kb) / (Number of C · Number of G)

5.2.8 Chromatin Immunoprecipitation

The ChIP protocol described in this section applies to the ChIP experiments on DRG for H3-K9ac or H3-K9me2, conducted by Dr. Elisa Floriddia and by the author (**Figures 21 and 22**). Further ChIP experiments on cerebellar granule cells (CGN) were conducted by Dr. Radhika Puttagunta (**Figures 24 C+D**) according to a slightly modified procedure [Puttagunta et al. (under revision)]. Briefly, ChIP on DRG was performed following a modified version of the Upstate ChIP Kit protocol. In particular, magnetic beads were used instead of Protein A/G agarose beads. From 6 mice for each condition, all L4-L5 DRG were dissected 1 day following either SNA or DCA (injury or sham) and collected in cold HBSS buffer. Cleaned DRG were fixed and chromatin cross-linked in 1 percent formaldehyde for 30 min at RT and stopped with 125 mM glycine. Fixed DRG were lysed in 400 µl ChIP SDS Lysis Buffer (Upstate ChIP Kit) and sonicated on ice to disrupt cross-linked chromatin. The sonication procedure was optimized to the following procedure: 8 times, 50 percent pulses for 10 s at 70 percent power applying a Bandelin Sonopuls GM70 type UW 70 sonication device with micropestle. Reverse cross-linked control samples were verified on agarose gel (fragment size range: 200 to 1,000 bp). Sheared chromatin samples were equally split into IP and IgG antibody control samples and diluted with ChIP Dilution Buffer including PhosSTOP

Phosphatase Inhibitor Cocktail (Roche). 1 percent of the diluted sample was kept as Input. Antibodies for H3-K9ac or H3-K9me2 (Cell Signaling) were added to the diluted samples and incubated overnight at 4 °C under agitation. Then, antibody-chromatin complexes were immunoprecipitated by adding 30 µl of Protein-G Magnetic Beads, incubated for 2 hours at 4 °C with rotation. Beads were pulled-down and washed accordingly to the manufacturer's protocol, as described before, and eluted in 300 µl of ChIP Elution Buffer (Input included from now on) by incubation for 30 min at 65 °C with gentle agitation. 200 mM NaCl and 0.2 mg/ml Proteinase K were added to the eluates and incubated for 2 hours at 65 °C. DNA was recovered by standard Phenol/Chloroform extraction and ethanol precipitation and resuspended in 20 µl of RNase-free water. Quantitative real-time PCR was run using ABsolute QPCR SYBR® Green ROX Mix (Thermo Scientific) on an ABI 7000 Fast Real Time PCR System (ABS/Life Technologies). Relative gene expression (fold changes) was calculated according to the standard delta-ct method from a triplicate dataset using the SEM, as previously reported [Tedeschi et al. 2009b; Tedeschi et al. 2009c]. Primers designed by Dr. E. Floriddia targeted the proximal promoter region within 1,000 bp upstream the TSS.

5.2.9 Primers and Design Software

All primers in **Table 6** target mouse sequences and were used as 100 µM stocks and 10 µM working dilutions in RNase-free water. Primers for SYBR Green qRT-PCR were either obtained from Weber, M. et al. (MeDIP verification), designed by me or colleagues from the research group, or obtained from the Primer Bank (http://pga.mgh.harvard.edu/primerbank/) [Weber et al. 2005]. Dr. E. Floriddia designed primers for RAG promoter ChIP (DRG) and partly for RAG mRNA. qRT-PCR primers for DM genes and for several RAGs were designed by the author. Primer sets with FAM probes for the TaqMan® Gene Expression Array were provided by ABS/Life Technologies. Other primers were provided on order by Invitrogen/Life Technologies (for MeDIP, ChIP, and qRT-PCR). Additional primers for RAG expression and ChIP on CGN were used by Dr. R. Puttagunta [Puttagunta et al. (under revision)]. **Table 7** displays the software tools used to design and verify primer sequences.

Table 6 – Primers used in this study. The different primer sequences were designed either by the author (LR, Ricco Lindner) or by colleagues from the author's research group (FE, Elisa Floriddia; TA, Andrea Tedeschi), or obtained from Weber et al. (WM), or from the Primer Bank (PrB) [Weber et al. 2005; Tedeschi et al. 2009b]. Primers for MeDIP or ChIP targeted mouse genomic DNA (*H19*) or the proximal gene promoter region. Primers for qRT-PCR or for the TaqMan Gene Expression Array targeted cDNA synthesized from mouse DRG mRNA. FAM probes were used for the TaqMan Array with primers obtained from Applied Biosystems (ABS)/Life Technologies. Src. Source

MeDIP	Target Gene	Tm	Sequence forward	Tm	Sequence reverse	Src.
genomic	beta-Actin	61 °C	AGCCAACTTTACGCCTAGCGT	63 °C	TCTCAAGATGGACCTAATACGGC	*WM*
	Spop/"CSa"	62 °C	TGGTTGGCATTTTATCCCTAGAAC	60 °C	GCAACATGGCAACTGGAAACA	*WM*
	H19.1	61 °C	ACATTCACACGAGCATCCAGG	60 °C	GCTCTTTAGGTTTGGCGCAAT	*WM*
	H19.2	60 °C	GCATGGTCCTCAAATTCTGCA	58 °C	GCATCTGAACGCCCCAATTA	*WM*
	H19.3	58 °C	TGCCAGAAAGCACAAAAGCC	58 °C	TGGCCCTTGGACATTGTCAT	*WM*
	H19.4	58 °C	GCCCAAATGCTGCCAACTT	61 °C	ACCATTCCAGAGGTGCACACA	*WM*

qRT-PCR	Target Gene Tm	Sequence forward	Tm	Sequence reverse	Src.
TaqMan	18S, human	GGAGGGCAAGTCTGGTGCCAGCAGC		*Hs99999901_s1*	*ABS*
	Acbd6	CAAGCAGGTCAAAGTTGGAAATTGC		*Mm00511524_m1*	*ABS*
	Actb	CCCTAGGCACCAGGGTGTGATGGTG		*Mm01205647_g1*	*ABS*
	Adra1d	CTTCGTCCTGCCTCTGGGTTCTCTG		*Mm01328600_m1*	*ABS*
	Agr3	ACCCCAGGACTTACCCATGTTGGTA		*Mm01291825_m1*	*ABS*
	Ak3l1	TGGCAAACTGCACAATTCTTGCCAG		*Mm00784745_s1*	*ABS*
	Ampd3	TACTGTGCAGGGATCACTGTGGAAG		*Mm00477495_m1*	*ABS*
	Angptl7	GCAGACCTCGGCAGATGCCATCTAC		*Mm01256626_m1*	*ABS*
	Arhgap10	CCACCACGCCAAGCCAGACCCGGCC		*Mm00518722_m1*	*ABS*
	Arl4c	TTAAGGGTGCAGTTGACTGTTAGTA		*Mm00844558_s1*	*ABS*
	Cbx4	TTCCAGAACAGGGAAAGGCAGGAGC		*Mm00483089_m1*	*ABS*
	Cdyl2	TGCAGTGCTGTGGTTTTGGAGGAGT		*Mm00512756_m1*	*ABS*
	Cul3	TTCAAACAGTTGCAGCCAAACAAGG		*Mm00516747_m1*	*ABS*
	D16Ertd472e	CGAGCTAAATCTCGAGGGAGTGCCA		*Mm00508954_m1*	*ABS*
	Dpp10	CAACCCATCAAGGTATTTCCTCTTG		*Mm01284946_m1*	*ABS*
	Dpysl5	GAGGGGCGTGGTTGGAGGAAAGATG		*Mm00491680_m1*	*ABS*
	Emid1	GCGCTGGAGGCCAAGGTGGCGGTGC		*Mm00499768_m1*	*ABS*
	Gapdh	GTGAACGGATTTGGCCGTATTGGGC		*Mm99999915_g1*	*ABS*
	Gnat1	ATTCAGCCCGGCAGGATGATGCCCG		*Mm00492388_g1*	*ABS*
	Kif21a	ACCTCAGGGCAAAATTATTAGAAAG		*Mm00497322_m1*	*ABS*
	Kif22	TTTCCTGAAGGCGAATCTCTTGAGC		*Mm00521174_g1*	*ABS*
	Kif3c	TGCCAGCTGGAGTGAATAACAGCCA		*Mm00492902_m1*	*ABS*
	Krt4	ACCAGATCAAGGTCCAGCAGCTCCA		*Mm00492996_g1*	*ABS*
	Maml3	AGGTCAACCAGTTTCAAGGTTCACC		*Mm01294189_m1*	*ABS*
	Map3k4	CACAGCCCTGTCACAGCTATCCATC		*Mm00442468_m1*	*ABS*
	Otop2	GGGGACAAAGTCGGCACCGGTCCAG		*Mm00555643_m1*	*ABS*
	Plxna3	AGTACCGTCAGGAGATCCTCACCTC		*Mm00501170_m1*	*ABS*
	Ptpn9	TTCCACTGCTACAGAGAAACAAGAA		*Mm00451036_m1*	*ABS*
	Rbpjl	GGGGAGTTGGACCAGGTCACCCCCA		*Mm00485631_m1*	*ABS*
	Sap130	CCTAGACCTGCAGGTGCCAAACCTA		*Mm00556995_m1*	*ABS*
	Slc10a4	CGGCGACATGAACCTCAGCATCATC		*Mm00557788_m1*	*ABS*
	Slc7a10	GGGCCTGGCTGGATTCCTACTGCTC		*Mm00502045_m1*	*ABS*
	Smarcc2	AGTCAAGGCCAAGCACTTGGCTGCA		*Mm01159912_m1*	*ABS*
	Stk3	AGGAAGAAAACTCGGATGAAGATGA		*Mm00490480_m1*	*ABS*
	Tprgl	CCGAAGTCGCTCAACAAGAGAGAAG		*Mm00509510_m1*	*ABS*
	Trpc1	GGCCCACTGCAGATTTCAATGGGAC		*Mm00441975_m1*	*ABS*
	Ubn2	CAGCCAGTGTGCAGTCCACAGCAGG		*Mm00723981_m1*	*ABS*
	Wnt2b	ACACGTCCTGGTGGTACATAGGGGC		*Mm00437330_m1*	*ABS*
	Ythdf1	ACAGTCCAATCCGAGTAACAGTTAC		*Mm00620538_m1*	*ABS*

qRT-PCR	Target Gene	Tm	Sequence forward	Tm	Sequence reverse	Src.
cDNA	Dnmt1	63 °C	GTGGTGTCTGTGAGGTCTGTC	63 °C	AAGTTAGGACACCTCCTCTTGAG	*RL*
	Dnmt3a	61 °C	AGGGAGGCTGAGAAGAAAGC	58 °C	GGCTGCTTTGGTAGCATTCT	*RL*
	Dnmt3b	61 °C	AGTTTCCGGCTACCAGGTCT	61 °C	TGTGCTGTCTCCATCTCTGC	*RL*
	Abl2	61 °C	ACCCAGCACGATCACTTTGC	60 °C	CGCAGCTTTTCACCTTTAGTGA	*RL*
	Cbx4	60 °C	GGATACGCAAGGGCAGAGT	61 °C	GAGCGTCGGGCAAAGGTG	*RL*
	Cdyl2	60 °C	TGCTGGCTGTTCCTCCTAC	61 °C	GACCTCTTGGCTGAAAGTCG	*RL*
	Cul3	61 °C	AAGGTGGTGGAGAGGGAACT	60 °C	GTCTTCAAACCATTTGGCACAC	*RL*
	Kif21a	60 °C	ACTTCCTGTCAATGGGCATCA	61 °C	TGCTGTCCTCCTCGTTTTCTG	*RL*
	Kif22	61 °C	CCTGCAACTAGCAAGGGAAG	61 °C	TGGCTCCTACAGCTCGATTTC	*RL*
	Kif3c	61 °C	TCCCATCCCAGATACAGAGC	61 °C	CCAGAAAGCTGTCCAACCTC	*RL*
	Maml3	60 °C	ACACATCTGGCTGGTTTTCCT	61 °C	TGGAAGTCTGGAGGGAGAGA	*RL*
	Plxna3	61 °C	CGCTGTTGATGGCAAGTCTGA	61 °C	GAAGGAGGCACTGACAAAGC	*RL*
	Sap130	60 °C	CACATTGGAGCTTCCCACTTA	61 °C	TCTGGTGGCTGAGACTGTTG	*RL*
	Smarca2	61 °C	TGAGAGGGTGGAGAAGCAGT	61 °C	GCAATGGTCTGGATGGTCTTG	*RL*
	Smarcc2	60 °C	TGAGGTCCCCAAGAAAGATGA	60 °C	AGGTTGCCTTCACCAATGTCA	*RL*
	Tprgl	61 °C	CAGATGGAACCCCTGGTCTA	61 °C	CTCTCCTTCTGGGCCTTCTT	*RL*
	ZA20d1	60 °C	GTGGCAGAAGGAATGGAATGAA	60 °C	ACATGAGCAAGGACGAAGACA	*RL*
	BDNF	61 °C	ATGGGGGTACTCTGAAACTCC	61 °C	TACTTCTTTCATGGGCGCCG	*FE*
	Basp1	69 °C	GGCGGCAGCGCTCCAACTCG	69 °C	CCGCCTGGGGTTCGCTCTCC	*FE*
	Chl1	65 °C	GAATTGCCATTATGTGGAAGAGGACT	67 °C	TTTTGGAACCCCTGGTACTATGAACTC	*FE*
	Galanin	61 °C	TGCAGTAAGCGACCATCCAG	61 °C	TCTTCTCCTTTGCGGCATCC	*FE*
	Gap43	62 °C	AAGCTACCACTGATAACTCGCC	62 °C	CTTCTTTACCCTCATCCTGTCG	*TA*
	L1cam	71 °C	ATGCTGCGGTACGTGTGGCCTCTC	69 °C	CCACTTGGGGGCACCCTCGG	*FE*
	Lgals1	71 °C	GCTGGTGGAGCAGGTCTCAGGAATCT	70 °C	AAGGTGATGCACTCCTCTGTGATGCTC	*FE*
	Stmn2	71 °C	AGACTCCTCTCTCGCTCTCTCCGC	70 °C	AGCCTCTTGAGACTTTCTTCGCTCCTC	*FE*
	Sprr1a	58 °C	TTGTGCCCCCAAAACCAAG	63 °C	GGCTCTGGTGCCTTAGGTTG	*PrB*
ChIP	**Target Gene**	**Tm**	**Sequence forward**	**Tm**	**Sequence reverse**	**Src.**
promoter	Basp1	56 °C	TTCCTAGGGTGCATTTCTTC	58 °C	ACAGATATCCGCTGGTTTTAG	*FE*
	Bdnf	63 °C	GGAGACTAGCGCCGATCTTC	63 °C	CGAGCCACTAGTTGCCCACA	*FE*
	Chl1	58 °C	TGGCTCTTAAATGGTTGTGTTAT	58 °C	TTCCATCATTCCTCAGAAAGG	*FE*
	Galanin	63 °C	AGCAGCGGTGAGTGACTCTGT	63 °C	GCGCTGCTGCCGCTATTTATG	*FE*
	Gap43	60 °C	CTGGGAAAGAGGAGAGTTAGA	58 °C	CTGACTTTCCGCACTGCATT	*FE*
	L1cam	61 °C	GCTGCACCATCCACTCTCTT	61 °C	TCACGACCATCTTGCTGTCAG	*FE*
	Lgals1	63 °C	CTGACTGGTCACCTCTGCTC	63 °C	CAGTCAGAAGACTCCACCCGA	*FE*
	Stmn2	61 °C	CAGCACCATTGGCCGATCAA	61 °C	GTCTGAGTAAGGCACTGAGTC	*FE*
	Sprr1a	63 °C	GAGGAGGAGGGTGACAGAGAA	63 °C	GGCATTGGGCAGCTGGCTTTT	*FE*

Table 7 – Software tools applied for primer design.

Software Tools	Webpage	Purpose
Primer3 v.0.4.0	http://frodo.wi.mit.edu/primer3/	Basic primer design
Esembl Genome Browser	www.ensemble.org	cDNA sequence
UniProtKB database	www.uniprot.org/uniprot/	Transcript check
OligoCalc	www.basic.northwestern.edu/biotools/oligocalc.html	Tm calculation, BLASTn
NetPrimer	www.premierbiosoft.com/netprimer/	Primer interactions
UCSC In-Silico PCR	http://genome.ucsc.edu/	Specificity, byproducts

5.2.10 Primary Cell Culture, Immunocytochemistry and Analysis, Western Blot, AAV Infection, Luciferase Assay

Methods applied by Dr. R. Puttagunta resulting in the data of **Figures 23, 24, and 25** are not described in detail here, instead it shall be referred to the submitted publication [Puttagunta et al. (under revision)]. Briefly, dissociated DRG neurons were cultured on glass coverslips coated with mouse laminin (Millipore) or on rat CNS myelin (4 μg/cm^2). Cultured cells were infected with either PCAF-GFP-AAV or GFP-AAV as control, both available in the research group, or AAV was injected into the sciatic nerve [KK Park et al. 2008]. Immunocytochemistry for DRG was performed as previously reported, using the marker of differentiated neurons, TUJ1 (TUBB3), and DAPI for nuclei [Puttagunta et al. 2011]. Outgrowth potential was assessed by image analysis of longest neurites from pictures taken with an Axiovert 200 microscope and an Axiocam MRm CCD camera (Zeiss), and analyses was done with the Neurolucida software (MicroBrightField). Substrate-dependent RAG expression upon PCAF overexpression or GFP control was assessed by qRT-PCR (**Figure 23 A to C**). In addition to DRG neurons, cerebellar granule neurons (CGN) were cultured on coverslips coated with Poly-D-lysine (PDL) or on CNS myelin, and infected with AAV-PCAF-GFP or AAV-GFP. CGN were prepared from cerebellum of 7-day-old C57Bl6/J mice following standard procedures [Puttagunta et al. 2011]. Neurite length analysis was performed analogous to DRG cultures (**Figure 23 D**). Total levels of H3-K9ac in cultured CGN on both substrates were assessed using antibodies for H3-K9ac (Cell Signaling) and GAPDH. ChIP was performed for CGN on PDL or myelin upon PCAF overexpression or GFP control. Quantitation of protein expression was performed by densitometry (Image J software). Promoter occupancy was assessed for several RAGs (**Figure 24**). Additionally, CGN cultured on PDL were treated for 24 hours with 5 μM Garcinol (Sigma-Aldrich), and immunocytochemistry was performed for TUJI (TUBB3), H3-K9ac, and DAPI. Neurite length was determined upon Garcinol treatment. CGN on PDL were further electroporated (Rat neuron nucleofactor kit, Amaxa Biosystems) with a Gap43-promoter luciferase reporter construct [Nguyen T, 2009 J Biol Chem]. All experiments were performed in triplicate, data was plotted as mean ± SEM, and significant differences were analyzed by ANOVA with Bonferroni post-hoc tests, Student's t-test or two-way ANOVA. Standard Western Blot procedure was performed by Dr. E. Floriddia for **Figure 20** using either an antibody for H3-K9/K14ac or H3-K9me2 (Cell Signaling).

6 Bibliography / List of References

Aapola, U., Lyle, R., et al. 2001. Isolation and initial characterization of the mouse Dnmt3l gene. *Cytogenet Cell Genet,* **92,** 122-126.

Abdanipour, A., Schluesener, H. J., et al. 2012. Effects of valproic acid, a histone deacetylase inhibitor, on improvement of locomotor function in rat spinal cord injury based on epigenetic science. *Iran Biomed J,* **16,** 90-100.

Abe, N. & Cavalli, V. 2008. Nerve injury signaling. *Curr Opin Neurobiol,* **18,** 276-283.

Adorjan, P., Distler, J., et al. 2002. Tumour class prediction and discovery by microarray-based DNA methylation analysis. *Nucleic Acids Res,* **30,** e21.

Akbik, F., Cafferty, W. B., et al. 2011. Myelin associated inhibitors: A link between injury-induced and experience-dependent plasticity. *Exp Neurol*.

Allan, S. M. & Rothwell, N. J. 2003. Inflammation in central nervous system injury. *Philos Trans R Soc Lond B Biol Sci,* **358,** 1669-1677.

Allfrey, V. G., Faulkner, R., et al. 1964. Acetylation and Methylation of Histones and Their Possible Role in the Regulation of Rna Synthesis. *Proc Natl Acad Sci U S A,* **51,** 786-794.

Amir, R. E., Van den Veyver, I. B., et al. 1999. Rett syndrome is caused by mutations in X-linked MECP2, encoding methyl-CpG-binding protein 2. *Nat Genet,* **23,** 185-188.

Antequera, F. 2003. Structure, function and evolution of CpG island promoters. *Cell Mol Life Sci,* **60,** 1647-1658.

Antequera, F. & Bird, A. 1993. Number of CpG islands and genes in human and mouse. *Proc Natl Acad Sci U S A,* **90,** 11995-11999.

Atwal, J. K., Pinkston-Gosse, J., et al. 2008. PirB is a functional receptor for myelin inhibitors of axonal regeneration. *Science,* **322,** 967-970.

Aubert, I., Ridet, J. L., et al. 1998. Expression of L1 and PSA during sprouting and regeneration in the adult hippocampal formation. *J Comp Neurol,* **399,** 1-19.

Auclair, G. & Weber, M. 2012. Mechanisms of DNA methylation and demethylation in mammals. *Biochimie,* **94,** 2202-2211.

Balasubramanyam, K., Altaf, M., et al. 2004. Polyisoprenylated benzophenone, garcinol, a natural histone acetyltransferase inhibitor, represses chromatin transcription and alters global gene expression. *J Biol Chem,* **279,** 33716-33726.

Bannister, A. J. & Kouzarides, T. 2011. Regulation of chromatin by histone modifications. *Cell Res,* **21,** 381-395.

Bareyre, F. M., Garzorz, N., et al. 2011. In vivo imaging reveals a phase-specific role of STAT3 during central and peripheral nervous system axon regeneration. *Proc Natl Acad Sci U S A,* **108,** 6282-6287.

Barker, D. L., Hansen, M. S., et al. 2004. Two methods of whole-genome amplification enable accurate genotyping across a 2320-SNP linkage panel. *Genome Res,* **14,** 901-907.

Bartels, S. J., Spruijt, C. G., et al. 2011. A SILAC-based screen for Methyl-CpG binding proteins identifies RBP-J as a DNA methylation and sequence-specific binding protein. *PLoS One,* **6,** e25884.

Barton, C. A., Hacker, N. F., et al. 2008. DNA methylation changes in ovarian cancer: implications for early diagnosis, prognosis and treatment. *Gynecol Oncol,* **109,** 129-139.

Bedford, M. T. & Clarke, S. G. 2009. Protein arginine methylation in mammals: who, what, and why. *Mol Cell,* **33,** 1-13.

Benfey, M. & Aguayo, A. J. 1982. Extensive elongation of axons from rat brain into peripheral nerve grafts. *Nature,* **296,** 150-152.

Benowitz, L. I. & Routtenberg, A. 1997. GAP-43: an intrinsic determinant of neuronal development and plasticity. *Trends Neurosci,* **20,** 84-91.

Benson, M. D., Romero, M. I., et al. 2005. Ephrin-B3 is a myelin-based inhibitor of neurite outgrowth. *Proc Natl Acad Sci U S A,* **102,** 10694-10699.

Berger, S. L. 2007. The complex language of chromatin regulation during transcription. *Nature,* **447,** 407-412.

Bernstein, B. E., Meissner, A., et al. 2007. The mammalian epigenome. *Cell,* **128,** 669-681.

Bernstein, E., Duncan, E. M., et al. 2006. Mouse polycomb proteins bind differentially to methylated histone H3 and RNA and are enriched in facultative heterochromatin. *Mol Cell Biol,* **26,** 2560-2569.

Berry, M. 1982. Post-injury myelin-breakdown products inhibit axonal growth: an hypothesis to explain the failure of axonal regeneration in the mammalian central nervous system. *Bibl Anat***,** 1-11.

Bestor, T. H. 2000. The DNA methyltransferases of mammals. *Hum Mol Genet,* **9,** 2395-2402.

Bhalala, O. G., Pan, L., et al. 2012. microRNA-21 regulates astrocytic response following spinal cord injury. *J Neurosci,* **32,** 17935-17947.

Bhutani, N., Burns, D. M., et al. 2011. DNA demethylation dynamics. *Cell,* **146,** 866-872.

Biermann, J., Grieshaber, P., et al. 2010. Valproic acid-mediated neuroprotection and regeneration in injured retinal ganglion cells. *Invest Ophthalmol Vis Sci,* **51,** 526-534.

Bilinski, P., Wojtyla, A., et al. 2012. Epigenetic regulation in drug addiction. *Ann Agric Environ Med,* **19,** 491-496.

Bird, A. 2002. DNA methylation patterns and epigenetic memory. *Genes Dev,* **16,** 6-21.

Bird, A. P. 1986. CpG-rich islands and the function of DNA methylation. *Nature,* **321,** 209-213.

Blesch, A., Lu, P., et al. 2012. Conditioning lesions before or after spinal cord injury recruit broad genetic mechanisms that sustain axonal regeneration: superiority to camp-mediated effects. *Exp Neurol,* **235,** 162-173.

Blits, B., Dijkhuizen, P. A., et al. 2000. Intercostal nerve implants transduced with an adenoviral vector encoding neurotrophin-3 promote regrowth of injured rat corticospinal tract fibers and improve hindlimb function. *Exp Neurol,* **164,** 25-37.

Boeke, J., Ammerpohl, O., et al. 2000. The minimal repression domain of MBD2b overlaps with the methyl-CpG-binding domain and binds directly to Sin3A. *J Biol Chem,* **275,** 34963-34967.

Bogdanovic, O. & Veenstra, G. J. 2009. DNA methylation and methyl-CpG binding proteins: developmental requirements and function. *Chromosoma,* **118,** 549-565.

Bomze, H. M., Bulsara, K. R., et al. 2001. Spinal axon regeneration evoked by replacing two growth cone proteins in adult neurons. *Nat Neurosci,* **4,** 38-43.

Bonfils, C., Beaulieu, N., et al. 2000. Characterization of the human DNA methyltransferase splice variant Dnmt1b. *J Biol Chem,* **275,** 10754-10760.

Bonilla, I. E., Tanabe, K., et al. 2002. Small proline-rich repeat protein 1A is expressed by axotomized neurons and promotes axonal outgrowth. *J Neurosci,* **22,** 1303-1315.

Bosse, F., Hasenpusch-Theil, K., et al. 2006. Gene expression profiling reveals that peripheral nerve regeneration is a consequence of both novel injury-dependent and reactivated developmental processes. *J Neurochem,* **96,** 1441-1457.

Bosse, F., Kury, P., et al. 2001. Gene expression profiling and molecular aspects in peripheral nerve regeneration. *Restor Neurol Neurosci,* **19,** 5-18.

Bradbury, E. J., Moon, L. D., et al. 2002. Chondroitinase ABC promotes functional recovery after spinal cord injury. *Nature,* **416,** 636-640.

Brandeis, M., Ariel, M., et al. 1993. Dynamics of DNA methylation during development. *Bioessays,* **15,** 709-713.

Brandeis, M., Frank, D., et al. 1994. Sp1 elements protect a CpG island from de novo methylation. *Nature,* **371,** 435-438.

Bretzner, F., Plemel, J. R., et al. 2010. Combination of olfactory ensheathing cells with local versus systemic cAMP treatment after a cervical rubrospinal tract injury. *J Neurosci Res,* **88,** 2833-2846.

Brot, S., Rogemond, V., et al. 2010. CRMP5 interacts with tubulin to inhibit neurite outgrowth, thereby modulating the function of CRMP2. *J Neurosci,* **30,** 10639-10654.

Broude, E., McAtee, M., et al. 1997. c-Jun expression in adult rat dorsal root ganglion neurons: differential response after central or peripheral axotomy. *Exp Neurol,* **148,** 367-377.

Buck-Koehntop, B. A. & Defossez, P. A. 2013. On how mammalian transcription factors recognize methylated DNA. *Epigenetics,* **8,** 131-137.

Bunge, M. B. 2001. Bridging areas of injury in the spinal cord. *Neuroscientist,* **7,** 325-339.

Buschmann, T., Martin-Villalba, A., et al. 1998. Expression of Jun, Fos, and ATF-2 proteins in axotomized explanted and cultured adult rat dorsal root ganglia. *Neuroscience,* **84,** 163-176.

Cafferty, W. B., McGee, A. W., et al. 2008. Axonal growth therapeutics: regeneration or sprouting or plasticity? *Trends Neurosci,* **31,** 215-220.

Caiafa, P. & Zampieri, M. 2005. DNA methylation and chromatin structure: the puzzling CpG islands. *J Cell Biochem,* **94,** 257-265.

Caroni, P. 1998. Neuro-regeneration: plasticity for repair and adaptation. *Essays Biochem,* **33,** 53-64.

Caroni, P. & Schwab, M. E. 1988a. Antibody against myelin-associated inhibitor of neurite growth neutralizes nonpermissive substrate properties of CNS white matter. *Neuron,* **1,** 85-96.

Caroni, P. & Schwab, M. E. 1988b. Two membrane protein fractions from rat central myelin with inhibitory properties for neurite growth and fibroblast spreading. *J Cell Biol,* **106,** 1281-1288.

Caspary, T. & Anderson, K. V. 2003. Patterning cell types in the dorsal spinal cord: what the mouse mutants say. *Nat Rev Neurosci,* **4,** 289-297.

Cazorla, M., Shegda, M., et al. 2012. Striatal D2 receptors regulate dendritic morphology of medium spiny neurons via Kir2 channels. *J Neurosci,* **32,** 2398-2409.

Cervoni, N., Bhattacharya, S., et al. 1999. DNA demethylase is a processive enzyme. *J Biol Chem,* **274,** 8363-8366.

Ch'ng, T. H., Uzgil, B., et al. 2012. Activity-dependent transport of the transcriptional coactivator CRTC1 from synapse to nucleus. *Cell,* **150,** 207-221.

Chahrour, M., Jung, S. Y., et al. 2008. MeCP2, a key contributor to neurological disease, activates and represses transcription. *Science,* **320,** 1224-1229.

Chedin, F. 2011. The DNMT3 family of mammalian de novo DNA methyltransferases. *Prog Mol Biol Transl Sci,* **101,** 255-285.

Chen, C., Ito, K., et al. 2011a. Distinct expression patterns of the subunits of the CCR4-NOT deadenylase complex during neural development. *Biochem Biophys Res Commun,* **411,** 360-364.

Chen, M. S., Huber, A. B., et al. 2000. Nogo-A is a myelin-associated neurite outgrowth inhibitor and an antigen for monoclonal antibody IN-1. *Nature,* **403,** 434-439.

Chen, T. 2011. Mechanistic and functional links between histone methylation and DNA methylation. *Prog Mol Biol Transl Sci,* **101,** 335-348.

Chen, W. G., Chang, Q., et al. 2003. Derepression of BDNF transcription involves calcium-dependent phosphorylation of MeCP2. *Science,* **302,** 885-889.

Chen, Y., Wang, H., et al. 2011b. HDAC-mediated deacetylation of NF-kappaB is critical for Schwann cell myelination. *Nat Neurosci,* **14,** 437-441.

Chen, Z. X. & Riggs, A. D. 2011c. DNA methylation and demethylation in mammals. *J Biol Chem,* **286,** 18347-18353.

Chestnut, B. A., Chang, Q., et al. 2011. Epigenetic regulation of motor neuron cell death through DNA methylation. *J Neurosci,* **31,** 16619-16636.

Chindasub, P., Lindsey, J. D., et al. 2013. Inhibition of histone deacetylases 1 and 3 protects injured retinal ganglion cells. *Invest Ophthalmol Vis Sci,* **54,** 96-102.

Chong, M. S., Reynolds, M. L., et al. 1994. GAP-43 expression in primary sensory neurons following central axotomy. *J Neurosci,* **14,** 4375-4384.

Christie, K. & Zochodne, D. 2013. Peripheral axon regrowth: New molecular approaches. *Neuroscience*.

Chrivia, J. C., Kwok, R. P., et al. 1993. Phosphorylated CREB binds specifically to the nuclear protein CBP. *Nature,* **365,** 855-859.

Clark, S. J., Harrison, J., et al. 1994. High sensitivity mapping of methylated cytosines. *Nucleic Acids Res,* **22,** 2990-2997.

Clatterbuck, R. E., Price, D. L., et al. 1994. Further characterization of the effects of brain-derived neurotrophic factor and ciliary neurotrophic factor on axotomized neonatal and adult mammalian motor neurons. *J Comp Neurol,* **342,** 45-56.

Cortellino, S., Xu, J., et al. 2011. Thymine DNA glycosylase is essential for active DNA demethylation by linked deamination-base excision repair. *Cell,* **146,** 67-79.

Costigan, M., Befort, K., et al. 2002. Replicate high-density rat genome oligonucleotide microarrays reveal hundreds of regulated genes in the dorsal root ganglion after peripheral nerve injury. *BMC Neurosci,* **3,** 16.

Cui, S. S., Yang, C. P., et al. 2003. Valproic acid enhances axonal regeneration and recovery of motor function after sciatic nerve axotomy in adult rats. *Brain Res,* **975,** 229-236.

D'Addario, C., Dell'Osso, B., et al. 2012. Selective DNA methylation of BDNF promoter in bipolar disorder: differences among patients with BDI and BDII. *Neuropsychopharmacology,* **37,** 1647-1655.

D'Alessio, A. C. & Szyf, M. 2006. Epigenetic tete-a-tete: the bilateral relationship between chromatin modifications and DNA methylation. *Biochem Cell Biol,* **84,** 463-476.

Dalton, S. R. & Bellacosa, A. 2012. DNA demethylation by TDG. *Epigenomics,* **4,** 459-467.

David, S. & Aguayo, A. J. 1981. Axonal elongation into peripheral nervous system "bridges" after central nervous system injury in adult rats. *Science,* **214,** 931-933.

Daxinger, L. & Whitelaw, E. 2012. Understanding transgenerational epigenetic inheritance via the gametes in mammals. *Nat Rev Genet,* **13,** 153-162.

Day, J. J. & Sweatt, J. D. 2010. DNA methylation and memory formation. *Nat Neurosci,* **13,** 1319-1323.

De Biase, A., Knoblach, S. M., et al. 2005. Gene expression profiling of experimental traumatic spinal cord injury as a function of distance from impact site and injury severity. *Physiol Genomics,* **22,** 368-381.

de Heredia, L. L. & Magoulas, C. 2012. Lack of the transcription factor C/EBPdelta impairs the intrinsic capacity of peripheral neurons for regeneration. *Exp Neurol,* **239,** 148-157.

De la Monte, S. M., Federoff, H. J., et al. 1989. GAP-43 gene expression during development: persistence in a distinctive set of neurons in the mature central nervous system. *Brain Res Dev Brain Res,* **46,** 161-168.

de Ruijter, A. J., van Gennip, A. H., et al. 2003. Histone deacetylases (HDACs): characterization of the classical HDAC family. *Biochem J,* **370,** 737-749.

Deaton, A. M. & Bird, A. 2011. CpG islands and the regulation of transcription. *Genes Dev,* **25,** 1010-1022.

Di Giovanni, S. 2006. Regeneration following spinal cord injury, from experimental models to humans: where are we? *Expert Opin Ther Targets,* **10,** 363-376.

Di Giovanni, S. 2009. Molecular targets for axon regeneration: focus on the intrinsic pathways. *Expert Opin Ther Targets,* **13,** 1387-1398.

Di Giovanni, S., De Biase, A., et al. 2005. In vivo and in vitro characterization of novel neuronal plasticity factors identified following spinal cord injury. *J Biol Chem,* **280,** 2084-2091.

Di Giovanni, S., Knoblach, S. M., et al. 2003. Gene profiling in spinal cord injury shows role of cell cycle in neuronal death. *Ann Neurol,* **53,** 454-468.

Diaz de Leon-Guerrero, S., Pedraza-Alva, G., et al. 2011. In sickness and in health: the role of methyl-CpG binding protein 2 in the central nervous system. *Eur J Neurosci,* **33,** 1563-1574.

Dillon, S. C., Zhang, X., et al. 2005. The SET-domain protein superfamily: protein lysine methyltransferases. *Genome Biol,* **6,** 227.

Ditor, D. S. & Hicks, A. L. 2009. Exercise therapy after spinal cord injury: the effects on heath and function. *Crit Rev Biomed Eng,* **37,** 165-191.

Dooley, D. M., Sharkey, J., et al. 1978. Treatment of demyelinating and degenerative diseases by electro stimulation of the spinal cord. *Med Prog Technol,* **6,** 1-14.

Down, T. A., Rakyan, V. K., et al. 2008. A Bayesian deconvolution strategy for immunoprecipitation-based DNA methylome analysis. *Nat Biotechnol,* **26,** 779-785.

Dulac, C. 2010. Brain function and chromatin plasticity. *Nature,* **465,** 728-735.

Dunn, D. B. & Smith, J. D. 1955. Occurrence of a new base in the deoxyribonucleic acid of a strain of Bacterium coli. *Nature,* **175,** 336-337.

Ehrlich, M. & Wang, R. Y. 1981. 5-Methylcytosine in eukaryotic DNA. *Science,* **212,** 1350-1357.

Emery, D. L., Royo, N. C., et al. 2003. Plasticity following injury to the adult central nervous system: is recapitulation of a developmental state worth promoting? *J Neurotrauma,* **20,** 1271-1292.

Endres, M., Meisel, A., et al. 2000. DNA methyltransferase contributes to delayed ischemic brain injury. *J Neurosci,* **20,** 3175-3181.

Esteller, M. 2008. Epigenetics in cancer. *N Engl J Med,* **358,** 1148-1159.

Fabes, J., Anderson, P., et al. 2007. Regeneration-enhancing effects of EphA4 blocking peptide following corticospinal tract injury in adult rat spinal cord. *Eur J Neurosci,* **26,** 2496-2505.

Fan, M., Mi, R., et al. 2001. Analysis of gene expression following sciatic nerve crush and spinal cord hemisection in the mouse by microarray expression profiling. *Cell Mol Neurobiol,* **21,** 497-508.

Fawcett, J. W. & Asher, R. A. 1999. The glial scar and central nervous system repair. *Brain Res Bull,* **49,** 377-391.

Fazzari, M. J. & Greally, J. M. 2004. Epigenomics: beyond CpG islands. *Nat Rev Genet,* **5,** 446-455.

Feng, J., Chang, H., et al. 2005. Dynamic expression of de novo DNA methyltransferases Dnmt3a and Dnmt3b in the central nervous system. *J Neurosci Res,* **79,** 734-746.

Feng, J. & Fan, G. 2009. The role of DNA methylation in the central nervous system and neuropsychiatric disorders. *Int Rev Neurobiol,* **89,** 67-84.

Feng, J., Fouse, S., et al. 2007. Epigenetic regulation of neural gene expression and neuronal function. *Pediatr Res,* **61,** 58R-63R.

Feng, J., Zhou, Y., et al. 2010. Dnmt1 and Dnmt3a maintain DNA methylation and regulate synaptic function in adult forebrain neurons. *Nat Neurosci,* **13,** 423-430.

Filbin, M. T. 2003. Myelin-associated inhibitors of axonal regeneration in the adult mammalian CNS. *Nat Rev Neurosci,* **4,** 703-713.

Finsterwald, C., Fiumelli, H., et al. 2010. Regulation of dendritic development by BDNF requires activation of CRTC1 by glutamate. *J Biol Chem,* **285,** 28587-28595.

Fischle, W., Franz, H., et al. 2008. Specificity of the chromodomain Y chromosome family of chromodomains for lysine-methylated ARK(S/T) motifs. *J Biol Chem,* **283,** 19626-19635.

Fischle, W., Wang, Y., et al. 2003. Molecular basis for the discrimination of repressive methyl-lysine marks in histone H3 by Polycomb and HP1 chromodomains. *Genes Dev,* **17,** 1870-1881.

Fisher, C. L. & Fisher, A. G. 2011. Chromatin states in pluripotent, differentiated, and reprogrammed cells. *Curr Opin Genet Dev,* **21,** 140-146.

Floriddia, E. M., Rathore, K. I., et al. 2012. p53 Regulates the neuronal intrinsic and extrinsic responses affecting the recovery of motor function following spinal cord injury. *J Neurosci,* **32,** 13956-13970.

Flynn, J., Glickman, J. F., et al. 1996. Murine DNA cytosine-C5 methyltransferase: pre-steady- and steady-state kinetic analysis with regulatory DNA sequences. *Biochemistry,* **35,** 7308-7315.

Fournier, A., Sasai, N., et al. 2012. The role of methyl-binding proteins in chromatin organization and epigenome maintenance. *Brief Funct Genomics,* **11,** 251-264.

Fujita, Y., Endo, S., et al. 2011. Myelin suppresses axon regeneration by PIR-B/SHP-mediated inhibition of Trk activity. *EMBO J,* **30,** 1389-1401.

Fujitani, M., Yamagishi, S., et al. 2004. P311 accelerates nerve regeneration of the axotomized facial nerve. *J Neurochem,* **91,** 737-744.

Fukada, M., Watakabe, I., et al. 2000. Molecular characterization of CRMP5, a novel member of the collapsin response mediator protein family. *J Biol Chem,* **275,** 37957-37965.

Fuks, F., Hurd, P. J., et al. 2003. The DNA methyltransferases associate with HP1 and the SUV39H1 histone methyltransferase. *Nucleic Acids Res,* **31,** 2305-2312.

Gao, Y., Deng, K., et al. 2004. Activated CREB is sufficient to overcome inhibitors in myelin and promote spinal axon regeneration in vivo. *Neuron,* **44,** 609-621.

Garcia-Cao, M., O'Sullivan, R., et al. 2004. Epigenetic regulation of telomere length in mammalian cells by the Suv39h1 and Suv39h2 histone methyltransferases. *Nat Genet,* **36,** 94-99.

Gardiner-Garden, M. & Frommer, M. 1987. CpG islands in vertebrate genomes. *J Mol Biol,* **196,** 261-282.

Gaub, P., Joshi, Y., et al. 2011. The histone acetyltransferase p300 promotes intrinsic axonal regeneration. *Brain,* **134,** 2134-2148.

Gaub, P., Tedeschi, A., et al. 2010. HDAC inhibition promotes neuronal outgrowth and counteracts growth cone collapse through CBP/p300 and P/CAF-dependent p53 acetylation. *Cell Death Differ,* **17,** 1392-1408.

Geremia, N. M., Pettersson, L. M., et al. 2010. Endogenous BDNF regulates induction of intrinsic neuronal growth programs in injured sensory neurons. *Exp Neurol,* **223,** 128-142.

Giger, R. J., Hollis, E. R., 2nd, et al. 2010. Guidance molecules in axon regeneration. *Cold Spring Harb Perspect Biol,* **2,** a001867.

Gold, J. D. & Pedersen, R. A. 1994. Mechanisms of genomic imprinting in mammals. *Curr Top Dev Biol,* **29,** 227-280.

Goldberg, J. L., Klassen, M. P., et al. 2002. Amacrine-signaled loss of intrinsic axon growth ability by retinal ganglion cells. *Science,* **296,** 1860-1864.

Goldberg, J. L., Vargas, M. E., et al. 2004. An oligodendrocyte lineage-specific semaphorin, Sema5A, inhibits axon growth by retinal ganglion cells. *J Neurosci,* **24,** 4989-4999.

Goldshmit, Y., Galea, M. P., et al. 2004. Axonal regeneration and lack of astrocytic gliosis in EphA4-deficient mice. *J Neurosci,* **24,** 10064-10073.

Goll, M. G., Kirpekar, F., et al. 2006. Methylation of tRNAAsp by the DNA methyltransferase homolog Dnmt2. *Science,* **311,** 395-398.

Goodman, R. H. & Smolik, S. 2000. CBP/p300 in cell growth, transformation, and development. *Genes Dev,* **14,** 1553-1577.

Goto, K., Numata, M., et al. 1994. Expression of DNA methyltransferase gene in mature and immature neurons as well as proliferating cells in mice. *Differentiation,* **56,** 39-44.

Graef, I. A., Wang, F., et al. 2003. Neurotrophins and netrins require calcineurin/NFAT signaling to stimulate outgrowth of embryonic axons. *Cell,* **113,** 657-670.

GrandPre, T., Nakamura, F., et al. 2000. Identification of the Nogo inhibitor of axon regeneration as a Reticulon protein. *Nature,* **403,** 439-444.

Gribble, S., Ng, B. L., et al. 2004. Chromosome paints from single copies of chromosomes. *Chromosome Res,* **12,** 143-151.

Grill, R., Murai, K., et al. 1997a. Cellular delivery of neurotrophin-3 promotes corticospinal axonal growth and partial functional recovery after spinal cord injury. *J Neurosci,* **17,** 5560-5572.

Grill, R. J., Blesch, A., et al. 1997b. Robust growth of chronically injured spinal cord axons induced by grafts of genetically modified NGF-secreting cells. *Exp Neurol,* **148,** 444-452.

Gris, P., Murphy, S., et al. 2003. Differential gene expression profiles in embryonic, adult-injured and adult-uninjured rat spinal cords. *Mol Cell Neurosci,* **24,** 555-567.

Guan, Z., Giustetto, M., et al. 2002. Integration of long-term-memory-related synaptic plasticity involves bidirectional regulation of gene expression and chromatin structure. *Cell,* **111,** 483-493.

Guo, J. U., Ma, D. K., et al. 2011a. Neuronal activity modifies the DNA methylation landscape in the adult brain. *Nat Neurosci,* **14,** 1345-1351.

Guo, J. U., Su, Y., et al. 2011b. Hydroxylation of 5-methylcytosine by TET1 promotes active DNA demethylation in the adult brain. *Cell,* **145,** 423-434.

Gutkovich, Y. E., Ofir, R., et al. 2010. Xenopus Meis3 protein lies at a nexus downstream to Zic1 and Pax3 proteins, regulating multiple cell-fates during early nervous system development. *Dev Biol,* **338,** 50-62.

Hackenberg, M., Barturen, G., et al. 2010. Prediction of CpG-island function: CpG clustering vs. sliding-window methods. *BMC Genomics,* **11,** 327.

Hannila, S. S. & Filbin, M. T. 2008. The role of cyclic AMP signaling in promoting axonal regeneration after spinal cord injury. *Exp Neurol,* **209,** 321-332.

Hansson, M. L., Behmer, S., et al. 2012. MAML1 acts cooperatively with EGR1 to activate EGR1-regulated promoters: implications for nephrogenesis and the development of renal cancer. *PLoS One,* **7,** e46001.

Harel, N. Y. & Strittmatter, S. M. 2006. Can regenerating axons recapitulate developmental guidance during recovery from spinal cord injury? *Nat Rev Neurosci,* **7,** 603-616.

Hashimshony, T., Zhang, J., et al. 2003. The role of DNA methylation in setting up chromatin structure during development. *Nat Genet,* **34,** 187-192.

Hatada, I., Namihira, M., et al. 2008. Astrocyte-specific genes are generally demethylated in neural precursor cells prior to astrocytic differentiation. *PLoS One,* **3,** e3189.

He, Z. & Koprivica, V. 2004. The Nogo signaling pathway for regeneration block. *Annu Rev Neurosci,* **27,** 341-368.

Heintz, N. 2004. Gene expression nervous system atlas (GENSAT). *Nat Neurosci,* **7,** 483.

Hendrich, B., Hardeland, U., et al. 1999. The thymine glycosylase MBD4 can bind to the product of deamination at methylated CpG sites. *Nature,* **401,** 301-304.

Herdegen, T., Skene, P., et al. 1997. The c-Jun transcription factor--bipotential mediator of neuronal death, survival and regeneration. *Trends Neurosci,* **20,** 227-231.

Hermann, A., Gowher, H., et al. 2004. Biochemistry and biology of mammalian DNA methyltransferases. *Cell Mol Life Sci,* **61,** 2571-2587.

Hoang, E., Bost-Usinger, L., et al. 1999. Characterization of a novel C-kinesin (KIFC3) abundantly expressed in vertebrate retina and RPE. *Exp Eye Res,* **69,** 57-68.

Hodawadekar, S. C. & Marmorstein, R. 2007. Chemistry of acetyl transfer by histone modifying enzymes: structure, mechanism and implications for effector design. *Oncogene,* **26,** 5528-5540.

Hokfelt, T., Zhang, X., et al. 1994. Messenger plasticity in primary sensory neurons following axotomy and its functional implications. *Trends Neurosci,* **17,** 22-30.

Holliday, R. & Pugh, J. E. 1975. DNA modification mechanisms and gene activity during development. *Science,* **187,** 226-232.

Horton, J. R., Upadhyay, A. K., et al. 2010. Enzymatic and structural insights for substrate specificity of a family of jumonji histone lysine demethylases. *Nat Struct Mol Biol,* **17,** 38-43.

Hou, S., Nicholson, L., et al. 2012. Dependence of regenerated sensory axons on continuous neurotrophin-3 delivery. *J Neurosci,* **32,** 13206-13220.

Hsieh-Li, H. M., Witte, D. P., et al. 1995. Gsh-2, a murine homeobox gene expressed in the developing brain. *Mech Dev,* **50,** 177-186.

Hsieh, J., Nakashima, K., et al. 2004. Histone deacetylase inhibition-mediated neuronal differentiation of multipotent adult neural progenitor cells. *Proc Natl Acad Sci U S A,* **101,** 16659-16664.

Huang, J., Sengupta, R., et al. 2007. p53 is regulated by the lysine demethylase LSD1. *Nature,* **449,** 105-108.

Huang, S. F., Ding, Y., et al. 2011. An experimental electro-acupuncture study in treatment of the rat demyelinated spinal cord injury induced by ethidium bromide. *Neurosci Res,* **70,** 294-304.

Huber, A. B. & Schwab, M. E. 2000. Nogo-A, a potent inhibitor of neurite outgrowth and regeneration. *Biol Chem,* **381,** 407-419.

Huebner, E. A. & Strittmatter, S. M. 2009. Axon regeneration in the peripheral and central nervous systems. *Results Probl Cell Differ,* **48,** 339-351.

Hyatt Sachs, H., Schreiber, R. C., et al. 2007. Activating transcription factor 3 induction in sympathetic neurons after axotomy: response to decreased neurotrophin availability. *Neuroscience,* **150,** 887-897.

Iaci, J. F., Vecchione, A. M., et al. 2007. Chondroitin sulfate proteoglycans in spinal cord contusion injury and the effects of chondroitinase treatment. *J Neurotrauma,* **24,** 1743-1759.

Ikehata, H., Kudo, H., et al. 2003. UVA induces C-->T transitions at methyl-CpG-associated dipyrimidine sites in mouse skin epidermis more frequently than UVB. *Mutagenesis,* **18,** 511-519.

Illingworth, R., Kerr, A., et al. 2008. A novel CpG island set identifies tissue-specific methylation at developmental gene loci. *PLoS Biol,* **6,** e22.

Iskandar, B. J., Nelson, A., et al. 2004. Folic acid supplementation enhances repair of the adult central nervous system. *Ann Neurol,* **56,** 221-227.

Iskandar, B. J., Rizk, E., et al. 2010. Folate regulation of axonal regeneration in the rodent central nervous system through DNA methylation. *J Clin Invest,* **120,** 1603-1616.

Jabbari, K. & Bernardi, G. 2004. Cytosine methylation and CpG, TpG (CpA) and TpA frequencies. *Gene,* **333,** 143-149.

Jeltsch, A. 2006. On the enzymatic properties of Dnmt1: specificity, processivity, mechanism of linear diffusion and allosteric regulation of the enzyme. *Epigenetics,* **1,** 63-66.

Jenkins, R., McMahon, S. B., et al. 1993. Expression of c-Jun as a response to dorsal root and peripheral nerve section in damaged and adjacent intact primary sensory neurons in the rat. *Eur J Neurosci,* **5,** 751-759.

Jenuwein, T. 2006. The epigenetic magic of histone lysine methylation. *FEBS J,* **273,** 3121-3135.

Jenuwein, T. & Allis, C. D. 2001. Translating the histone code. *Science,* **293,** 1074-1080.

Jiang, Y., Jakovcevski, M., et al. 2010. Setdb1 histone methyltransferase regulates mood-related behaviors and expression of the NMDA receptor subunit NR2B. *J Neurosci,* **30,** 7152-7167.

Jin, B., Kim, G., et al. 2004. Microarray analysis of gene regulation in the Hepa1c1c7 cell line following exposure to the DNA methylation inhibitor 5-aza-2'-deoxycytidine and 2,3,7,8-tetrachlorodibenzo-p-dioxin. *Toxicol In Vitro,* **18,** 659-664.

Jin, Q., Yu, L. R., et al. 2011. Distinct roles of GCN5/PCAF-mediated H3K9ac and CBP/p300-mediated H3K18/27ac in nuclear receptor transactivation. *EMBO J,* **30,** 249-262.

Jones, L. L., Oudega, M., et al. 2001. Neurotrophic factors, cellular bridges and gene therapy for spinal cord injury. *J Physiol,* **533,** 83-89.

Jones, T. B., McDaniel, E. E., et al. 2005. Inflammatory-mediated injury and repair in the traumatically injured spinal cord. *Curr Pharm Des,* **11,** 1223-1236.

Juliandi, B., Abematsu, M., et al. 2010. Epigenetic regulation in neural stem cell differentiation. *Dev Growth Differ,* **52,** 493-504.

Jurkowska, R. Z., Jurkowski, T. P., et al. 2011a. Structure and function of mammalian DNA methyltransferases. *Chembiochem,* **12,** 206-222.

Jurkowska, R. Z., Rajavelu, A., et al. 2011b. Oligomerization and binding of the DNMT3A DNA methyltransferase to parallel DNA molecules, heterochromatic localization and role of DNMT3L. *J Biol Chem*.

Kadoya, K., Tsukada, S., et al. 2009. Combined intrinsic and extrinsic neuronal mechanisms facilitate bridging axonal regeneration one year after spinal cord injury. *Neuron,* **64,** 165-172.

Kamei, Y., Xu, L., et al. 1996. A CBP integrator complex mediates transcriptional activation and AP-1 inhibition by nuclear receptors. *Cell,* **85,** 403-414.

Kartasova, T., Darwiche, N., et al. 1996. Sequence and expression patterns of mouse SPR1: Correlation of expression with epithelial function. *J Invest Dermatol,* **106,** 294-304.

Kato, K., Maesawa, C., et al. 2009. DNA hypomethylation at the CpG island is involved in aberrant expression of the L1 cell adhesion molecule gene in colorectal cancer. *Int J Oncol,* **35,** 467-476.

Kazantseva, A., Sepp, M., et al. 2009. N-terminally truncated BAF57 isoforms contribute to the diversity of SWI/SNF complexes in neurons. *J Neurochem,* **109,** 807-818.

Khoshnan, A. & Patterson, P. H. 2012. Elevated IKKalpha accelerates the differentiation of human neuronal progenitor cells and induces MeCP2-dependent BDNF expression. *PLoS One,* **7,** e41794.

Kim, J. E., Li, S., et al. 2003. Axon regeneration in young adult mice lacking Nogo-A/B. *Neuron,* **38,** 187-199.

Kim, J. E., Liu, B. P., et al. 2004. Nogo-66 receptor prevents raphespinal and rubrospinal axon regeneration and limits functional recovery from spinal cord injury. *Neuron,* **44,** 439-451.

Kinney, S. R. & Pradhan, S. 2011. Regulation of expression and activity of DNA (cytosine-5) methyltransferases in mammalian cells. *Prog Mol Biol Transl Sci,* **101,** 311-333.

Kiryu-Seo, S. & Kiyama, H. 2011. The nuclear events guiding successful nerve regeneration. *Front Mol Neurosci,* **4,** 53.

Klesse, L. J. & Parada, L. F. 1999. Trks: signal transduction and intracellular pathways. *Microsc Res Tech,* **45,** 210-216.

Klimaschewski, L., Tran, T. D., et al. 1994. Plasticity of postganglionic sympathetic neurons in the rat superior cervical ganglion after axotomy. *Microsc Res Tech,* **29,** 120-130.

Klose, R. J. & Bird, A. P. 2006a. Genomic DNA methylation: the mark and its mediators. *Trends Biochem Sci,* **31,** 89-97.

Klose, R. J., Kallin, E. M., et al. 2006b. JmjC-domain-containing proteins and histone demethylation. *Nat Rev Genet,* **7,** 715-727.

Klug, M., Heinz, S., et al. 2010. Active DNA demethylation in human postmitotic cells correlates with activating histone modifications, but not transcription levels. *Genome Biol,* **11,** R63.

Knoll, J. H., Nicholls, R. D., et al. 1989. Angelman and Prader-Willi syndromes share a common chromosome 15 deletion but differ in parental origin of the deletion. *Am J Med Genet,* **32,** 285-290.

Kochanek, S., Renz, D., et al. 1993. DNA methylation in the Alu sequences of diploid and haploid primary human cells. *EMBO J,* **12,** 1141-1151.

Komashko, V. M., Acevedo, L. G., et al. 2008. Using ChIP-chip technology to reveal common principles of transcriptional repression in normal and cancer cells. *Genome Res,* **18,** 521-532.

Kordi-Tamandani, D. M., Sahranavard, R., et al. 2012. DNA methylation and expression profiles of the brain-derived neurotrophic factor (BDNF) and dopamine transporter (DAT1) genes in patients with schizophrenia. *Mol Biol Rep,* **39,** 10889-10893.

Kouzarides, T. 2007. Chromatin modifications and their function. *Cell,* **128,** 693-705.

Kriaucionis, S. & Heintz, N. 2009. The nuclear DNA base 5-hydroxymethylcytosine is present in Purkinje neurons and the brain. *Science,* **324,** 929-930.

Kriukiene, E., Liutkeviciute, Z., et al. 2012. 5-Hydroxymethylcytosine--the elusive epigenetic mark in mammalian DNA. *Chem Soc Rev,* **41,** 6916-6930.

Kronenberg, G., Colla, M., et al. 2009. Folic acid, neurodegenerative and neuropsychiatric disease. *Curr Mol Med,* **9,** 315-323.

Kronenberg, G. & Endres, M. 2010. Neuronal injury: folate to the rescue? *J Clin Invest,* **120,** 1383-1386.

Kubo, T., Yamashita, T., et al. 2002. Analysis of genes induced in peripheral nerve after axotomy using cDNA microarrays. *J Neurochem,* **82,** 1129-1136.

Kurihara, D., Ueno, M., et al. 2010. Expression of galectin-1 in immune cells and glial cells after spinal cord injury. *Neurosci Res,* **66,** 265-270.

Kwok, R. P., Lundblad, J. R., et al. 1994. Nuclear protein CBP is a coactivator for the transcription factor CREB. *Nature,* **370,** 223-226.

Lachner, M., O'Carroll, D., et al. 2001. Methylation of histone H3 lysine 9 creates a binding site for HP1 proteins. *Nature,* **410,** 116-120.

Lan, F. & Shi, Y. 2009. Epigenetic regulation: methylation of histone and non-histone proteins. *Sci China C Life Sci,* **52,** 311-322.

Lander, E. S., Linton, L. M., et al. 2001. Initial sequencing and analysis of the human genome. *Nature,* **409,** 860-921.

LaPlant, Q., Vialou, V., et al. 2010. Dnmt3a regulates emotional behavior and spine plasticity in the nucleus accumbens. *Nat Neurosci,* **13,** 1137-1143.

Latasa, M. J., Ituero, M., et al. 2010. Retinoic acid regulates myelin formation in the peripheral nervous system. *Glia,* **58,** 1451-1464.

Laurent, L., Wong, E., et al. 2010. Dynamic changes in the human methylome during differentiation. *Genome Res,* **20,** 320-331.

Lee, D. H., O'Connor, T. R., et al. 2002. Oxidative DNA damage induced by copper and hydrogen peroxide promotes CG-->TT tandem mutations at methylated CpG dinucleotides in nucleotide excision repair-deficient cells. *Nucleic Acids Res,* **30,** 3566-3573.

Lee, J. K. & Zheng, B. 2011. Role of myelin-associated inhibitors in axonal repair after spinal cord injury. *Exp Neurol*.

Lehnertz, B., Ueda, Y., et al. 2003. Suv39h-mediated histone H3 lysine 9 methylation directs DNA methylation to major satellite repeats at pericentric heterochromatin. *Curr Biol,* **13,** 1192-1200.

Lernmark, A., Ducat, L., et al. 1990. Family cell lines available for research. *Am J Hum Genet,* **47,** 1028-1030.

Levenson, J. M., Roth, T. L., et al. 2006. Evidence that DNA (cytosine-5) methyltransferase regulates synaptic plasticity in the hippocampus. *J Biol Chem,* **281,** 15763-15773.

Li, B., Carey, M., et al. 2007a. The role of chromatin during transcription. *Cell,* **128,** 707-719.

Li, B., Zhou, J., et al. 2007b. Polycomb protein Cbx4 promotes SUMO modification of de novo DNA methyltransferase Dnmt3a. *Biochem J,* **405,** 369-378.

Li, M. Y., Lai, F. J., et al. 2009. Dramatic co-activation of WWOX/WOX1 with CREB and NF-kappaB in delayed loss of small dorsal root ganglion neurons upon sciatic nerve transection in rats. *PLoS One,* **4,** e7820.

Li, W., Calfa, G., et al. 2012. Activity-dependent BDNF release and TRPC signaling is impaired in hippocampal neurons of Mecp2 mutant mice. *Proc Natl Acad Sci U S A,* **109,** 17087-17092.

Lilja, T., Heldring, N., et al. 2013. Like a rolling histone: epigenetic regulation of neural stem cells and brain development by factors controlling histone acetylation and methylation. *Biochim Biophys Acta,* **1830,** 2354-2360.

Lin, S. E., Oyama, T., et al. 2002. Identification of new human mastermind proteins defines a family that consists of positive regulators for notch signaling. *J Biol Chem,* **277,** 50612-50620.

Lindsay, R. M. 1988. Nerve growth factors (NGF, BDNF) enhance axonal regeneration but are not required for survival of adult sensory neurons. *J Neurosci,* **8,** 2394-2405.

Lindsay, S., Monk, M., et al. 1985. Differences in methylation on the active and inactive human X chromosomes. *Ann Hum Genet,* **49,** 115-127.

Lindwall, C. & Kanje, M. 2005. The role of p-c-Jun in survival and outgrowth of developing sensory neurons. *Neuroreport,* **16,** 1655-1659.

Lister, R., Pelizzola, M., et al. 2009. Human DNA methylomes at base resolution show widespread epigenomic differences. *Nature,* **462,** 315-322.

Liu, D. X., Nath, N., et al. 2005. Regulation of neuron survival and death by p130 and associated chromatin modifiers. *Genes Dev,* **19,** 719-732.

Liu, F., Sun, W. W., et al. 2009. Effects of electro-acupuncture on NT-4 expression in spinal dorsal root ganglion and associated segments of the spinal dorsal horn in cats subjected to adjacent dorsal root ganglionectomy. *Neurosci Lett,* **450,** 158-162.

Liu, R. Y. & Snider, W. D. 2001. Different signaling pathways mediate regenerative versus developmental sensory axon growth. *J Neurosci,* **21,** RC164.

Lockett, G. A., Wilkes, F., et al. 2010. Brain plasticity, memory and neurological disorders: an epigenetic perspective. *Neuroreport,* **21,** 909-913.

Lubin, F. D., Roth, T. L., et al. 2008. Epigenetic regulation of BDNF gene transcription in the consolidation of fear memory. *J Neurosci,* **28,** 10576-10586.

Lv, L., Han, X., et al. 2012. Valproic acid improves locomotion in vivo after SCI and axonal growth of neurons in vitro. *Exp Neurol,* **233,** 783-790.

Lv, L., Sun, Y., et al. 2011. Valproic acid improves outcome after rodent spinal cord injury: potential roles of histone deacetylase inhibition. *Brain Res,* **1396,** 60-68.

Ma, D. K., Jang, M. H., et al. 2009. Neuronal activity-induced Gadd45b promotes epigenetic DNA demethylation and adult neurogenesis. *Science,* **323,** 1074-1077.

Ma, D. K., Marchetto, M. C., et al. 2010. Epigenetic choreographers of neurogenesis in the adult mammalian brain. *Nat Neurosci,* **13,** 1338-1344.

Macdonald, J. L., Verster, A., et al. 2010. MBD2 and MeCP2 regulate distinct transitions in the stage-specific differentiation of olfactory receptor neurons. *Mol Cell Neurosci,* **44,** 55-67.

Maezawa, I., Swanberg, S., et al. 2009. Rett syndrome astrocytes are abnormal and spread MeCP2 deficiency through gap junctions. *J Neurosci,* **29,** 5051-5061.

Mager, J. & Bartolomei, M. S. 2005. Strategies for dissecting epigenetic mechanisms in the mouse. *Nat Genet,* **37,** 1194-1200.

Mahalik, T. J., Carrier, A., et al. 1992. The expression of GAP43 mRNA during the late embryonic and early postnatal development of the CNS of the rat: an in situ hybridization study. *Brain Res Dev Brain Res,* **67,** 75-83.

Maksakova, I. A., Mager, D. L., et al. 2008. Keeping active endogenous retroviral-like elements in check: the epigenetic perspective. *Cell Mol Life Sci,* **65,** 3329-3347.

Makwana, M. & Raivich, G. 2005. Molecular mechanisms in successful peripheral regeneration. *FEBS J,* **272,** 2628-2638.

Mantyh, P. W. 2006. Cancer pain and its impact on diagnosis, survival and quality of life. *Nat Rev Neurosci,* **7,** 797-809.

Margueron, R., Trojer, P., et al. 2005. The key to development: interpreting the histone code? *Curr Opin Genet Dev,* **15,** 163-176.

Marklund, N., Fulp, C. T., et al. 2006. Selective temporal and regional alterations of Nogo-A and small proline-rich repeat protein 1A (SPRR1A) but not Nogo-66 receptor (NgR) occur following traumatic brain injury in the rat. *Exp Neurol,* **197,** 70-83.

Martin, C. & Zhang, Y. 2005. The diverse functions of histone lysine methylation. *Nat Rev Mol Cell Biol,* **6,** 838-849.

Martinowich, K., Hattori, D., et al. 2003. DNA methylation-related chromatin remodeling in activity-dependent BDNF gene regulation. *Science,* **302,** 890-893.

Mason, K., Liu, Z., et al. 2012. Chromatin and epigenetic modifications during early mammalian development. *Anim Reprod Sci,* **134,** 45-55.

Mason, M. R., Lieberman, A. R., et al. 2003. Corticospinal neurons up-regulate a range of growth-associated genes following intracortical, but not spinal, axotomy. *Eur J Neurosci,* **18,** 789-802.

Mason, M. R., Lieberman, A. R., et al. 2002. Transcriptional upregulation of SCG10 and CAP-23 is correlated with regeneration of the axons of peripheral and central neurons in vivo. *Mol Cell Neurosci,* **20,** 595-615.

Masuda, T., Yaginuma, H., et al. 2009. Netrin-1 signaling for sensory axons: Involvement in sensory axonal development and regeneration. *Cell Adh Migr,* **3,** 171-173.

Masui, T., Swift, G. H., et al. 2010. Replacement of Rbpj with Rbpjl in the PTF1 complex controls the final maturation of pancreatic acinar cells. *Gastroenterology,* **139,** 270-280.

Masumi, A., Wang, I. M., et al. 1999. The histone acetylase PCAF is a phorbol-ester-inducible coactivator of the IRF family that confers enhanced interferon responsiveness. *Mol Cell Biol,* **19,** 1810-1820.

Mattson, M. P. & Shea, T. B. 2003. Folate and homocysteine metabolism in neural plasticity and neurodegenerative disorders. *Trends Neurosci,* **26,** 137-146.

Maunakea, A. K., Nagarajan, R. P., et al. 2010. Conserved role of intragenic DNA methylation in regulating alternative promoters. *Nature,* **466,** 253-257.

Maurice, T., Duclot, F., et al. 2008. Altered memory capacities and response to stress in p300/CBP-associated factor (PCAF) histone acetylase knockout mice. *Neuropsychopharmacology,* **33,** 1584-1602.

McDonel, P., Costello, I., et al. 2009. Keeping things quiet: roles of NuRD and Sin3 co-repressor complexes during mammalian development. *Int J Biochem Cell Biol,* **41,** 108-116.

McGraw, C. M., Samaco, R. C., et al. 2011. Adult Neural Function Requires MeCP2. *Science*.

McGraw, J., Oschipok, L. W., et al. 2004. Galectin-1 expression correlates with the regenerative potential of rubrospinal and spinal motoneurons. *Neuroscience,* **128,** 713-719.

McKeon, R. J., Schreiber, R. C., et al. 1991. Reduction of neurite outgrowth in a model of glial scarring following CNS injury is correlated with the expression of inhibitory molecules on reactive astrocytes. *J Neurosci,* **11,** 3398-3411.

Meaney, M. J. & Ferguson-Smith, A. C. 2010. Epigenetic regulation of the neural transcriptome: the meaning of the marks. *Nat Neurosci,* **13,** 1313-1318.

Meier-Stiegen, F., Schwanbeck, R., et al. 2010. Activated Notch1 target genes during embryonic cell differentiation depend on the cellular context and include lineage determinants and inhibitors. *PLoS One,* **5,** e11481.

Meissner, A., Mikkelsen, T. S., et al. 2008. Genome-scale DNA methylation maps of pluripotent and differentiated cells. *Nature,* **454,** 766-770.

Mendez-Gomez, H. R. & Vicario-Abejon, C. 2012. The homeobox gene Gsx2 regulates the self-renewal and differentiation of neural stem cells and the cell fate of postnatal progenitors. *PLoS One,* **7,** e29799.

Mikkelsen, T. S., Ku, M., et al. 2007. Genome-wide maps of chromatin state in pluripotent and lineage-committed cells. *Nature,* **448,** 553-560.

Millan, M. J. 2013. An epigenetic framework for neurodevelopmental disorders: From pathogenesis to potential therapy. *Neuropharmacology,* **68,** 2-82.

Miller, A. L. 2003. The methionine-homocysteine cycle and its effects on cognitive diseases. *Altern Med Rev,* **8,** 7-19.

Miller, C. A. & Sweatt, J. D. 2007. Covalent modification of DNA regulates memory formation. *Neuron,* **53,** 857-869.

Minoguchi, S., Taniguchi, Y., et al. 1997. RBP-L, a transcription factor related to RBP-Jkappa. *Mol Cell Biol,* **17,** 2679-2687.

Miranda, T. B. & Jones, P. A. 2007. DNA methylation: the nuts and bolts of repression. *J Cell Physiol,* **213,** 384-390.

Mo, Q. 2012. A fully Bayesian hidden Ising model for ChIP-seq data analysis. *Biostatistics,* **13,** 113-128.

Momparler, R. L. & Bovenzi, V. 2000. DNA methylation and cancer. *J Cell Physiol,* **183,** 145-154.

Monsey, M. S., Ota, K. T., et al. 2011. Epigenetic alterations are critical for fear memory consolidation and synaptic plasticity in the lateral amygdala. *PLoS One,* **6,** e19958.

Montolio, M., Messeguer, J., et al. 2009. A semaphorin 3A inhibitor blocks axonal chemorepulsion and enhances axon regeneration. *Chem Biol,* **16,** 691-701.

Moore, D. L., Apara, A., et al. 2011a. Kruppel-like transcription factors in the nervous system: Novel players in neurite outgrowth and axon regeneration. *Mol Cell Neurosci*.

Moore, D. L., Blackmore, M. G., et al. 2009. KLF family members regulate intrinsic axon regeneration ability. *Science,* **326,** 298-301.

Moore, D. L. & Goldberg, J. L. 2011b. Multiple transcription factor families regulate axon growth and regeneration. *Dev Neurobiol*.

Moreau-Fauvarque, C., Kumanogoh, A., et al. 2003. The transmembrane semaphorin Sema4D/CD100, an inhibitor of axonal growth, is expressed on oligodendrocytes and upregulated after CNS lesion. *J Neurosci,* **23,** 9229-9239.

Mueller, B. K., Yamashita, T., et al. 2006. The role of repulsive guidance molecules in the embryonic and adult vertebrate central nervous system. *Philos Trans R Soc Lond B Biol Sci,* **361,** 1513-1529.

Mukhopadhyay, G., Doherty, P., et al. 1994. A novel role for myelin-associated glycoprotein as an inhibitor of axonal regeneration. *Neuron,* **13,** 757-767.

Munoz, P. C., Aspe, M. A., et al. 2010. Correlations of recognition memory performance with expression and methylation of brain-derived neurotrophic factor in rats. *Biol Res,* **43,** 251-258.

Nagai, K., Miyake, K., et al. 2005. A transcriptional repressor MeCP2 causing Rett syndrome is expressed in embryonic non-neuronal cells and controls their growth. *Brain Res Dev Brain Res,* **157,** 103-106.

Nakayama, J., Rice, J. C., et al. 2001. Role of histone H3 lysine 9 methylation in epigenetic control of heterochromatin assembly. *Science,* **292,** 110-113.

Namihira, M., Nakashima, K., et al. 2004. Developmental stage dependent regulation of DNA methylation and chromatin modification in a immature astrocyte specific gene promoter. *FEBS Lett,* **572,** 184-188.

Nan, X., Ng, H. H., et al. 1998. Transcriptional repression by the methyl-CpG-binding protein MeCP2 involves a histone deacetylase complex. *Nature,* **393,** 386-389.

Nangle, M. R. & Keast, J. R. 2011. Semaphorin 3A inhibits growth of adult sympathetic and parasympathetic neurones via distinct cyclic nucleotide signalling pathways. *Br J Pharmacol,* **162,** 1083-1095.

Nasu-Nishimura, Y., Hayashi, T., et al. 2006. Role of the Rho GTPase-activating protein RICS in neurite outgrowth. *Genes Cells,* **11,** 607-614.

Navarro, X., Vivo, M., et al. 2007. Neural plasticity after peripheral nerve injury and regeneration. *Prog Neurobiol,* **82,** 163-201.

Neumann, S., Bradke, F., et al. 2002. Regeneration of sensory axons within the injured spinal cord induced by intraganglionic cAMP elevation. *Neuron,* **34,** 885-893.

Ng, H. H., Jeppesen, P., et al. 2000. Active repression of methylated genes by the chromosomal protein MBD1. *Mol Cell Biol,* **20,** 1394-1406.

Ng, S. S., Yue, W. W., et al. 2009. Dynamic protein methylation in chromatin biology. *Cell Mol Life Sci,* **66,** 407-422.

Ng, Y. P., Cheung, Z. H., et al. 2006. STAT3 as a downstream mediator of Trk signaling and functions. *J Biol Chem,* **281,** 15636-15644.

Nguyen, T., Lindner, R., et al. 2009. NFAT-3 is a transcriptional repressor of the growth-associated protein 43 during neuronal maturation. *J Biol Chem,* **284,** 18816-18823.

Nicholls, R. D., Knoll, J. H., et al. 1989. Genetic imprinting suggested by maternal heterodisomy in nondeletion Prader-Willi syndrome. *Nature,* **342,** 281-285.

Nilsson, A., Moller, K., et al. 2005. Early changes in gene expression in the dorsal root ganglia after transection of the sciatic nerve; effects of amphiregulin and PAI-1 on regeneration. *Brain Res Mol Brain Res,* **136,** 65-74.

Nishino, J., Yamashita, K., et al. 2004. Meteorin: a secreted protein that regulates glial cell differentiation and promotes axonal extension. *EMBO J,* **23,** 1998-2008.

O'Doherty, A. M., Rutledge, C. E., et al. 2011. DNA methylation plays an important role in promoter choice and protein production at the mouse Dnmt3L locus. *Dev Biol*.

Ogryzko, V. V., Schiltz, R. L., et al. 1996. The transcriptional coactivators p300 and CBP are histone acetyltransferases. *Cell,* **87,** 953-959.

Oka, M., Rodic, N., et al. 2006. CpG sites preferentially methylated by Dnmt3a in vivo. *J Biol Chem,* **281,** 9901-9908.

Okano, M., Bell, D. W., et al. 1999. DNA methyltransferases Dnmt3a and Dnmt3b are essential for de novo methylation and mammalian development. *Cell,* **99,** 247-257.

Ozturk, G. & Tonge, D. A. 2001. Effects of leukemia inhibitory factor on galanin expression and on axonal growth in adult dorsal root ganglion neurons in vitro. *Exp Neurol,* **169,** 376-385.

Park, K. K., Liu, K., et al. 2008. Promoting axon regeneration in the adult CNS by modulation of the PTEN/mTOR pathway. *Science,* **322,** 963-966.

Park, K. Y., Fletcher, J. R., et al. 2011. Epigenetic regulation of the calcitonin gene-related peptide gene in trigeminal glia. *Cephalalgia,* **31,** 614-624.

Parthun, M. R. 2007. Hat1: the emerging cellular roles of a type B histone acetyltransferase. *Oncogene,* **26,** 5319-5328.

Pasterkamp, R. J., Anderson, P. N., et al. 2001. Peripheral nerve injury fails to induce growth of lesioned ascending dorsal column axons into spinal cord scar tissue expressing the axon repellent Semaphorin3A. *Eur J Neurosci,* **13,** 457-471.

Pearson, A. G., Gray, C. W., et al. 2003. ATF3 enhances c-Jun-mediated neurite sprouting. *Brain Res Mol Brain Res,* **120,** 38-45.

Pedersen, M. T. & Helin, K. 2010. Histone demethylases in development and disease. *Trends Cell Biol,* **20,** 662-671.

Pei, Z., Wang, B., et al. 2011. Homeobox genes Gsx1 and Gsx2 differentially regulate telencephalic progenitor maturation. *Proc Natl Acad Sci U S A,* **108,** 1675-1680.

Ponger, L. & Mouchiroud, D. 2002. CpGProD: identifying CpG islands associated with transcription start sites in large genomic mammalian sequences. *Bioinformatics,* **18,** 631-633.

Pradhan, S., Bacolla, A., et al. 1999. Recombinant human DNA (cytosine-5) methyltransferase. I. Expression, purification, and comparison of de novo and maintenance methylation. *J Biol Chem,* **274,** 33002-33010.

Pruss, H., Wenzel, M., et al. 2003. Kir2 potassium channels in rat striatum are strategically localized to control basal ganglia function. *Brain Res Mol Brain Res,* **110,** 203-219.

Puttagunta, R., Schmandke, A., et al. 2011. RA-RAR-{beta} counteracts myelin-dependent inhibition of neurite outgrowth via Lingo-1 repression. *J Cell Biol,* **193,** 1147-1156.

Qiu, J., Cafferty, W. B., et al. 2005. Conditioning injury-induced spinal axon regeneration requires signal transducer and activator of transcription 3 activation. *J Neurosci,* **25,** 1645-1653.

Qiu, J., Cai, D., et al. 2002. Spinal axon regeneration induced by elevation of cyclic AMP. *Neuron,* **34,** 895-903.

Qiu, J., Cai, D., et al. 2000. Glial inhibition of nerve regeneration in the mature mammalian CNS. *Glia,* **29,** 166-174.

Qureshi, I. A., Mattick, J. S., et al. 2010. Long non-coding RNAs in nervous system function and disease. *Brain Res,* **1338,** 20-35.

Raisman, G. 2004. Myelin inhibitors: does NO mean GO? *Nat Rev Neurosci,* **5,** 157-161.

Raivich, G., Bohatschek, M., et al. 2004. The AP-1 transcription factor c-Jun is required for efficient axonal regeneration. *Neuron,* **43,** 57-67.

Rajendran, G., Shanmuganandam, K., et al. 2011. Epigenetic regulation of DNA methyltransferases: DNMT1 and DNMT3B in gliomas. *J Neurooncol,* **104,** 483-494.

Rasband, M. N., Park, E. W., et al. 2001. Distinct potassium channels on pain-sensing neurons. *Proc Natl Acad Sci U S A,* **98,** 13373-13378.

Rea, S., Eisenhaber, F., et al. 2000. Regulation of chromatin structure by site-specific histone H3 methyltransferases. *Nature,* **406,** 593-599.

Reik, W., Collick, A., et al. 1987. Genomic imprinting determines methylation of parental alleles in transgenic mice. *Nature,* **328,** 248-251.

Reik, W., Dean, W., et al. 2001. Epigenetic reprogramming in mammalian development. *Science,* **293,** 1089-1093.

Reimer, M. & Kanje, M. 1999. Peripheral but not central axotomy promotes axonal outgrowth and induces alterations in neuropeptide synthesis in the nodose ganglion of the rat. *Eur J Neurosci,* **11,** 3415-3423.

Riccio, A., Ahn, S., et al. 1999. Mediation by a CREB family transcription factor of NGF-dependent survival of sympathetic neurons. *Science,* **286,** 2358-2361.

Rice, J. C., Briggs, S. D., et al. 2003. Histone methyltransferases direct different degrees of methylation to define distinct chromatin domains. *Mol Cell,* **12,** 1591-1598.

Richardson, P. M., McGuinness, U. M., et al. 1980. Axons from CNS neurons regenerate into PNS grafts. *Nature,* **284,** 264-265.

Richardson, P. M., Miao, T., et al. 2009. Responses of the nerve cell body to axotomy. *Neurosurgery,* **65,** A74-79.

Riggs, A. D. 1975. X inactivation, differentiation, and DNA methylation. *Cytogenet Cell Genet,* **14,** 9-25.

Robertson, K. D., Uzvolgyi, E., et al. 1999. The human DNA methyltransferases (DNMTs) 1, 3a and 3b: coordinate mRNA expression in normal tissues and overexpression in tumors. *Nucleic Acids Res,* **27,** 2291-2298.

Rodriguez-Paredes, M. & Esteller, M. 2011. Cancer epigenetics reaches mainstream oncology. *Nat Med,* **17,** 330-339.

Roopra, A., Qazi, R., et al. 2004. Localized domains of G9a-mediated histone methylation are required for silencing of neuronal genes. *Mol Cell,* **14,** 727-738.

Roshanpour, F., Pourmirza, R., et al. 2012. Traumatic spinal cord lesions: impact of comprehensive nursing care. *J Inj Violence Res,* **4**.

Rossi, F., Gianola, S., et al. 2007. Regulation of intrinsic neuronal properties for axon growth and regeneration. *Prog Neurobiol,* **81,** 1-28.

Sachs, H. H., Wynick, D., et al. 2007. Galanin plays a role in the conditioning lesion effect in sensory neurons. *Neuroreport,* **18,** 1729-1733.

Sakurai, T., Dorr, N. P., et al. 2011. Haploinsufficiency of Gtf2i, a gene deleted in Williams Syndrome, leads to increases in social interactions. *Autism Res,* **4,** 28-39.

Samaco, R. C. & Neul, J. L. 2011. Complexities of Rett Syndrome and MeCP2. *J Neurosci,* **31,** 7951-7959.

Santini, V., Kantarjian, H. M., et al. 2001. Changes in DNA methylation in neoplasia: pathophysiology and therapeutic implications. *Ann Intern Med,* **134,** 573-586.

Saxonov, S., Berg, P., et al. 2006. A genome-wide analysis of CpG dinucleotides in the human genome distinguishes two distinct classes of promoters. *Proc Natl Acad Sci U S A,* **103,** 1412-1417.

Schecterson, L. C. & Bothwell, M. 1992. Novel roles for neurotrophins are suggested by BDNF and NT-3 mRNA expression in developing neurons. *Neuron,* **9,** 449-463.

Schirmer, U., Fiegl, H., et al. 2013. Epigenetic regulation of L1CAM in endometrial carcinoma: comparison to cancer--testis (CT-X) antigens. *BMC Cancer,* **13,** 156.

Schneider, R., Bannister, A. J., et al. 2002. Unsafe SETs: histone lysine methyltransferases and cancer. *Trends Biochem Sci,* **27,** 396-402.

Schnell, L., Schneider, R., et al. 1994. Neurotrophin-3 enhances sprouting of corticospinal tract during development and after adult spinal cord lesion. *Nature,* **367,** 170-173.

Schnell, L. & Schwab, M. E. 1990. Axonal regeneration in the rat spinal cord produced by an antibody against myelin-associated neurite growth inhibitors. *Nature,* **343,** 269-272.

Scholz, J. & Woolf, C. J. 2007. The neuropathic pain triad: neurons, immune cells and glia. *Nat Neurosci,* **10,** 1361-1368.

Schoofs, T. & Muller-Tidow, C. 2011. DNA methylation as a pathogenic event and as a therapeutic target in AML. *Cancer Treat Rev*.

Schreyer, D. J. & Skene, J. H. 1993. Injury-associated induction of GAP-43 expression displays axon branch specificity in rat dorsal root ganglion neurons. *J Neurobiol,* **24,** 959-970.

Schwab, M. E. 2004. Nogo and axon regeneration. *Curr Opin Neurobiol,* **14,** 118-124.

Schwab, M. E., Kapfhammer, J. P., et al. 1993. Inhibitors of neurite growth. *Annu Rev Neurosci,* **16,** 565-595.

Schwartz, M. 1987. Molecular and cellular aspects of nerve regeneration. *CRC Crit Rev Biochem,* **22,** 89-110.

Seijffers, R., Mills, C. D., et al. 2007. ATF3 increases the intrinsic growth state of DRG neurons to enhance peripheral nerve regeneration. *J Neurosci,* **27,** 7911-7920.

Seira, O., Gavin, R., et al. 2010. Neurites regrowth of cortical neurons by GSK3beta inhibition independently of Nogo receptor 1. *J Neurochem,* **113,** 1644-1658.

Serman, A., Vlahovic, M., et al. 2006. DNA methylation as a regulatory mechanism for gene expression in mammals. *Coll Antropol,* **30,** 665-671.

Sgado, P., Ferretti, E., et al. 2012. The atypical homeoprotein Pbx1a participates in the axonal pathfinding of mesencephalic dopaminergic neurons. *Neural Dev,* **7,** 24.

Shadiack, A. M. & Zigmond, R. E. 1998. Galanin induced in sympathetic neurons after axotomy is anterogradely transported toward regenerating nerve endings. *Neuropeptides,* **32,** 257-264.

Shahbazian, M. D., Antalffy, B., et al. 2002. Insight into Rett syndrome: MeCP2 levels display tissue- and cell-specific differences and correlate with neuronal maturation. *Hum Mol Genet,* **11,** 115-124.

Sharma, A., Moore, M., et al. 1999. The NeuroD1/BETA2 sequences essential for insulin gene transcription colocalize with those necessary for neurogenesis and p300/CREB binding protein binding. *Mol Cell Biol,* **19,** 704-713.

Sharma, R. P., Gavin, D. P., et al. 2010. CpG methylation in neurons: message, memory, or mask? *Neuropsychopharmacology,* **35,** 2009-2020.

Sharma, R. P., Grayson, D. R., et al. 2005. Chromatin, DNA methylation and neuron gene regulation--the purpose of the package. *J Psychiatry Neurosci,* **30,** 257-263.

Shein, N. A. & Shohami, E. 2011. Histone deacetylase inhibitors as therapeutic agents for acute central nervous system injuries. *Mol Med,* **17,** 448-456.

Shen, Y., Tenney, A. P., et al. 2009. PTPsigma is a receptor for chondroitin sulfate proteoglycan, an inhibitor of neural regeneration. *Science,* **326,** 592-596.

Shen, Z. L., Lassner, F., et al. 2000. Cellular activity of resident macrophages during Wallerian degeneration. *Microsurgery,* **20,** 255-261.

Shi, Y. 2007. Histone lysine demethylases: emerging roles in development, physiology and disease. *Nat Rev Genet,* **8,** 829-833.

Shi, Y. J., Matson, C., et al. 2005. Regulation of LSD1 histone demethylase activity by its associated factors. *Mol Cell,* **19,** 857-864.

Silver, J. & Miller, J. H. 2004. Regeneration beyond the glial scar. *Nat Rev Neurosci,* **5,** 146-156.

Singh, R. P., Shiue, K., et al. 2009. Cellular epigenetic modifications of neural stem cell differentiation. *Cell Transplant,* **18,** 1197-1211.

Singleton, M. K., Gonzales, M. L., et al. 2011. MeCP2 is required for global heterochromatic and nucleolar changes during activity-dependent neuronal maturation. *Neurobiol Dis,* **43,** 190-200.

Sivasankaran, B., Degen, M., et al. 2009. Tenascin-C is a novel RBPJkappa-induced target gene for Notch signaling in gliomas. *Cancer Res,* **69,** 458-465.

Skene, J. H. & Willard, M. 1981. Axonally transported proteins associated with axon growth in rabbit central and peripheral nervous systems. *J Cell Biol,* **89,** 96-103.

Smith-Thomas, L. C., Stevens, J., et al. 1995. Increased axon regeneration in astrocytes grown in the presence of proteoglycan synthesis inhibitors. *J Cell Sci,* **108 (Pt 3),** 1307-1315.

Smith, D. S. & Skene, J. H. 1997. A transcription-dependent switch controls competence of adult neurons for distinct modes of axon growth. *J Neurosci,* **17,** 646-658.

Smith, Z. D. & Meissner, A. 2013. DNA methylation: roles in mammalian development. *Nat Rev Genet,* **14,** 204-220.

Song, X. Y., Li, F., et al. 2008. Peripherally-derived BDNF promotes regeneration of ascending sensory neurons after spinal cord injury. *PLoS One,* **3,** e1707.

Soriano, F. X. & Hardingham, G. E. 2011. In cortical neurons HDAC3 activity suppresses RD4-dependent SMRT export. *PLoS One,* **6,** e21056.

Spannhoff, A., Hauser, A. T., et al. 2009. The emerging therapeutic potential of histone methyltransferase and demethylase inhibitors. *ChemMedChem,* **4,** 1568-1582.

Springer, J. E. 2002. Apoptotic cell death following traumatic injury to the central nervous system. *J Biochem Mol Biol,* **35,** 94-105.

Starkey, M. L., Davies, M., et al. 2009. Expression of the regeneration-associated protein SPRR1A in primary sensory neurons and spinal cord of the adult mouse following peripheral and central injury. *J Comp Neurol,* **513,** 51-68.

Sterner, D. E. & Berger, S. L. 2000. Acetylation of histones and transcription-related factors. *Microbiol Mol Biol Rev,* **64,** 435-459.

Stoll, G., Griffin, J. W., et al. 1989. Wallerian degeneration in the peripheral nervous system: participation of both Schwann cells and macrophages in myelin degradation. *J Neurocytol,* **18,** 671-683.

Strickland, I. T., Richards, L., et al. 2011. Axotomy-induced miR-21 promotes axon growth in adult dorsal root ganglion neurons. *PLoS One,* **6,** e23423.

Su, A. I., Wiltshire, T., et al. 2004. A gene atlas of the mouse and human protein-encoding transcriptomes. *Proc Natl Acad Sci U S A,* **101,** 6062-6067.

Sui, L., Wang, Y., et al. 2012. Epigenetic regulation of reelin and brain-derived neurotrophic factor genes in long-term potentiation in rat medial prefrontal cortex. *Neurobiol Learn Mem,* **97,** 425-440.

Sung, Y. J., Chiu, D. T., et al. 2006. Activation and retrograde transport of protein kinase G in rat nociceptive neurons after nerve injury and inflammation. *Neuroscience,* **141,** 697-709.

Tachibana, M., Matsumura, Y., et al. 2008. G9a/GLP complexes independently mediate H3K9 and DNA methylation to silence transcription. *EMBO J,* **27,** 2681-2690.

Takahashi, S., Inatome, R., et al. 2003. Isolation and expression of a novel mitochondrial septin that interacts with CRMP/CRAM in the developing neurones. *Genes Cells,* **8,** 81-93.

Takizawa, T., Nakashima, K., et al. 2001. DNA methylation is a critical cell-intrinsic determinant of astrocyte differentiation in the fetal brain. *Dev Cell,* **1,** 749-758.

Tanabe, K., Bonilla, I., et al. 2003. Fibroblast growth factor-inducible-14 is induced in axotomized neurons and promotes neurite outgrowth. *J Neurosci,* **23,** 9675-9686.

Tao, X., Finkbeiner, S., et al. 1998. Ca2+ influx regulates BDNF transcription by a CREB family transcription factor-dependent mechanism. *Neuron,* **20,** 709-726.

Tawa, R., Ono, T., et al. 1990. Changes of DNA methylation level during pre- and postnatal periods in mice. *Differentiation,* **45,** 44-48.

Taylor, A. M., Berchtold, N. C., et al. 2009. Axonal mRNA in uninjured and regenerating cortical mammalian axons. *J Neurosci,* **29,** 4697-4707.

Tedeschi, A. & Di Giovanni, S. 2009a. The non-apoptotic role of p53 in neuronal biology: enlightening the dark side of the moon. *EMBO Rep,* **10,** 576-583.

Tedeschi, A., Nguyen, T., et al. 2009b. A p53-CBP/p300 transcription module is required for GAP-43 expression, axon outgrowth, and regeneration. *Cell Death Differ,* **16,** 543-554.

Tedeschi, A., Nguyen, T., et al. 2009c. The tumor suppressor p53 transcriptionally regulates cGKI expression during neuronal maturation and is required for cGMP-dependent growth cone collapse. *J Neurosci,* **29,** 15155-15160.

Teng, F. Y. & Tang, B. L. 2006. Axonal regeneration in adult CNS neurons--signaling molecules and pathways. *J Neurochem,* **96,** 1501-1508.

Tian, F., Hu, X. Z., et al. 2009. Dynamic chromatin remodeling events in hippocampal neurons are associated with NMDA receptor-mediated activation of Bdnf gene promoter 1. *J Neurochem,* **109,** 1375-1388.

Tochiki, K. K., Cunningham, J., et al. 2012. The expression of spinal methyl-CpG-binding protein 2, DNA methyltransferases and histone deacetylases is modulated in persistent pain states. *Mol Pain,* **8,** 14.

Tollefsbol, T. O. & Hutchison, C. A., 3rd 1995. Mammalian DNA (cytosine-5-)-methyltransferase expressed in Escherichia coli, purified and characterized. *J Biol Chem,* **270,** 18543-18550.

Tonra, J. R., Curtis, R., et al. 1998. Axotomy upregulates the anterograde transport and expression of brain-derived neurotrophic factor by sensory neurons. *J Neurosci,* **18,** 4374-4383.

Trapp, B. D., Andrews, S. B., et al. 1989. Co-localization of the myelin-associated glycoprotein and the microfilament components, F-actin and spectrin, in Schwann cells of myelinated nerve fibres. *J Neurocytol,* **18,** 47-60.

Tremblay, K. D., Duran, K. L., et al. 1997. A 5' 2-kilobase-pair region of the imprinted mouse H19 gene exhibits exclusive paternal methylation throughout development. *Mol Cell Biol,* **17,** 4322-4329.

Trewick, S. C., McLaughlin, P. J., et al. 2005. Methylation: lost in hydroxylation? *EMBO Rep,* **6,** 315-320.

Tsankova, N. M., Berton, O., et al. 2006. Sustained hippocampal chromatin regulation in a mouse model of depression and antidepressant action. *Nat Neurosci,* **9,** 519-525.

Tsuda, Y., Kanje, M., et al. 2011. Axonal outgrowth is associated with increased ERK 1/2 activation but decreased caspase 3 linked cell death in Schwann cells after immediate nerve repair in rats. *BMC Neurosci,* **12,** 12.

Tsukada, Y., Fang, J., et al. 2006. Histone demethylation by a family of JmjC domain-containing proteins. *Nature,* **439,** 811-816.

Tucker, K. L. 2001. Methylated cytosine and the brain: a new base for neuroscience. *Neuron,* **30,** 649-652.

Turek-Plewa, J. & Jagodzinski, P. P. 2005. The role of mammalian DNA methyltransferases in the regulation of gene expression. *Cell Mol Biol Lett,* **10,** 631-647.

Upadhyay, A. K. & Cheng, X. 2011. Dynamics of histone lysine methylation: structures of methyl writers and erasers. *Prog Drug Res,* **67,** 107-124.

Uribe-Lewis, S., Woodfine, K., et al. 2011. Molecular mechanisms of genomic imprinting and clinical implications for cancer. *Expert Rev Mol Med,* **13,** e2.

Vogel, T., Stoykova, A., et al. 2006. Differential expression of polycomb repression complex 1 (PRC1) members in the developing mouse brain reveals multiple complexes. *Dev Dyn,* **235,** 2574-2585.

Wagener, R., Kobbe, B., et al. 2001. Characterization of the mouse matrilin-4 gene: a 5' antiparallel overlap with the gene encoding the transcription factor RBP-l. *Genomics,* **76,** 89-98.

Wakatsuki, S., Saitoh, F., et al. 2011. ZNRF1 promotes Wallerian degeneration by degrading AKT to induce GSK3B-dependent CRMP2 phosphorylation. *Nat Cell Biol,* **13,** 1415-1423.

Walker, B. A., Ji, S. J., et al. 2012. Intra-axonal translation of RhoA promotes axon growth inhibition by CSPG. *J Neurosci,* **32,** 14442-14447.

Wallberg, A. E., Pedersen, K., et al. 2002. p300 and PCAF act cooperatively to mediate transcriptional activation from chromatin templates by notch intracellular domains in vitro. *Mol Cell Biol,* **22,** 7812-7819.

Wang, J., Hevi, S., et al. 2009. The lysine demethylase LSD1 (KDM1) is required for maintenance of global DNA methylation. *Nat Genet,* **41,** 125-129.

Wang, Z., Andrade, N., et al. 2012. Meteorin is a chemokinetic factor in neuroblast migration and promotes stroke-induced striatal neurogenesis. *J Cereb Blood Flow Metab,* **32,** 387-398.

Wang, Z., Zang, C., et al. 2008. Combinatorial patterns of histone acetylations and methylations in the human genome. *Nat Genet,* **40,** 897-903.

Watanabe, D., Uchiyama, K., et al. 2006. Transition of mouse de novo methyltransferases expression from Dnmt3b to Dnmt3a during neural progenitor cell development. *Neuroscience,* **142,** 727-737.

Watson, P., Black, G., et al. 2001. Angelman syndrome phenotype associated with mutations in MECP2, a gene encoding a methyl CpG binding protein. *J Med Genet,* **38,** 224-228.

Weber, M., Davies, J. J., et al. 2005. Chromosome-wide and promoter-specific analyses identify sites of differential DNA methylation in normal and transformed human cells. *Nat Genet,* **37,** 853-862.

Weber, M., Hellmann, I., et al. 2007. Distribution, silencing potential and evolutionary impact of promoter DNA methylation in the human genome. *Nat Genet,* **39,** 457-466.

Weishaupt, N., Blesch, A., et al. 2012. BDNF: the career of a multifaceted neurotrophin in spinal cord injury. *Exp Neurol,* **238,** 254-264.

Wilkins, R. J. 1988. Genomic imprinting and carcinogenesis. *Lancet,* **1,** 329-331.

Wilkinson, L. S., Davies, W., et al. 2007. Genomic imprinting effects on brain development and function. *Nat Rev Neurosci,* **8,** 832-843.

Windebank, A. J. & Poduslo, J. F. 1986. Neuronal growth factors produced by adult peripheral nerve after injury. *Brain Res,* **385,** 197-200.

Wong, C. M., Wong, C. C., et al. 2011. Transcriptional repressive H3K9 and H3K27 methylations contribute to DNMT1-mediated DNA methylation recovery. *PLoS One,* **6,** e16702.

Wong, K., Zhang, J., et al. 2004. Nerve growth factor receptor signaling induces histone acetyltransferase domain-dependent nuclear translocation of p300/CREB-binding protein-associated factor and hGCN5 acetyltransferases. *J Biol Chem,* **279,** 55667-55674.

Wong, L. F., Yip, P. K., et al. 2006. Retinoic acid receptor beta2 promotes functional regeneration of sensory axons in the spinal cord. *Nat Neurosci,* **9,** 243-250.

Wossidlo, M., Arand, J., et al. 2010. Dynamic link of DNA demethylation, DNA strand breaks and repair in mouse zygotes. *EMBO J,* **29,** 1877-1888.

Wu, D., Raafat, M., et al. 2011. MicroRNA machinery responds to peripheral nerve lesion in an injury-regulated pattern. *Neuroscience,* **190,** 386-397.

Wu, F., Xing, D., et al. 2008. Enhanced rat sciatic nerve regeneration through silicon tubes implanted with valproic acid. *J Reconstr Microsurg,* **24,** 267-276.

Wu, J., Wang, S. H., et al. 2007a. Diverse histone modifications on histone 3 lysine 9 and their relation to DNA methylation in specifying gene silencing. *BMC Genomics,* **8,** 131.

Wu, J. I., Lessard, J., et al. 2007b. Regulation of dendritic development by neuron-specific chromatin remodeling complexes. *Neuron,* **56,** 94-108.

Wu, L., Sun, T., et al. 2002. Identification of a family of mastermind-like transcriptional coactivators for mammalian notch receptors. *Mol Cell Biol,* **22,** 7688-7700.

Wu, S. C. & Zhang, Y. 2010. Active DNA demethylation: many roads lead to Rome. *Nat Rev Mol Cell Biol,* **11,** 607-620.

Xenaki, G., Ontikatze, T., et al. 2008. PCAF is an HIF-1alpha cofactor that regulates p53 transcriptional activity in hypoxia. *Oncogene,* **27,** 5785-5796.

Xu, W., Edmondson, D. G., et al. 1998. Mammalian GCN5 and P/CAF acetyltransferases have homologous amino-terminal domains important for recognition of nucleosomal substrates. *Mol Cell Biol,* **18,** 5659-5669.

Yakovlev, A. G. & Faden, A. I. 1995. Molecular biology of CNS injury. *J Neurotrauma,* **12,** 767-777.

Yamauchi, J., Miyamoto, Y., et al. 2007. Gadd45a, the gene induced by the mood stabilizer valproic acid, regulates neurite outgrowth through JNK and the substrate paxillin in N1E-115 neuroblastoma cells. *Exp Cell Res,* **313,** 1886-1896.

Yang, P. & Yang, Z. 2012. Enhancing intrinsic growth capacity promotes adult CNS regeneration. *J Neurol Sci,* **312,** 1-6.

Yang, X. J. & Seto, E. 2007. HATs and HDACs: from structure, function and regulation to novel strategies for therapy and prevention. *Oncogene,* **26,** 5310-5318.

Yang, X. J. & Seto, E. 2008. The Rpd3/Hda1 family of lysine deacetylases: from bacteria and yeast to mice and men. *Nat Rev Mol Cell Biol,* **9,** 206-218.

Yiu, G. & He, Z. 2006. Glial inhibition of CNS axon regeneration. *Nat Rev Neurosci,* **7,** 617-627.

Ylera, B., Erturk, A., et al. 2009. Chronically CNS-injured adult sensory neurons gain regenerative competence upon a lesion of their peripheral axon. *Curr Biol,* **19,** 930-936.

Yu, B., Zhou, S., et al. 2013. Altered long noncoding RNA expressions in dorsal root ganglion after rat sciatic nerve injury. *Neurosci Lett,* **534,** 117-122.

Yu, N. K., Baek, S. H., et al. 2011. DNA methylation-mediated control of learning and memory. *Mol Brain,* **4,** 5.

Zagrebelsky, M., Buffo, A., et al. 1998. Retrograde regulation of growth-associated gene expression in adult rat Purkinje cells by myelin-associated neurite growth inhibitory proteins. *J Neurosci,* **18,** 7912-7929.

Zhang, B., West, E. J., et al. 2008. HDAC inhibitor increases histone H3 acetylation and reduces microglia inflammatory response following traumatic brain injury in rats. *Brain Res,* **1226,** 181-191.

Zhang, H. Y., Zheng, S. J., et al. 2011. MicroRNAs 144, 145, and 214 are down-regulated in primary neurons responding to sciatic nerve transection. *Brain Res,* **1383,** 62-70.

Zhang, Y., Bo, X., et al. 2005. Growth-associated protein GAP-43 and L1 act synergistically to promote regenerative growth of Purkinje cell axons in vivo. *Proc Natl Acad Sci U S A,* **102,** 14883-14888.

Zhang, Y., Roslan, R., et al. 2000. Expression of CHL1 and L1 by neurons and glia following sciatic nerve and dorsal root injury. *Mol Cell Neurosci,* **16,** 71-86.

Zhao, Y., Katzman, R. B., et al. 2007. The notch regulator MAML1 interacts with p53 and functions as a coactivator. *J Biol Chem,* **282,** 11969-11981.

Zhou, F. Q., Walzer, M. A., et al. 2004. Turning on the machine: genetic control of axon regeneration by c-Jun. *Neuron,* **43,** 1-2.

Zhou, L., Baumgartner, B. J., et al. 2003. Neurotrophin-3 expressed in situ induces axonal plasticity in the adult injured spinal cord. *J Neurosci,* **23,** 1424-1431.

Zhu, B., Benjamin, D., et al. 2001. Overexpression of 5-methylcytosine DNA glycosylase in human embryonic kidney cells EcR293 demethylates the promoter of a hormone-regulated reporter gene. *Proc Natl Acad Sci U S A,* **98,** 5031-5036.

Zhu, Q., Wang, L., et al. 2012. Increased expression of DNA methyltransferase 1 and 3a in human temporal lobe epilepsy. *J Mol Neurosci,* **46,** 420-426.

Zhubi, A., Veldic, M., et al. 2009. An upregulation of DNA-methyltransferase 1 and 3a expressed in telencephalic GABAergic neurons of schizophrenia patients is also detected in peripheral blood lymphocytes. *Schizophr Res,* **111,** 115-122.

Zibetti, C., Adamo, A., et al. 2010. Alternative splicing of the histone demethylase LSD1/KDM1 contributes to the modulation of neurite morphogenesis in the mammalian nervous system. *J Neurosci,* **30,** 2521-2532.

Zocchi, L. & Sassone-Corsi, P. 2012. SIRT1-mediated deacetylation of MeCP2 contributes to BDNF expression. *Epigenetics,* **7,** 695-700.

Zuo, J., Ferguson, T. A., et al. 1998. Neuronal matrix metalloproteinase-2 degrades and inactivates a neurite-inhibiting chondroitin sulfate proteoglycan. *J Neurosci,* **18,** 5203-5211.

7 Appendix

7.1 Supplementary Tables

Table S1 – Complete list of hyper- and hypomethylated genes upon sciatic nerve axotomy (SNA) or dorsal column axotomy (DCA) for each time point were filtered from the complete Roche/NimbleGen microarray dataset. An extreme scenario was applied to filter genes with Methylation Values (MV) of +5 or -5 regarding only single conditions, pre-filtered for the corresponding naive value (0 or 1 out of 3 hits for hypermethylated genes; 2 or 3 out of 3 hits for hypomethylated genes). Altogether 179 genes were filtered, 105 hypermethylated and 74 hypomethylated.

NCBI	Gene	SNA 1 day			SNA 3 days			SNA 7 days			DCA 1 day			DCA 3 days			DCA 7 days			N
Gene ID	Symbol	Inj	Sh	MV	Inj	Sh	MV	Inj	Sh	MV	Inj	Sh	MV	Inj	Sh	MV	Inj	Sh	MV	
HYPOmethylated genes after 1 day upon Sciatic nerve axotomy (SNA) - with Naive 3 or 2 - 5 Genes																				
11421	Ace	0	2	-5	1	1	-1	2	2	-2	2	2	-2	3	2	0	3	2	0	3
71991	Ercc8	0	2	-5	1	0	2	2	1	1	0	1	-3	1	1	-1	2	2	-2	2
14685	Gnat1	0	2	-5	2	2	-2	3	2	0	3	2	0	3	2	0	3	2	0	3
16682	Krt2-4	0	2	-5	0	2	-5	0	0	0	3	1	3	3	1	3	3	2	0	2
19668	Rbpsuhl	0	2	-5	0	2	-5	1	0	2	3	2	0	3	1	3	2	2	-2	3
HYPOmethylated genes after 3 day upon Sciatic nerve axotomy (SNA) - with Naive 3 or 2 - 14 Genes																				
11639	Ak3l1	2	0	4	0	2	-5	0	0	0	2	1	1	3	1	3	2	2	-2	2
11717	Ampd3	2	1	1	0	2	-5	2	2	-2	1	2	-4	3	1	3	2	2	-2	3
320982	Arl4c	3	1	3	0	2	-5	2	0	4	3	2	0	3	2	0	3	2	0	3
619306	B430319F04	2	1	1	0	2	-5	2	2	-2	1	2	-4	3	1	3	2	2	-2	3
66142	Cox7b	2	1	1	0	2	-5	0	0	0	2	0	4	2	0	4	2	2	-2	3
234796	Klhl36	2	2	-2	0	2	-5	1	1	-1	1	1	-1	2	2	-2	3	2	0	3
16682	Krt2-4	0	2	-5	0	2	-5	0	0	0	3	1	3	3	1	3	3	2	0	2
230654	Lrrc41	3	1	3	0	2	-5	0	0	0	1	1	-1	2	0	4	1	1	-1	2
272381	Lrrc4b	3	1	3	0	2	-5	1	0	2	2	1	1	1	1	-1	3	1	3	2
67075	Magt1	2	1	1	0	2	-5	0	0	0	2	0	4	2	0	4	2	2	-2	3
229877	Rap1gds1	1	2	-4	0	2	-5	0	0	0	1	1	-1	0	0	0	2	1	1	2
19668	Rbpsuhl	0	2	-5	0	2	-5	1	0	2	3	2	0	3	1	3	2	2	-2	3
75841	Rnf139	1	2	-4	0	2	-5	0	0	0	1	1	-1	2	1	1	1	1	-1	2
66576	Uqcrh	3	1	3	0	2	-5	0	0	0	1	1	-1	2	0	4	1	1	-1	2
HYPOmethylated genes after 7 day upon Sciatic nerve axotomy (SNA) - with Naive 3 or 2 - 5 Genes																				
320237	6330419J24	1	1	-1	2	1	1	0	2	-5	3	1	3	2	2	-2	3	0	5	2
109050	6530418L21	3	2	0	1	1	-1	0	2	-5	2	2	-2	2	1	1	3	2	0	2
66071	Ethe1	1	0	2	3	1	3	0	2	-5	1	2	-4	0	1	-3	2	0	4	2
93759	Sirt1	1	1	-1	1	1	-1	0	2	-5	3	2	0	1	2	-4	1	0	2	2
270028	Tmem28	1	2	-4	2	0	4	0	2	-5	1	1	-1	1	2	-4	1	2	-4	2

NCBI Gene ID	Gene Symbol	SNA 1 day			SNA 3 days			SNA 7 days			DCA 1 day			DCA 3 days			DCA 7 days			N
		Inj	Sh	MV	Inj	Sh	MV	Inj	Sh	MV	Inj	Sh	MV	Inj	Sh	MV	Inj	Sh	MV	
HYPOmethylated genes after 1 day upon Dorsal column axatomy (DCA) - with Naive 3 or 2 - 8 Genes																				
654824	Ankrd37	0	0	0	0	0	0	1	1	-1	0	2	-5	2	0	4	2	0	4	2
72685	Dnajc6	2	2	-2	3	1	3	3	1	3	0	2	-5	1	1	-1	3	2	0	2
94245	Dtnbp1	1	1	-1	2	0	4	1	0	2	0	2	-5	1	0	2	0	2	-5	2
140703	Emid1	2	2	-2	3	2	0	3	2	0	0	2	-5	3	1	3	3	2	0	3
14159	Fes	1	0	2	3	2	0	2	0	4	0	2	-5	1	0	2	2	2	-2	2
625424	LOC625424	1	0	2	1	2	-4	2	1	1	0	2	-5	1	0	2	2	1	1	2
231290	Slc10a4	2	2	-2	2	2	-2	1	1	-1	0	2	-5	1	1	-1	2	2	-2	2
22414	Wnt2b	2	0	4	1	0	2	2	0	4	0	2	-5	1	1	-1	0	1	-3	2
HYPOmethylated genes after 3 days upon Dorsal column axatomy (DCA) - with Naive 3 or 2 - 6 Genes																				
11550	Adra1d	1	1	-1	3	0	5	1	0	2	1	1	-1	0	2	-5	1	2	-4	2
57444	Isg20	2	1	1	2	2	-2	3	0	5	3	1	3	0	2	-5	2	1	1	2
118451	Mrps2	2	0	4	2	0	4	0	0	0	2	0	4	0	2	-5	1	0	2	2
67938	Mylc2b	2	0	4	0	0	0	0	0	0	1	1	-1	0	2	-5	0	0	0	2
56274	Stk3	3	2	0	3	1	3	1	0	2	1	1	-1	0	2	-5	2	2	-2	2
387515	Tas2r144	2	1	1	0	1	-3	1	1	-1	0	1	-3	0	2	-5	0	1	-3	2
HYPOmethylated genes after 7 days upon Dorsal column axatomy (DCA) - with Naive 3 or 2 - 36 Genes																				
67326	1700037H04	0	1	-3	0	0	0	0	0	0	1	1	-1	1	0	2	0	2	-5	3
66528	2210020M01	0	0	0	2	1	1	0	1	-3	2	2	-2	1	0	2	0	2	-5	3
70793	4631402N15	1	1	-1	1	0	2	0	1	-3	0	1	-3	2	1	1	0	2	-5	2
327824	5330438D12	2	2	-2	1	1	-1	0	0	0	3	2	0	3	1	3	0	2	-5	2
381155	9630014M24	3	2	0	1	0	2	1	0	2	2	1	1	0	1	-3	0	2	-5	2
11419	Accn2	1	1	-1	2	0	4	0	0	0	0	1	-3	0	0	0	0	2	-5	2
110355	Adrbk1	3	1	3	2	0	4	0	0	0	0	1	-3	0	0	0	0	2	-5	2
11702	Amd1	0	0	0	1	0	2	2	0	4	0	1	-3	1	1	-1	0	2	-5	2
11703	Amd2	0	0	0	1	0	2	2	0	4	0	1	-3	1	1	-1	0	2	-5	2
11877	Arvcf	3	0	5	2	1	1	0	0	0	0	1	-3	0	0	0	0	2	-5	3
72068	Cnot2	2	2	-2	1	1	-1	0	0	0	3	2	0	3	1	3	0	2	-5	2
231464	Cnot6l	1	1	-1	1	0	2	1	1	-1	3	1	3	2	2	-2	0	2	-5	2
13123	Cyp7b1	1	1	-1	1	1	-1	1	0	2	0	0	0	0	0	0	0	2	-5	3
94245	Dtnbp1	1	1	-1	2	0	4	1	0	2	0	2	-5	1	0	2	0	2	-5	2
67148	FAM103A1	1	1	-1	1	0	2	0	0	0	0	0	0	0	1	-3	0	2	-5	2
70363	Fam135b	0	0	0	2	0	4	0	1	-3	0	1	-3	1	1	-1	0	2	-5	2
381353	Gm996	3	2	0	2	1	1	1	0	2	2	2	-2	3	1	3	0	2	-5	2
14886	Gtf2i	3	2	0	2	1	1	0	0	0	2	1	1	2	1	1	0	2	-5	3
72692	Hnrpll	2	1	1	3	0	5	1	0	2	2	1	1	3	2	0	0	2	-5	2
53602	Hpcal1	2	2	-2	2	2	-2	0	0	0	1	1	-1	2	2	-2	0	2	-5	2
16004	Igf2r	2	0	4	1	0	2	0	0	0	0	0	0	0	0	0	0	2	-5	2
16573	Kif5b	0	1	-3	2	0	4	0	0	0	1	1	-1	3	1	3	0	2	-5	2
380916	Lrch1	3	2	0	2	1	1	0	0	0	3	1	3	3	1	3	0	2	-5	2
26921	Map4k4	1	2	-4	1	1	-1	0	1	-3	2	1	1	0	0	0	0	2	-5	2
17537	Mrg2/Meis3	3	2	0	2	1	1	1	0	2	0	1	-3	0	1	-3	0	2	-5	2
216856	Nlgn2	1	0	2	1	0	2	0	0	0	0	0	0	0	0	0	0	2	-5	3
70510	Rnf167	0	0	0	0	0	0	0	0	0	0	1	-3	0	0	0	0	2	-5	2
76816	Sdccag8	3	1	3	2	1	1	0	0	0	3	2	0	3	2	0	0	2	-5	2
208431	Shroom4	2	0	4	2	0	4	0	0	0	0	0	0	0	0	0	0	2	-5	2
67863	Slc25a11	0	0	0	0	0	0	0	0	0	0	1	-3	0	0	0	0	2	-5	2
24066	Spry4	3	2	0	1	0	2	1	0	2	2	1	1	0	1	-3	0	2	-5	2
66079	Tmem42	3	0	5	2	0	4	0	0	0	0	1	-3	0	0	0	0	2	-5	2
67808	Tprgl	1	1	-1	2	2	-2	2	2	-2	3	2	0	3	1	3	0	2	-5	3
68728	Trp53inp2	3	2	0	1	0	2	0	0	0	1	1	-1	0	0	0	0	2	-5	3
320538	Ubn2	2	1	1	2	1	1	2	1	1	1	1	-1	3	1	3	0	2	-5	2
56491	Vapb	0	1	-3	3	0	5	0	0	0	2	1	1	1	1	-1	0	2	-5	2

NCBI Gene ID	Gene Symbol	SNA 1 day Inj	Sh	MV	SNA 3 days Inj	Sh	MV	SNA 7 days Inj	Sh	MV	DCA 1 day Inj	Sh	MV	DCA 3 days Inj	Sh	MV	DCA 7 days Inj	Sh	MV	N
HYPERmethylated genes after 1 day upon Sciatic nerve axatomy (SNA) - with Naive 0 or 1 - 36 Genes																				
69380	1700013G24	3	0	5	0	0	0	1	0	2	0	0	0	1	0	2	0	0	0	0
70419	2810408A11	3	0	5	0	0	0	0	0	0	2	0	4	0	0	0	0	0	0	0
67642	4930515G01	3	0	5	2	0	4	0	0	0	1	1	-1	0	0	0	1	0	2	1
442825	A230083G16	3	0	5	0	0	0	0	0	0	1	0	2	0	0	0	0	0	0	1
72482	Acbd6	3	0	5	0	0	0	0	0	0	0	0	0	0	0	0	0	0	0	1
271813	Agbl2	3	0	5	2	0	4	2	1	1	2	1	1	1	0	2	1	0	2	1
68420	Ankrd13a	3	0	5	2	0	4	0	0	0	1	1	-1	0	0	0	1	0	2	1
12418	Cbx4	3	0	5	1	1	-1	0	0	0	0	0	0	1	1	-1	0	0	0	0
53951	Ccdc75	3	0	5	0	1	-3	1	2	-4	3	0	5	3	1	3	2	1	1	1
68119	Cmtm3	3	0	5	2	1	1	1	0	2	2	2	-2	2	2	-2	3	1	3	1
432508	Cpsf6	3	0	5	2	1	1	0	1	-3	1	1	-1	1	1	-1	1	0	2	1
26554	Cul3	3	0	5	1	1	-1	0	0	0	0	0	0	0	0	0	0	0	0	1
13177	Dci	3	0	5	2	1	1	1	0	2	2	0	4	1	0	2	0	2	-5	1
14118	Fbn1	3	0	5	2	0	4	0	2	-5	1	0	2	0	1	-3	0	0	0	0
98970	Fibcd1	3	0	5	0	0	0	0	0	0	1	1	-1	1	0	2	0	0	0	1
319448	Fndc3a	3	0	5	0	1	-3	0	0	0	1	1	-1	2	0	4	0	2	-5	1
14360	Fyn	3	0	5	0	1	-3	0	0	0	1	1	-1	1	0	2	0	0	0	0
57265	Fzd2	3	0	5	0	0	0	0	0	0	1	0	2	0	0	0	0	0	0	0
26431	Git2	3	0	5	2	0	4	0	0	0	1	1	-1	0	0	0	1	0	2	1
380629	Heca	3	0	5	0	0	0	0	0	0	1	1	-1	1	1	-1	0	0	0	1
110033	Kif22	3	0	5	1	1	-1	3	0	5	0	0	0	0	0	0	1	0	2	0
338372	Map3k9	3	0	5	2	0	4	1	1	-1	3	1	3	3	1	3	3	1	3	1
70083	Metrn	3	0	5	0	0	0	0	0	0	1	1	-1	0	0	0	0	1	-3	1
216860	Neurl4	3	0	5	0	0	0	0	0	0	2	0	4	0	0	0	0	0	0	0
18619	Penk1	3	0	5	0	0	0	0	0	0	1	1	-1	0	1	-3	0	0	0	0
19271	Ptprj	3	0	5	0	0	0	0	0	0	1	0	2	0	0	0	0	1	-3	0
269003	Sap130	3	0	5	1	0	2	0	0	0	0	0	0	2	1	1	0	0	0	0
140740	Sec63	3	0	5	2	2	-2	1	0	2	3	2	0	3	2	0	2	1	1	1
59049	Slc22a17	3	0	5	0	1	-3	0	0	0	3	0	5	3	2	0	1	2	-4	1
53896	Slc7a10	3	0	5	0	2	-5	1	1	-1	0	0	0	0	0	0	1	1	-1	1
68094	Smarcc2	3	0	5	0	0	0	0	0	0	0	0	0	0	0	0	0	1	-3	1
21423	Tcfe2a	3	0	5	0	1	-3	0	1	-3	1	1	-1	1	0	2	0	1	-3	1
68944	Tmco1	3	0	5	3	1	3	3	0	5	2	1	1	3	1	3	1	1	-1	1
68027	Tmem178	3	0	5	2	0	4	1	1	-1	3	1	3	2	2	-2	0	0	0	0
78784	Tnrc4	3	0	5	2	0	4	0	0	0	1	1	-1	1	0	2	1	0	2	0
22063	Trpc1	3	0	5	0	0	0	0	0	0	0	1	-3	2	0	4	1	1	-1	1
HYPERmethylated genes after 3 days upon Sciatic nerve axatomy (SNA) - with Naive 0 or 1 - 17 Genes																				
192136	AF397014	0	1	-3	3	0	5	2	0	4	2	1	1	1	1	-1	0	1	-3	1
12325	Camk2g	2	2	-2	3	0	5	0	0	0	1	1	-1	1	1	-1	0	1	-3	0
75796	Cdyl2	0	1	-3	3	0	5	0	0	0	0	0	0	0	1	-3	0	1	-3	1
12739	Cldn3	1	2	-4	3	0	5	2	2	-2	2	1	1	3	1	3	3	2	0	0
224897	Dpp9	3	2	0	3	0	5	1	0	2	2	1	1	1	1	-1	1	2	-4	1
14236	Foxn2	3	1	3	3	0	5	3	2	0	3	2	0	2	2	-2	2	0	4	1
74105	Gga2	0	1	-3	3	0	5	2	1	1	1	0	2	2	1	1	3	1	3	1
56295	Higd1a	1	0	2	3	0	5	0	1	-3	1	2	-4	3	1	3	2	1	1	1
16570	Kif3c	3	1	3	3	0	5	2	1	1	0	0	0	0	0	0	2	0	4	1
269513	Nkain3	1	1	-1	3	0	5	0	0	0	0	1	-3	1	1	-1	0	0	0	0
18145	Npc1	0	0	0	3	0	5	0	0	0	1	0	2	3	2	0	0	0	0	1
18741	Pitx2	2	0	4	3	0	5	3	2	0	1	1	-1	3	0	5	3	1	3	1
56294	Ptpn9	2	2	-2	3	0	5	0	0	0	1	1	-1	0	1	-3	0	1	-3	1
244882	Tnfaip8l3	2	1	1	3	0	5	1	1	-1	2	2	-2	3	2	0	2	1	1	1
66308	Ttdn1	0	1	-3	3	0	5	2	0	4	2	1	1	1	1	-1	0	1	-3	1
230796	Wdtc1	2	2	-2	3	0	5	0	0	0	1	1	-1	1	1	-1	1	2	-4	1
228994	Ythdf1	2	0	4	3	0	5	0	0	0	0	1	-3	0	0	0	0	0	0	1
HYPERmethylated genes after 7 days upon Sciatic nerve axatomy (SNA) - with Naive 0 or 1 - 6 Genes																				
654812	Angptl7	1	0	2	0	1	-3	3	0	5	0	0	0	0	0	0	0	0	0	0
73167	Arhgap8	1	1	-1	0	0	0	3	0	5	1	0	2	0	0	0	1	1	-1	1
69046	Hbld2	3	1	3	2	1	1	3	0	5	3	2	0	3	2	0	2	0	4	1
110033	Kif22	3	0	5	1	1	-1	3	0	5	0	0	0	0	0	0	1	0	2	0
239766	Rtp1	0	0	0	0	0	0	3	0	5	0	0	0	0	0	0	0	0	0	0
68944	Tmco1	3	0	5	3	1	3	3	0	5	2	1	1	3	1	3	1	1	-1	1

NCBI Gene ID	Gene Symbol	SNA 1 day Inj	Sh	MV	SNA 3 days Inj	Sh	MV	SNA 7 days Inj	Sh	MV	DCA 1 day Inj	Sh	MV	DCA 3 days Inj	Sh	MV	DCA 7 days Inj	Sh	MV	N
HYPERmethylated genes after 1 day upon Dorsal column axatomy (DCA) - with Naive 0 or 1 - 10 Genes																				
56068	Ammecr1	2	1	1	0	1	-3	0	0	0	3	0	5	0	1	-3	0	0	0	0
53951	Ccdc75	3	0	5	0	1	-3	1	2	-4	3	0	5	3	1	3	2	1	1	1
54419	Cldn6	1	0	2	1	0	2	1	1	-1	3	0	5	2	2	-2	2	2	-2	1
231413	Grsf1	1	0	2	2	1	1	1	1	-1	3	0	5	3	2	0	1	0	2	0
14843	Gsh2	1	0	2	2	0	4	0	1	-3	3	0	5	0	0	0	0	1	-3	1
433586	Maml3	0	1	-3	0	0	0	0	1	-3	3	0	5	0	2	-5	1	0	2	0
19072	Prep	3	2	0	2	1	1	2	1	1	3	0	5	0	1	-3	1	0	2	1
59049	Slc22a17	3	0	5	0	1	-3	0	0	0	3	0	5	3	2	0	1	2	-4	1
27279	Tnfrsf12a	1	0	2	1	0	2	1	1	-1	3	0	5	2	2	-2	2	2	-2	1
229603	Za20d1	0	1	-3	2	1	1	1	0	2	3	0	5	3	0	5	2	0	4	0
HYPERmethylated genes after 3 days upon Dorsal column axatomy (DCA) - with Naive 0 or 1 - 16 Genes																				
78514	Arhgap10	1	0	2	0	0	0	0	2	-5	2	2	-2	3	0	5	0	0	0	0
23806	Arih1	1	0	2	1	0	2	0	2	-5	0	1	-3	3	0	5	1	0	2	0
276905	Armc7	0	0	0	1	1	-1	3	1	3	2	1	1	3	0	5	3	0	5	1
71458	Bcor	1	1	-1	2	0	4	1	1	-1	1	1	-1	3	0	5	0	0	0	0
320169	Cdh29	0	0	0	1	0	2	0	0	0	1	1	-1	3	0	5	2	0	4	0
65254	Dpysl5	2	0	4	0	2	-5	0	0	0	2	2	-2	3	0	5	1	0	2	0
67102	Eurl	0	0	0	0	0	0	0	0	0	1	0	2	3	0	5	0	0	0	0
15432	Hoxd12	0	0	0	1	0	2	2	1	1	0	0	0	3	0	5	1	2	-4	0
16564	Kif21a	3	1	3	0	0	0	0	0	0	0	1	-3	3	0	5	0	0	0	1
26407	Map3k4	0	0	0	0	0	0	0	0	0	1	0	2	3	0	5	0	0	0	1
18741	Pitx2	2	0	4	3	0	5	3	2	0	1	1	-1	3	0	5	3	1	3	1
276952	Rasl10b	3	1	3	1	1	-1	1	2	-4	1	1	-1	3	0	5	1	1	-1	0
78748	Rassf10	1	0	2	1	0	2	2	2	-2	1	1	-1	3	0	5	1	1	-1	0
50850	Spast	0	0	0	1	0	2	0	0	0	2	0	4	3	0	5	0	0	0	1
53382	Txnl1	0	0	0	1	0	2	1	0	2	0	0	0	3	0	5	0	0	0	1
229603	Za20d1	0	1	-3	2	1	1	1	0	2	3	0	5	3	0	5	2	0	4	0
HYPERmethylated genes after 3 days upon Dorsal column axatomy (DCA) - with Naive 0 or 1 - 20 Genes																				
403205	Agr3	0	0	0	0	0	0	0	0	0	0	0	0	0	0	0	3	0	5	1
228998	Arfgap1	1	1	-1	1	1	-1	2	1	1	0	0	0	0	0	0	3	0	5	1
276905	Armc7	0	0	0	1	1	-1	3	1	3	2	1	1	3	0	5	3	0	5	1
12330	Canx	2	1	1	0	1	-3	1	1	-1	1	2	-4	2	2	-2	3	0	5	1
12843	Col1a2	1	1	-1	2	2	-2	3	2	0	2	0	4	0	0	0	3	0	5	0
382056	Crtc1	0	1	-3	0	0	0	1	2	-4	2	1	1	1	0	2	3	0	5	0
243376	Doxl2	2	2	-2	3	2	0	3	2	0	1	1	-1	3	1	3	3	0	5	0
269109	Dpp10	0	0	0	1	1	-1	0	1	-3	0	1	-3	1	1	-1	3	0	5	1
72349	Dusp3	2	2	-2	3	2	0	3	2	0	3	2	0	3	2	0	3	0	5	1
68135	Eif3s3	0	1	-3	1	1	-1	3	1	3	1	0	2	2	1	1	3	0	5	0
98221	Ga17	0	0	0	3	1	3	1	1	-1	1	1	-1	2	1	1	3	0	5	0
16506	Kcnd1	0	0	0	0	2	-5	3	2	0	2	0	4	2	2	-2	3	0	5	0
237091	Lhfpl1	0	0	0	0	0	0	2	2	-2	1	1	-1	2	0	4	3	0	5	0
637749	LOC637749	0	0	0	1	1	-1	0	1	-3	0	1	-3	1	1	-1	3	0	5	1
17215	Mcm3	0	0	0	0	0	0	2	2	-2	0	1	-3	0	0	0	3	0	5	0
14767	Nmur1	2	0	4	2	2	-2	1	0	2	0	0	0	0	0	0	3	0	5	0
237987	Otop2	0	0	0	0	0	0	0	0	0	0	0	0	0	0	0	3	0	5	0
18846	Plxna3	1	1	-1	1	0	2	0	1	-3	1	0	2	0	1	-3	3	0	5	0
94090	Trim9	0	1	-3	2	0	4	2	1	1	1	1	-1	2	1	1	3	0	5	0
268470	Ube2z	3	2	0	2	2	-2	1	1	-1	2	0	4	0	1	-3	3	0	5	1

Table S2 – Complete list of functional annotation analysis of hyper- and hypomethylated genes. 10 major functional categories were determined. Two categories were of specific interest, 'Transcription/Chromatin' and '(Neural) Development/Differentiation/Cell Cycle'. Genes were further grouped for their methylation status. Genes with known roles in the nervous system or in axonal regeneration were highlighted in red.

NCBI Gene ID	Gene Symbol	Condition	Protein name
Transcription/Chromatin			
68420	Ankrd13a	hyper for SNA 1D	Ankyrin repeat domain-containing protein 13A
12418	Cbx4	hyper for SNA 1D	E3 SUMO-protein ligase CBX4
75796	Cdyl2	hyper for SNA 3D	Chromodomain protein, Y chromosome-like 2 E
14236	Foxn2	hyper for SNA 3D	Forkhead box protein N2
18741	Pitx2	hyper for SNA 3D	Pituitary homeobox 2
269003	Sap130	hyper for SNA 1D	Histone deacetylase complex subunit SAP130
68094	Smarcc2	hyper for SNA 1D	BAF170-SWI/SNF complex 170 kDa subunit SMARCC2
21423	Tcfe2a	hyper for SNA 1D	Transcription factor E2-alpha
230796	Wdtc1	hyper for SNA 3D	WD and tetratricopeptide repeats protein 1
228994	Ythdf1	hyper for SNA 3D	YTH domain family protein 1
71991	Ercc8	hypo for SNA 1D	DNA excision repair protein ERCC-8
66071	Ethe1	hypo for SNA 7D	Protein ETHE1, mitochondrial
19668	Rbpsuhl/Rbpjl	hypo for SNA 1D,3D	Recombining binding protein suppressor of hairless-like protein
93759	Sirt1	hypo for SNA 7D	NAD-dependent deacetylase sirtuin-1
71458	Bcor	hyper for DCA 3D	BCL-6 corepressor
382056	Crtc1	hyper for DCA 7D	CREB-regulated transcription coactivator 1
14843	Gsh2	hyper for DCA 1D	GS homeobox 2
15432	Hoxd12	hyper for DCA 3D	Homeobox protein Hox-D12
17215	Mcm3	hyper for DCA 7D	DNA replication licensing factor MCM3
18741	Pitx2	hyper for DCA 3D	Pituitary homeobox 2
72068	Cnot2	hypo for DCA 7D	CCR4-NOT transcription complex subunit 2
14886	Gtf2i	hypo for DCA 7D	General transcription factor II-I
17537	Mrg2	hypo for DCA 7D	Cbp/p300-interacting transactivator 4
68728	Trp53inp2	hypo for DCA 7D	Tumor protein p53-inducible nuclear protein 2
(Neural) Development/Differention/Cell Cycle			
14360	Fyn	hyper for SNA 1D	Proto-oncogene tyrosine-protein kinase Fyn
380629	Heca	hyper for SNA 1D	HEPACAM family member 2
70083	Metrn	hyper for SNA 1D	Meteorin
216860	Neurl4	hyper for SNA 1D	Neuralized-like protein 4
66308	Ttdn1/Mplkip	hyper for SNA 3D	M-phase-specific PLK1-interacting protein
65254	Dpysl5	hyper for DCA 3D	Dihydropyrimidinase-related protein 5
Cell Structure/ECM/Cytoskeleton			
12739	Cldn3	hyper for SNA 3D	Claudin-3
14118	Fbn1	hyper for SNA 1D	Fibrillin-1
319448	Fndc3a	hyper for SNA 1D	Fibronectin type-III domain-containing protein 3a
110033	Kif22	hyper for SNA 1D,7D	Kinesin-like protein KIF22
16570	Kif3c	hyper for SNA 3D	Kinesin-like protein KIF3C
16682	Krt2-4	hypo for SNA 1D,3D	Keratin, type II cytoskeletal 4
272381	Lrrc4b	hypo for SNA 3D	Leucine-rich repeat-containing protein 4B
54419	Cldn6	hyper for DCA 1D	Claudin-6
320169	Cdh29/Cdhr4	hyper for DCA 3D	Cadherin-related family member 4 (new Gene ID 69398)
12843	Col1a2	hyper for DCA 7D	Collagen alpha-2(I) chain
16564	Kif21a	hyper for DCA 3D	Kinesin-like protein KIF21A
50850	Spast	hyper for DCA 3D	Spastin
11877	Arvcf	hypo for DCA 7D	Armadillo repeat protein deleted in velocardiofacial syndr. hom.
94245	Dtnbp1	hypo for DCA 1D,7D	Dysbindin
140703	Emid1/Emu1	hypo for DCA 1D	EMI domain-containing protein 1
16573	Kif5b	hypo for DCA 7D	Kinesin-1 heavy chain
67938	Mylc2b	hypo for DCA 3D	Myosin regulatory light chain MRLC2
216856	Nlgn2	hypo for DCA 7D	Neuroligin-2
76816	Sdccag8	hypo for DCA 7D	Serologically defined colon cancer antigen 8
208431	Shroom4	hypo for DCA 7D	shroom family member 4

NCBI Gene ID	Gene Symbol	Condition	Protein name
Signal Transduction			
70419	2810408A11Rik	hyper for SNA 1D	Novel protein similar to protein phosphatase Ppp1r2
271813	Agbl2	hyper for SNA 1D	Cytosolic carboxypeptidase 2
654812	Angptl7	hyper for SNA 7D	Angiopoietin-related protein 7
73167	Arhgap8	hyper for SNA 7D	Rho GTPase-activating protein 8
12325	Camk2g	hyper for SNA 3D	Calcium/calmodulin-dependent protein kinase type II gamma
68119	Cmtm3	hyper for SNA 1D	CKLF-like MARVEL transmembrane domain-containing protein 3
224897	Dpp9	hyper for SNA 3D	Dipeptidyl peptidase 9
98970	Fibcd1	hyper for SNA 1D	Fibrinogen C domain-containing protein 1
57265	Fzd2	hyper for SNA 1D	Frizzled-2
26431	Git2	hyper for SNA 1D	ARF GTPase-activating protein GIT2
338372	Map3k9	hyper for SNA 1D	Mitogen-activated protein kinase kinase kinase 9
18619	Penk1	hyper for SNA 1D	Proenkephalin-A
56294	Ptpn9	hyper for SNA 3D	Tyrosine-protein phosphatase non-receptor type 9
19271	Ptprj	hyper for SNA 1D	Receptor-type tyrosine-protein phosphatase eta
11421	Ace	hypo for SNA 1D	Angiotensin-converting enzyme 2
320982	Arl4c	hypo for SNA 3D	ADP-ribosylation factor-like protein 4C
14685	Gnat1	hypo for SNA 1D	Guanine nucleotide-binding protein G(t) subunit alpha-1
229877	Rap1gds1	hypo for SNA 3D	Rap1 GTPase-GDP dissociation stimulator 1
75841	Rnf139	hypo for SNA 3D	RING finger protein 139
78514	Arhgap10	hyper for DCA 3D	Rho GTPase-activating protein 10
72349	Dusp3	hyper for DCA 7D	Dual specificity protein phosphatase 3
26407	Map3k4	hyper for DCA 3D	Mitogen-activated protein kinase kinase kinase 4
14767	Nmur1	hyper for DCA 7D	Neuromedin-U receptor 1
18846	Plxna3	hyper for DCA 7D	Plexin-A3
276952	Rasl10b	hyper for DCA 3D	Ras-like protein family member 10B
78748	Rassf10	hyper for DCA 3D	Ras association domain-containing protein 10
27279	Tnfrsf12a	hyper for DCA 1D	Tumor necrosis factor receptor superfamily member 12A
229603	Za20d1/Out7b	hyper for DCA 1D,3D	OTU domain-containing protein 7B
110355	Adrbk1	hypo for DCA 7D	Beta-adrenergic receptor kinase 1
72685	Dnajc6	hypo for DCA 1D	Putative tyrosine-protein phosphatase auxilin
14159	Fes	hypo for DCA 1D	Proto-oncogene tyrosine-protein kinase Fes/Fps
53602	Hpcal1	hypo for DCA 7D	Hippocalcin-like protein 1
26921	Map4k4	hypo for DCA 7D	Mitogen-activated protein kinase kinase kinase kinase 4
24066	Spry4	hypo for DCA 7D	SPRY domain-containing protein 4
387515	Tas2r144	hypo for DCA 3D	Taste receptor type 2 member 40
22414	Wnt2b	hypo for DCA 1D	Protein Wnt-2b
Protein Modification			
26554	Cul3	hyper for SNA 1D	Cullin-3
234796	Klhl36	hypo for SNA 3D	Kelch-like protein 36
230654	Lrrc41	hypo for SNA 3D	Leucine-rich repeat-containing protein 41
23806	Arih1	hyper for DCA 3D	Protein ariadne-1 homolog
19072	Prep	hyper for DCA 1D	Presequence protease 1, chloroplastic/mitochondrial
268470	Ube2z	hyper for DCA 7D	Ubiquitin-conjugating enzyme E2 Z
70510	Rnf167	hypo for DCA 7D	E3 ubiquitin-protein ligase RNF167
320538	Ubn2	hypo for DCA 7D	Ubinuclein-2
Translation/mRNA processing			
432508	Cpsf6	hyper for SNA 1D	Cleavage and polyadenylation specificity factor subunit 6
78784	Tnrc4	hyper for SNA 1D	CUG-BP- and ETR-3-like factor 3
68135	Eif3s3	hyper for DCA 7D	Eukaryotic translation initiation factor 3 subunit H
98221	Ga17/Eif3m	hyper for DCA 7D	Eukaryotic translation initiation factor 3 subunit M
231413	Grsf1	hyper for DCA 1D	G-rich sequence factor 1
231464	Cnot6l	hypo for DCA 7D	CCR4-NOT transcription complex subunit 6-like
72692	Hnrpll	hypo for DCA 7D	Heterogeneous nuclear ribonucleoprotein L-like
57444	Isg20	hypo for DCA 3D	Interferon-stimulated gene 20 kDa protein
118451	Mrps2	hypo for DCA 3D	28S ribosomal protein S2, mitochondrial

NCBI Gene ID	Gene Symbol	Condition	Protein name
Transport/Ion channels			
140740	Sec63	hyper for SNA 1D	Translocation protein SEC63 homolog
59049	Slc22a17	hyper for SNA 1D	Solute carrier family 22 member 17
53896	Slc7a10	hyper for SNA 1D	Asc-type amino acid transporter 1 (
22063	Trpc1	hyper for SNA 1D	Short transient receptor potential channel 1 (TrpC1)
74105	Gga2	hyper for SNA 3D	ADP-ribosylation factor-binding protein GGA2
269513	Nkain3	hyper for SNA 3D	Na+/K+ transporting ATPase subunit beta-1-interacting protein 3
18145	Npc1	hyper for SNA 3D	Niemann-Pick C1 protein
239766	Rtp1	hyper for SNA 7D	Receptor-transporting protein 1
67075	Magt1	hypo for SNA 3D	Magnesium transporter protein 1
228998	Arfgap1	hyper for DCA 7D	Arfgap1 protein
12330	Canx	hyper for DCA 7D	Calnexin
269109	Dpp10	hyper for DCA 7D	Inactive dipeptidyl peptidase 10
16506	Kcnd1	hyper for DCA 7D	Potassium voltage-gated channel subfamily D member 1
59049	Slc22a17	hyper for DCA 1D	Solute carrier family 22 member 17
94090	Trim9	hyper for DCA 7D	E3 ubiquitin-protein ligase TRIM9
11419	Accn2	hypo for DCA 7D	Amiloride-sensitive cation channel 2, neuronal
11550	Adra1d	hypo for DCA 3D	Alpha-1D adrenergic receptor
16004	Igf2r	hypo for DCA 7D	Cation-independent mannose-6-phosphate receptor
231290	Slc10a4	hypo for DCA 1D	Sodium/bile acid cotransporter 4
67863	Slc25a11	hypo for DCA 7D	Mitochondrial 2-oxoglutarate/malate carrier protein (OGCP)
67808	Tprgl	hypo for DCA 7D	Tumor protein p63-regulated gene 1-like protein
56491	Vapb	hypo for DCA 7D	Vesicle-associated membrane protein-associated protein B/C
Metabolism			
72482	Acbd6	hyper for SNA 1D	Acyl-CoA-binding domain-containing protein 6
13177	Dci	hyper for SNA 1D	3,2-trans-enoyl-CoA isomerase, mitochondrial
69046	Hbld2	hyper for SNA 7D	Iron-sulfur cluster assembly 1 homolog, mitochondrial
11639	Ak3l1	hypo for SNA 3D	Adenylate kinase isoenzyme 4, mitochondrial
11717	Ampd3	hypo for SNA 3D	AMP deaminase 3
66142	Cox7b	hypo for SNA 3D	Cytochrome c oxidase subunit 7B, mitochondrial
66576	Uqcrh	hypo for SNA 3D	Cytochrome b-c1 complex subunit 6, mitochondrial
56068	Ammecr1	hyper for DCA 1D	AMMECR1-like protein
243376	Doxl2	hyper for DCA 7D	Diamine oxidase-like protein 2
433586	Maml3	hyper for DCA 1D	Mastermind-like protein 3
53382	Txnl1	hyper for DCA 3D	Thioredoxin-like protein 1
11702	Amd1	hypo for DCA 7D	S-adenosylmethionine decarboxylase proenzyme 1
11703	Amd2	hypo for DCA 7D	S-adenosylmethionine decarboxylase proenzyme 2
13123	Cyp7b1	hypo for DCA 7D	Cytochrome P450 7B1

NCBI Gene ID	Gene Symbol	Condition	Protein name
Stress response/Apoptosis			
56295	Higd1a	hyper for SNA 3D	HIG1 domain family member 1A
244882	Tnfaip8l3	hyper for SNA 3D	Tumor necrosis factor, alpha-induced protein 8-like protein 3
56274	Stk3	hypo for DCA 3D	Serine/threonine-protein kinase 3
Others/Unknown			
69380	1700013G24Rik	hyper for SNA 1D	Putative uncharacterized protein
67642	4930515G01Rik	hyper for SNA 1D	Putative uncharacterized Protein
442825	A230083G16Rik	hyper for SNA 1D	Putative uncharacterized protein
192136	AF397014	hyper for SNA 3D	Putative uncharacterized protein
53951	Ccdc75	hyper for SNA 1D	Coiled-coil domain-containing protein 75
68944	Tmco1	hyper for SNA 1D,7D	Transmembrane and coiled-coil domain-containing protein 1
68027	Tmem178	hyper for SNA 1D	Transmembrane protein 178
320237	6330419J24Rik	hypo for SNA 7D	Putative uncharacterized protein
109050	6530418L21Rik	hypo for SNA 7D	Putative uncharacterized protein
619306	B430319F04Rik	hypo for SNA 3D	Putative uncharacterized protein
270028	Tmem28	hypo for SNA 7D	Transmembrane protein FAM155B
403205	Agr3	hyper for DCA 7D	Anterior gradient homolog 3 (Xenopus laevis)
276905	Armc7	hyper for DCA 3D,7D	Armadillo repeat-containing protein 7
53951	Ccdc75	hyper for DCA 1D	Coiled-coil domain-containing protein 75
67102	Eurl	hyper for DCA 3D	Protein EURL homolog
237091	Lhfpl1	hyper for DCA 7D	Lipoma HMGIC fusion partner-like 1 protein
637749	LOC637749	hyper for DCA 7D	Putative uncharacterized protein
237987	Otop2	hyper for DCA 7D	Otopetrin-2
67326	1700037H04Rik	hypo for DCA 7D	Putative uncharacterized protein
66528	2210020M01Rik	hypo for DCA 7D	Putative uncharacterized protein
70793	4631402N15Rik	hypo for DCA 7D	Putative uncharacterized protein
327824	5330438D12Rik	hypo for DCA 7D	Putative uncharacterized protein
381155	9630014M24Rik	hypo for DCA 7D	Putative uncharacterized protein
654824	Ankrd37	hypo for DCA 1D	Ankyrin repeat domain-containing protein 37
67148	FAM103A1	hypo for DCA 7D	Protein FAM103A1
70363	Fam135b	hypo for DCA 7D	Protein Fam135b
381353	Gm996	hypo for DCA 7D	Gene model 996, (NCBI)
625424	LOC625424	hypo for DCA 1D	Putative uncharacterized protein
380916	Lrch1	hypo for DCA 7D	Leu-rich repeat and calponin homology domain-contain. protein 1
66079	Tmem42	hypo for DCA 7D	Transmembrane protein 42

Table S3 – DNA methylation analysis for selected genes in association with regeneration, chromatin remodeling, and transcription. From a total number of 73 investigated RAGs, genes for chromatin-modifying enzymes, and transcription factors, most were not significantly methylated at their proximal promoter. Only few genes exhibited a weak or extreme status of hyper- or hypomethylation for some conditions but none were differentially methylated. This list makes no claim to completeness.

NCBI	Gene	SNA 1 day			SNA 3 days			SNA 7 days			DCA 1 day			DCA 3 days			DCA 7 days			N
Gene ID	Symbol	Inj	Sh	MV	Inj	Sh	MV	Inj	Sh	MV	Inj	Sh	MV	Inj	Sh	MV	Inj	Sh	MV	
Regeneration-associated genes (RAGs)																				
70350	Basp1	0	0	0	0	0	0	0	0	0	0	0	0	0	0	0	0	0	0	0
12064	Bdnf	0	0	0	0	0	0	0	0	0	0	0	0	0	0	0	0	0	0	0
12310	Calca	0	0	0	0	0	0	0	0	0	0	0	0	0	0	0	0	0	0	0
12661	Chl1	0	0	0	0	0	0	0	0	0	0	0	0	0	0	0	0	0	0	0
14419	Gal	0	0	0	0	0	0	0	1	-3	1	0	2	0	0	0	1	0	2	0
14427	Galr1	0	0	0	1	0	2	1	0	2	0	0	0	0	0	0	0	0	0	0
14428	Galr2	0	0	0	0	0	0	0	0	0	0	0	0	0	0	0	0	0	0	0
14429	Galr3	0	0	0	0	1	-3	0	1	-3	0	0	0	1	1	-1	0	0	0	0
14432	Gap43	0	0	0	0	0	0	0	0	0	0	0	0	0	0	0	0	0	0	0
16728	L1cam	0	0	0	0	0	0	0	0	0	0	0	0	0	0	0	0	0	0	0
16852	Lgals1	0	0	0	0	0	0	0	0	0	0	0	0	2	1	1	0	1	-3	0
16878	Lif	3	2	0	3	2	0	3	2	0	3	2	0	3	2	0	3	2	0	2
16880	Lifr	0	0	0	0	0	0	0	0	0	0	0	0	0	0	0	0	0	0	0
17136	Mag	0	0	0	0	0	0	0	0	0	0	0	0	0	0	0	0	0	0	0
18049	Ngfb	0	1	-3	0	0	0	0	0	0	0	0	0	0	0	0	0	0	0	0
18053	Ngfr	0	0	0	0	0	0	0	0	0	0	0	0	0	0	0	0	0	0	0
20753	Sprr1a	0	0	0	0	0	0	0	0	0	0	0	0	0	0	0	0	0	0	0
20257	Stmn2	0	0	0	0	0	0	0	0	0	0	1	-3	0	0	0	0	0	0	0
Transcription factors																				
14281	c-Fos	0	0	0	0	0	0	0	0	0	0	0	0	0	0	0	0	0	0	0
16476	c-Jun	0	2	-5	0	0	0	0	0	0	0	0	0	0	0	0	0	0	0	0
12912	Creb1	0	0	0	0	0	0	0	0	0	0	0	0	0	0	0	0	0	0	0
54446	Nfat5	0	0	0	0	0	0	0	0	0	0	0	0	0	0	0	0	0	0	0
18018	Nfatc1	0	0	0	0	0	0	0	0	0	0	1	-3	0	0	0	0	0	0	0
18019	Nfatc2	0	0	0	0	0	0	0	0	0	0	0	0	0	0	0	0	0	0	0
18021	Nfatc3	0	0	0	0	0	0	0	0	0	0	0	0	0	0	0	0	0	0	0
73181	Nfatc4	0	0	0	0	0	0	0	0	0	0	0	0	0	0	0	0	0	0	0
18033	Nfkb1	0	0	0	0	0	0	0	0	0	0	0	0	0	0	0	0	0	0	0
18034	Nfkb2	3	2	0	3	2	0	3	2	0	3	2	0	3	2	0	2	2	-2	2
18035	Nfkbia	2	0	4	0	0	0	0	0	0	1	0	2	0	0	0	0	0	0	0
18036	Nfkbib	0	0	0	0	0	0	0	0	0	0	0	0	0	0	0	0	0	0	0
18037	Nfkbie	2	1	1	1	2	-4	1	0	2	1	0	2	1	1	-1	0	1	-3	0
18038	Nfkbil1	0	0	0	0	0	0	0	0	0	0	0	0	0	0	0	0	0	0	0
72749	Nfkbil2	0	0	0	0	0	0	0	0	0	0	0	0	0	0	0	0	0	0	0
80859	Nfkbiz	0	0	0	0	0	0	0	0	0	0	0	0	0	0	0	0	0	0	0
22059	Trp53	0	0	0	0	0	0	0	0	0	1	1	-1	2	2	-2	0	0	0	1
22061	Trp63	0	0	0	0	0	0	0	0	0	0	0	0	0	0	0	0	0	0	0
22062	Trp73	0	0	0	0	0	0	0	0	0	0	0	0	0	0	0	0	0	0	0

NCBI	Gene	SNA 1 day			SNA 3 days			SNA 7 days			DCA 1 day			DCA 3 days			DCA 7 days			N
Gene ID	Symbol	Inj	Sh	MV	Inj	Sh	MV	Inj	Sh	MV	Inj	Sh	MV	Inj	Sh	MV	Inj	Sh	MV	
Chromatin modifying enzymes																				
12705	Cited1	0	0	0	0	0	0	0	0	0	0	0	0	0	0	0	0	0	0	0
17684	Cited2	0	0	0	0	0	0	0	0	0	0	0	0	0	0	0	0	0	0	0
56222	Cited4	1	0	2	1	1	-1	2	2	-2	1	1	-1	2	1	1	2	1	1	0
12914	Crebbp	1	0	2	0	0	0	0	0	0	0	0	0	0	0	0	0	0	0	0
58521	Cri1	0	0	0	0	0	0	0	0	0	0	0	0	0	0	0	0	0	0	0
386655	Cri2	0	0	0	0	0	0	0	0	0	0	0	0	0	0	0	0	0	0	0
13433	Dnmt1	0	0	0	0	0	0	2	1	1	1	0	2	2	0	4	0	0	0	1
13434	Dnmt2	0	0	0	0	0	0	0	0	0	0	0	0	0	0	0	0	0	0	0
13435	Dnmt3a	0	0	0	0	0	0	0	0	0	0	0	0	0	0	0	0	0	0	0
13436	Dnmt3b	0	0	0	0	0	0	0	0	0	0	0	0	0	0	0	0	0	0	0
54427	Dnmt3l	0	0	0	0	0	0	0	0	0	0	0	0	0	0	0	0	0	0	0
328572	Ep300	1	0	2	1	1	-1	0	0	0	0	0	0	1	0	2	0	0	0	1
14056	Ezh2	1	0	2	0	0	0	0	0	0	1	0	2	0	0	0	0	0	0	0
14534	Gcn5l2/Kat2a	0	0	0	0	0	0	0	0	0	0	0	0	0	1	-3	0	0	0	0
433759	Hdac1	0	0	0	0	0	0	0	0	0	0	0	0	0	0	0	0	0	0	0
170787	Hdac10	0	0	0	0	0	0	1	2	-4	1	0	2	1	1	-1	1	0	2	0
232232	Hdac11	2	1	1	0	1	-3	1	0	2	3	2	0	1	0	2	0	0	0	0
15182	Hdac2	0	0	0	0	0	0	0	0	0	0	0	0	0	0	0	0	0	0	0
15183	Hdac3	0	0	0	0	0	0	0	0	0	0	0	0	0	0	0	0	0	0	0
208727	Hdac4	0	0	0	0	0	0	0	0	0	0	0	0	0	0	0	0	0	0	0
15184	Hdac5	3	2	0	2	2	-2	0	0	0	3	1	3	1	1	-1	1	2	-4	3
15185	Hdac6	0	0	0	0	0	0	0	0	0	0	0	0	0	0	0	0	0	0	0
56233	Hdac7a	0	0	0	0	0	0	0	0	0	1	0	2	0	0	0	0	0	0	0
70315	Hdac8	0	0	0	0	0	0	0	0	0	0	0	0	0	0	0	0	0	0	0
79221	Hdac9	0	0	0	0	0	0	0	0	0	0	0	0	0	0	0	0	0	0	0
104263	Jmjd1a	0	0	0	0	0	0	0	0	0	0	0	0	0	0	0	0	0	0	0
230674	Jmjd2a	0	0	0	0	0	0	0	0	0	0	0	0	0	0	0	0	0	0	0
193796	Jmjd2b	0	0	0	0	0	0	0	0	0	0	0	0	0	0	0	0	0	0	0
76804	Jmjd2c	0	0	0	0	0	0	0	0	0	0	0	0	0	0	0	0	0	0	0
244694	Jmjd2d	0	0	0	0	0	0	0	0	0	0	0	0	0	0	0	0	0	0	0
216850	Jmjd3	0	0	0	0	0	0	0	0	0	0	0	0	0	0	0	0	0	0	0
194952	Jmjd4	0	0	0	0	0	0	0	0	0	0	0	0	0	0	0	0	0	0	0
77035	Jmjd5	0	0	0	0	0	0	0	0	0	0	0	0	0	0	0	0	0	0	0
18519	Pcaf/Kat2b	0	0	0	0	0	0	0	0	0	0	0	0	0	0	0	0	0	0	0
20937	Suv39h1	0	0	0	0	0	0	0	0	0	0	0	0	0	0	0	0	0	0	0
64707	Suv39h2	0	0	0	0	0	0	0	0	0	0	0	0	0	0	0	0	0	0	0

Table S4 – Detailed list of CpG island (CGI) analysis for selected RAGs and selected differentially methylated genes. Genomic sequences together with the 5 kb promoter region upstream of the transcription start site (TSS) of 15 RAGs, 18 differentially methylated genes, and 2 housekeeping genes were analyzed (ENSEMBL genome browser). Almost all genes exhibited one or more CGIs within the proximal gene promoter region or around the TSS Housekeeping genes are highlighted in blue (Ref), RAGs in green (RAG), and differentially methylated genes in red (DM). As an indicator for the CpG content, normalized CpG were calculated as obs/exp CpG ratio for the 3 kb region around the TSS. The size of regular CGIs is given in black, that of combined CGIs in red, and that of significant CGIs smaller than 200 bp in italic (can be included in combined CGIs). Several prominent CGIs were found close to the 3'-UTR region potentially belonging to other transcription units. Values for sizes are given in basepairs, and positions are given in base pairs (bp) relative to the TSS. CGIs were identified with the CPGPlot online tool. Standard parameters of CGI identification were applied (with the exception of selectively allowing a CGI size smaller than 200 bp).

Gene	Ensembl ID	Gene size	Tr. Start (to TSS)	Window CGI	CGI start (to TSS)	CGI size (approx.)	Norm. CpG (3 kb, TSS)
Actb (Ref)	ENSMUSG00000029580	3.640	+1,068	100	-116	1.300	0,65
Gapdh (Ref)	ENSMUSG00000057666	4.615	+694	100	*-2.265*	*110*	0,40
					664	*337*	
					1.008	530	
					1.573	*120*	
					5.834	*110*	
					7.671	*120*	
Adra1d (DM)	ENSMUSG00000027335	16.436	+115	100	-599	1770	0,68
					8.392	*110*	
					15.806	470	
Arhgap10 (DM)	ENSMUSG00000037148	267.542	+124	100/200	-607	1230	0,70
					216.500	460	
Basp1 (RAG)	ENSMUSG00000045763	50.480	+48,856	100	-1.233	780	0,72
					-287	1.640	
					31301	*110*	
					36316	*110*	
					41.213	*110*	
					48.679	930	
					54.692	*280*	
Bdnf (RAG)	ENSMUSG00000048482	52.348	+48,703	100	*-1.170*	*760*	0,56
					1.304	260	
					2.513	470	
					3.365	260	
					17.661	210	
					18.657	900	
					20.360	*150*	
					48.719	*520*	
Calca/Cgrp1 (RAG)	ENSMUSG00000030669	4.878	+1,145	100	1.212	350	0,29
Cbx4 (DM)	ENSMUSG00000039989	8.649	+204	100	-4.951	1.170	0,67
					-3.489	240	
					-1.534	*390*	
					-361	1.150	
					5.407	210	
					4.832	540	
					7.137	*100*	

Gene	Ensembl ID	Gene size	Tr. Start (to TSS)	Window CGI	CGI start (to TSS)	CGI size (approx.)	Norm. CpG (3 kb, TSS)
Chl1 (RAG)	ENSMUSG00000030077	238.802	+131,095	100	*-51*	*110*	0,38
					1.273	*340*	
					25.588	*140*	
					70.150	260	
					70.633	640	
					192.174	*110*	
					208.712	280	
					209.211	260	
					228.644	*110*	
Cul3 (DM)	ENSMUSG00000004364	75.558	+169	100	-639	1.250	0,81
Emid1 (DM)	ENSMUSG00000034164	45.993	+35	100	-308	470	0,44
					15.558	*110*	
Galanin (RAG)	ENSMUSG00000024907	4.554	+360	100	-168	360	0,28
Gap43 (RAG)	ENSMUSG00000047261	92.210	+149	100	*-240*	*333*	0,36
					26.831	*150*	
					84.772	*110*	
Gnat1 (DM)	ENSMUSG00000034837	5.116	+44	100	*-4.469*	*480*	0,37
					-3.236	*150*	
					2.470	1.250	
Kif3c (DM)	ENSMUSG00000020668	41.363	+849	100	-53	370	0,46
					940	*100*	
					1.902	*230*	
Kif22 (DM)	ENSMUSG00000030677	14.689	+19	100	-158	440	0,44
					6.470	*130*	
					9.022	*110*	
					14.841	2.260	
					17.787	*110*	
L1cam (RAG)	ENSMUSG00000031391	27.075	+11,030	100	*-456*	*120*	0,35
					-44	260	
Lgals1 (RAG)	ENSMUSG00000068220	3.741	+71	100	1.291	360	0,30
					8.134	540	
Lif (RAG)	ENSMUSG00000034394	14.958	+9,042	100	9.025	920	0,18
					11.399	*100*	
Maml3 (DM)	ENSMUSG00000061143	427.281	+748	100/200	-554	890	0,74
					721	2160	
					34.904	240	
					96.978	210	
					174.302	210	
					403.144	210	
Map3k4 (DM)	ENSMUSG00000014426	91.126	+120	100/200	-181	830	0,68
					33.515	320	
					34.435	460	
					90.819	220	
Matn4 (DM)	ENSMUSG00000016995	15.532	+3,240	100	-3.298	610	0,37
	(overlap with Rbpjl)				*269*	*150*	
					1.887	*100*	
					4.117	480	
					4.922	*110*	
					6.666	940	
					8.875	*140*	
					10.440	740	
					15.018	340	

Gene	Ensembl ID	Gene size	Tr. Start (to TSS)	Window CGI	CGI start (to TSS)	CGI size (approx.)	Norm. CpG (3 kb, TSS)
Nrg2 (RAG)	ENSMUSG00000060275	179.702	+309	100/200	*-2.181*	*100*	0,52
					-406	1.330	
					128.403	630	
					178.453	850	
Rbpjl (DM)	ENSMUSG00000017007	12.308	+103	100	-4.951	240	0,39
					-3.075	*110*	
					-2.637	480	
					-28	*100*	
					1.539	*150*	
					4.652	610	
					11.163	260	
Sap130 (DM)	ENSMUSG00000024260	88.691	+1,617	100	-398	1530	0,65
					281	*140*	
Slc10a4 (DM)	ENSMUSG00000029219	7.780	+163	100	-82	710	0,49
					2.752	110	
					5.006	*290*	
					6.487	730	
Slit1 (RAG)	ENSMUSG00000025020	143.409	+257	100/200	*-3.906*	*110*	0,47
					-201	810	
Smarcc2 (DM)	ENSMUSG00000025369	30.938	+91	100	-796	1440	0,76
					9.474	*410*	
					21.134	*110*	
					23.448	*100*	
Sprr1a (RAG)	ENSMUSG00000050359	1.940	+1,202	100	- - -	- - -	0,04
Stmn2 (RAG)	ENSMUSG00000027500	52.078	+85	100	*-12*	*150*	0,36
					593	220	
					2.025	*110*	
					32.437	*110*	
Tnfrsf12A (RAG)	ENSMUSG00000023905	2.003	+29	100	*-2.429*	*440*	0,53
					-1.686	*120*	
					-151	420	
					568	200	
					3.474	460	
Tprgl (DM)	ENSMUSG00000029030	3.182	+37	100	-559	960	0,64
Trp53 (RAG)	ENSMUSG00000059552	11.515	+6,541	100	-1.925	1050	0,70
					133	220	
					600	700	
					4.598	*110*	
					7.919	*270*	
					9.226	*120*	
					10.252	*100*	
Wnt2b (DM)	ENSMUSG00000027840	16.905	+237	100	-812	1180	0,55
					5.696	*100*	
					6.894	*180*	
					8.488	*350*	
					10.557	*100*	
Ythdf1 (DM)	ENSMUSG00000038848	16.573	+239	100	-197	910	0,59
					9.761	*140*	
					16.275	*110*	

7.2 List of Abbreviations

#	number of
®	registered trademark
°C	degree Celcius
µg	microgram
µl	microliter
µM	micromolar
3'	3-prime end
5-HT	5-hydroxytryptamin
5'	5-prime end
5'-Aza-dC	DNMT inhibitor
A	adenosine
A260/280	absorption at 260 or 280 nm
aa	amino acids
AAV	adeno-associated virus
Ab	antibody
Abb.	Abbildung
ac	acetylated
AdoMet	S-adenosyl-l-methionine
Arg	arginine
AU	arbitrary units
bp	base pair(s)
BSA	bovine serum albumin
C	cytosine
C5	carbon number 5 (of cytosine)
cAMP	cyclic adenosine monophosphate
cDNA	copy DNA
CGI	CpG island
CGN	cerebellar granule neurons
ChIP	chromatin immuoprecipitation
cm	centimeter
CNS	central nervous system
CpG	cytosine-guanidine dinucleotide
CST	corticospinal tract
Cy3/Cy5	fluorophores; cyanine dyes
D	Day (eg 1D)
DAPI	fluorescent stain, 4',6-diamidino-2-phenylindole
DCA	dorsal column axotomy
DM	differentially methylated
DNA	deoxyribonucleic acid
DNMT	De novo methyltransferase
dNTP	deoxyribonucleotide triphosphate
DRG	dorsal root ganglion (ganglia)
DTT	dithiothreitol
E3 SUMO	ubiquitn ligase-like for SUMO1 (Small ubiquitin-related modifier 1)
eg	exempli gratia, 'for example'
EDTA	ehylenediaminetetraacetic acid
ESC	embryonic stem cells
et al.	et alii
EtOH	ethanol
FAM	fluorophore, 6-carboxyfluorescein
FC	fold change
g	gram
G	guanidine
gDNA	genomic DNA
GFP	green fluorescent protein
H3 (eg)	histone 3 (for example)
HAT	histone acetyltransferase
HBSS	Hank's Buffered Salt Solution
HCl	hydrochloric acid
HDAC	histone deacetylase
HKMT	histone lysine methyltransferase
ICR	imprinting control region
IP	immunoprecipitated (sample)
In	Input sample
K9 (eg)	lysine 9 (for example)
kb	kilobase pairs
KDM	lysine demethylase
kg	kilogram
L	liter
L4-L6 DRG	lumbar DRG number 4 to 6
LiCl	lithium chloride
log2/log10	logarithm to the base 2 or 10
Lys	lysine
M	molar
MBD	methyl-CpG binding domain
MBP	methyl-CpG binding protein
me2/3	mono/di-/trimethylated
MeDIP	methylated DNA immunoprecipitation
mg	milligram
min	minute(s)
ml	milliliter
mm	millimeter
mM	millimolar
mRNA	messenger RNA
MV	methylation value
n	replicate number of animals or experiments
NaCl	sodium chloride
NaOAc	sodium acetate
nBAF	a SWI/SNF-type complex in post-mitotic neurons
npBAF	a SWI/SNF-type complex in neural stem or progenitor cells
NCOR2	nuclear receptor corepressor 2
ng	nanogram
nM	nanomolar

NMDA	N-methyl-D-aspartate
NP-40	Nonidet P-40 (octyl phenoxypolyethoxylethanol).
NPC	neural precursor cells
NSC	neural stem cells
NuRD	nucleosome remodelling and histone deacetylase
O2	oxygen
obs/exp	observed to expected ration or CpG island analysis
Oligo(dT)	oligo deoxythymidine
ONC	optic nerve crush
p	phosphate group
PBS	phosphate buffered saline
PCR	polymerase chain reaction
PDL	poly-D-lysine
pH	measure of acidity or basicity of an aqueous solution
PHD	Plant Homeo Domain
PNS	peripheral nervous system
PRC1	Polycomb Repressive Complex 1
ProK	proteinase K
qRT-PCR	quantitative real-time PCR
RA	retinoic acid
RAG	regeneration-associated gene
RCOR1	REST corepressor 1
REST	RE1-silencing transcription factor
RGC	retinal ganglia cell
RNA	ribonucleic acid
RNase	ribonuclease
RT	room temperature
s	second(s)
SDS	sodium dodecyl sulfate
SEM	Standard error of mean
SET	Su(var)3-9, Enhancer-of-zeste and Trithorax
SNA	sciatic nerve axotomy
STD	Standard deviation
T	thymidine
T9/T10	thoracic vertebrae number 9 or 10
TE	Tris/EDTA buffer
TM	trademark
TSA	trichostatin A
TSS	transcription start site
TUJ1	Tubulin, beta 3 class III (TUBB3)
U	unit(s)
VPA	valproic acid
WGA	whole genome amplification

Abbreviations for mouse genes (italic) or for proteins (capital letters) are indicated in the text according to the recommended standard (see MGI database: http://www.informatics.jax.org/).

7.3 List of Figures

7.4 List of Tables

7.5 Publications and congress presentations

(2013) Submitted to Neurotherapeutics
Epigenetic regulation of axon outgrowth and regeneration in CNS injury: the first steps forward
Lindner R, Puttagunta P, and Di Giovanni S

(2013), Submitted to Nature Letters (under revision)
PCAF-dependent epigenetic changes promote axonal regeneration in the central nervous system.
Puttagunta P, Tedeschi A, Soria MG, **Lindner R**, Gaub P, Rathore K, Joshi Y, Nguyen T, Schmandke T, Bradke F, and Di Giovanni S

J Neurochem. 2012 Aug;122(4):844-55. Epub 2012 Jul 9. (PMID: 22671705)
A novel cross-talk between endothelin and ErbB receptors controlling glutamate transporter expression in astrocytes.
Glisic D, Lehmann C, Figiel M, Ödemis V, **Lindner R**, Engele J

Cell Physiol Biochem. 2010;25(6):723-32. Epub 2010 May 18. (PMID: 20511718)
The serum and glucocorticoid inducible kinases SGK1-3 stimulate the neutral amino acid transporter SLC6A19.
Böhmer C, Sopjani M, Klaus F, **Lindner R**, Laufer J, Jeyaraj S, Lang F, Palmada M

Cell Physiol Biochem. 2010;25(2-3):187-94. Epub 2010 Jan 12. (PMID: 20110679)
Regulation of the glutamate transporter EAAT4 by PIKfyve.
Alesutan IS, Ureche ON, Laufer J, Klaus F, Zürn A, **Lindner R**, Strutz-Seebohm N, Tavaré JM, Boehmer C, Palmada M, Lang UE, Seebohm G, Lang F

J Biol Chem. 2009 Jul 10;284(28):18816-23. Epub 2009 May 14. (PMID: 19443652)
NFAT-3 is a transcriptional repressor of the growth-associated protein 43 during neuronal maturation.
Nguyen T, **Lindner R**, Tedeschi A, Forsberg K, Green A, Wuttke A, Gaub P, Di Giovanni S

Cell Physiol Biochem. 2009;24(5-6):361-8. Epub 2009 Nov 4. (PMID: 19910676)
Regulation of the glutamate transporter EAAT2 by PIKfyve.
Gehring EM, Zurn A, Klaus F, Laufer J, Sopjani M, **Lindner R**, Strutz-Seebohm N, Tavaré JM, Boehmer C, Palmada M, Lang UE, Seebohm G, Lang F

Neurochem Int. 2009 May-Jun;54(5-6):372-7. (PMID: 19418632)
Regulation of the Na(+)-coupled glutamate transporter EAAT3 by PIKfyve.
Klaus F, Gehring EM, Zürn A, Laufer J, **Lindner R**, Strutz-Seebohm N, Tavaré JM, Rothstein JD, Boehmer C, Palmada M, Gruner I, Lang UE, Seebohm G, Lang F

Cell Physiol Biochem. 2009;23(1-3):25-36. Epub 2009 Feb 18. (PMID: 19255497)
The C-terminal PDZ-binding motif in the Kv1.5 potassium channel governs its modulation by the Na+/H+ exchanger regulatory factor 2.
Laufer J, Boehmer C, Jeyaraj S, Knuwer M, Klaus F, **Lindner R**, Palmada M, Lang F

Cell Physiol Biochem. 2008;22(5-6):705-14. Epub 2008 Dec 9. (PMID: 19088452)
The peptide transporter PEPT2 is targeted by the protein kinase SGK1 and the scaffold protein NHERF2.
Boehmer C, Palmada M, Klaus F, Jeyaraj S, **Lindner R**, Laufer J, Daniel H, Lang F

Cell Physiol Biochem. 2008;22(5-6):591-600. Epub 2008 Dec 9. (PMID: 19088441)
Modulation of the voltage-gated potassium channel Kv1.5 by the SGK1 protein kinase involves inhibition of channel ubiquitination.
Boehmer C, Laufer J, Jeyaraj S, Klaus F, **Lindner R**, Lang F, Palmada M

J Physiol. 2008 Mar 15;586(6):1539-47. Epub 2008 Jan 17. (PMID: 18202099)
Up-regulation of hypertonicity-activated myo-inositol transporter SMIT1 by the cell volume-sensitive protein kinase SGK1.
Klaus F, Palmada M, **Lindner R**, Laufer J, Jeyaraj S, Lang F, Boehmer C

J Cell Mol Med. 2008 Apr;12(2):622-38. Epub 2007 Dec 5. (PMID: 18053084)
Oval cell proliferation in p16INK4a expressing mouse liver is triggered by chronic growth stimuli.
Ueberham E, **Lindner R**, Kamprad M, Hiemann R, Hilger N, Woithe B, Mahn D, Cross M, Sack U, Gebhardt R, Arendt T, Ueberham U.

FEBS Lett. 2007 Dec 11;581(29):5586-90. Epub 2007 Nov 20. (PMID: 18005662)
Regulation of the epithelial calcium channel TRPV6 by the serum and glucocorticoid-inducible kinase isoforms SGK1 and SGK3.
Böhmer C, Palmada M, Kenngott C, **Lindner R**, Klaus F, Laufer J, Lang F.

2010/07: *FENS Forum of European Neuroscience – Poster*

2008/03: *Annual Meeting of the Deutsche Physiologische Gesellschaft 2008 in Cologne – Talk*

2007/03: *Annual Meeting of the Deutsche Physiologische Gesellschaft 2007 in Hannover – Poster*

7.6 Curriculum Vitae

See the following pages